Seasonal variability of ionic concentrations in surface snow and elution processes in snow-firn packs at the PGPI site on Glacier No. 1 in eastern Tianshan, China

Zhongqin Li[1], Ross Edwards[2], E. Mosley-Thompson[3], Feiteng Wang[1], Zhibao Dong[1], Xiaoni You[1], Huilin Li[1], Chuanjin Li[1], and Yuman Zhu[1]
([1]*Tianshan Glaciological Station/ Laboratory of Ice Core and Cold Regions Environment, CAREERI, CAS, Lanzhou 730000, China. E-mail: Lizq@lzb.ac.cn*
[2]*Desert Research Institute, Raggio Parkway, Reno, NV 89512, USA*
[3]*Byrd Polar Research Center, the Ohio State University, Columbus, OH 43210, USA*)

ABSTRACT: To investigate the effects of both non-meltwater and meltwater-related post-depositional processes on chemical species within the snow-firn pack, a research program, Program for Glacier Processes Investigation, was initiated in July 2002 by the Tianshan Glaciological Station. The seasonal variability of the ionic concentrations in surface snow samples and ion elution behavior in the snow-firn pack were assessed from surface samples collected year-round and 1,011 samples collected from a snowpit at weekly intervals from September 2003 through September 2004. The results indicate that elevated ionic concentrations in spring and summer result from Asian dust storm-derived aerosol input and other aerosols entrained in precipitation. Potential sources of these chemical species are explored using correlation and factor analyses. The elution sequence through the snow-firn pack was determined to be $SO_4^{2-} > Ca^{2+} > Na^+ > NO_3^- > Cl^- > K^+ > Mg^{2+} > NH_4^+$. The elution of ions at the sampling site was found to be driven primarily by air temperature and became evident when a diurnal mean temperature of -3.6 °C was attained. At 0.3 °C all of the year-round new ionic input was leached from the snow.

INTRODUCTION

Chemical records from alpine ice cores provide an invaluable source of paleoclimatic and environmental information (Thompson and others, 1995, 1998; Ginot, 2001). Not only are the atmospheric chemical composition and depositional processes recorded, but post-depositional processes within the snow/firn stratum, especially when melt occurs, are recorded as well. To investigate the effects of depositional processes and meltwater-related post-depositional processes on chemical species in the snow-firn pack, a research program, Program for Glacier

Processes Investigation (PGPI), was launched in July 2002 by the Tianshan Glaciological Station (TGS), Chinese Academy of Sciences (CAS). An observational and experimental site (henceforth the PGPI site) was carefully located in a percolation zone of the east branch of Glacier No. 1 at the headwaters of the Urumqi River at an altitude of 4,130 meters above sea level (masl). Aerosol, surface snow, and snowpit samples were collected on a weekly basis at the PGPI site using established techniques to prevent contamination. They were then transported frozen to the TGS laboratory. At the same time, a variety of observations of the snow-firn pack physical properties and experiments on meltwater were made. Over the duration of the sampling campaign (September 2003 to September 2004) snow-firn density and temperature were measured along a snow pit wall and *in-situ* air temperature was continuously observed using a thermometer screen. Most of the samples were analyzed for major ions and insoluble microparticles while oxygen isotopic ratios (ä^{18}O), trace metals, and carbonaceous particles (organic and black carbon, OC and BC, respectively) were analyzed for selected samples. A suite of samples was also archived (frozen) for future analyses. This study focused on both the seasonal variability of the major ionic concentrations in surface snow and the elution processes in the snow-firn pack, and constituted a basic research component of the PGPI.

METHODOLOGY

Glacier No. 1 (43°06• N, 86°49• E) is located at the headwaters of the Urumqi River in the eastern Tianshan mountains of central Asia that are surrounded by vast desert areas: the Taklimakan to the south, the Gurbantunggut Desert in the Junggar basin to the north, and the Gobi Desert to the east. With a typical continental climate, the westerly jet stream prevails across these high mountains. Glacier No. 1 is a northwest-facing valley glacier composed of east and west branches covering 1.73 km^2. The annual equilibrium line altitude (ELA) has averaged approximately 4,055 masl from 1959 to 2003 (Li, 2003) and the mean annual precipitation is about 645.8 mm a^{-1} on the east branch (Wang and Zhang, 1985; Yang and others, 1988, 1992). The PGPI site was situated at 4,130 masl, with no direct wintertime exposure to sunshine due to the shadowing effect of the mountain ridges. The mean annual air temperature and precipitation at the site were -9.1 °C and 700 mm water equivalent (w.e.), respectively, during the experimental period. Maximum precipitation occurs in summer at the same time as maximum snow melt. The floor of the snow-firn pack at this site is composed of superimposed ice that is typically formed in the glacial percolation zone or superimposed ice zone. The ice is characterized by clear, impermeable, opaque ice with spherical bubbles of 1 to 5 mm diameter. Field observations indicate that the snow depth of the percolation zone typically ranges from about 1.5 m in the late summer to about 3 m in the late spring. During winter it remains stable due to snow compaction, snow drifting and sublimation. In the early summer, as air temperatures rise to ~0°C, the upper part of the snow layer begins to melt, leading to rapid thinning. The melt originates primarily from the accumulation received in the previous autumn. In late summer to early autumn, melting dominates and affects the entire

annual layer and even the previous year's accumulation. The meltwater infiltrates the underlying firn layers, reaching the firn that overlies the impermeable ice formed in the previous year. The meltwater fills the pores of the firn and is refrozen, thus forming superimposed ice. The complete transformation of fresh snow to superimposed ice at the site took 41 to 47 months (You and others, 2005; Wang and others, 2005). Some of the meltwater also pooled on the surface and eventually drained away from the site.

Samples were collected weekly and every effort was made to collect fresh, well-preserved surface snow (i.e. snow not affected by post-depositional processes such as sublimation or melting) to facilitate our investigation of the seasonality in the chemical composition of both precipitation and dry deposition. During the winter season when there was insufficient snowfall, the top three centimeters were sampled. However, if an accumulation event occurred prior to the scheduled sampling, we collected the top one centimeter of fresh snow. During the summer, there was usually sufficient fresh snow available, and samples no more than two days old were collected from the top 3 to 5 cm. Over the year a total of 54 surface snow samples were collected, however, nine samples were discarded for analysis because of problems associated with *in-situ* melting. A pit was also sampled weekly from top to bottom at ten centimeter increments 54 times during the year which resulted in a total of 1,011 samples. After each sampling session, the pit was refilled and then re-excavated seven days later. The wall was then cut back by at least 50 cm before the next round of sample collection.

Strict procedures were followed during sampling and transportation to prevent contamination, including using disposable polyethylene gloves, oronasal masks, and pre-cleaned polyethylene sample containers. All samples were transported frozen to the TGS laboratory. Blanks were made at each step in the process to ensure that the cumulative contamination remained below the baseline of each measured chemical species.

Samples were analyzed for major ions (Na^+, K^+, Ca^{2+}, Mg^{2+}, NH_4^+, Cl^-, SO_4^{2-}, NO_3^-, and $HCOO^-$) by ion chromatography (Dionex DX-320), while concentrations and size distributions of insoluble microparticles were analyzed by an AccuSizer 780A (0.5 to 400 μm measurement range with an uncertainty less than 5%). These methods have been described by Zhao and Li (2004) and Zhu and others (2005).

SEASONAL VARIATIONS OF MAJOR IONS IN SURFACE SNOW

Seasonal variability

The major ion concentrations and insoluble microparticles in the surface snow samples are presented in Figure 1. The ionic balances △C (total cation equivalents minus total anion equivalents) for the 45 samples averaged 36.1 μeq. L^{-1}, accounting for 60% of the total anion content. Linear regression on all the samples showed that the calcium and △C correlate well (R^2=0.97, N=45, $p < 0.01$), suggesting that the △C represents primarily the carbonate/bicarbonate in the snow (Wake, 1992).

The seasonal variability of the surface snow ion chemistry was found to reflect seasonal

inputs of impurities from the atmosphere. Figure 1 demonstrates that Cl^-, Na^+, K^+, SO_4^{2-}, and Ca^{2+} have similar seasonal variations and we categorized them as Group 1. All elements in Group 1 had low concentrations during the period from September 2003 to late March 2004 and high concentrations from April throughout the summer. Group 1 profiles also contained sequential concentration peaks that were associated with precipitation events. During this period the baseline concentration of the ions rose only slightly, suggesting that the concentration increases resulted from precipitation events rather than from an increase in their atmospheric abundance. Insoluble microparticles (dust) in the samples were dominated by particles less than 1.5 μm in diameter. The microparticle and Mg^{2+} concentrations (both categorized as Group 2) were highly linearly correlated ($R = 0.74$, $N=45$, $p < 0.01$; see Table 1), and exhibited a trend very similar to that of Group 1 species before late July. However, in August there were several prominent Mg^{2+} and dust peaks that were absent in the concentrations of Group 1 species. The concentrations of NO_3^-, NH_4^+, and $HCOO^-$ were poorly correlated with those of the other ionic species (Fig. 1) so they were categorized as Group 3. In detail, NO_3^- concentration peaks were prominent during February to March, and in June and August 2004, while relatively high NH_4^+ concentrations appeared during September to October 2003 and from spring to early summer 2004. A reduced baseline emerged during winter 2003 and persisted for much of the summer (2004). Most $HCOO^-$ and NH_4^+ peaks overlap during the study period, but a more pronounced increase of $HCOO^-$ concentration occurred during mid-March to mid-June 2004. In addition, a sharp $HCOO^-$ peak appeared in early December, coinciding with increased wind speeds.

Seasonal variability in the chemical composition of the surface snow was closely associated with climatic and environmental characteristics in the region. For example, cold frontal systems frequently sweep across the region during late March to early May (spring) producing large dust storms (Gao and others, 1992; Li and others, 1994; Wake and others, 1994). This stormy period is followed by the summer precipitation maximum (May through September) that accounts for approximately 90 percent of the annual precipitation. During the rest of the year, the climate regime is cold and dry. Both the spring dust storms and summer precipitation can bring terrestrial impurities to the glacier surface, as reflected by the ionic concentration profiles, especially for Groups 1 and 2, in which the explicit increases during April and early May strongly coincide with period of greatest wind intensity (Figure 1). This suggests that the ionic concentration increases result from the input of local-to-regional dust aerosols derived by strong winds. Most concentration peaks of Group 1 and 2 species overlap throughout the study period, suggesting similar transport and deposition processes. However the amplitudes of the peaks are different, especially during the precipitation events after July 2004 (summer). As the highest concentrations coincide with the largest precipitation events, they likely result primarily from wet deposition and long range transport to the glacier in August. The peaks of Mg^{2+} and insoluble microparticles in the snow samples also support this interpretation. Among the Group 3 species, NO_3^- concentrations are generally out of phase with those in Groups 1 and 2, indicating that it may have different source and depositional mechanisms. NH_4^+ and $HCOO^-$ peaks slightly overlap Group 1 elements (particularly with K^+), but have different amplitudes.

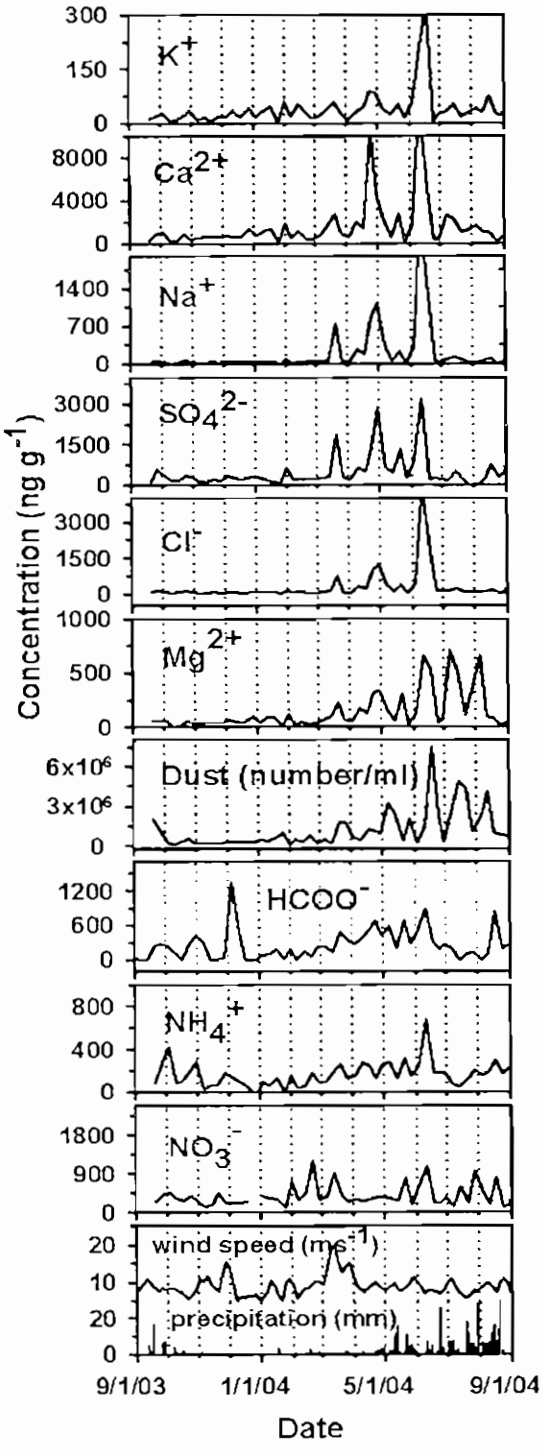

Figure 1. Temporal variations of major ions and dust in surface snow, compared with contemporaneous precipitation and wind speed in this area.

Correlation among the various chemical species

The interrelationship of the chemical species in the snow pack was further investigated using correlation matrices (Table 1) and factor analysis (Table 2). Table 1 presents the matrix of R values for the elements measured in the surface snow. The significant correlations ($R \geqslant 0.7$, 2-tailed, p=0.01, N=45) are highlighted with bold type. To connect these elements to their sources, correlations among the elements were further investigated using factor analysis (Table 2).

Table 1. The correlation matrix for the elements in surface snow

Elements	NH_4^+	Dust	NO_3^-	Cl^-	SO_4^{2-}	Mg^{2+}	Ca^{2+}	Na^+	K^+	$HCOO^-$
NH_4^+	—									
Dust	0.36	—								
NO_3^-	0.53	0.33	—							
Cl^-	0.70*	0.62	0.47	—						
SO_4^{2-}	0.67	0.56	0.62	0.78	—					
Mg^{2+}	0.32	0.74	0.23	0.55	0.36	—				
Ca^{2+}	0.54	0.85	0.30	0.85	0.65	0.65	—			
Na^+	0.65	0.63	0.32	0.97	0.72	0.58	0.89	—		
K^+	0.45	0.49	0.33	0.76	0.48	0.58	0.67	0.76	—	
$HCOO^-$	0.55	0.38	0.45	0.50	0.67	0.20	0.40	0.41	0.36	—

*The bold type indicates that the correlation is significant ($R \geqslant 0.7$) at the 0.01 level (2-tailed).

Table 2. Factor loading matrix for the elements in surface snow

Factors were extracted by principal components analysis, with varimax rotation to produce the final factor loadings.Bold type indicates the highest factor loading

Elements	*Communality*	*Factor loadings*		
		Factor 1	Factor 2	Factor 3
NH_4^+	*0.740*	0.557	0.665	0.033
Dust	*0.902*	0.278	0.266	0.868
NO_3^-	*0.775*	-0.014	0.849	0.231
Cl^-	*0.941*	0.806	0.411	0.351
SO_4^{2-}	*0.828*	0.463	0.742	0.250
Mg^{2+}	*0.825*	0.314	0.041	0.852
Ca^{2+}	*0.892*	0.668	0.241	0.623
Na^+	*0.962*	0.865	0.268	0.376
K^+	*0.711*	0.753	0.155	0.346
$HCOO^-$	*0.668*	0.306	0.757	0.034
Fraction of variance (%)		32.06	26.68	23.70

Factor 1 loadings are highest for Cl^-, Ca^{2+}, Na^+, and K^+, and except for SO_4^{2-} all are Group 1 elements that are significantly correlated with each other. This factor is interpreted as a local-plus-regional source component. Potential sources include local mineral aerosols entrained in the atmosphere by the strong winds that prevail during spring along with a more regional Asian dust flux. Previous studies indicate that local bare rocks and glacial sediments are readily available sources for the elements in Group 1 (Luo and Wang, 1983; Williams and others, 1992; Hou and others, 2002).

Factor 2 loadings are highest for NH_4^+, NO_3^-, SO_4^{2-}, and $HCOO^-$, and except for SO_4^{2-} all are Group 3 elements that are also correlated with each other. This factor is interpreted as an anthropogenic source component that includes emissions from fossil fuel combustion and biomass burning, livestock manure, and commercial and natural fertilizers. Mineral dust commonly acts as a carrier for these pollutants (Li and others, 1995, 1999). Although the region is relatively unpopulated, Glacier No. 1 is situated only 105 km from Urumqi, the provincial capital of Xinjiang Uyger Autonomous Region, with more than two million inhabitants. Also the town of Houxia is only 50 km away in the Urumqi River valley. In addition, the Urumqi-Koehler road passes only a few kilometers from the study site. We suspect that these sources must be largely responsible for the anthropogenically derived compounds deposited on the glacier. Atmospheric pollutants from Urumqi may be transported to the glacier by the low-level regional atmospheric circulation. Clouds from the factories in the town Houxia drift into the river valley and periodically reach Glacier No. 1 by the valley winds (Wake and others, 1992; Lee and others, 2003).

Factor 3 loadings are highest for Mg^{2+} and dust content (Group 2), and the two elements are also significantly linear correlated ($R = 0.74$, 2-tailed, $p=0.01$, $N=45$; see Table 1). This factor is interpreted as a long-distance source component, mainly deposited by wet deposition. Potential sources for this group are mineral dust and evaporite aerosols entrained along the trajectory of the air masses that bring moisture to the region.

Evidently, Ca^{2+} and SO_4^{2-} have more potential sources than other species, making it difficult to attribute them to a particular group. Within Group 1, Ca^{2+} was highly correlated with the elements in Group 2 and had a very high loading (0.623) on factor 3, indicating that the long-distance sources are also a major contributor. The position of the Tianshan Mountains relative to the large desert basins with predominantly calcareous material (Dregne, 1968) provides strong evidence for a desert dust source for Ca^{2+}. In addition to its anthropogenic sources, SO_4^{2-} can be widely derived from terrestrial materials, e.g., pyrite minerals and evaporites, on local and regional scales. A documented record of SO_4^{2-} in an ice core from Glacier No. 1 demonstrates that natural sources associated with mineral dust aerosols are basic contributors of SO_4^{2-} in snow, but anthropogenic sources also have a large impact on the snow chemistry (Annual Report 2003/2004 of Tianshan Glaciological Station, unpublished data, 2006).

ELUTION PROCESS

For most low- to mid-latitude mountain glaciers, snow transforms to ice through infiltration and refreezing processes. Specifically, meltwater infiltrates downward to the bottom of a snow pack where it refreezes as infiltration ice in the percolation zone (Shumskii, 1964; Paterson, 1994). As the meltwater percolates vertically, elution occurs and the chemical species within the firn are redistributed by differential transportation toward the base of the snow pack. If temperatures at the snow pack floor are sufficiently cold the chemical species can be sequentially incorporated into the infiltration ice. This is called the elution process. Under certain conditions, this depositional sequence may be preserved in the glacier; otherwise, the chemical record is destroyed by percolation. Due to elution, the original chemical composition of the snow pack is altered. Previous studies suggest that the elution effect homogenizes the snow chemistry and reduces the resolution of the ice core record, thereby diminishing the value of alpine ice core studies (Johannessen and Henriksen, 1978; Brimblecombe and others, 1985, 1987; Bales and others, 1989; Hewitt and others, 1991). Figure 2 demonstrates the modification of the SO_4^{2-} concentration profile by snowmelt at the PGPI site during the ablation season. As this is a typical result of the elution effect, the PGPI has focused much attention on this process.

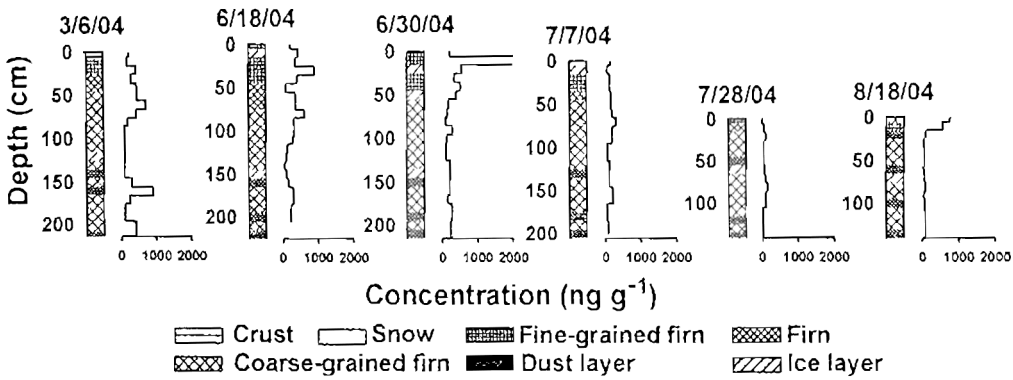

Figure 2. Profiles illustrate the temporal variation of SO_4^{2-} concentrations in the snow-firn pack at the PGPI site and confirm that they are severely modified by snowmelt during the ablation season.

Elution sequence

As described in various field and laboratory studies, ions are leached from snow and firn with different efficiencies, and the elution sequence can be determined by comparing the concentration ratios between different ions (Brimblecombe and others, 1987; Tranter and others, 1992; Eichler and others, 2001; Iizuka and others, 2002). Figure 3 presents variations of Mg^{2+}, NO_3^-, and SO_4^{2-} that provide examples of ionic concentration changes in the snow-firn pack. As explicit changes occurred from April 24, 2004 to June 25, 2004 this was selected as the study period. In the summer ablation season, all ions reached their lowest concentrations and thereafter remained stable until late August. Compared with other ions,

Mg^{2+} demonstrated very little variation over this interval (Figure 3), indicating that it was leached less efficiently from the snow. Therefore $Mg2^{+}$ was selected as the reference species for determination of the elution sequence.

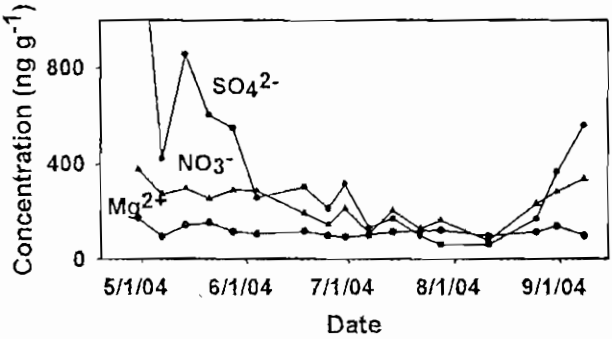

Figure 3. Concentration variations of Mg^{2+}, NO_3^- and SO_4^{2-} during the ablation season.

The temporal variation of the ratio between the concentration of each ion, relative to that of Mg^{2+}, is shown in Figure 4 along with the linear trend. The slopes of the linear regression reflect the relative preferences of the ions to Mg^{2+} during the elution process. Thus, by comparing these slopes, the following elution sequence was obtained: $SO_4^{2-} > Ca^{2+} > Na^+ > NO_3^- > Cl^- > K^+ > Mg^{2+} > NH_4^+$, which is generally in good agreement with previous studies (e.g. Brimblecombe and others, 1985, 1987; Tranter and others, 1992; Hou, 2000). The elution preference varies depending on specific characteristics of the chemical species, such as the initial concentration in the snow, the rearrangement processes during snow metamorphism, the capability to form volatile compounds, and the solubility in firn. As in many studies, NH_4^+ was found to be relatively immobile with respect to the percolating meltwater and thus it is placed at the end of the elution sequence. This observation likely reflects the fact that NH_4^+ is incorporated into the ice lattice (it is highly soluble in ice) as noted by Eichler and others (2001). As noted earlier Mg^{2+} also is relatively immobile. The strong correlation between the concentration peaks in Mg^{2+} and dust layers in the 54 successive pit profiles suggest that much of the Mg^{2+} is bound to the surface of the dust particles so that it is less susceptible to leaching during elution than other cation species that are located at ice grain boundaries and thus more easily washed out by meltwater. However, future studies are needed for a better explanation of the elution processes.

Relationship between the elution process and air temperature

Temperature can be used as a predictor for the elution process in many cases. Quantifying the linkage between the elution process and *in-situ* air temperature has the potential to provide a useful tool for evaluating the effect of elution, and thus for assessing ice core quality over a wide range of locations. The magnitude of elution can be presented by variations in the total ionic concentration (TIC) of the snow-firn pack. TIC was acquired at weekly intervals by accumulating mass-weighted mean concentrations of all major ions in the snow-firn pack. A

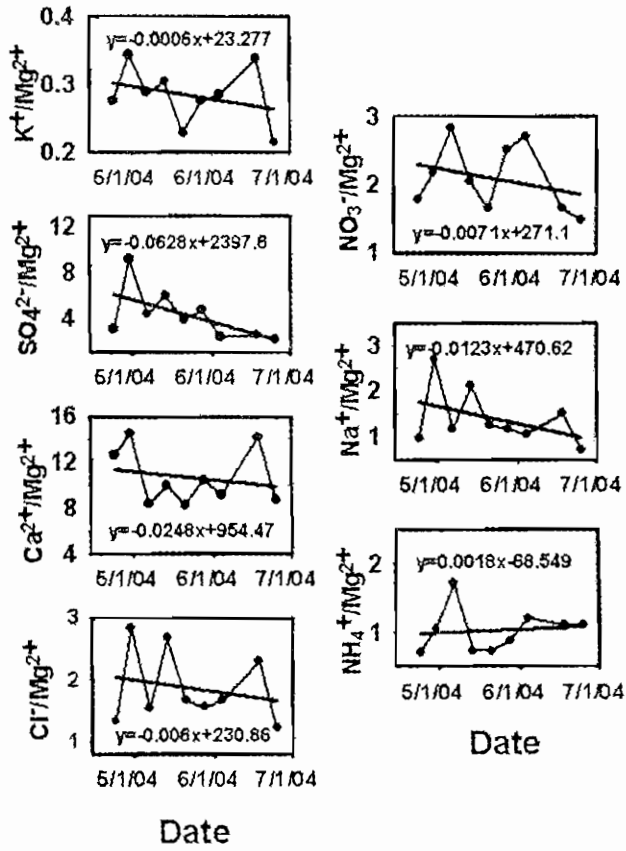

Figure 4. Temporal variations of the ratios of Ca^{2+}, Na^{+}, K^{+}, NH_4^{+}, Cl^{-}, SO_4^{2-}, and NO_3^{-} relative to Mg^{2+} are shown along with their linear trend.

lower TIC indicates that more of the snow's chemical burden is leached out thus reflecting intensive elution. The converse also holds. The value of TIC at the end of the 2003 ablation season (around mid-August) was 985 ng g^{-1} (dashed line in Figure 5). It increased gradually during winter 2003, and then rose rapidly during spring 2004. The TIC values peaked in early May, reaching a maximum of 5,883 ng g^{-1}. The corresponding diurnal mean air temperature at the turning point was approximately -3.6 °C (T_1). As temperature continued to rise, TIC continued to decrease, and around early July, it was approaching the lowest value of the previous year, suggesting that all ionic inputs since the previous fall were completely leached out by elution. The corresponding temperature at this point (T_2) was approximately 0.3 °C. All relevant data discussed above are presented in Figure 5. T_1 and T_2 are suggested to be important reference temperatures for elution at the PGPI site, such that elution started when the diurnal mean temperature reached -3.6 °C, but when the temperature rose to 0.3 °C, all new, year-round ionic inputs were leached out of the snow. The TIC has a general inverse correlation with air temperature ($R^2 = 0.36$, N=19, $P<0.01$) during the elution period, which is evident in Figure 6.

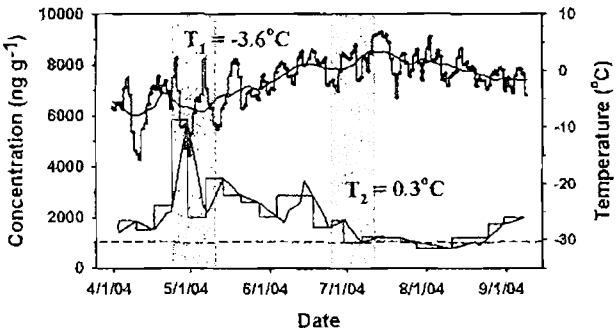

Figure 5. Comparison of the total ionic concentrations (TIC) in snow-firn pack and in-situ diurnal mean temperature. Left shaded column designates the time elution started, where the diurnal mean temperature was about -3.6 °C. Right shaded column designates the time TIC reached its lowest value in the previous year, indicated by the dashed line, where the diurnal mean temperature was about 0.3 °C.

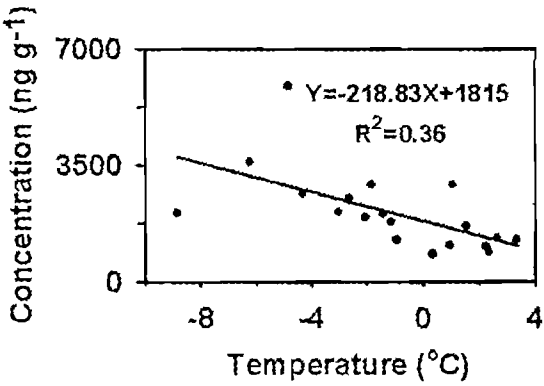

Figure 6. The relationship between total ionic concentrations (TIC) in the snow-firn pack and diurnal mean temperature during the ablation period.

CONCLUSIONS

From this investigation we conclude that the major ions in Glacier No. 1 snow can be categorized into three groups based on their seasonal behavior and characteristic relationships that were explored using correlation and factor analysis. The potential sources for these groups were identified as earth surface materials at the local to regional scale, long-distance sources (primarily Asian dust storms), and anthropogenic sources. Some elements, such as Ca^{2+} and SO_4^{2-}, appear to have multiple sources. Secondly, the elution sequence, $SO_4^{2-} > Ca^{2+} > Na^+ > NO_3^- > Cl^- > K^+ > Mg^{2+} > NH_4^+$, was determined by comparing the temporal trends in their concentration ratio relative to Mg^{2+}. Quantitative analysis of the relationship between *in- situ* air temperature and total ionic concentration in snow-firn pack at the study site revealed that elution is initiated when the diurnal mean temperature reaches about -3.6 °C. When the temperature rises above 0.3 °C, all the new, year-round ionic inputs are leached from the snow.

ACKNOWLEDGEMENTS

This research was supported by the National Natural Science Foundation of China (40371028; 40571033; 40121101; J0130084), CAS and CAREERI (2003101; 2004102; kzcx3-sw-341; 052062). We also thank Michael Bender and two anonymous reviewers for their useful comments and helpful suggestions. Support for this research has been provided under the Program for Glacier Processes Investigation (PGPI) conducted by the Tianshan Glaciological Station (TGS), Chinese Academy of Sciences (CAS).

REFERENCES

[1] Bales, R.C., R.E. Davies and D.A. Stanley. 1989. Ion elution through shallow homogeneous snow. *Water Resour. Res.*, **25**, 1869-1877.

[2] Brimblecombe, P., M. Tranter, P.W. Abrahams, I. Blackwood, T.D. Davies and C.E. Vincent. 1985. Relocation and preferential elution of acidic solute through the snowpack of a small, remote, high-altitude Scottish catchment. *Ann. Glaciol.*, **7**, 141-147.

[3] Brimblecombe, P., S.L. Clegg, T.D. Davies, D. Shooter and M. Tranter. 1987. Observations of the preferential loss of major ions from melting snow and laboratory ice. *Water Res.*, **21**, 1279-1286.

[4] Dregne, H.E. 1986. Surface material of desert environments. In McGinnies, W.G., B.J. Bram and P. Paylore, *eds. Deserts of the World*. University of Arizona Press. 287-377.

[5] Eichler, A., M. Schwikowski and W. Heine. 2001. Meltwater-induced relocation of chemical species in Alpine firn. *Tell.*, **53**(B), 192-203.

[6] Gao, Y., R. Arimoto, R.A. Duce, D.S. Lee and M.Y. Zhou. 1992. Relationships between the dust concentrations over eastern Asia and the remote north Pacific. *J. Geophys. Res.*, **97** (D9), 9867-9872.

[7] Ginot, P. 2001. Glaciochemical study of ice cores from Andean glaciers. (Ph.D. thesis, University of Bern.)

[8] Hewitt, A.D., J.H. Cragin and S.C. Colbeck. 1991. Effects of crystal metamorphosis on the elution of chemical species from snow. *In: Proceedings of the 48th Annual Eastern Snow Conference*. Guelph, Ontario, 2-10 June.

[9] Hou, S. 2000. Preliminary results of ion elution experiments of winter snow at the Headwaters of the Urumqi River. *J. Glaciol. and Geocryol.*, **22**(4), 362-365. [In Chinese]

[10] Hou, S. and D. Qin. 2002. The effect of postdepositional process on the chemical profiles of snow pits in the percolation zone. *Cold Regions Sci. Tech.*, **34**, 111-116.

[11] Johannessen, M. and A. Henriksen. 1978. Chemistry of snow meltwater: Changes in concentration during melting. *Water Resour. Res.*, **4**, 615-619.

[12] Lee, X., D. Qin, G. Jiang, K. Duan and H. Zhou. 2003. Atmospheric pollution of a remote area of Tianshan Mountain: Ice core record. *J. Geophys. Res.*, **108**(D14), 4406-4416.

[13] Li, Z., T. Yao and Z. Xie. 1994. Modern atmospheric environmental records in Guliya Ice Cap of

Qing-zang (Tibet) Plateau. *Chin. Sci. Bull.*, **40** (10), 874-875.

[14] Li, Z., T. Yao and Z. Xie. 1995. Study on SO_4^{2-} and NO_3^- in Atmospheric Aerosol. *Adv. Geosci.*, **10**(1), 289-295. [In Chinese]

[15] Li, Z., G. Lu, B. Liu and H. Fu. 1999. Ice core dust particulate by XPS-SEM/ED AX--Impact of dust particulate on SO_4^{2-} and NO_3^- record in ice cores. *Chin. Sci. Bull.*, **44**(15), 1424-1427.

[16] Li, Z., T. Han, Z. Jing, H. Yang and K. Jiao. 2003. A summary of 40-year observed variation facts of climate and Glacier No. 1 at the headwaters of Urumqi River. *J. Glaciol. Geocryol.*, **25**(2), 117-123. [In Chinese]

[17] Iizuka Y., M. Igarashi, K. Kamiyama, H. Motoyama and O. Watanabe. 2002. Ratios of Mg^{2+}/Na^+ in snowpack and an ice core at Austfonna ice cap, Svalbard, as an indicator of seasonal melting. *J. Glaciol.*, **48**(162), 452-460.

[18] Luo, H. 1983. Hydrochemical features of the Glacier No.1 in the source region of Urumqi River, Tianshan. *J. Glaciol. and Geocryol.*, **5**(2), 55-64. [In Chinese]

[19] Paterson. W. S. B. 1994. *The physics of glaciers, 3rd edition.* Oxford, Pergamon Press.

[20] Shumskii, P. A. 1964. *Principles of structural glaciology. Translated from the Russian by David Kraus.* New York, Dover Publications.

[21] Thompson, L.G., E. Mosley-Thompson, M.E. Davis, P. Lin, V. Mikhalenko and J. Dai. 1995. A 1,000-year climatic ice-core record from the Guliya ice cap, China: its relationship to global climate variability. *Ann. Glaciol.*, **21**, 175-181.

[22] Thompson, L.G., M.E. Davis, E. Mosley-Thompson, T. A. Sowers, K. A. Henderson, V. S. Zagorodnov, P. Lin, V. N. Mikhalenko, R.K. Campen, J.F. Bolzan, J. Cole-Dai and B. Francou. 1998. 25,000-year tropical climate history from Bolivian ice cores, *Sci.*, **282**, 1858-1864.

[23] Tranter, M., S. Tsiouris, T.D. Davies and H,G. Jones. 1992. A laboratory investigation of the leaching of solute from snowpack by rainfall. *Hydrol. Process*, **6**, 169-178.

[24] Wake, C.P., P. A. Mayewski, P. Wang, Q. Yang, J. Hang and Z. Xie. 1992. Anthropogenic sulfate and Asian dust signals in snow from Tien Shan, northwest China. *Ann. Glaciol.*, **16**, 45-52.

[25] Wake C.P., P.A. Mayewski, Z. Li, J. Han and D. Qin. 1994. Modern eolian dust deposition in central Asia. *Tell.*, **46**(B), 220-233.

[26] Wang, D. and P. Zhang. 1985. Climate in Urumqi River valley, Tianshan. *J. Glaciol. Geocryol.*, **7**(3), 239-248. [In Chinese]

[27] Wang, F., Z. Li, X. You and C. Li. 2006. Snow to ice evolution process observation and study at percolation zone on Glacier No. 1 at Urumqi river head. *J. Glaciol. Geocryol.*, In press. [In Chinese]

[28] Williams, M.W., K.A. Tonnessen, J.M. Melac and D. Yang. 1992. Sources and spatial variation of the chemical composition of snow in the Tianshan, China. *Ann. Glaciol.*, **16**, 25-32.

[29] Yang, D., T. Jiang, Y. Zhang and E. Kang. 1988. Analysis and correction of errors in precipitation measurement at the head of Urumqi River. *J. Glaciol. Geocryol.*, **10**, 384-399. [In Chinese]

[30] Yang, D., E. Kang and F. Blumer. 1992. Characteristics of precipitation in the source area of the Urumqi River basin. *J. Glaciol. Geocryol.*, **14**(3), 258-266. [In Chinese]

[31] You, X., Z. Li and F. Wang. 2005. Study on time scale of snow–ice transformation through snow layer tracing method-take Glacier No. 1 at the headwaters of Urumqi River as an example. *J. Glaciol. Geocryol.*, **27**(6), 853-860. [In Chinese]

[32] Zhao, Z. and Z. Li. 2004. Determination of soluble ions in atmospheric aerosol by ion chromatography Mod. *Sci. Inst.*, **5**, 46-49. [In Chinese]

[33] Zhu, Y., Z. Li and X. You. 2006. Application and technique in glacier by AccuSizer 780A Optical Particle Sizer. *J. Glaciol. Geocryol.*, In press. [In Chinese]

Seasonal evolution of aerosol stratigraphy in Glacie No. 1 percolation zone, eastern Tianshan, China

WANG Feiteng, LI Zhongqin, YOU Xiaoni, LI Chuanjin,
LI Huilin, LI Xiangying, ZHU Yuman

Tianshan Glaciological Station/Key Laboratory of Ice Core and Cold Regions Environment, CAREER, CAS, Lanzhou 730000, China. Email: qianj@lzb.ac.cn

ABSTRACT: The processes involved in the evolution of vertical profiles of Mg^{2+}, Ca^{2+} and microparticle concentrations, as well as their seasonal variation in surface snow, was studied by weekly sampling a snow pit from September 2003 to September 2004 on Glacier No.1 in the eastern Tianshan. The development of the microparticle and Mg^{2+} and Ca^{2+} stratigraphy in the snow pit are closely related to the physical development of the snow-firn pack. The sampling site is located at 4130 m asl in the percolation zone of the glacier, and in addition to the effects of sublimation and wind erosion, melting plays a crucial role in both the physical and chemical evolution processes. During the winter season, soluble aerosol concentrations in the surface layers are altered slightly by sublimation and wind erosion, and the concentrations are further modified as the wet season begins in late April. In contrast, soluble aerosol stratigraphy in the deeper layers remains relatively unchanged through the winter. In early summer, as melting occurs in the upper part of the snow-firn pack, meltwater carries chemical species to different depths in the underlying snow-firn layers, such that at the end of the ablation season, all of the surface cations might be leached out from the upper layers. In addition, the possible source of calcium and magnesium is discussed in this paper.

INTRODUCTION

Ice core chemistry records contain climatic and environmental information over a wide range of time-scales. The records preserved in glaciers, however, are not only determined by the atmospheric concentration of the physical and chemical species and the processes involved in their deposition, but also by post-depositional processes such as melting, percolation, sublimation, wind filtration through firn (which involves mass loss, addition and/or exchange) and diffusion (Dibb, 1996; Waddington and others, 1996; Wolff, 1996; Ginot and others, 2001; Stichler and others,2001; Schotterer and others, 2004; Schulz and de Jong, 2004).

In order to better understand the deposition and post-depositional processes controlling the chemical signals recorded in glacial snow and ice, the Program for Glacier Processes Investigation (PGPI) has examined the seasonal variation and evolution of Mg^{2+}, Ca^{2+} and microparticle concentrations in 54 profiles collected over 12 months from a snow pit on Glacier

No.1, located in the eastern Tianshan in northwestern China. Several similar studies have been accomplished on other alpine glaciers, (e.g.; Psenner and Nickus, 1986; Neftel and others, 1987; Puxbaum 1989; Maupetit and others, 1993; Winiwarter and others, 1998; Kuhn and others, 1998; Lizuka and others, 2002; Pohjola and others, 2002; Schotterer and others, 2004), but only a few studies (Hou and others, 1996, 1999, 2002) have been conducted in this region of the Tianshan.

THE SETTING AND GLACIOLOGY OF THE SAMPLING SITE

Glacier No.1 is located at the Urümqi riverhead adjacent to the vast deserts and dried lakes of central Asia and far from densely populated areas. The glacier itself is composed of east and west branches which flow around a mass of exposed bedrock and moraine sediment, the chemical composition of which is rich in such species as sodium, calcium, magnesium and iron (Luo, 1983). The prevailing westerlies flow over the mountain range, however the topography distorts the windflow into cyclonic and anticyclonic circulation patterns up to 4000 m asl (meters above sea level). Near the surface, the local valley winds prevail from March through September (Zhang and others, 1994). Typically, 90% of the precipitation in this region occurs between May and September.

From 1959 to 2003, the annual equilibrium line (ELA) of the glacier has averaged approximately 4055 m asl. An observation and experimental site was carefully chosen in a percolation zone of the east branch of Glacier No. 1 (where the ice surface slopes about 6^{o}) above the ELA at 4130 m asl. Here the overshadowing of the mountain ridges prevents any direct exposure to sunshine in the winter. During the sampling period, the mean annual air temperature was about -9.1°C and the precipitation (i.e. snowfall) was approximately 700 mm water equivalent.

The stratigraphic sequence of the pit from top to bottom can be described as fresh snow, coarse-grained snow, fine-grained firn, firn and coarse-grained firn. The fresh snow and coarse-grained snow were derived from the accumulation of the most recent year, while the underlying firn layers were from previous years. The floor of the pit was made of "infiltration-congelation ice" (Shumskii, 1964), or superimposed-ice (Paterson, 1994), which was characterized by clear and impermeable opaque ice with spherical bubbles ~1 to 5 mm in diameter. The depth typically ranged from about 1.5 m as the study began in the late summer to about 3 m in the late spring, but during the winter it remained stable because of snow compaction, drifting and sublimation. In the early summer, as air temperature rose to ~0^{o}C, the upper part of the snow layer began to melt, which led to a rapid thinning. The melting primarily involved the accumulation from the previous autumn. During the late summer to the early autumn, the melting impacted the entire annual layer, and even included the underlying accumulation from the previous year. The meltwater infiltrated to the underlying firn layers, reaching the impermeable superimposed ice formed the previous year. The water filled the pores and was refrozen to form new superimposed ice, while some of the meltwater pooled on the ice surface and eventually drained off.

METHODOLOGY

At the PGPI site, both surface snow and snow pit samples were collected from September 2003 to September 2004 on a weekly basis. We tried to collect the fresh snow and well-preserved surface snow (i.e. snow that was not affected by post-depositional processes such as sublimation or melting) at the sampling site each week to investigate the chemical seasonality in precipitation and dry deposition. Therefore, during the winter season when there was insufficient snowfall, we usually sampled the topmost three centimeters. However, if an accumulation event occurred prior to the sampling, we collected the top one centimeter of the fresh snow. During the summer, there was usually sufficient fresh snow available, and samples from accumulation that was no more than two days old were usually collected from the top 3 to 5 cm. Over the year a total of 54 surface snow samples were retrieved, however, nine samples were discarded for analysis because of problems associated with *in situ* melting.

The pit was also sampled from top to bottom at ten centimeter increments 54 times during the year on a weekly basis to yield a total of 1,011 samples. After each session, the pit was refilled and seven days later was re-excavated. The wall was then scaled back by at least 50 cm before the next round of collecting. A strict protocol was followed during this procedure to prevent contamination, including the use of disposable polyethylene gloves, masks, and precleaned polyethylene sample containers. All the samples were transported in insulated boxes to the Tianshan Glaciological Station (TGS) laboratory, and were kept frozen until analysis.

Insoluble particles, Ca^{2+} and Mg^{2+} were analyzed in the TGS laboratory. All sample handling was done in a Class 100 clean room in order to minimize contamination. The Ca^{2+} and Mg^{2+} concentrations were measured by ion chromatography using a Dionex DX-320 system with a CS12A separation column. The detection limits of Mg^{2+} and Ca^{2+} are 0.8 ng g^{-1} and 0.75 ng g^{-1}, respectively (Zhao and Li, 2004). Microparticle concentrations and size distributions were measured with an AccuSizer 780A which uses Single Particle Optical Sensing (SPOS) technology and measures in 8 to 512 size channels, with an error of less than 5% in the 0.5-400 μm measuring range. Prior to analysis, samples were melted at room temperature while the pipeline and AccuSizer system were cleaned with Milli-Q water until the background particle count was below 50 per mL.

RESULTS AND DISCUSSION

Processes involved in the postdepositional modification of the aerosol stratigraphy

Although the processes involved in the post-depositional modification of the insoluble and soluble aerosols were different, the stratigraphy of the pits indicate that the dust layers occurred coincidently with increases in Ca^{2+} and Mg^{2+}, which suggests that these species were not leached out from the dust. The linear correlation coefficient (r) of each ion with the large particles (>10ì m in diameter) is significant; for Mg^{2+}, r=0.74 and for Ca^{2+}, r=0.85 (2-tailed, p=0.01, N=107). Slight seasonal differences in the microparticle, Mg^{2+} and Ca^{2+} concentrations in the surface snow may be due to the aerosols being derived from separate sources. However, after

being deposited into the snow, they experienced post-depositional alteration mainly controlled by meltwater percolation. It was determined that the development of the aerosol stratigraphies was closely related to the physical development of the snow-firn pack such that both experienced a similar evolution process (Fig.1).

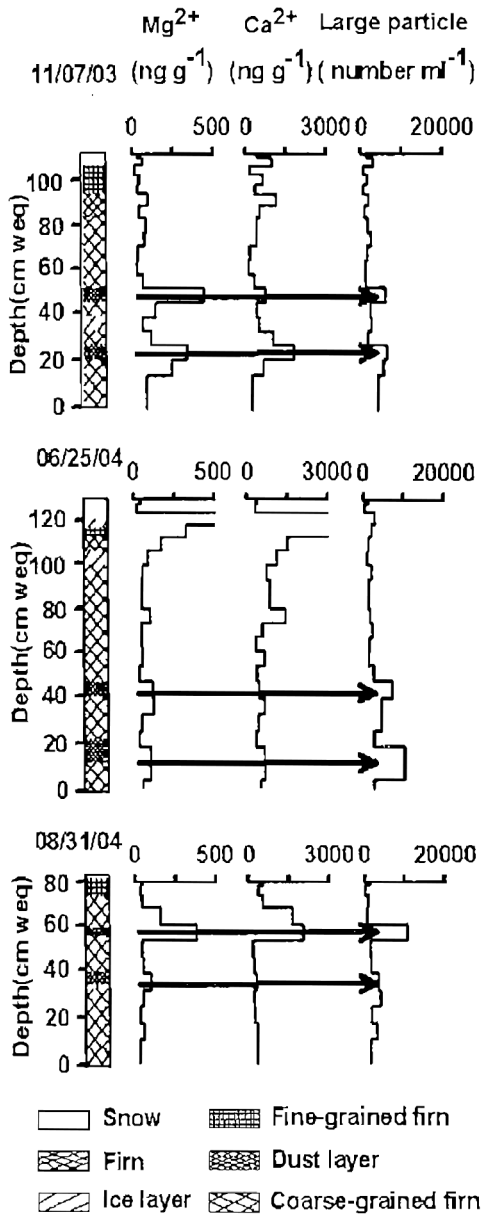

Fig.1 The relationship between the snow stratigraphy and the Mg^{2+}, Ca^{2+}, and large particle concentration profiles in the snow pit on selected sampling days. These profiles were selected from among the 54 that were created from the weekly sampling in order to illustrate seasonal changes. Y-axis presents height (cm weq) above the surface of the superimposed ice.

Figure 2 illustrates the evolution processes of the Mg^{2+} in the snow pits from September 2003 to September 2004 (the evolution processes of $Ca2^{+}$ and microparticle in the snowpit are identical to Mg^{2+}). In mid-September 2003, there were three marked Mg^{2+} peaks (P1, P2 and P3) in the firn at heights of 89, 62 and 34 cm, respectively above the superimposed ice. From mid-September to mid-November 2003, P1, P2 and P3 moved downward to heights of 80, 55, and 16 cm, respectively from the bottom of the pit, and this movement was mainly related to snow compaction. During the period from mid-Nov 2003 to late April 2004, several small concentration peaks in the upper part of the snow pits appeared. This resulted from limited precipitation, low temperatures and weak evaporation (Ginot and others, 2001; Stichler and others, 2001; Schulz and de Jong, 2004) at the site, which enabled post-depositional processes such as sublimation and dry deposition to become more dominant. As the temperature increased from April to late May, meltwater appeared in the pit, which attenuated the peaks as they moved downward. At the same time, the increasing precipitation resulted in successive

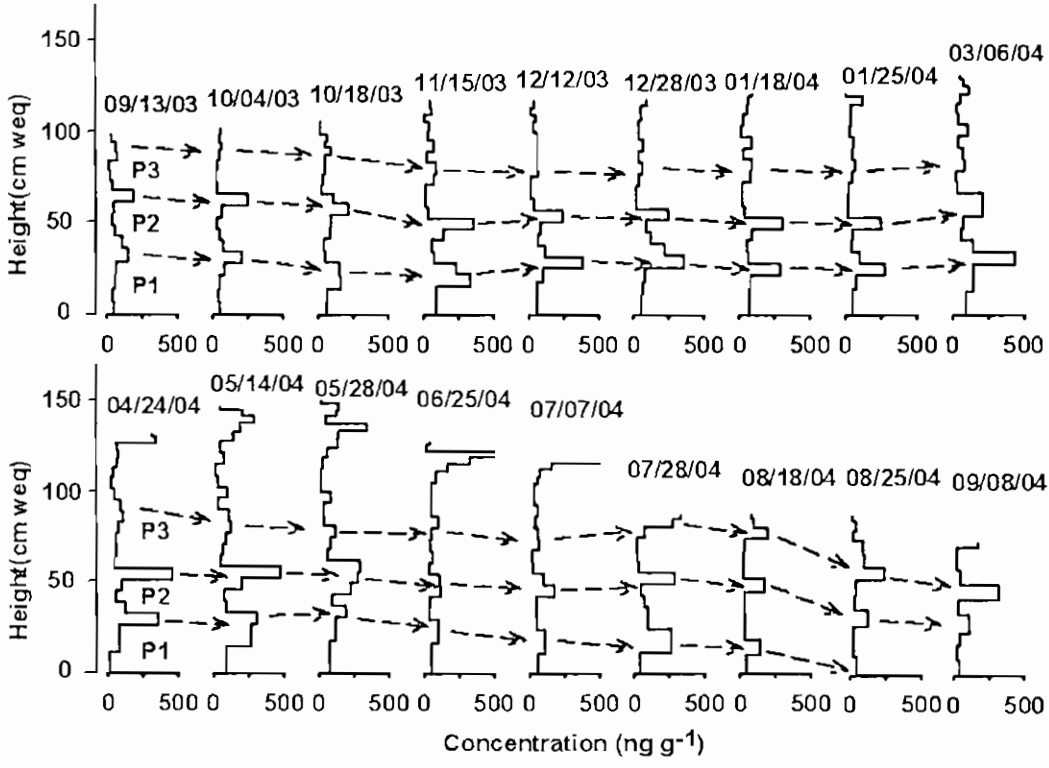

Fig.2 The evolution process of vertical profiles of Mg^{2+} in snow pits from13th September 2003 to 8th September 2004. P1, P2 and P3 indicate Mg^{2+} concentration peaks. Y-axis presents the height (cm weq) above the surface of the superimposed ice. The September 2003 superimposed ice height (0 as plotted here) remained constant until approximately mid-June 2004, when the height increased as new ice was added by refreezing of percolating meltwater. These profiles were selected from among the 54 that were created from the weekly sampling in order to illustrate seasonal changes.

concentration peaks at about 10 to 30 cm below the surface. In the summer (June to August), as meltwater percolated through the pit, it leached the ions, including Ca^{2+} and Mg^{2+} (Brimblecombe and others, 1985, 1987; Tranter and others, 1992; Eichler and others, 2001). During this period, the upper part of the snow pit experienced the most post-depositional alteration. With increasing temperature, larger volumes of meltwater began to percolate deeper into the pit along with the Mg^{2+}, which is indicated by the displacement and reduced concentration of the peaks. When the water encountered the superimposed ice in the bottom of the coarse-grained firn layer, it refroze resulting in accretion (mass gain) at the superimposed ice surface . This strong ablation caused the melding of the P3 layer with the surface layers. At the end of the August, P1 merged into the superimposed ice at the bottom of the pit and was henceforth preserved in the glacier. By the beginning of September 2004, there were only two peaks observed in the snow pit. This demonstrates that in spite of considerable loss of Mg^{2+} through post-depositional processes, the general information is still preserved.

Seasonal variations of dust, Mg^{2+} and Ca^{2+} in the surface snow

Dust and chemical species are removed from the atmosphere through dry and wet deposition (Heather, 2004). For both types of deposition, precipitation and wind are the main control factors on Glacier No.1. Once aerosols accumulate on the glacier surface, they undergo post-depositional alteration, which is mainly influenced by temperature and meltwater percolation. Surface samples collected from the uppermost 1 to 5 cm of surface snow were examined to investigate the chemical seasonality in precipitation and dry deposition, and are shown in Figure 3. The concentrations of all three species were low from October to the end of March, then were elevated from April to June. After that, they show different characteristics; Ca^{2+} rapidly decreased in June, but Mg^{2+} and, to a lesser extent, dust peaked along with August snowfall.

Data from the Daxigou Meteorological Station (3539 m asl), located three kilometers away from Glacier No.1, show that the atmospheric stability, temperature, local valley wind strength, and the precipitation were related to the insoluble and soluble aerosol concentrations in the surface snow. This can be seen in Figure 3 where the peak in surface snow concentrations is associated with wind speed peaks and the precipitation. The high concentrations between May and June may be attributed to the local valley wind, which could potentially cause more dust input into the atmosphere and result in increased Ca^{2+} and Mg^{2+} concentrations. The juxtaposition of high dust and Mg^{2+} concentrations in July and August 2004 may have been due to the transport of these species from remote areas by moisture advection, which suggests that the Mg^{2+} concentration in the surface snow may be related to the dust coming from these remote regions. In winter, the low concentrations coincide with the temperature inversions and stable atmospheric stratification, similar to conditions that are observed in the Alps (Maupetit, 1995; Kuhn and others, 1998).

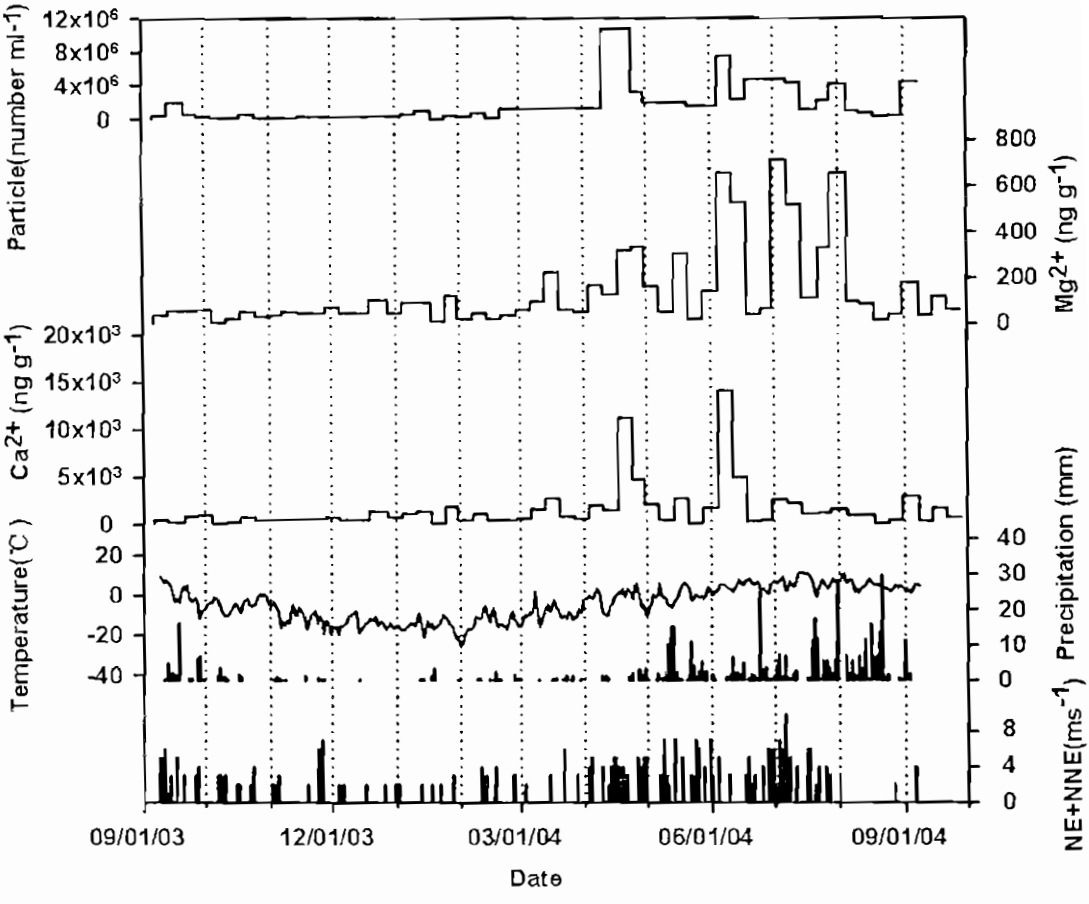

Fig.3 Seasonal changes in calcium, magnesium and insoluble particle concentrations in surface snow and daily variability of temperature, precipitation and the prevailing wind speed versus time from September 2003 to September 2004 recorded at the Daxigou Meteorological Station.

Possible sources of Ca^{2+} and Mg^{2+}

The sources of the Ca^{2+} and Mg^{2+} in Glacier No.1 can be assessed by examining the correlation between various ions in the snow, as well as the atmospheric circulation pattern that brings moisture to the region. Based on the correlation matrix of ions captured from the surface snow at the site, we observe that the linear correlation of Ca^{2+} with electric conductivity and pH are 0.97 and 0.77, respectively (2-tailed, p=0.01, N=45). This indicates that the main components of the atmospheric dust are calcium-rich minerals, which probably come from the weathering of local rocks, as well as from the surrounding desert. Magnesium and dust are significantly correlated (R = 0.74) (2-tailed, p=0.01, N=45), which suggests that the Mg^{2+} source is more distant and may be mainly related to precipitation events.

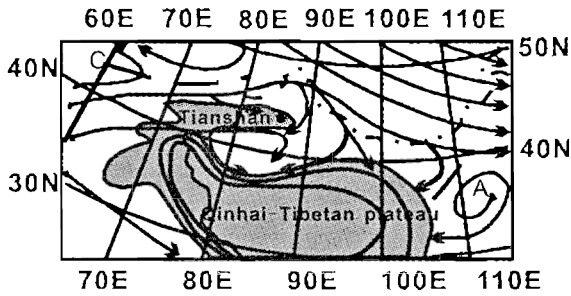

Fig.4. Mean air mass trajectory at 1500 m above the Tianshan Mountains and surrounding areas during the spring season from 1960–1969 (modified from Li ,1991). The location of the study site is indicated by the black circle. "A" indicate anticyclone, "C" indicate cyclone, the dashed line is national boundaries.

Prevailing westerlies dominate the air circulation over the study area (Fig. 4), and westerly winds are especially dominant over the eastern Tianshan Mountains when the circum-Arctic vortex is stronger (Zhang and others, 1987; Hu and Jiang, 1989; Qiu, 1993; Jiang, 2002). Therefore, moisture travels through this region from west to east. Along with this pattern of atmospheric circulation the aerosols, which include Mg^{2+} and Ca^{2+}, are blown from the inland deserts and transported to the study area by this strong airflow. This suggests that long-range transport accounts for part of the Ca^{2+} that is present in the snow pits.

SUMMARY

Long-term Mg^{2+}, Ca^{2+} and microparticle data from snow pits were examined to determine the depositional and post-depositional processes that occur on Glacier No. 1 at the Urümqi riverhead in eastern Tianshan, China. During the winter, the formation of the vertical stratigraphy of the microparticle, Mg^{2+} and Ca^{2+} concentrations in the upper layers of the glacier were mainly related to snow compaction, sublimation and dry deposition. During the summer, the snow in the pit experienced the maximum post-depositional alteration through the percolation of the meltwater; however, alteration deeper in the snow pit was very slight and the general information was still preserved.

The seasonal changes in the concentrations of calcium and magnesium in surface snow display a characteristic sequence of low and high values. Low values of Ca^{2+} and Mg^{2+} were observed during the winter from November to April. In May, the concentrations increased to several times those of the winter, peaked in June, and then rapidly decreased through August. Through the Autumn the concentrations appear to have been stable. The possible sources of Ca^{2+} may primarily be the local rocks and secondarily from a more remote source; while Mg^{2+} may be primarily from a remote source.

ACKNOWLEDEMENTS

This research was supported by the National Natural Science Foundation of China (40371028; 40571033; 40121101) and The Cold and Arid Regions Environmental and

Engineering Research Institute (CACX2003101). We also thank Patrick Ginot, Douglas Hardy, and an anonymous reviewer for their useful comments and helpful suggestions, and Mary Davis and Tracy Mashiotta for language editing. Support for this research has been provided under the Program for Glacier Processes Investigation (PGPI) conducted by the Tianshan Glaciological Station (TGS), Chinese Academy of Sciences (CAS).

REFERENCES

[1] Brimblecombe, P., M. Tranter, P.W. Abrahams, L. Blackwood, T.D. Davies and C.E. Vincent. 1985. Relocation and preferential elution of acidic solute through the snowpack of a small, remote, high-altitude Scottish catchment. *Ann. Glaciol.*, **7**, 141-147.

[2] Brimblecombe, P., S.L. Clegg, T.D. Davies, D. Shooter and M. Tranter. 1987. Servation of the preferential loss of major ions from melting snow and laboratory ice. *Water Res.*, **21**, 1279-1286.

[3] Dibb, J.E. 1996. Overview of field data on the deposition of aerosol-associated species to the surface snow of polar glaciers, particularly recent work in Greenland. In Wolff, E.W. and R.C. Bales, *eds. Chemical exchange between the atmosphere and polar snow*. Berlin, Springer-Verlag, 249-274. (NATO ASI Series I: Global Environmental Change 43.)

[4] Eichler, A., M. Schwikowski and H. W. Gaggeler. 2001. Meltwater-induced relocation of chemical species in Alpine firn. *Tell.*, **53**(B), 192-203.

[5] Ginot, P., C. Kull, M. Schwikowski, U. Schotterer and H.W. Gaggeler. 2001. Effects of postdepositional processes on snow composition of a subtropical glacier (Cerro Tapado, Chilean Andes). *J. Geophys. Res.*, **106**(23), 32375-32386.

[6] H.A. Raymond, S-M Yi and N. Moumen. 2004. Quantifying the dry deposition of reactive nitrogen and sulfur containing species in remote areas using a surrogate surface analysis approach. *Atmos. Env.*, **38**, 2687–2697.

[7] Hou, S., D. Qin and J. Ren. 1996. Different post-deposition processes of NO_3^- in snow layers in East Antarctica and on the northern Qinghai-Tibetan Plateau. *Ann. Glaciol.*, **29**, 73-76.

[8] Hou, S. and D. Qin. 1999. The ion elution effect on the main ion profiles of the glacier snowpacks. *Sci. Geol. Sin.*, **19**(6), 536-542. [In Chinese]

[9] Hou, S. and D. Qin. 2002. The effect of postdepositional process on the chemical profiles of snow pits in the percolation zone. *Cold Regions Sci. Tech.*, **34**, 111-116.

[10] Hu, R. and F. Jiang. 1989. *Snow avalanche in Tian Shan Mountains, China.* People's Transportation Press, Beijing, 1-18. [In Chinese]

[11] Jiang, F., C. Zhu, W. Wei and A. Osamu. 2002. Some results of snow chemical surveys in the Kunnes River valley, East Tienshan mountains, China. *Atmos. Env.*, **36**, 4941-4949.

[12] Kuhn, M., U. Nickus and H. Schellander. 1998. Seasonal variation of ion concentration in a high alpine snow pack. *Atmos. Env.*, **32**, 4041-4051.

[13] Iizuka Y., M. Igarashi, K. Kamiyama, H. Motoyama and O. Watanabe. 2002. Ratios of Mg^{2+}/Na^+ in snowpack and an ice core at Austfonna ice cap, Svalbard, as an indicator of seasonal melting. *J.Glaciol.*, **48**(162), 452-460.

[14] Luo, H. 1983. Hydrochemical features of the Glacier No.1 in the source region of Urumqi River, Tianshan.

J. Glaciol. and Geocryol., **5**(2), 55-64. [In Chinese]

[15] Maupetit, F., D. Wagenbach, K. Geis, M. Schwikowsky, U. Baltensperger, H.W. Gäggeler, A. Novo, G.C. Rossi, U. Nickus, M. Kuhn, V. Trockner, G. Bendetta, W. Winiwarter and H. Puxbaum. 1993. Chemical composition of Alpine glacier snow during 1991SNOSP campaign: An overview of its spatial variability. *Proceedings EUROTRAC Symposium*, 1992, 757.

[16] Maupetit, F., D. Wagenbach, P. Weddeling and R. Delmas. 1995. Seasonal fluxes of major ions to a high altitude cold alpine glacier. *Atmos. Env.*, **29**, 1-9.

[17] Neftel, A., A. Sigg and F. Zurcher. 1987. Acid deposition in a snow field at 2500 m a.s.l. in Switzerland. In: Angletti, G. and G. Restelli, *eds. Physico-Chemical Behaviour of Atmospheric Pollutants*, Air Pollution Research 2, 500-510, Reidel, Dordrecht.

[18] Paterson. W. S. B. 1994. *The physics of glaciers, 3rd edition.* Oxford, Pergamon Press.

[19] Pohjola, V.A., J.C. Moore, E. Isaksson, T. Jauhiainen, R.S.W. van de Wal, T. Maetma, H.A.J. Meijer and R. Vaikmae. 2002. Effect of periodic melting on geochemical and isotopic signals in an ice core from Lomonosovfonna, Svalbard. *J.Geophys.Res.*, **107** (D4), 0-10.

[20] Psenner, R. and U. Nickus. 1986. Snow chemistry of a glacier in the Central Eastern Alps (Hintereisferner, Tyrol, Austria). *Zeitschrift für Gletscherkunde und Glazialgeologie*, **22**, 1-18.

[21] Puxbaum, H. 1989. *ALPTRAC. EUROTRAC Annual Report, Part 3.* Garmisch-Partenkirchen.

[22] Qiu, J. 1993. Study on characters of snow climate in middle mountains of Western Tianshan with examples from the valley of Kunnes River. In *Geographical Symposium of Arid Zone, No. 3.* Beijing, Science Press, 123–132. [In Chinese]

[23] Schotterer, U., W. Stichler and P. Ginot. 2004. The influence of post-depositional effects on ice core studies: examples from the Alps, Andes, and Altai. In L. De Wayne Cecil, J. R. Green and L. G. Thompson,*eds. Earth Paleoenvironments: Records preserved in Mid- and Low-Latitude Glaciers.* Dordrecht, etc., Kluwer, 39-60.

[24] Schulz, O. and C. de Jong. 2004. Snowmelt and sublimation: field experiments and modeling in the High Atlas Mountains of Morocco. *Hydrol. Earth Syst. Sc.*, **8**(6), 1076-1089.

[25] Shumskii, P. A. 1964. *Principles of structural glaciology. Translated from the Russian by David Kraus.* New York, Dover Publications.

[26] Stichler, W., U. Schotterer, K. Frohlich, P. Ginot, C. Kull, H. Gaggeler and B. Pouyaud. 2001. Influence of sublimation on stable isotope records recovered from high-altitude glaciers in the tropical Andes. *J. Geophys. Res.*, **106**(19), 22613-22620.

[27] Tranter, M., S. Tsiouris, T.D. Davies and H.G. Jones. 1992. A laboratory investigation of the leaching of solute from snowpack by rainfall. *Hydrol. Process.*, **6**, 169-178.

[28] Waddington, E.D., J. Cunningham and S. L. Harder. 1996. The effects of snow ventilation on chemical concentrations. In Wolff, E.W. and R.C. Bales, *eds. Chemical exchange between the atmosphere and polar snow.* Berlin, Springer-Verlag, 405-451. (NATO ASI Series I: Global Environmental Change 43.)

[29] Winiwarter, W., H. Puxbaum, W. Schöner, R. Böhm, R.Werner, W. Vitovec and A. Kasper. 1998. Concentration of ionic compounds in the wintertime deposition: Results and trends from the Austrian Alps over 11 years (1983-1993). *Atmos. Env.*, **32**, 4031-4040.

[30] Wolff, E.W. 1996. Location, movement and reactions of impurities in solid ice. In Wolff, E.W. and R.C.

Bales, *eds. Chemical exchange between the atmosphere and polar snow*. Berlin, Springer-Verlag, 541-560. (NATO ASI Series I: Global Environmental Change 43.)

[31] Zhang, J. and J. Deng. 1987. *An outline of Precipitation in Xinjiang*. Beijing, Meteorology Press, 89-117. [In Chinese]

[32] Zhang, Y., E. Kang and C. Liu. 1994. The climatic features of Tianshan Urumqi River valley. *J. Glaciol. Geocryol.*, **16**(4), 333-341. [In Chinese]

[33] Zhao, Z. and Z. Li. 2004. Determination of soluble ions in atmospheric aerosol by ion chromatography. *Mod. Sci. Inst.*, **5**, 46-49. [In Chinese]

Atmosphere-to-snow-to-firn transfer of NO_3^- on Glacier No. 1, eastern Tienshan, China

Zhongping ZHAO, Zhongqin LI, Feiteng WANG, Huilin LI, and Yuman ZHU
Tianshan Glaciological Station/Key Laboratory of Ice Core and Cold Regions Environment, CAREER, CAS, Lanzhou 730000, China. Email: qianj@lzb.ac.cn

ABSTRACT: In order to understand deposition and post-depositional processes controlling atmospheric NO_x recorded in glacial snow and firn, NO_3^-, an oxidation product of NO_x, was investigated in atmospheric aerosol, surface snow, and snow-firn pack on the Glacier No. 1 in eastern Tien Shan, China, from September 2002 to September 2004. In this paper, seasonal changes in both aerosol and snow NO_3^- and their relationship are discussed. The snow pit data indicates that during winter, the formation of vertical NO_3^-stratigraphy in the upper layers of the glacier is mainly related to snow compaction, sublimation and dry deposition. The greatest post-depositional alteration of NO_3^- in the snowpack was found to occur during summer through the percolation of meltwater. The mobility of NO_3^- in the snowpack was compared with $Mg^{2+}$and was found to be eluted downward through the snow at a much faster rate than Mg^{2+}. Compared with other remote glaciers, relatively high snow NO_3^- concentrations were found at the Glacier No. 1.

INTRODUCTION

Glaciers are excellent archives of atmospheric constituent depositions. However, in order to interpret these records the atmospheric transfer function and effect of post-depositional processes need to be known. Being reversibly deposited in the snow, the transfer function for NO_3^- involves multiple post-depositional processes, e.g., the particularly low NO_3^- concentrations that reflected re-emission of NO_3^- from snow after deposition were detected in deep layers at Antarctic sites like Dome C, Vostok, and in the Dominian Range (Mayewski and Legrand, 1990; De Angelis and Legrand, 1995; Wolff and others, 1998). NO_3^- is assumed to be essentially or partly deposited as HNO_3, and it can be also released from the snow surface as HNO_3. The gas phase HNO_3 within snow possibly undergoes reversible exchange with atmosphere and should eventually equilibrate with its atmospheric levels. This phenomenon seems to be typical for low-accumulation snow fields (De Angelis and Legrand, 1995). In high-accumulation snow fields, there may be insufficient time to reach equilibrium before new snowfalls (Bales and Choi, 1996). However, as observed in Greenland, NO_3^- escaped from the snow layer within a few days of deposition. This suggests post-depositional processes may alsc be important sites with higher accumulation rates, given the right conditions.

To investigate the effects of depositional processes and meltwater-related post-depositional processes on NO_3^- in an alpine glacier, NO_3^- concentrations in aerosol, surface snow, and evolution processes in a snow-firn pack were investigated on the Glacier No. 1, located at eastern Tien Shan, the northwestern China. The investigation was undertaken as part of the Program for Glacier Processes Investigations (PGPI), which was initiated in July 2002 by the Tianshan Glaciological Station (TGS). Several publications presented the transfer function of NO_3^- between atmosphere and snow, and post-depositional processes in other glaciers (e.g., Baltensperger and others, 1993; Dibb and others, 1994; Mulvaney and others, 1998; Rothlisberger and others, 2000; Ginot and others, 2001; Preunkert and others, 2003; Burkhart and others, 2004). However, no similar research has been previously conducted at the eastern Tien Shan.

SAMPLING SITE

In a frame of the PGPI, an observation site (PGPI site) was established in the percolation zone of the Glacier No. 1 east branch (43.05• N; 86.49• E, 4,130 m a.s.l.), 3 kmsouth-west from the Daxigon meteorological station (3,539 m a.s.l.). The depth of snow-firn pack at PGPI site typically ranged from 1.5 m in late summer to 3 m in late spring, containing three to four year snow deposits. The floor of the snow-firn pack was formed by superimposed ice, a clear and impermeable opaque ice with spherical bubbles approximately 1 to 5 mm in diameter. The samples of atmospheric aerosol, glacier surface snow, and snow-firn pit at the PGPI site were concurrently collected on a weekly basis.

Eastern Tien Shan is surrounded by vast desert areas (Figure 1). The Glacier No. 1 located at the headwaters of the Urumqi River is surrounded by barren rock and frozen ground with sparse vegetation. The forest zone at this area spreads between 2,900 m a.s.l. and 1,500 m a.s.l. the mean annual precipitation at snow line elevation (approximate 4,055 m a.s.l.) is 646 mm a^{-1}. Maximum precipitation in eastern Tien Shan occurred in summer, from May to September (90%). The western atmospheric circulation patterns are prevailing over the eastern Tien Shan during a year, however from March through September there are very distinctive valley winds (Zhang and others, 1994). One large city and a few small towns are along the Urumqi River basin. The large city Urumqi is located in 100 km on the east from the PGPI site, which is the capital of Xinjiang Uyger Autonomous Region and a large industrial city with more than two million populations. A small town Houxia, 50 km northeastern from PGPI site in Urumqi River basin, has two power stations and one cement factory working on local coal since 1958.

DATA & METHODS

Fifty-five aerosol samples were retrieved from 27th of December 2002 to 21st of February 2004 on a weekly basis during dry clear weather. These samples were collected with 2-μm pore size, 47-mm-diameter Zefluor™ Teflon filters (Gelman sciences), which were placed facing down in a cylindrical polyethylene protective cover. Air was drawn by a 12-V diaphragm pump with a line flow meter. The measured air volumes were corrected for ambient temperature and

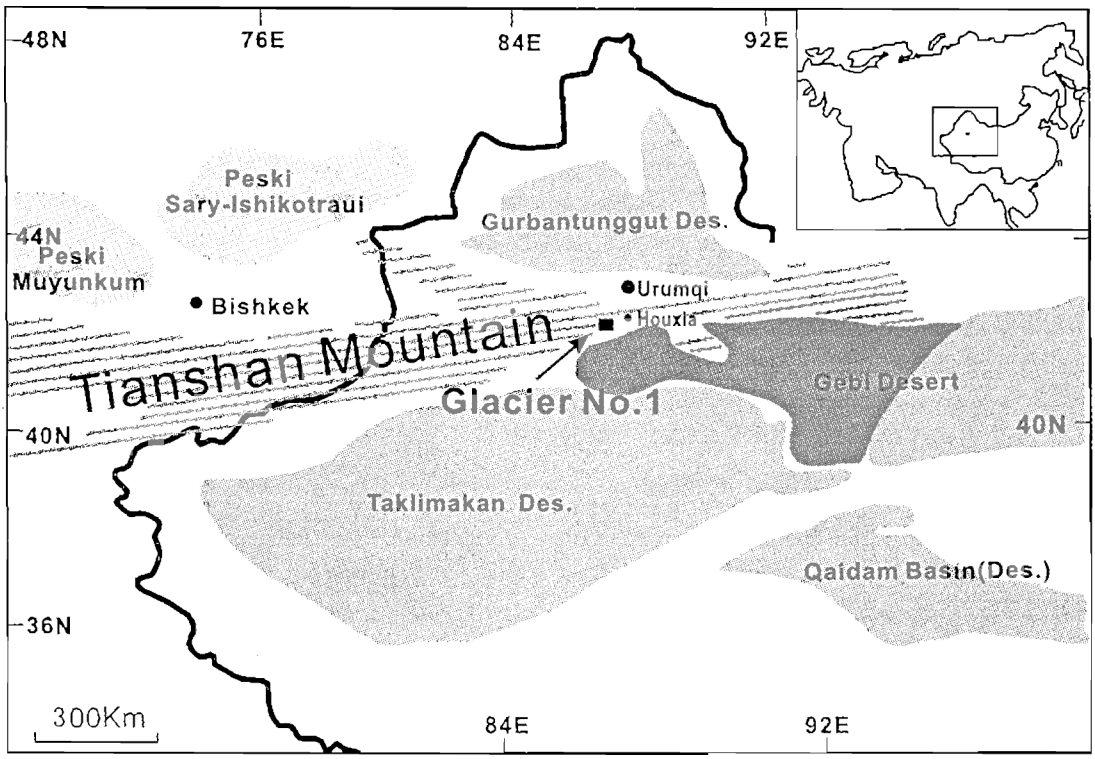

Figure 1. Geographic environment around the east Tianshan (modified from Lee and others, 2003) showing the vicinity of the study site to the deserts, Gobis and the city of Urumqi. The stippled areas designate deserts and Gobis that were drawn in the same scale as the surrounding areas.

pressure and converted into standard cubic meters (m^3). For the mean flow rate of 1.27 m^3 h^{-1}, the velocity at the face of the filter was sufficiently high that the particle collection efficiency (for particles as small as 0.035 μm) was greater than 97 percent (Liu and others, 1984). Strict procedures were followed during sampling and transportation to prevent contamination both in field and the laboratory, including using disposable polyethylene gloves, oronasal masks, and precleaned polyethylene sample containers. The filter cartridges were loaded and packed to clean plastic bags in the Class 100 clean TGS lab and transported to the field in air-tight containers. After sampling, the filters were removed from the cartridges and placed in pre-cleaned, air-tight glass bottles. Blank filters were handled in the same manner as the samples. To analyze the major ion concentrations, the sample and blank filters were wetted by 0.2-ml ultra-pure alcohol. The soluble components were then extracted with 25-ml aliquots of deionized Milli-Q water. The detection limits for NO_3^- in aerosol were 0.18 neq/m^3. Detailed sampling methods and analytical techniques of aerosol were described by Shrestha and others (1997, 2000) and Zhao and Li (2004).

One-hundred-seven (107) surface snow samples (usually 1 to 5 cm of uppermost snow) were collected at the PGPI site at seven-day intervals from September 14, 2002 to September 28, 2004. The surface snow consisted mainly of fresh snow during summer (the wet season) and of

relatively old snow during winter because of sporadic precipitation (dry season). During surface sampling an effort was made to collect the fresh snow and well-preserved surface snow (i.e., snow that was not affected by post-depositional processes such as sublimation or melting) at the sampling site each week to investigate the chemical seasonality in precipitation and dry deposition. Therefore, during the winter season when there was insufficient snowfall, we usually sampled the topmost three centimeters. However, if an accumulation event occurred prior to the sampling, we collected the top one centimeter of the fresh snow. During the summer season, there was usually sufficient fresh snow available, and samples from accumulation that was no more than two days old were usually collected from the top 3 to 5 cm.

The snow-firn pit was concurrently sampled from top to bottom with 10-cm resolution to yield a total of 1,011 samples from September 2003 to September 2004. The snow pit wall was scaled back by at least 50 cm before the collection of samples, and the pit was refilled after each sampling campaign.

Snow samples were kept frozen in the field, during transportation, and in laboratory before the analysis. The analysis of duplicate samples as well as field and laboratory blanks indicates that sample contamination during sample collection, transport, and subsequent analytical procedures is negligible. Both aerosol and snow samples were analyzed in the TGS laboratory, using a Dionex Ion Chromatograph model DX-320. Detailed methods were described by Buck and others (1992), Wake and Mayewski (1993), and Zhao and Li (2004).

RESULTS AND DISCUSSION

Variations in aerosol and surface snow

The concentrations of NO3- in aerosol and surface snow samples are shown in Figure 2. The concentration of NO_3^- in aerosol has been averaged by 6 neq/m^3, fluctuating from the values below the detection limit (0.18 neq/m^3) to a maximum of 31.3 neq/m^3. The 74% of the values were found less than 15 neq/m^3. The received result exhibits somewhat seasonal variability with mean values for spring, summer, autumn, and winter of 3.9, 5.0, 13.0, and 4.7 neq/m^3, respectively. The highest aerosol concentrations were revealed in autumn. Most likely, the high NO_3^- concentrations in the autumn resulted from polluted air masses drifted from Urumqi and Houxia. Pollution from these cities visually observed along the Urumqi River basin during the valley winds (Lee and others, 2003).

Note that NO_3^- is removed from the atmosphere through dry and wet deposition. For both types of deposition strongly depend on meteorological parameters, such as precipitation, wind, etc. Figure 2 shows that the concentration of NO_3^- in the surface snow was very high from mid-September to the end of October 2002, then decreased and remained stable until the beginning of April 2003. On the 5th of April 2003, a sharp peak occurred. From the middle of May to the end of August 2003, the NO_3^- concentration was characterized by several peaks, then displayed small variability by the end of January 2004. From the beginning of February to October 2004, in spite of a short, stable period during April and May, the NO_3^- concentration was characterized by successive high peaks, but returned to a similar baseline.

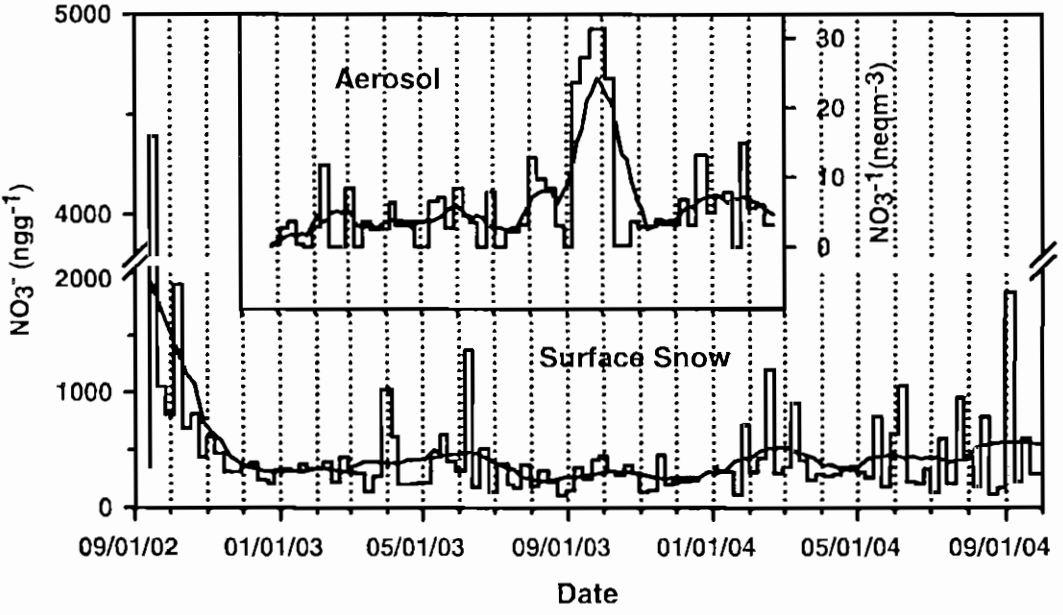

Figure 2. NO_3^- concentrations and its variation trends in aerosol and surface snow samples collected on the Glacier No. 1, eastern Tianshan. The smoothed curve is generated form negative exponential smoother with sampling proportion 0.1 and polynomial degree 1.

During observed period, the NO_3^- seasonal variability in surface snow was ambiguous. The average concentrations of NO_3^- in spring and summer are very similar: 390.9 ng/g and 392.4 ng/g respectively. In autumn the value is 657 ng/g, much higher than it in other seasons. During winter, NO_3^- appears to be relatively stable with lowest average value of 348 ng/g. The mean concentration for all samples is 446.4 ng/g (7.2μeq/L).

During summer the surface snow samples consisted mainly of fresh snow (the wet season). In comparison the surface snow samples collected during winter was relatively old because of sporadic precipitation (dry season). Surface snow in winter experiences more post-depositional effect that includes dry deposition, wind erosion, sublimation and condensation processes. It has been observed that surface snow usually has higher NO_3^- value than ageing snow collected in snow pit that was subjected to elution alternation. The surface snow can be redistributed by wind. which considerable effects on NO_3^- concentrations in snow, e.g., the fact that snow drift can scavenge particles from the lower levels of the troposphere may lead to the increase of NO_3^- concentration in snow (Wolff and others, 1998).

Relationship between NO_3^- in surface snow and aerosol

The linear relationship between the NO_3^- concentrations in surface snow and aerosol was found only during the winter (December 2003 to mid-February 2004; Figure 3), whereas the regression coefficient R is 0.89 (N=10, $p < 0.01$). There is no correlation between these parameters in spring and summer. Similar cases have been observed at other alpine sites (e.g.,

Baltensperger and others, 1993).

Most likely, the discrepancy in NO_3^- concentration between aerosol and surface snow can be interpreted by different depositional processes. During the summer, due to sufficient snowfalls, the NO_3^- concentration in surface snow is determined by two sources: NO_3^- within precipitation and NO_3^- scavenged from air by precipitation. Low concentrations of NO_3^- in aerosol during the wet season could hint to a scavenging effect, i.e., an efficient removal of aerosol particles during persistent precipitation, possibly resulting in significant dilution of NO_3^- and HNO_3 in air and enrichment of those in snow. This case might have happened on the sampling days of May 8, June 26, and July 12, 2003. On these dates the NO_3^- concentrations in aerosol were too low to be detected possibly because the samples were collected after a long period of continuous precipitation. During the winter, because of scarce snowfall, volatilization/sublimation and dry deposition appeared to be the main factors affecting NO_3^- concentration in surface snow. These post-depositional processes apparently enhanced the relationship of NO_3^- between aerosol and surface snow.

In spite of a difference in the NO_3^- concentrations in concurrently collected aerosol and surface snow samples, the NO_3^- concentration in the aerosol evidently shows a similar trend with that in surface snow (Figure 2), suggesting that the low-frequency variation trend of atmospheric NO_x may have been preserved in the surface snow. Thus, the relationship between NO_3^- in the aerosol and snow appears indirectly presented because the complexity of the processes. The similarity of the NO_3^- trends and variability in the aerosol and surface snow is an evidence of this relationship.

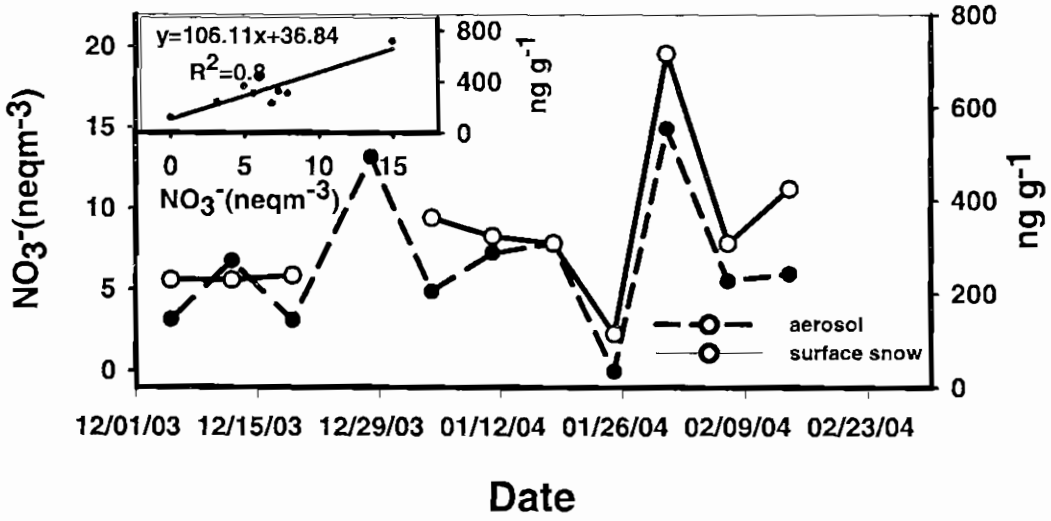

Figure 3. Comparison of NO_3^- in surface snow with aerosol, and linear regression calculated for period from December 2003 to mid-February 2004.

Evolution processes in snow-firn

Figure 4 shows the evolution process of NO_3^- in snow-firn pack at the PGPI site from October 2003 to September 2004. To compare with different species the Mg^{2+} profile is also included in the figure. Mg^{2+} represents a mineral aerosol source. Figure 4 illustrates that there were two prominent NO_3^- peaks (P1 and P2) in the snowpit at the beginning of October 2003. The lower peak (P1) was formed before the middle of September 2003 and the upper one (P2) was found to be shaped by intense precipitation at the end of September 2003. From the middle of November 2003 to the late April 2004, the positions of P1 and P2 remained relatively stable with a slight sinking towards to the superimposed ice surface, which could be caused by snow compaction. Several small peaks of concentration, in the upper part of the snow pits appear as the result of limited precipitation, low temperatures, and weak evaporation, which enabled post-depositional processes such as sublimation and dry deposition to become more dominant.

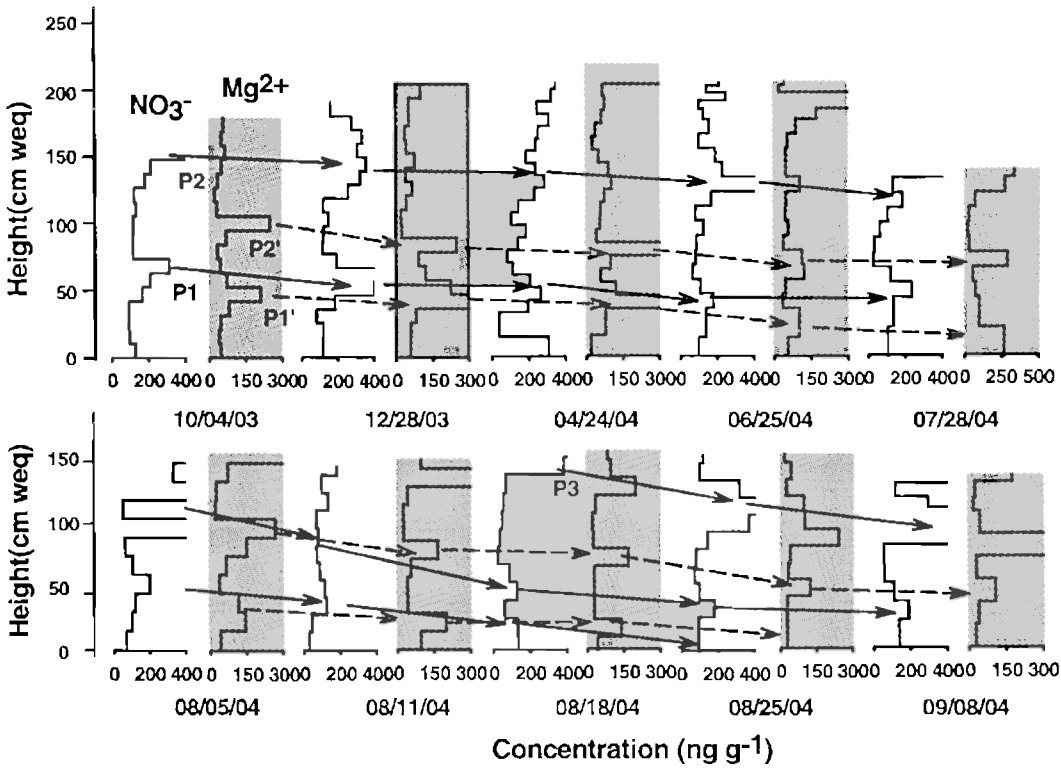

Figure 4. The evolution process of vertical profiles of NO_3^- and Mg^{2+} in snow pits from September 4, 2003 till September 8, 2004. The P1, P2 and P3 indicate NO_3^- concentration peaks, and P1 and P2 indicate Mg^{2+} concentration peaks. Y-axis presents the height (cm weq) above the superimposed ice surface.

From April to the end of May, as temperature increased, meltwater appeared in the snow pit, which attenuated the peaks somewhat as they moved downward. At the same time, the increasing precipitation resulted in successive concentration peaks at about 10 to 30 cm below

he surface. In the summer (June to August), as meltwater percolated through the snow-firn pit, t leached ions, including the NO_3^- and Mg^{2+}. During this period, the upper part of the pit experienced the most post-depositional alteration. With increasing temperature, larger volumes of meltwater began to percolate deeper into the pit along with the NO_3^- and Mg^{2+}, which is indicated by displacement and reduction in concentration of the peaks. When meltwater encountered the superimposed ice at the bottom of the coarse firn layer, it refroze, resulting in the rise of the superimposed ice surface. The extensive ablation caused the compaction of the concentration peaks. At the end of the August, P1 merged into the superimposed ice at the bottom of the pit and was henceforth preserved in the glacier as new annual layer. This demonstrates that in spite of considerable loss of NO_3^- and Mg^{2+} through post-depositional processes, the general information is still preserved in the snowpit. Around mid-August, a new peak (P3) emerged in the upper layer of the pit, and quickly sank downwards.

In comparison with Mg^{2+}, the NO_3^- appeared to be preferentially leached downward in the snowpit. This is clearly illustrated during the period from June to August 2004 as elution intensified. On the June 25, both P1 and P2 were located above P1′ and P2′ (the two peaks were traced in Mg^{2+} concentration profiles) in the pit, but in the profiles of August 25, both P1 and P2 were found in positions below P1′ and P2′,which indicated that NO_3^- was more efficiently leached downward. Most likely, the reason that Mg^{2+} was relatively immobile during elution is because that a relatively large portion of Mg^{2+} was locked in dust layers in the snow-firn pit. This portion of Mg^{2+} appeared to be less efficiently leached during elution than those of solutes that were located mainly at snow grain boundaries and were easily washed out by meltwater. Except for the alternation of NO_3^- in the snowpit, a part of the NO_3^- trapped in the snow deposits as volatile NO_3^-, like HNO_3, was inevitably re-emitted during the evolution process toward the atmosphere.

Table 1. Comparison of NO_3^- in surface snow with other remote glacier areas.

Site	Elevation (m asl)	Periods of record	Sample type	Mean concentration (μeq/L)	Source
East Dronning Maud Land, East Antarctica	1,800 to 3,000	Jan. 1986 to Jan. 1987	Drifting snow	2.69	Osada (1994)
Halley station, Coastal Antarctica		Jul. 1990 to Feb. 1993	Surface snow	1.55	Mulvaney and others (1998)
Neumayer station, Coastal Antarctica		a year long	Fresh snow	1.24	Mulvaney and others (1998)
Summit, Greenland	3,203	a year long	Surface snow	2.9	Burkhart and others (2004)
East Rongbuk Glacier, Mt. Everest, central Himalayas	5,800 to 6,500	Aug. and Sep. 1998	Fresh snow	1.14	Kang and others (2004)
Glacier No. 1, east Tianshan	4,130	Sep. 2002 to Sep. 2004	Surface snow	7.2	This work

Spatial comparisons

Table 1 represents the means NO_3^- concentrations in snow of different glaciers. It is noted that Antarctic data are generally lower than 1.6 μeq/L. Drifting snow in Antarctica may become enriched in NO_3^- compared with new deposited snow (Wolff and others, 1998). The lowest reported snow NO_3^- level was found at East Rongbuk Glacier during the monsoon season (northern slope of Mt. Everest), lower than in Antarctic and Greenland snow. Actually, the highest ion concentrations in the East Rongbuk Glacier occur in spring (pre-monsoon season), resulting from dust aerosol input during the dust-storms observed mainly in April and May in western China, and the lowest concentrations occur in late summer (monsoon season), reflecting not only decreased dust deposition, but also the effect of elution (Kang and others, 2004). Comparing all the sites, the concentration of NO_3^- in Glacier No. 1 is much higher. This may be attributed to the transport of terrestrial dust and anthropogenic emissions into the area.

With respect to the Glacier No. 1, the concentrations of NO_3^- in Inilchek glacier (42°12.5′N; 80°12.2′E) in central Tien Shan provide a comparable dataset. Table 2 presents seasonal NO_3^- values of Inilchek glacier from a firn-ice core recovered in 1998 from the accumulation zone at an altitude of 5,100 m asl (Aizen and others 2004).

Table 2. Seasonal average values of NO_3^- in Glacier No. 1 and Inilchek glacier.

	NO_3^- in Glacier No. 1 (μeq/L)	NO_3^- in Inilchek glacier (μeq/L)
Spring	6.3	5.0
Summer	6.3	5.0
Autumn	10.6	6.0
Winter	5.6	4.0
Mean	7.2	5.25

While the seasonal variation of NO_3^- in Glacier No. 1 and Inilchek glacier are similar, the values of NO_3^- in Glacier No. 1 are generally higher. On the Inilchek Glacier, the changes in NO_3^- in spring and summer were associated with increasing frequency of northwestern advection, which originated over the southern Urals and passed through western Kazakhstan. Both western Kazakhstan and the southern Urals are industrial areas and potential sources of pollution (Aizen and others, 2004). For both areas, anthropogenic pollution, including emission from fossil fuel combustion and biomass burning, livestock manure, and commercial and natural fertilizers may be the principal source of NO_3^-. Mineral dust acts as a carrier for these pollutants (Li and others, 1995, 1999) and may be partially responsible for high levels of NO_3^- in these two areas, since both areas are impacted by regional and local Asian dust.

SUMMARY

A two-year study of NO_3^- from aerosol, surface snow, and snowpits was conducted to determine the depositional and post-depositional processes that occur on the Glacier No. 1 at the

Urumqi riverhead in eastern Tien Shan. The concentrations of nitrite in both surface snow and aerosol display ambiguous seasonal changes. Low values are commonly observed during winter, and relatively high concentrations during autumn. Sources of the NO_3^- include local-to-regional anthropogenic emissions, which may be enhanced by transport in dust storms. No significant correlation of NO_3^- concentrations in concurrently collected aerosol and surface snow samples is found except for the dry season from December 2003 to mid-February 2004. However, the NO_3^- concentration in the aerosol evidently shows a similar trend with that in surface snow, suggesting that the low-frequency variation trend of atmospheric NO_x may have been preserved in the surface snow. Long-term NO_3^- data from snowpits indicate that during winter, the formation of the vertical NO_3^- stratigraphy in the upper layers of the glacier is mainly related to snow compaction, sublimation, and dry deposition. During summer, the snow in the pit experiences the maximum post-depositional alteration through the percolation of the meltwater, and NO_3^- is observed to be more efficiently leached downward than Mg^{2+}. Compared with other regions, the NO_3^- concentration in the Glacier No. 1 is relatively high.

AKNOWLEDGEMENTS

This research was supported by the National Natural Science Foundation of China (40371028; 40571033; 40121101; J0130084) and CAS & CAREERI (CACX2003101; KZCX3-SW-341). We also thank Vladimir Aizen, Daniel R. Joswiak, Rod March and Ross Edwards for their useful comments and helpful suggestions. Support for this research has been provided under the Program for Glacier Processes Investigation (PGPI) conducted by the Tianshan Glaciological Station (TGS), Chinese Academy of Sciences (CAS).

REFERENCES

[1] Aizen, V.B., E.M. Aizen, J.M. Melack, K.J. Kreutz, and L.D. Cecil. 2004. Association between atmospheric circulation patterns and firn-ice core records from the Inilchek glacierized area, central Tien Shan, Asia. *J. Geophys. Res.*, 109(D8), doi:10. 1029/2003JD003894.

[2] Bales, R.C., and J. Choi. 1996. Conceptual framework for interpretation of exchange processes. In Chemical Exchange between the Atmosphere and Polar Snow, E.W. Wolff and R.C. Bales (eds.). *NATO ASI Ser.*, I, 43, 319-338.

[3] Baltensperger, U., M.Schwikowski, H.W. Gaggeler, D.T. Jost, J. Beer,U. Siegenthaler, D. Wagenbach, H.J. Hofmann and H.A. Synal. 1993. Transfer of atmospheric constituents onto an Alpine snow field. *Atmos. Environ.* 27A, 12, 1881-1890.

[4] Buck, C.F., P.A. Mayewski, M.J. Spencer, S.I. Whitlow, M.S. Twickler, and D. Barrett. 1992. Determination of major ions in snow and ice cores by ion chromatography. *J. Chromatogr.*, 594, 225-228.

[5] Burkhart, J.F., M. Hutterli, R.C. Bales, and J.R. McConnell. 2004. Seasonal accumulation timing and preservation of nitrate in firn at Summit, Greenland. *J. Geophys. Res.*, 109, D19302,

doi:10.1029/2004JD004658.

[6] De Angelis, M., and M. Legrand. 1995. Preliminary investigations of depositional effects on HCl, HNO_3, and organic acids in polar firn layers. In Ice Core Studies of Global Biogeochemical Cycles, R.J. Delmas (ed.). *NATO ASI Ser.*1, 30, 361-385.

[7] Dibb, J.E., W.T. Robertand, and M.H. Bergin.1994. Soluble acidic species in air and snow at Summit, Greenland. *Geophys. Res. Lett.*, 21 (15), 1627-1630.

[8] Ginot, P., C. Kull, M. Schwikoski, U. Schotterer, H.W. Gaggeler., Christoph Kull, Margit Schwikowski. 2001. Effects of postdepositional processes on snow composition of a subtropical glacier (Cerro Tapado, Chilean Andes). *J. Geophys. Res.*, 106(D23), 32375-32386.

[9] Kang, S., P. A. Mayewski, D. Qin, S.A. Sneed, J. Ren, and D. Zhang. 2004. Seasonal differences in snow chemistry from the vicinity of Mt. Everest, central Himalayas. *Atmos. Environ.*, 38, 2819-2829.

[10] Lee, X., D. Qin, G. Jiang, K. Duan, and H. Zhou. 2003. Atmospheric pollution of a remote area of Tianshan Mountain: Ice core record. *J. Geophys. Res.*, 108 (D14), 4406-4416.

[11] Li, Z., T. Yao, and Zi Xie. 1995. Study on SO_4^{2-} and NO_3^- in atmospheric aerosol. *Adv. Geosci.*, 10(1), 289-295. [In Chinese]

[12] Li, Z., G. Lu, and B. Liu. 1999. Ice core dust particulate by XPS-SEM/EDAX -- Impact of dust particulate on SO_4^{2-} and NO_3^- record in ice cores. *Chin. Sci. Bull.*, 44(15), 1424-1427.

[13] Liu, B.Y.H., D.Y.H. Pui, and K.L. Rubow. 1984. Characteristics of air sampling filter media. In Aerosols in the mining and industrial work environments, Vol. 3, Instrumentation (V.A. Marple V.A. and B.Y.U. Liu, eds.). *Ann Arbor Science*, MI, 989-1037.

[14] Mayewski, P.A., and M. Legrand.1990. Recent increase in nitrate concentration of Antarctic snow. *Nature*, 346, 258-260.

[15] Mulvaney, R., D. Wagenbach, and E.W. Wolff. 1998. Postdepositional change in snowpack nitrate from observation of year-round near-surface snow in coastal Antarctica. *J. Geophys. Res.*, 103(D9), 11021-11030.

[16] Osada, K. 1994. Seasonal variations of major ionic concentration levels in drifting-snow samples obtained from east Dronning Maud Land, East Antarctica. *Ann. Glaciol.*, 20, 226-230.

[17] Preunkert, S., D. Wagenbach, and M. Legrand. 2003. A seasonally revolved alpine ice core record of nitrate: Comparison with anthropogenic inventories and estimation of preindustrial emissions of NO in Europe. *J. Geophys. Res.*, 108

[18] Rothlisberger, R., M.A. Hutterli, S. Sommer, E.W.Wolff, and R. Mulvaney. 2000. Factors controlling nitrate in ice cores: Evidence from the Dome C deep ice core. *J. Geophys. Res.*, 105(D16), 20565-20572.

[19] Shrestha, A.B., C.P. Wake, and J.E. Dibb.1997. Chemical composition of aerosol and snow in the high Himalaya during the summer monsoon season. *Atmos. Environ.*, 31(17), 2815-2826.

[20] Shrestha, A.B., C.P. Wake, J.E. Dibb, P. A. Mayewski, S. I. Whitlow, G. R. Carmichael, M. Ferm. 2000. Seasonal variations in aerosol concentrations and compositions in the Nepal Himalaya. *Atmos. Environ.*, 34,3349-3363.

[21] (D21),4681,doi:10.1029/2003JD003475.

[22] Wake, C.P., P.A. Mayewski. 1993. The spatial variation of Asian dust and marine aerosol contributions to glaciochemical signals in central Asia. In: G. Young (ed.), International Symposium on Snow and Glacier Hydrology. Kathmandu. *IAHS Publication*, 218, 385-402.

[23] Wolff, E.W., J.S. Hall, R. Mulvaney, E.C. Pasteur, D. Wagenbach, and M. Legrand. 1998. Relationship between chemistry of air, fresh snow and firn cores for aerosol species in coastal Antarctica. *J. Geophys. Res.*, 103(D9), 11057-11070.

[24] Zhang, Y., E. Kang, and C. Liu. 1994. Mountain climate analysis in Urumqi River valley, Tianshan. *J. Glacio. Geocryol.*, 16, 333-341. [In Chinese]

[25] Zhao, Z., and Z. Li. 2004. Determination of soluble ions in atmospheric aerosol by ion chromatography. *Mod. Sci. Inst.*, 5, 46-49. [In Chinese]

近期乌鲁木齐河源 1 号冰川成冰带及雪层剖面特征研究

李向应，李忠勤，尤晓妮，王飞腾，李传金，朱宇漫

(中国科学院寒区旱区环境与工程研究所天山冰川观测试验站/
冰冻圈与环境联合重点实验室，甘肃 兰州 730000)

摘　要：冰川成冰带特征和冰川表面雪层剖面特征反映了冰川的基本特性，是冰川学研究的基本内容之一。天山乌鲁木齐河源 1 号冰川（以下简称 1 号冰川）的成冰带研究最初始于上世纪 60 年代初，谢自楚等将 1 号冰川自下而上划分为 4 个成冰带。1988 年，王晓军等发现，由于气候变暖，冰川上部的冷渗浸—重结晶带消失，被渗浸带所取代。因而，在刘潮海等 1989 年的研究中，将 1 号冰川划分为 3 个成冰带。上世纪 90 年代中期以来，气温升高给 1 号冰川带来了有观测记录以来最深刻的变化，由此造成成冰带的变化和冰川表面雪层剖面特征的变化是人们十分关注的问题。本文对近期 1 号冰川的成冰带进行了划分，并通过大量雪坑资料，研究论述了目前 1 号冰川雪层剖面的层位特征。研究发现，由于气候变暖，剖面特征和成冰带谱有由“冷”向“暖”的转化趋势。同时还发现，1 号冰川东支顶部发生了强烈的消融现象，该处已由渗浸带转化为具有强烈消融特征的局部消融区。

关键词：1 号冰川　成冰带　雪层剖面　雪坑

1　引言

冰川成冰带特征和雪层剖面特征反映了冰川的基本特性，是冰川学研究的基本内容之一。冰川的形成是通过不同的成冰过程将雪转变成冰而实现的，前人对此作了许多研究[1, 2]。1955 年，舒姆斯基首次提出冰川成冰带的概念，根据成冰作用的不同划分出 7 种成冰带[3]：重结晶带、再冻结—重结晶带、冷渗浸—重结晶带、暖渗浸—重结晶带、渗浸带、渗浸—冻结带和消融带。随后，Paterson 又将其归纳为 5 个成冰带[4]，即：干雪带、渗浸带、湿雪带、附加冰带和消融带。在我国，有关成冰带的研究前人已经做了很多工作，主要集中在祁连山[5]、天山[6]、阿尔泰山、西昆仑山、喜马拉雅山、藏东南地区和横断山区等[7-9]的冰川上。而其中对 1 号冰川成冰带的研究是开展最早且最为详细的冰川之一。初始于 1965 年，谢自楚等根据雪—粒雪层的构造特征，将 1 号冰川自下而上划分为 4 个成冰带[3]：消融带、渗浸—冻结带、渗浸带和冷渗浸—重结晶带。1988 年，王晓军等[10]通过对冷渗浸带雪层剖面特征的研究发现，由于气候变暖，冰川上部的冷渗浸—重结晶带消失，被渗浸带所取代。因而在 1989 年，刘潮海等根据冰雪积累量随高度变化的特征将 1 号冰川自下而上重新划分为 3 个成冰带[11]：消融带（依据有无附加冰的形成再分为消融下带和消融上带）、渗浸—冻结带和渗浸带。此外，王晓军、刘潮海等人[10-11]对 1 号冰川不同区域的雪层剖面特征也进行了研究，其不同成冰带内雪层剖面的主要特征为消融带的雪层剖面中没有多年

积雪，消融下带有冰川冰出露，消融上带存在附加冰，且皆为季节性的；渗浸—冻结带的成冰作用完全为融水的渗浸和冻结所控制，附加冰大量发育；渗浸带内长期存在粒雪，雪—粒雪层较厚，粒雪层内含有大量渗浸冰片和冰透镜体。

自上世纪 90 年代中期以来，乌鲁木齐河源区气温升高给 1 号冰川带来有观测记录以来最深刻的变化[12]。1958－2003 年的 45 a 间，1 号冰川的年物质平衡量平均为－222.0 mm（约－40.8×10^4 m^3），累积物质平衡量达到－9991.5 mm，亦即这期间冰川减薄了 11 m 多，累积亏损量达 1.838×10^4 m^3。1 号冰川面积在 1962－2004 年的 42 a 间减少 0.242 km^2，为 12.4%，并呈加速减小趋势。1962 年至今，1 号冰川东支末端共退缩 175.2 m，西支共退缩 197.6 m，冰川表面运动速度减缓。1986 年以来，冰川年均径流深较之以前翻了近一番。在这种情形下，1 号冰川的成冰带和雪层剖面特征发生了怎样的变化是众所关心的问题。本研究根据近期取得的 1 号冰川东、西支共 32 个雪坑的雪层剖面资料，并结合近年来天山冰川观测试验站的观测资料对近期 1 号冰川的成冰带和雪层剖面特征进行了专门研究。

2　研究方法和资料

为研究成冰带和雪层剖面特征，于 2004 年 8－11 月间，分别自东、西支末端沿 1 号冰川主流线方向直至顶部总共挖取雪坑 32 个。在挖取过程中，对每个雪坑的雪层剖面特征进行详细观测和记录，并统一整理，将各个雪坑的雪层剖面绘成柱状剖面图进行对比分析研究。此外按海拔高度对雪坑进行统一编号：东支为 E1，E2，…，E20；西支为 W1，W2，…，W12。雪坑所在的位置、海拔、坡度及雪坑编号详见图 1 和表 1（其中雪坑编号、海拔及挖取雪坑的时间在柱状剖面图顶部已注明）。另外，根据雪层剖面的层位特征和附加冰出现的区域范围，并参考多年零平衡线平均海拔高度对成冰带进行划分。需要说明的是：首先，为满足计算机绘图软件的要求，在绘图过程中使用另一套雪层剖面图例；其次，本文中的表层雪厚度指风板,风吹雪和新雪的厚度；雪坑深度或雪层剖面厚度在消融带、渗浸－冻结带和渗浸带分别指表层雪面距冰川冰面、附加冰面和粒雪冰面的距离。

表 1　雪坑编号

Table 1.　Serial number of snow-pits

		雪坑编号															
		E1	E2	E3	E4	E5	E6	E7	E8	E10	E12	E13	E14	E15	E18	E19	E20
东支	海拔（m）	3890	3923	3965	4004	4043	4055	4060	4065	4080	4116	4126	4130	4134	4187	4224	4225
	坡度（°）	5	12.5	12	11	17	—	18	16	11	28	25	26	30	—	0	0
		W1	W2	W3	W4	W5	W6	W7	W8	W9	W10	W11	W12				
西支	海拔（m）	3926	3976	4013	4045	4085	4200	4224	4232	4246	4250	4276	4484				
	坡度（°）	—	—	—	—	—	—	31	32	30	30	32	0				

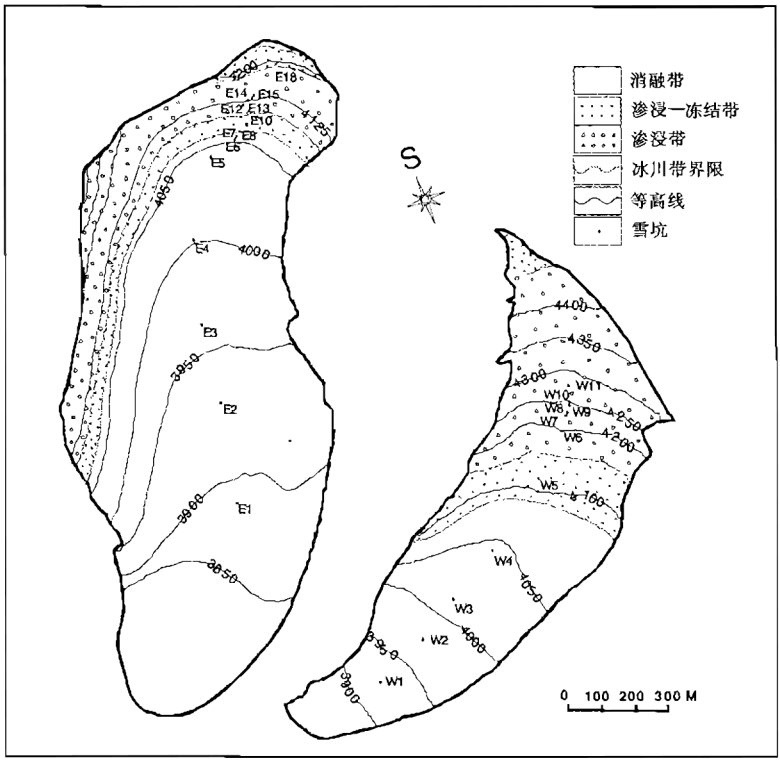

图 1 1 号冰川雪坑位置及成冰带分布

Figure 1. Position of snow-pits and distribution of ice formation zones on Glacier No.1

3 结果与讨论

3.1 雪层剖面的总体变化特征

图 2 表示雪坑深度自冰舌末端至冰川顶部随海拔的变化。雪层剖面厚度的变化受气温和降水的共同作用，即厚度与气温呈反相关，与降水呈正相关[13]。另外与雪坑所在位置的地形也有关系。由图 2 看出，1 号冰川东支的雪层剖面厚度自冰舌末端至海拔 4060m 处逐渐增大，随之减小，后又增大直至海拔 4080m 处；在海拔 4080m－4116m 雪层剖面厚度有较小的减小趋势，然后迅速增大直至粒雪盆厚壁处（海拔 4125 左右）达到最大，后又快速减小至顶部达到最小。西支自冰舌末端至海拔 4200m 处呈缓慢的增大趋势，从海拔 4200m 开始厚度快速增大至粒雪盆厚壁处（海拔 4276m 左右）达到最大，后又快速减小至顶部达到最小。结合雪层剖面变化特征发现，细粒雪层和粗粒雪层厚度的变化规律同于雪层剖面厚度的变化，不同的是粗粒雪层厚度随海拔的增大趋势大于细粒雪层，如图 4—图 8。

污化面按其形成季节的不同分为冬春季污化和夏季污化[14]。冬春季污化是由于冬季降雪很少，同一冰雪面长期暴露于大气中，经风力搬运来自于远处的沙尘和周围山体表面的风化碎屑物质迁移、沉降于冰雪表面而形成，颜色呈淡黄色，一般被春季降雪覆盖。夏季污化一般形成于夏末，融水在渗浸过程中携带雪层剖面中不同层位的污化物迁移、滞留于某一层位而形成，颜色为黄色，一般被秋季降雪覆盖。如图 3，1 号冰川雪层剖面中的污化层数目随海拔升高明显增多，污化层深度显著增大。东、西支分别大致在海拔 4050m 和

4200m 以下，雪层剖面中只有一个污化层，颜色较浅，污化层的最大深度在 50cm 左右。东支在海拔 4050m－4150m，西支在海拔 4210m－4260m，污化层数目较多，东支最多有 4 个，西支最多有 5 个；东、西支污化层的最大深度分别为 160cm 和 210cm。东、西支分别自海拔 4150m，4270m 至顶部，雪坑中的污化层的数目减少为一个，且污化的深度变浅。

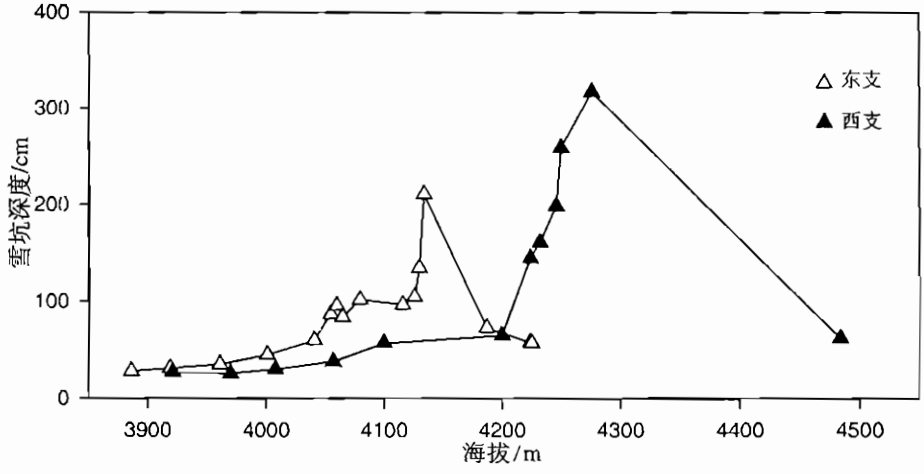

图 2　雪坑深度随海拔的变化

Figure 2.　Depth variation of snow-pits with altitude

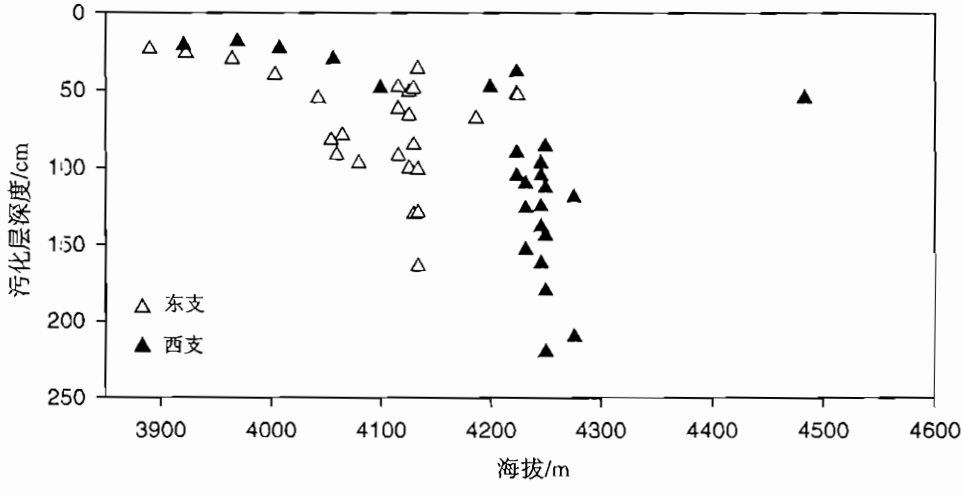

图 3　雪层剖面中的污化层深度随海拔的变化

Figure 3.　Depth variation of dust layers with altitude

雪层剖面的层位特征反映了冰川不同海拔区域积累、消融程度的差异和成冰作用的不同。在高海拔区域（如图 7 和图 8，东支在 4116m—4134m，西支在 4224m—4276m），雪层剖面主要由风板—新雪—细粒雪—中粒雪—粗粒雪组成；在海拔较低处和西支顶部区域（如图 4，图 5 和图 6，东支在 3923m—4080m，西支在 3976m—4200m 和 4484m 左右），

雪层剖面较为简单，主要由新雪（风板）—细粒雪—粗粒雪组成；在冰舌末端和东支顶部区域（如图 4 和图 5，东支在 3890m 以下和 4224m 左右，西支在 3926m 以下），层位剖面最简单，主要由风板—中粒雪—粗粒雪组成。

目前 1 号冰川顶部的冰雪特征较为显著（图 4 中 E19 和 E20）[15]，东支为：（1）雪层厚度较小（约 40cm），局部区域的冰川冰面直接外露；（2）层位剖面简单，以中粒雪和粗粒雪为主，无新雪和细粒雪层（如雪坑 E19，海拔 4224m；雪坑 E20，海拔 4225m）；（3）雪层剖面中只有一个污化层，位于冰川冰面上部，颜色很深，为强污化。这与冰川消融的加剧和气温持续升高，造成冰川冷储减少有很大关系。气候持续转暖，加之东支顶部冰川朝南，不远处存在裸露岩石，大量接受太阳辐射，造成冰雪消融强度增大，消融量剧烈增加。在西支（如图 6 中的雪坑 W12），（1）雪坑深度较小（约 55cm），较之东支稍大；剖面特征比东支复杂，有新雪和细粒雪发育；（2）雪层剖面中仅有一个污化层，位于附加冰面上部，强度弱，颜色很浅，需仔细辨认才能识别。这表明西支顶部冰雪的消融强度远小于东支顶部。

3.2 各成冰带的范围

根据野外观测，1 号冰川东、西支挖取的雪坑中附加冰出现的范围可知，1 号冰川东、西支消融带和渗浸—冻结带的界限分别在海拔 4066m 和 4089m 处，这与近十年来零平衡线的平均值 4084m 相差不大[16-17]。野外观测发现雪坑 E10（海拔 4080m）下部有明显的附加冰存在，附加冰上部有一层颜色较深的污化面；同时在雪坑 E12（海拔 4116m）中发现，雪坑下部的冰层性质发生了明显变化，附加冰上部出现一层 2-3cm 厚的粒雪冰；由此可以确定东支粒雪线的高度应在雪坑 E10（海拔 4080m）与 E12（海拔 4116m）之间，取其平均值为 4098m，同理可确定西支的粒雪线在海拔 4136m 处。由此可以确定 1 号冰川东、西支渗浸-冻结带和渗浸带的界限分别在海拔 4098m 和 4136m 处。

根据上述成冰带的划分结果，可将 1 号冰川自下而上划分成三个成冰带：（1）消融带（东支在海拔 4066m 以下和顶部的局部区域，西支在海拔 4089m 以下）。（2）渗浸—冻结带（东支在海拔 4066m—4098m 和渗浸带上限至顶部的局部消融区下限之间，西支在海拔 4089m—4136m 和顶部的局部区域）。（3）渗浸带（东支在海拔 4098m 至粒雪盆上部的渗浸—冻结带下限之间；西支在海拔 4136m 至顶部的局部渗浸—冻结区下限之间）。各成冰带的具体范围及分布状况见图 1。

3.3 各成冰带的基本特征

（1）消融带

根据上述成冰带的区域范围划分结果：雪坑 E1（海拔 3890m）—E8（海拔 4065m），E19（海拔 4224m）—E20（海拔 4225m）和 W1（海拔 3926m）—W5（海拔 4085m）位于消融带。消融带内年物质平衡为负，降水不能长时间保存。夏季消融强烈时期，冰川吸收的热量可融化掉全部粒雪和部分冰川冰，东支顶部和西支冰舌末端表现最为明显。融水沿冰川表面向地势低处汇集成河，在下部形成较大的水道，表面形成一道道小水沟。污化物随融水的流动在冰川表面形成球形颗粒物，一部分随融水的流失而进入河道。

消融带的表层雪厚度和雪层剖面厚度均较小，其最大厚度东支分别为 26.5cm 和 88.5cm（如图 4，雪坑 E5，E7），西支分别为 26cm 和 48.5cm（如图 5，雪坑 W5）。平均厚度东支分别为 11cm 和 49cm，西支分别为 13.5cm 和 28.2cm。它们的厚度随海拔升高缓慢的增大。这是由于消融带海拔低，坡度小，地势平坦，接受日照时间长和单位面积的辐射量多

的缘故。在消融带中、下部，雪层剖面特征非常单一。具体表现为有的雪层剖面中无细粒雪层而有粗粒雪层（图 5 雪坑 W1，海拔 3926m），有的雪层剖面中无粗粒雪层但有细粒雪层（如图 4，雪坑 E1，海拔 3890m）。这是由于在较高的温度条件下，细粒雪和粗粒雪没有充足的时间变质转化便消融流失。在消融带上部，细粒雪层下部为粗粒雪层，粗粒雪层的厚度随海拔的升高明显增加，而细粒雪层厚度变化不大，且细粒雪层和粗粒雪层距表层雪面的距离均逐渐增大。其原因为在相当的气候条件下粗粒雪层比细粒雪层的深度相对较大，保存的时间比细粒雪较长。消融带的雪层剖面中只有一个污化层（如图 4，图 5），位于冰川冰面上，颜色很深，为强污化，有的污化物已经进入冰内。污化层深度较小，但相对其它雪坑而言，雪坑 E19 和 E20 的污化层深度较大，分别为 57cm 和 58cm。这是大量冰雪融水携带不同层位的污化物渗浸、迁移的结果：一部分污化物随融水流失，一部分在气温较低时重新冻结而进入冰川冰内。

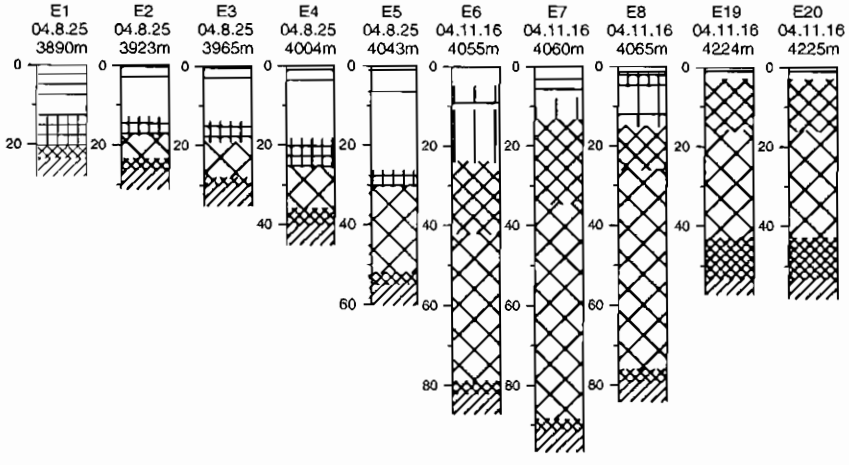

图 4　1 号冰川东支消融带的雪坑层位剖面

Figure 4.　Stratigraphy profiles of snow-pits in ablation zone at the east branch on Glacier No.1

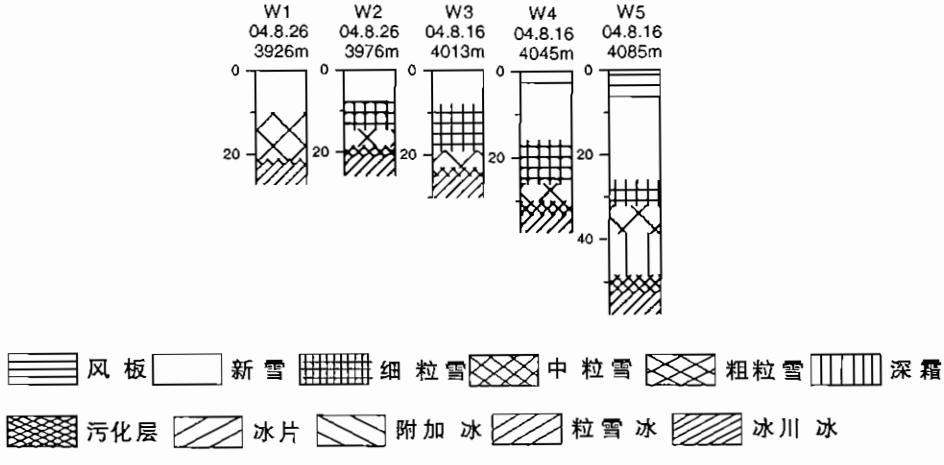

图 5　1 号冰川西支消融带的雪坑层位剖面

Figure 5.　Stratigraphy profiles of snow-pits in ablation zone at the west branch on Glacier No.1

（2）渗浸—冻结带(附加冰带)

E10（海拔 4080m），E18（海拔 4187m）和 W12（海拔 4484m）位于渗浸—冻结带。此带内年物质平衡为正，雪层中有较多的附加冰发育。在夏末消融强烈时期大量附加冰消融并出露，大部分融水沿附加冰面流失，少部分形成渗浸冰片和冰透镜体。成冰作用完全被融水的渗浸和冻结控制，成冰速度快，时间短，成冰量大（以夏季为主）。另外，在粒雪盆上部靠近冰川顶部出现了大范围的渗浸—冻结带，这是由于靠近冰川顶部区域的海拔较高，日照强烈，风力较大的缘故。渗浸－冻结带的雪层厚度较薄（约 60cm），附加冰面有较强的污化层。如图 6 雪坑 E18（海拔 4187m）。

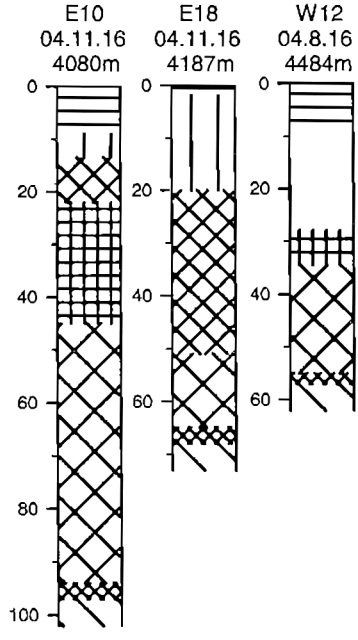

图 6 1 号冰川渗浸—冻结带的雪坑层位剖面

Figure 6. Stratigraphy profiles of snow-pits in superimposed-ice zone on Glacier No.1

渗浸—冻结带的雪层剖面，细粒雪层和粗粒雪层厚度都介于其它两成冰带之间，如雪坑 E10（海拔 4080m）分别为 102cm，23cm 和 49cm。这是由于此带的海拔高度，消融强度和物质积累量均介于其它两成冰带之间，且此带的渗浸冻结作用较强，大部分融水参与了粒雪的改造，在冰面形成附加冰，少部分融水沿冰面形成径流而损失。雪层剖面中只有一个污化层（如图 6），位于附加冰面，颜色较深，强度较大。污化层深度介于其它两成冰带之间。其原因同于在消融带的形成原因。

（3）渗浸带(湿雪带)

E12（海拔 4116m）—E15（海拔 4134m），W6（海拔 4200m）—W11（海拔 4276m）位于渗浸带。渗浸带内年物质平衡为正，雪—粒雪层较厚，雪层下部含有较多渗浸冰片和冰透镜体。雪层内温度较低，除在夏季温度可至 0℃以上外，其它季节全在 0℃或 0℃以下。成冰作用以暖型为主，但在冬季冷型占优势，不过成冰量很少。夏季融水不能全部冻结在本带内，少部分融水沿粒雪冰面流失。

与其它两成冰带相比，渗浸带的表层雪厚度和雪层剖面的最大厚度东支分别为 21cm

和 206cm，西支分别为 28cm 和 312cm；其平均厚度东支分别为 17cm 和 117cm，西支分别为 16cm 和 166cm。此外，表层雪和雪层剖面厚度随海拔的升高显著增大。这是由于渗浸带海拔高，消融强度弱，积累量大的缘故。另外由于地形的原因，风吹雪的影响也可能使表层雪和雪层剖面的厚度增大。此带的细粒雪层和粗粒雪层厚度最大，且细粒雪层远小于粗粒雪层厚度。细粒雪层的最大厚度东、西支分别为 28cm 和 76cm（图 7 雪坑 E13，海拔 4126m；图 8 雪坑 W11，海拔 4276m）；粗粒雪层的最大厚度东、西支分别为 155cm 和 208cm（图 7 雪坑 E15，海拔 4134m；图 8 雪坑 W11，海拔 4276m）。这是由于此带位于粒雪盆后壁的凹陷地带，温度低（年平均气温在 0℃以下）；在气候变化正常的年份（2002 年例外）季节降水可长时间保存，不易发生消融变质作用。此外，雪－冰转化时间较长，粗粒雪转化为冰较细粒雪转化为粗粒雪的时间更长。研究发现[13、18]，细粒雪转化为粗粒雪的时间夏季一般为 20 天—3 个月，冬季一般为 4.5 个月；粗粒雪转化为冰一般为 3 年零 4 个月。

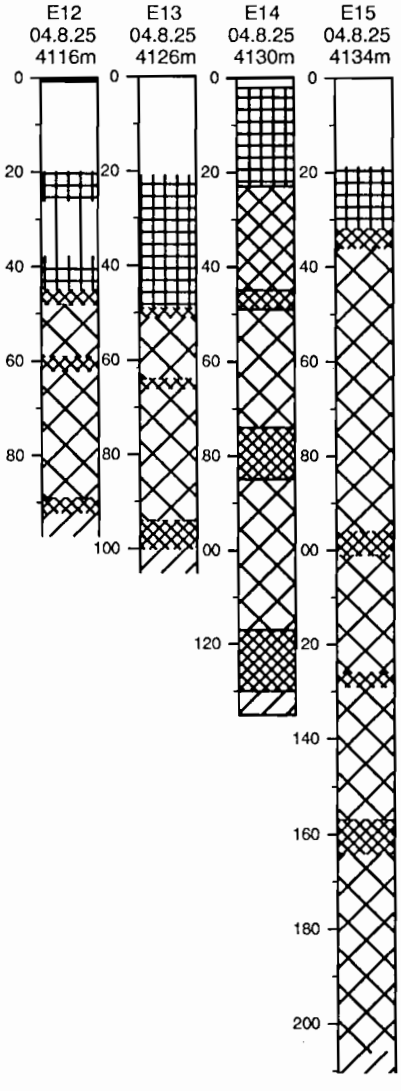

图 7　1 号冰川东支渗浸带的雪坑层位剖面

Figure 7.　Stratigraphy profiles of snow-pits in percolation zone at the east branch on Glacier No.1

相对消融带和渗浸—冻结带而言，渗浸带雪层剖面中污化层的数目最多，深度最大。如图7、图8，东、西支雪层剖面中的污化层数目最多分别为4层和5层，最大深度分别为157cm和220cm。污化层距粒雪冰面的距离随海拔的升高逐渐减小，污化层距粒雪冰面越近强度越大，颜色也越深。这是由于渗浸带内融水的渗浸冻结作用很弱，污化层虽发生迁移但很难叠加，随着季节性降水的积累保存于不同层位。另外，渗浸带的物质积累量随着海拔的升高不断增大，雪层厚度逐渐增加，密实化作用渐次增强，从而导致污化层间的粒雪更加密实和粒雪中孔隙体积减小，粒雪层的厚度减薄，污化层与粒雪冰面的距离逐渐缩小。

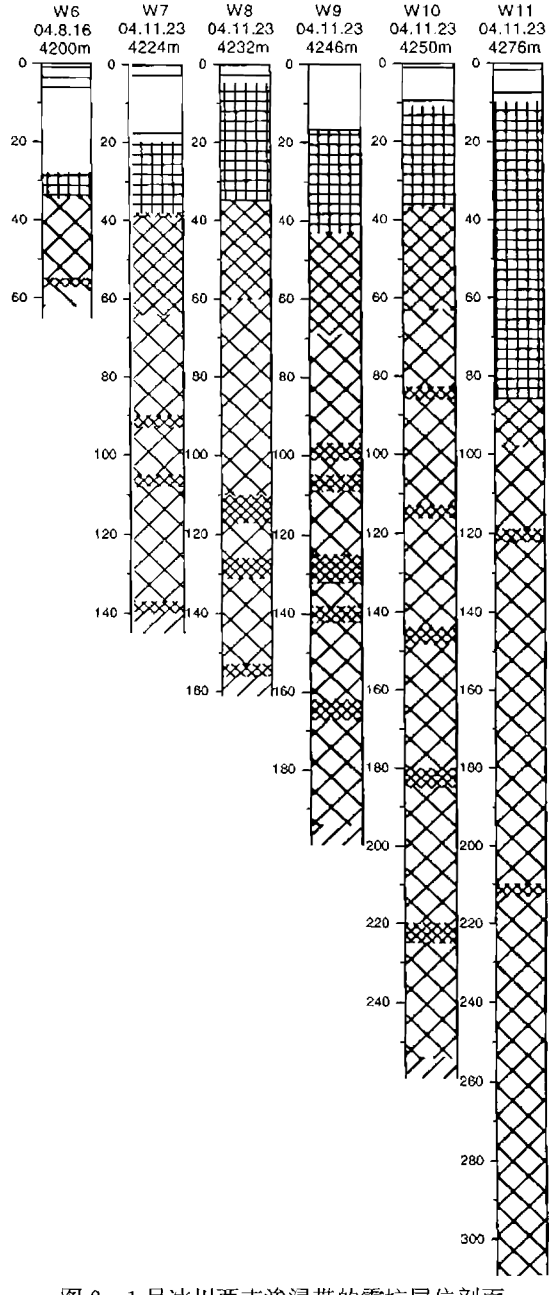

图8 1号冰川西支渗浸带的雪坑层位剖面

Figure 8. Stratigraphy profiles of snow-pits in percolation zone at the west branch on Glacier No.1

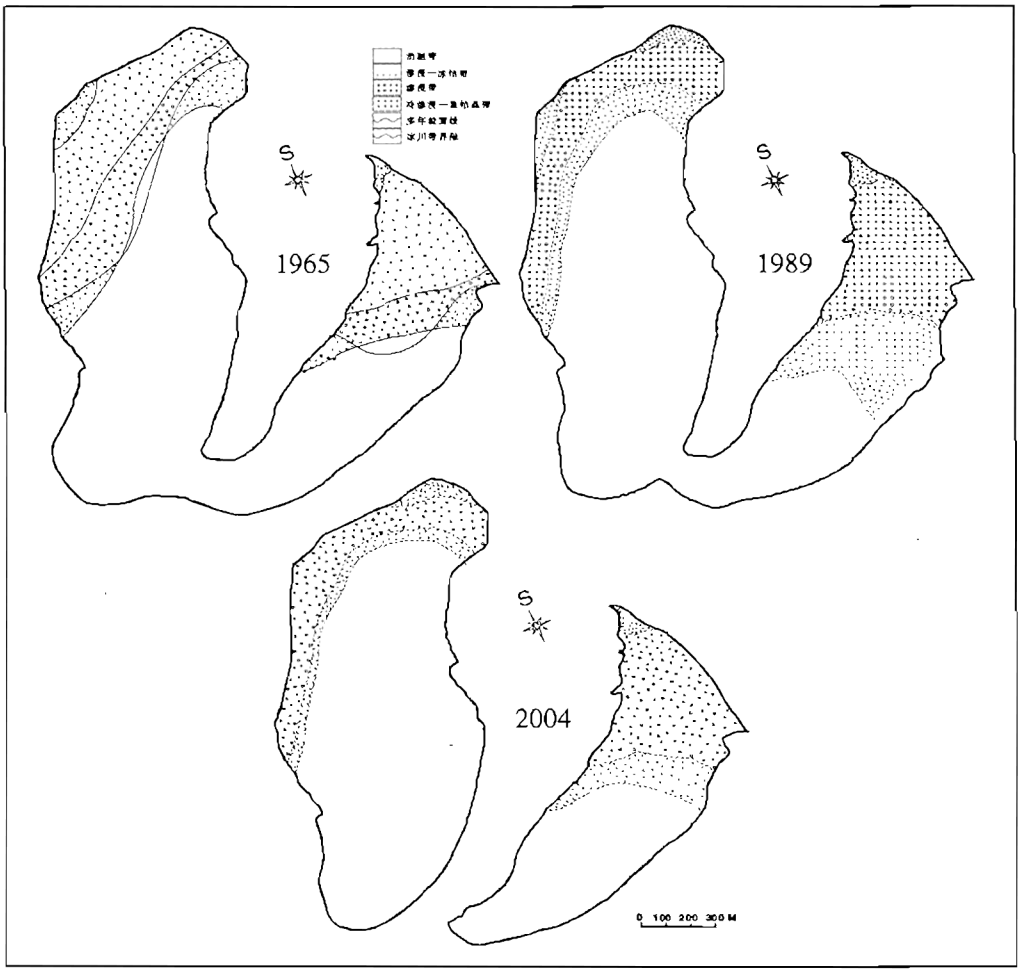

图 9　1 号冰川不同时期的成冰带图

Figure 9.　Ice formation zones on Glacier No.1 in different periods

3.4　不同时期雪层剖面特征和成冰带谱的比较

上世纪 80 年代中期以来，西部开始出现明显的气候转型现象[19]。乌鲁木齐河源区气温升高，1 号冰川强烈消融，逐年退缩，成冰带谱和雪层剖面特征发生了显著变化。主要表现在：雪层剖面厚度变薄，层位变得简单。1965 年和 1989 年渗浸－冻结带雪层中大量发育的渗浸冰片、冰透镜体、深霜现已大大减少，代之以细粒雪和粗粒雪为主，并间或有少量的冰片和深霜。层位剖面间的界限变得模糊，不易分辨，但细粒雪和粗粒雪层的界限较为清楚。这主要是由于随着气温升高冰川消融加剧，雪线上升，不同海拔区域的消融量增大，积累量减少。而且渗浸冻结作用的增强对雪层受融水改造的影响增大，雪层中的渗浸冰片、冰透镜体不能长期保存而消融流失。1 号冰川的成冰带与 1965 年和 1989 年相比除具备以前成冰带的基本特征外，又出现了一些新的特点。尤其在东支顶部偏西北方向约有 5m 厚的冰川冰出露，消融强烈，类似于西支冰舌末端裸露的冰川冰壁，而且在出露的冰川冰南面有冰川融水聚集形成的面积约 30m^2 的水域，水面已结冰，冰层很厚，人可在

上面行走。这说明 1989 年存在于东支顶部的渗浸—冻结带，现局部已转化为具有强烈消融特征的局部消融区。这些现象表明目前 1 号冰川的雪层剖面特征和成冰带谱具有由冷向暖的转化趋势。另外，根据李忠勤，李传金等[12、20]的研究发现 1996 年以来 1 号冰川的消融区有扩大趋势，本世纪初成冰带之间的界限明显上移，2004 年 8 月的观测资料发现冰舌末端已达 4074m，较 1962 年（4000m）升高了 74 米，渗浸带上限位置达到 4093m，达到各研究时期的最高，且各成冰带面积显著减小。

4 结论

近期研究发现，随着乌鲁木齐河源区气温升高，1 号冰川的成冰带谱和雪层剖面特征具有由冷向暖的转化趋势。（1）雪层剖面厚度随海拔升高逐渐增大，靠近冰川顶部又明显减小；细粒和粗粒雪层厚度的变化规律同于雪层剖面，不同的是粗粒雪层厚度的增大趋势大于细粒雪层；雪层剖面中的污化层数目随海拔升高而增多，深度增大，但靠近高海拔区域污化层数目和深度明显减少和减弱。（2）在高海拔区域，雪层剖面主要由风板—新雪—细粒雪—中粒雪—粗粒雪组成；在低海拔区域和西支顶部，主要由新雪（风板）—细粒雪—粗粒雪组成；在冰舌末端和东支顶部区域，主要由风板—中粒雪—粗粒雪组成。雪层剖面组成以粒雪（细粒雪和粗粒雪）为主，粗粒雪在雪层中所占比例随着海拔升高而增大；深霜、冰片和冰透镜体较以前大为减少，只有在部分渗浸带区域的雪层中有发育；雪层中的渗浸冻结作用较以前增强，污化层数目减少，颜色变深，强度更高。（3）目前 1 号冰川的成冰带谱为：消融带（东支在海拔 4066m 以下和顶部的局部区域，西支在海拔 4089m 以下）；渗浸—冻结带（东支在海拔 4066m—4098m 和渗浸带上限至顶部的局部消融区下限之间，西支在海拔 4089m—4136m 和顶部的局部区域）；渗浸带（东支在海拔 4098m 至粒雪盆上部的渗浸—冻结带下限之间；西支在海拔 4136m 至顶部的局部渗浸—冻结区下限之间）。值得关注的是东支顶部的局部区域现已转化为具有强烈消融特征的局部消融区。

致谢：本项研究是天山冰川观测试验站开展的雪冰现代过程研究项目的一部分，是在全体观测和研究人员集体努力下完成的。在此对参加本项研究的每一个观测人员以及项目组人员焦克勤，杨惠安，韩添丁，赵中平，李慧林，张坤，钱军，张明军等表示衷心感谢。

参考文献（references）：

[1] Yao Tandong,Pu Jianchen,Wang Ninglian,et al.A new type of ice formation zone found in the Himalayas.Chinese Science Bulletin[J],1999,Vol.44 No 5:467—473.[姚檀栋,薄健辰,王宁练,等.中国境内又一种新成冰作用的发现.科学通报[J],1998,43（1）:94～97.]

[2] Kalesnik C U.An Introduction to Glaciology[M].Lanzhou:Lanzhou Institute of Glaciology and Geocryology,CAS,1982:13-17,28-40.[卡列斯尼克 C B.冰川学概论[M].兰州：中国科学院冰川冻土研究所.1982:13-17,28-40.]

[3] Xie Zichu,Huang Maohuan,et al.A evolution of the snow-snowgrains layer and ice formation in the Glacier No.1 at the headwaters of the Urumqi River,Tianshan[A].An studies of glaciology and hydrology on the Urumqi River,Tianshan[C].Beijing:Science Press,1965,1-14.[谢自楚,黄茂恒,等.天山乌鲁木齐河源 1 号冰川雪-粒雪层的演变及成冰作用[A].天山乌鲁木齐河冰川与水文研究[C].北京:科学出版社,1965,1-14.]

[4] W.S.B.Paterson.The Physics of Glaciers.Beijing:Science Press,1987,3-12.[W.S.B.佩特森.冰川物理学.北京:科

学出版社,1987,3-12.]

[5] Xie Zichu,Wu Guanghe,*et al*.Ice formation process in glacier of Qilian mountain. [谢自楚,伍光和,等.祁连山冰川的成冰作用.中国科学院兰州冰川冻土所集刊.1984:27－40.]

[6] Liu Chaohai,Xie Zichu,et al.Ice formation in Tianshan Glaciers.Beijing:Science Press,1996:96-115.[刘潮海,谢自楚,等.《天山冰川作用》.北京:科学出版社,1996,96-115.]

[7] Xie Zichu,Wang Zongtai.Ice formation process in northern Everest area.Investigation reports in Everest area[C].1975:8-13.[谢自楚,王宗太.珠穆朗玛峰地区北坡成冰作用.见:珠穆朗玛峰地区科学考察报告[C](1966-1968).1975:8-13.]

[8] Xie Zichu.Snow and ice formation process in northern xixiabangma peak.Investigtation reports in xixiabangma area. Beijing:science press[C],1982,45-59.[谢自楚.希夏邦马峰北坡的积雪和成冰作用.见: 希夏邦马峰地区科学考察报告[C].北京:科学出版社,1982:45-59.]

[9] Shi Yafeng,et al.An Introduction to the Glaciers in China Contents.Beijing:science press,1988,55—65.[施雅风,等.中国冰川概论.北京:科学出版社,1988,55—65.]

[10] Wang Xiaojun,Wang Zhongxiang,Xie Zichu.A Change trend of recent climatic on the Tianshan regions from the change of the past 28 years of the glacier No.1 at the Urumqi River headwater,Tianshan.Chinese[J] Science Bulletin,1988,9:693-696.[王晓军,王仲祥,谢自楚.从乌鲁木齐河源 1 号冰川二十八年来的变化看天山地区近期气候变化趋势.科学通报,1988,第 9 期,693－696.]

[11] Liu Chaohai,M.B.ÄÞ Ðæåðî Â.Study on processes of mass balance of Glacier No.1 at the headwaters of Urumqi River,Tianshan[J]. Annual Report on the Work At Tianshan Glaciological Station[M],1989(8):1—23.[刘潮海,久尔盖洛夫.乌鲁木齐河源 1 号冰川物质平衡过程研究[J].天山冰川站年报[M],1989(8):1—23.]

[12] Li Zhongqin,Han Tianding,Jing Zhefan,et al.A summary of 40-year observed variation facts of climate and Glacier No.1 at the headwaters of Urumqi River,Tianshan,China[J].Journal of Glaciology and Geocryology,2003,25(2):117-123.[李忠勤,韩添丁,井哲帆,等.乌鲁木齐河源区气候变化和 1 号冰川 40a 观测事实[J].冰川冻土,2003,25(2):117-123.]

[13] Wang Feiteng,Li Zhongqin,You Xiaoni,et al.Studying on ice formation process of surface snow layer in accumulation area of Glacier No.1 at the Ürümqi river head, Tianshan Mts[J].Journal of Glaciology and Geocryology,2005,27:In press.[王飞腾,李忠勤,尤晓妮,等.天山乌鲁木齐河源 1 号冰川积累区表面雪层演化成冰过程的观测研究[J].冰川冻土,2005,27:待刊.]

[14] Yang Daqing,Jiang Tong,Zhang Yinsheng,et al.Analysis and correction of errors in precipitation measurement at the heat of the Urumqi River,tianshan[J].Journal of Glaciology and Geocryology, 1988,10(4):384-399.[杨大庆,姜彤,张寅生,等.天山乌鲁木齐河源降水观测误差分析及其修正.冰川冻土,1988,10(4):384－399.]

[15] Li Zhongqin.A Glacier Melt Water Pool Was Discovered at Summit of East Branch of Glacier No.1 at Urumqi River Head,Tianshan Mts.,Xinjiang[J]. Journal of Glaciology and Geocryology,2005,27(1): 150-152.[李忠勤.天山乌鲁木齐河源 1 号冰川东支顶部出现冰面湖[J].冰川冻土,2005,27(1):150-152.]

[16] Yang Huian,Li Zhongqin,Jiao Keqin.Mass balance of Glacier No.1 at headwaters of Urumqi River in 1999-2002[J]. Annual Report on the Work At Tianshan Glaciological Station[M],1999-2002(16):9-103.[杨惠安,李忠勤,焦克勤.天山乌鲁木齐河源 1 号冰川 2000－2002 年物质平衡[J],天山冰川站年报,1999-2002,16:93-103.]

[17] Yang Huian,Li Zhongqiin,Ye Baisheng,et al.Study on Mass Balance and Process of Glacier No.1 at the Headwaters of the Urumqi River in the Past 44 years[J].Arid and Geography,2005,28(1):76-80.[杨惠安,李忠勤,

叶柏生,等.过去 44 年乌鲁木齐河源一号冰川物质平衡结果及其过程研究[J].干旱区地理,2005,28(1):76-80.]

[18] You Xiaoni,Li Zhongqin,Wang Feiteng,et al.Study on Time Scale of Snow – Ice transformation through Snow Layer tracing method—Take Glacier No.1 at the Headwaters of Ürümqi River as an Example[J]. Journal of Glaciology and Geocryology,2005,27:In press. [尤晓妮,李忠勤,王飞腾,等.利用雪层层位跟踪法研究暖型成冰作用的年限问题--以乌鲁木齐河源 1 号冰川为例[J].冰川冻土,2005,27:待刊.]

[19] Shi Yafeng,Shen Yongping, Hu Ruji.Preliminary study on signal,impact and foreground of climate shift from warm-dry to warm-humid in the Northwest China[J].Journal of Glaciology and Geocryology,2002. 24(3):220-226.[施雅风,沈永平,胡汝骥.西北气候由暖干向暖湿转型的信号、影响和前景初步探讨[J].冰川冻土,2002,24(3):220-226.]

[20] Li Chuanjin,Li Zhongqin,Wang Feiteng,et al. A Contrast of the Ice Forming Time, Zones and the Stratigraphic Profiles of Snow Pits in Different Time of Glacier No.1 at the Headwater of the Urumqi River ,Tianshan[J].Journal of Glaciology and Geocryology,2005,27:In press.[李传金,李忠勤,王飞腾,等.乌鲁木齐河源 1 号冰川不同时期雪层剖面及成冰带对比研究[J].冰川冻土,2005,27:待刊.]

Study on Ice Formation Zones and Stratigraphy Profiles of Snow-pits on Glacier No.1 at the Headwaters of Urumqi River

Li Xiangying, Li Zhongqin, You Xiaoyi, Wang Feiteng, Li Chuanjin, Zhu Yuman

(Tianshan Glaciological Station/Key Laboratory of Ice Core and Cold Regions Environment, CAREERI, CAS, Lanzhou Gansu 730000, China)

Abstract: Characteristics of ice formation zones on glacier and stratigraphy profiles of snow-pits that relected basic features of glaciers is one of the basic contents of glacier studies. The study of ice formation zones on Glacier No.1 at the headwaters of Urumqi River, Tianshan began first at the beginning of the 60s of the 20th century, Xie Zichu and Huang Maohuan,etc, divided Glacier No.1 into four ice formation zones. In 1988, Wang Xiaojun, etc, found that cold-percolation-recrystal zone on Glacier No.1 that disappeared has been replaced by percolation zone. Therefore, in1989, Liu Chaohai, etc, divided Glacier No.1 into three ice formation zones. Huge change happened on Glacier No.1 because of temperature increase since the 90s of the 20th century, which results in changes of ice formation zones and stratigraphy profiles of snow-pits on Glacier No.1 is a key question that people pay it more attention. This paper presents division of ice formation zones and physical characters of stratigraphy profiles by study of a series of snow-pits on Glacier No.1. It found that characters of stratigraphy profiles and ice formation zones on Glacier No.1 have a transformation trend from cold to warm. In addition, A strong ablation phenomenon has happened in the top of east branch, which has transformed into ablation area from percolation zone.

Key words: Glacier No.1, ice formation zones, strigraphy profiles, snow-pits

天山乌鲁木齐河源 1 号冰川雪坑中 pH 值和电导率的季节变化与淋溶过程

李向应[1]，李忠勤[1]，陈正华[2]，赵中平[1]，尤晓妮[1]，朱宇漫[1]

(1. 中国科学院寒区旱区环境与工程研究所冰芯与寒区环境重点实验室，
天山冰川观测试验站,甘肃 兰州 730000;
2. 兰州大学资源环境学院,甘肃 兰州 730000)

摘　要：自 2002 年 9 月 14 日至 2004 年 9 月 28 日，在天山乌鲁木齐河源 1 号冰川积累区雪坑中连续观测取样，频率为 1 次/周。对表层雪样品和粒雪坑样品的 pH 值和电导率进行了分析。结果表明，表层雪的 pH 值和电导率具有明显的季节变化趋势，与本区域的主导山谷风风向 NE 和 ENE 密切相关。在春季，由于尘暴发生频率的增加，表层雪的 pH 值呈现较强碱性，电导率达到最大值；在冬季，由于原生气溶胶向次生气溶胶的转化，pH 值呈现较弱碱性，电导率达到最小值。在后沉积过程中（2003 年 10 月 4 日－2004 年 9 月 8 日），雪坑中不同时期的 pH 值和电导率呈现不同的季节变化特征和淋溶过程。电导率的峰值 P1 进入粒雪冰的时间比与它相对应的大粒径（直径>10μm）微粒浓度的峰值提前 40 天左右；在有的雪坑中，pH 值和电导率的峰值出现在污化层附近，与污化层的位置有较好的一致性，说明污化层对可溶性离子的淋溶作用可能有一定的影响。相关分析表明，Ca^{2+}是影响表层雪中 pH 值和电导率变化的最主要离子。

关键词：1 号冰川；雪坑；pH 值；电导率；季节变化；淋溶过程

0　引言

冰川内部包含有丰富的古大气化学信息，在恢复其记录的过程中，冰芯记录以其分辨率高、保真度强、气候环境信息丰富、时间序列长等独特优点占据了非常重要的地位[1-3]。格陵兰和南极冰盖钻取的冰芯包含有成百上千年以前的大气化学信息，这为重建和恢复古大气化学记录提供了手段[4-7]。极地冰芯 pH 值和电导率的研究满足了重建古大气化学纪录的要求[8-10]。Wolff 等[9] 和效存德等[11]对南、北极和青藏高原雪冰内的电导以及大气化学载荷的相关关系做了比较细致的工作。研究指出，格陵兰冰芯中的电导记录是大气酸度背景值的反映，由暖期（冰呈酸性）向冷期（冰呈碱性）有着明显的变化；冰芯中的酸度主要受有中和能力的碱性粉尘数量的控制。然而，青藏高原雪冰电导率主要依赖于地壳来源的碱性矿物盐类杂质（如 Ca^{2+}、Mg^{2+}、SO_4^{2-}等），与雪冰酸度（即 H^+）呈反相关；极地冰盖雪冰电导率依赖于海洋性来源的酸根离子（如 Cl^-、SO_4^{2-}等），与雪冰酸度成正相关。但在北极地区，雪冰电导率与各离子的关系存在着复杂的地域分异。姚檀栋等[12]和盛文坤等[13-14]对青藏高原雪冰内的 pH 值和电导率也开展了诸多研究工作。指出，青藏高原冰雪化学性质多呈碱性，冰雪的比电导与 pH 值呈正相关关系，与 H^+浓度呈负相关关系，使比电导增大的因素是碱性尘埃中的可溶盐。古里雅冰芯 pH 值呈碱性的变化主要受 CO_2 气体及尘埃中可溶性碳酸盐的控制。若冰芯中电导率与 pH 值呈平行变化趋势，说明相应时期的

气候环境相对较稳定、风暴较小；若电导率和 pH 值呈相反变化趋势，说明气候环境不稳定、风暴强烈。此外，降水多、气候环境相对较湿润，冰芯中的 pH 值较低，电导率也较低；降水少、气候环境相对较干旱，冰芯中的 pH 值较高，电导率也较高。候书贵等[15]和李心清等[16]对天山乌鲁木齐河源 1 号冰川雪冰中的 pH 值和电导率也进行了研究。认为在消融率较大和融水渗浸作用较强的内陆地区，pH 值和电导率记录仍可合理的反演沉积时的大气环境状况；并且指出 1 号冰川冰芯的 pH 值较自然降水的要高，且较世界其它偏远地区的也高是由于矿物性粉尘的强力输入，尤其是碳酸盐。然而，在山地冰川中依据 pH 值和电导率进行雪－冰现代过程的研究还很少，这主要是由于长期观测和连续取样条件的限制。鉴于此，本文依托中国科学院天山冰川观测试验站和乌鲁木齐市大西沟气象站对天山乌鲁木齐河源 1 号冰川雪坑中 pH 值和电导率在后沉积过程中的季节变化和淋溶过程进行了详细研究，并结合大西沟气象站的气象资料（气温、降水、风速风向、相对湿度、大气压等）对影响 pH 值和电导率的因素进行了具体分析。

1 取样点位置

天山乌鲁木齐河源 1 号冰川（43°06′ N, 86°49′ E）位于中亚的东天山，即天山东部。东天山位于欧洲大陆中部，四周被沙漠和戈壁包围：东面有蒙古的沙漠和戈壁，南面有位于塔里木盆地的塔克拉玛干沙漠，西面有萨雷－伊施科特劳等中亚地区的沙漠，北面有位于准格尔盆地的古尔班通古特沙漠[16]（图 1）。东天山地处荒漠环境、植被覆盖面积极小；但在天山某一海拔高度带上仍具有不同程度的植被覆盖，在山谷底部海拔 1500m－2900m 的山地环境中存在自然林带，在海拔 2900m 以上是高山草垫、贫瘠的岩石和冰川沉积物，海拔 3000m 以上是永久冻结带[17]。在典型大陆性气候条件下，西风带在天山上空起着主导作用，地形的影响使西风带在海拔 4000m 以上处于气旋与反气旋的循环之中，近地表局地的山谷风在每年的 3-9 月盛行[18-19]。天山乌鲁木齐河源 1 号冰川是一条山谷冰川，由东（1.12 km^2）、西（0.61 km^2）两支组成，总面积 1.73 km^2，平均海拔 4330m[20]。1 号冰川东、西支及整个冰川多年平均零平衡线高度分别为：4016m、4095m 和 4056m；西支零平衡线高度平均高于东支，但相对变幅比东支小[21]。自 1993 年 1 号冰川完全分为两支，特别是 1996 年以后，气温持续升高（冬季升温更加明显），零平衡线呈现显著的升高趋势[22]；冰川冰舌部分，东支年退缩量、变幅均较小，西支退缩量明显大于东支[23]。除了气温升高在冰川退缩中的支配作用外[24]，冰川分离后冰舌末端更加陡峭和冰面、冰下河发育等因素也是造成冰川退缩速度显著增大的原因。年平均气温为-9.1 ℃，降水为 700mm a^{-1}，降水主要发生在 5－9 月，冰川消融在这段时期也达到最大。野外观测表明，采样点所在的渗浸带雪坑的深度在 1.5m（夏末）－3m（春末）内波动变化。冬季由于雪的密实化、风吹雪和升华作用的影响，雪坑的深度较为稳定、变化不大。夏初随着气温上升到 0℃，雪坑上部的雪层开始融化，雪坑深度迅速减小。在夏末至秋初这段时期，由于消融加剧，融水下渗，对下部雪层、甚至上一年的积累产生影响[25]。

2 样品采集和分析

样品采集于天山乌鲁木齐河源 1 号冰川东支渗浸带积累区海拔 4130m 处的雪坑中，大约 100 个表层雪样品（2002 年 9 月 14 日-2004 年 9 月 28 日）和 1018 个粒雪坑样品（2003

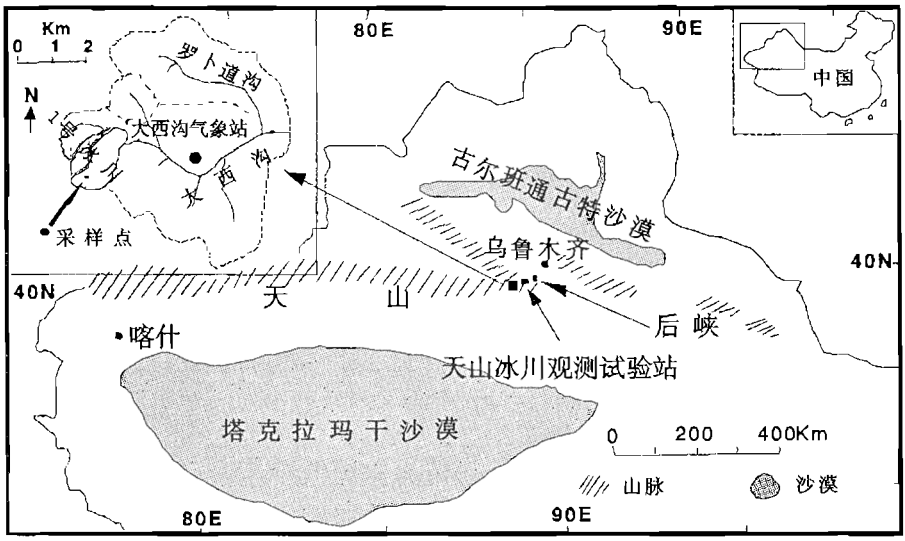

图 1　研究区域的地理位置

Figure 1.　Maps showing the study area.

年 10 月 4 日-2004 年 9 月 8 日）在本项研究中得以分析和应用，取样频率为 1 次/周。表层雪样品取自雪坑顶部表层 5cm 处，粒雪坑样品在取完表层雪样品后，沿雪坑剖面继续向下以每 10cm 间距连续取样直至粒雪冰面。样品在采集和运输的过程中均采取严格的操作规范，包括使用聚乙烯手套和面具等以避免污染。采样后雪坑被重新填埋、直至下次采样时在上次采样位置重新挖开并向前挖进 0.5m 左右，在与上次相同的层位上取样。雪冰样品在冷冻状态下装入聚乙烯塑料瓶中，装完样品后立即封闭以避免蒸发和扩散。样品保持在冷冻状态下置于绝缘的铁箱中被运输到中国科学院寒区旱区环境与工程研究所天山冰川观测试验站实验室进行 pH 值、电导率和化学离子等的分析。空白实验表明，不同季节相邻雪坑间的离子浓度具有较高的相关性，说明在样品的采集、运输和测量过程中样品没有受到污染。pH 值和电导率使用 PHJS-4A(0.001)和 DDSJ-308A (0.001)测量；在仪器使用前，均应用 pH 值为 6.86 和 9.18 的标准缓冲溶液对仪器的电极进行校正；在样品测量前，首先用部分样品对电极进行清洗，每个样品测量完后再用去离子水清洗，后浸入新鲜和静止的样品中，5 分钟后得到经温度补偿后的 pH 值。应用光学粒径监测仪(AccuSizer 780A)对微粒的大小和浓度进行分析，使用离子色谱仪（DX-320）对雪－粒雪样品中主要化学离子（Cl^-、NO_3^-、SO_4^{2-}、Na^+、NH_4^+、K^+、Mg^{2+}和 Ca^{2+}等）的浓度进行测量。本文着重对分析测定结果中的 pH 值和电导率进行专项研究。

3　结果与讨论

3.1　季节变化

图 2 表示表层雪中 pH 值和电导率随时间的变化规律。如图 2 所示，表层雪的 pH 值在春、夏、秋、冬季的变化范围分别为：6.14-8.05、5.79-7.61、6.08-7.02、5.91-6.88；电导率的变化范围分别为：4.43-63.1 μs/cm(春季)、2.14-95.5 μs/cm(夏季)、2.94-17.77 μs/cm (秋季)、2.85-20.3 μs/cm(冬季)。表层雪的 pH 值在春、夏、秋、冬季的平均值分别为：6.99、

6.62、6.56、6.45；电导率的平均值分别为：22.73 μ s/cm(春季)、13.93 μ s/cm(夏季)、7.41 μ s/cm(秋季)、6.87 μ s/cm(冬季)。此外，表层雪中 pH 值和电导率的年平均值分别为 5.66 和 12.74 μ s/cm。

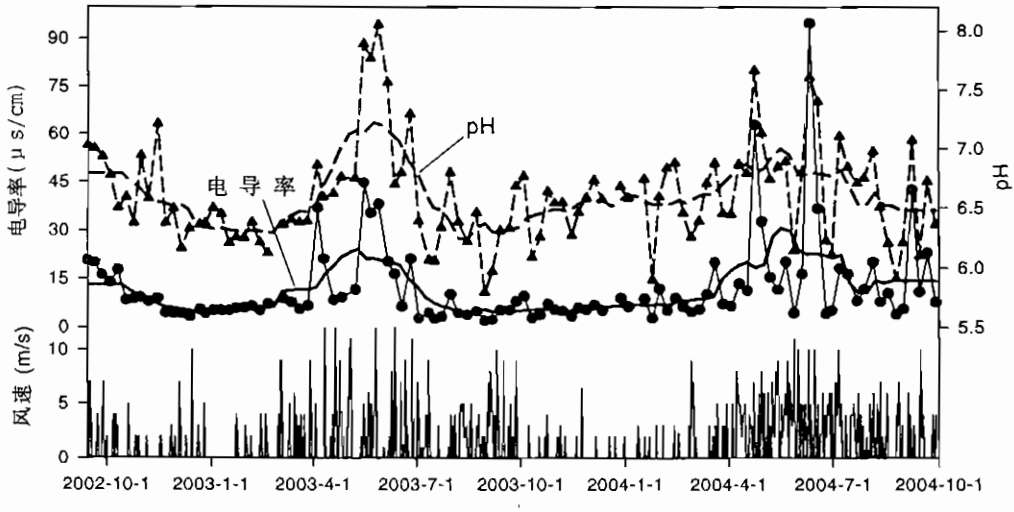

图 2 表层雪中的 pH 值和电导率随时间的变化以及与风速风向 (NE 和 ENE) 的关系

Figure 2. Variations of pH and electrical conductivity in surface snow in relation to valley wind (in NE and ENE direction).

由上述可知，表层雪 pH 值和电导率在不同季节的平均值自春季至冬季逐渐减小，进入冬季达到最小；pH 值在春季和冬季分别呈现出较强和较弱的碱性，电导率在春季和冬季分别达到最大值和最小值。具体来说，pH 值在春季（2003 年 5 月 29 日和 2004 年 4 月 24 日）达到一年中的最大值；电导率在春季（2003 年 5 月 16 日）和夏季（2004 年 6 月 11 日）达到一年中的最大值，分别为 44.9 μ s/cm 和 95.5 μ s/cm。一般来说，表层雪的 pH 值和电导率在春季（4 月和 5 月）和夏初（6 月）较高，在夏末（8 月和 9 月）较低。表层雪的 pH 值和电导率从 2003 年夏末到 2004 年夏初逐渐升高、达到一年中的最大，然后在 2004 年夏末迅速减小，随后又逐渐升高。这是由于：在春季和夏初，乌鲁木齐河源区尘暴发生的频率增加，大气中的粉尘载量增大，可溶性化学离子的沉降作用增强；在夏末，由于温度升高并达到一年中的最大，淋溶作用增强，大量融水产生，这时表层雪中大部分可溶性离子随融水径流而流失。在秋季和冬季，尘暴发生的频率较小，大气中的粉尘载量较为稳定，且气溶胶由原生向次生转化，可溶性离子沉降作用减弱，所以表层雪的 pH 值和电导率相对于春季和夏末较小，但比夏末较大[26]。

表层雪的 pH 值和电导率主要受冰川所在区域大气中的可溶性离子控制。可溶性离子通常在粉尘的吸附作用下，由于尘扬作用，被大气气流携带、输送至冰川上空的大气中，后通过干、湿沉降方式降落至冰川表面。因此，表层雪中的可溶性离子在一定程度上与大气气流的季节性特征密切相关，对表层雪中 pH 值和电导率的大小起着重要作用。乌鲁木齐河源 1 号冰川所在的东天山地区主要受西风带控制，由于地形的影响，西风带在海拔 4000m 以上处于气旋与反气旋的循环之中，西风带对远距离及较远距离的大气粉尘输送起

着重要作用。但是，由于 1 号冰川区近地表局地的山谷风在每年的 3-9 月盛行[18-19]，远距离及较远距离的大气粉尘在西风带的作用下到达冰川上方，在山谷风盛行季节，沉降过程必然受到山谷风季节性特征的影响。先前的研究[17,19,25]表明，1 号冰川上方大气粉尘中总的离子载量主要受局地和局域性来源的粉尘影响，而且局地裸露的岩石和冰川沉积物是这些粉尘的主要源地。这些局地来源的粉尘在向大气输送的过程中，局地山谷风起着至关重要的作用。因此，局地山谷风的季节特征必然与 1 号冰川区大气中可溶性离子载量有着密切联系。基于大西沟气象站山谷风的风速风向资料（图 1）可知，SSE、SSW、WSW、ENE 和 NE 是 1 号冰川所在区域的主要风向。通过对表层雪 pH 值、电导率与大西沟气象站主要风向的季节性特征变化进行对比分析，发现风向 NE 和 ENE 的季节变化特征与表层雪中 pH 值和电导率的季节变化特点具有很好的季节一致性。山谷风 NE 和 ENE 在春季（4 月和 5 月）和夏初（6 月）的高峰值与表层雪的 pH 值和电导率在同时期的峰值有较好的对应关系，与秋、冬季节较低的值也保持较好的一致性（图 2）。这说明，山谷风风向 NE 和 ENE 与表层雪的 pH 值和电导率的确有着密切的联系，关于其内部联系的机制将在以后的研究中予以讨论。同时从另一方面也说明，表层雪中的 pH 值和电导率主要受局地和局域源的粉尘控制。

3.2　淋溶过程

图 3 为 pH 值和电导率（2003 年 10 月 4 日－2004 年 9 月 8 日）在雪坑中的淋溶过程。据李忠勤等[25]和王飞腾等[27]的研究，雪坑中化学离子的淋溶序列为：$SO_4^{2-} > Ca^{2+} > Na^+ > NO_3^- > Cl^- > K^+ > Mg^{2+} > NH_4^+$；$Mg^{2+}$ 相对于其它化学离子淋溶速度较慢，Mg^{2+}浓度峰值的变化与大粒径（直径>10μm）微粒浓度峰值的变化具有较好的一致性，而且它们的浓度峰值与雪坑中的污化层也有着较好的对应。因此，在本研究中用 Mg^{2+} 浓度的峰值变化和大粒经微粒浓度的峰值变化作为参考来研究pH值和电导率在雪坑中的淋溶过程和淋溶规律。

如图 3 所示，pH 值和电导率的峰值通常出现在雪坑的顶部；在消融季节，pH 值和电导率的峰值向雪坑底部移动的速度较快，在其它季节移动的速度较慢，直至最后进入粒雪冰内。本研究中，我们通过跟踪电导率峰值在雪坑中的变化来研究 pH 值和电导率在雪坑中的淋溶过程和淋溶规律。图 3 中的三条实线是我们跟踪的电导率的三个较为明显的峰值，分别为 P1，P2 和 P3，它们分别位于雪坑 T1（2003 年 10 月 4 日）的上部、中部和下部。起初，三个峰值 P1，P2 和 P3 距雪坑 T1 底部粒雪冰面的距离分别为 170cm、100cm 和 50cm。在秋初至夏初这段时期（2003 年 10 月 4 日－2004 年 5 月 28 日），即雪坑 T1-T9，峰值 P1，P2 和 P3 在雪坑中较为明显，呈现稳定的波动趋势。其中，在 W1 时期（2003 年 10 月 4 日－2004 年 1 月 25 日），除峰值 P1、P2 和 P3 大于 10μs/cm 外，雪坑中电导率的其它值均小于 10μs/cm。这是由于，此段时期的气温完全保持在 0℃以下（平均气温为-11.9℃），几乎没有降水产生（图 4）。这说明，W1 时期内雪坑中几乎没有融水产生，雪坑中的 pH 值和电导率在一定程度上可以反映它们在大气中的初始水平。在 W2 时期（2004 年 3 月 20 日－2004 年 5 月 28 日），位于峰值 P1、P2 和 P3 之上、电导率其它较高的峰值突然出现在雪坑 T5－T8 的顶部，而且这些峰值均大于 20μs/cm（图 3，粗箭头所示）。这是由于，W2 时期的温度升高（平均温度为-4.1℃），个别天数的温度达 0℃以上（图 4）。也就是说，随着温度在 W2 时期的升高，尽管降水也有所增加，但雪坑中仍有少量的融水产生、并引起了部分可溶性离子的迁移。

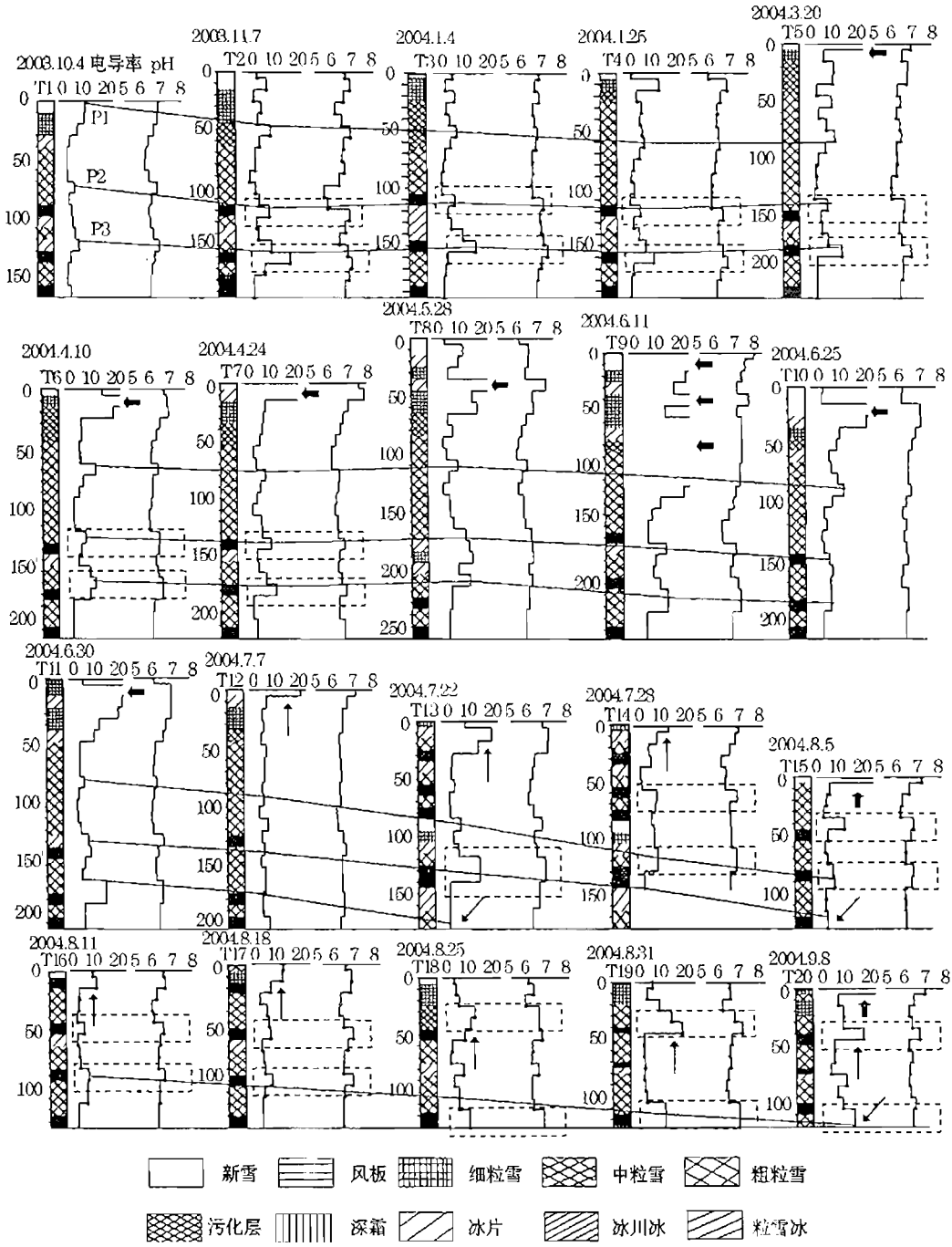

图 3 雪坑中 pH 值和电导率的层位剖面

Figure 3. The successive profiles of pH and electrical conductivity in snow-pits.

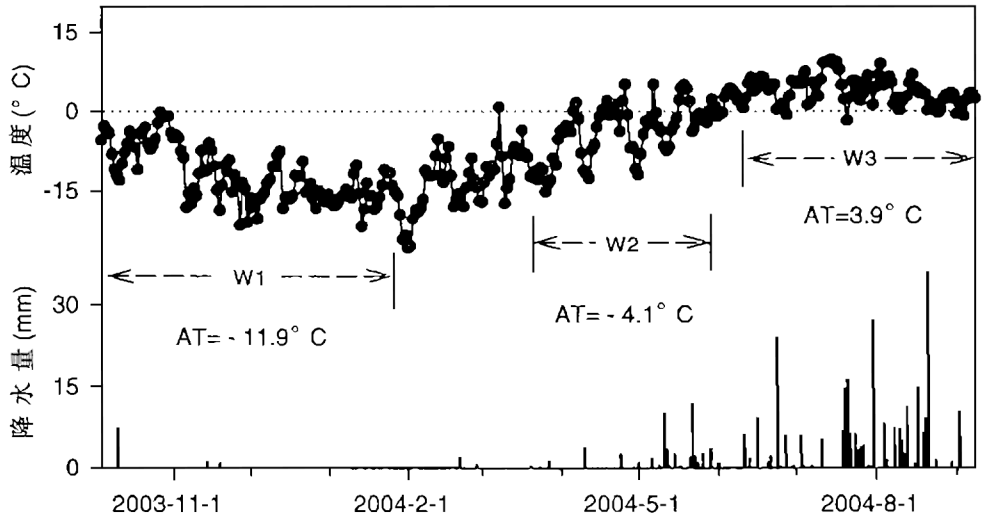

图4 气温和降水随时间的变化.AT分别表示W1、W2、W3时期内的平均气温.

Figure 4. Variations of temperature and precipitation. AT show the average temperature in the corresponding periods W1、W2 and W3 respectively, the dashed line indicates the 0℃ level.

在W3时期(2004年6月11日－2004年9月8日),气温几乎全部上升到0℃以上(平均温度为3.9℃)(图4)。其中，在6月11日至6月30日这段时期，较多的融水产生，融水对可溶性离子的影响加强。在融水的作用下，可溶性离子向雪坑下部移动、聚集，相应的电导率峰值（P1、P2和P3除外）不断增加，大多数峰值出现在雪坑的上部和中部，尤其在雪坑T9中表现的最为显著。此时，峰值P1、P2和P3在雪坑中仍较为明显，它们距雪坑T11底部粒雪冰面的距离分别为125cm、75cm和40cm。在7月7日至9月8日这段时期，峰值P1、P2和P3在雪坑中不易辨别，它们距雪坑T12底部粒雪冰面的距离明显减小，分别为111cm、71cm和35cm。此外，尽管有两个大于20μs/cm的峰值出现在雪坑T15（8月5日）和T20（9月8日）中（图3，粗箭头所示），电导率的其它峰值总体上仍呈现出稳定的波动趋势，此时峰值P1、P2和P3在雪坑中不显著，其它峰值在10-20μs/cm范围内变动（图3，细箭头所示）。这说明，此时融水对可溶性离子的影响较小，因为这段时期的气温完全达到0℃以上、且达到了一年中的最大值，大多数可溶性离子已随着融水的径流而流失，尽管此段时期内的降水也达到了一年中的最大值（图4）。很明显，在气温与降水的共同作用下，降水相对于气温对可溶性离子的影响较弱。

另外，峰值P1、P2和P3分别在2004年7月末（T13）、8月初（T15）和9月初（T20）进入粒雪冰中（图3，斜箭头所示）。峰值P1进入粒雪冰的时间比与它相对应的、距粒雪冰面最近的大粒径微粒浓度的峰值进入粒雪冰的时间提前约 40 天。这是由于大粒径微粒浓度的峰值与污化层有较好的一致性，在一定程度上反映了不溶性离子的淋溶作用；而电导率峰值的变化反映了总的可溶性离子的淋溶作用，同时可溶性离子的淋溶速度大于不溶性离子。此外发现，大多数雪坑中的pH值和电导率峰值通常出现在污化层附近，并且在某些雪坑中与污化层的位置具有较好的一致性（图 3，矩形方框所示）。这意味着污化层

对可溶性离子的淋溶过程可能有一定的影响。pH 值的淋溶过程与电导率的淋溶过程非常相似（图 3），它们在表层雪中的相关系数(r=0.752)可以说明这一点，所以关于 pH 值的淋溶过程不再作详细的论述。

3.3 影响因素

冰川融水的电导率为估算总的可溶性离子浓度和它们在雪坑中的深度分布提供了一个简单、方便、有效的方法，尤其是在以碳酸盐为主的地区[28]。pH 是水溶液酸、碱度的一个指标，可表示为：$pH = -\log a$（a - 活度）。表层雪中的化学成分来源于干、湿沉降，它们与气溶胶中的化学成分密切相关[14]。

表 1 表层雪中各种化学成分之间的相关系数

Table 1 Correlation coefficients of pH and electrical conductivity between different chemical species in surface snow.

	NH_4^+	NO_3^-	Cl^-	SO_4^{2-}	Mg^{2+}	Ca^{2+}	Na^+	k^+	pH
电导率	0.446	0.313	0.885	0.727	0.660	0.960	0.879	0.716	0.752
NH_4^+		0.490	0.464	0.610	0.161	0.322	0.413	0.483	0.338
NO_3^-			0.380	0.674	0.191	0.215	0.242	0.323	0.241
Cl^-				0.720	0.559	0.792	0.956	0.729	0.520
SO_4^{2-}					0.390	0.623	0.662	0.551	0.531
Mg^{2+}						0.631	0.575	0.511	0.624
Ca^{2+}							0.820	0.638	0.779
Na^+								0.734	0.524
K^+									0.532

在 0.01 置信度下显著相关(n=107)

表 1 给出表层雪的 pH 值和电导率与化学离子之间的相关系数。与 pH 值的相关系数大于 0.600 的离子有 Mg^{2+} (r=0.624) 和 Ca^{2+} (r=0.779)；与电导率的相关系数大于 0.700 的离子有 Cl^- (r=0.885)、SO_4^{2-} (r=0.727)、Ca^{2+} (r=0.960)、Na^+ (r=0.879) 和 K^+ (r=0.716)；这说明 Mg^{2+}、Ca^{2+} 和 Cl^-、SO_4^{2-}、Ca^{2+}、Na^+、K^+分别是控制表层雪中 pH 值和电导率的主要离子，而 Ca^{2+}是最主要的离子。Ca^{2+}是大气粉尘一个很好的替代指标，也是表层雪中最主要的离子，占离子总载量的 56%；其它离子为：SO_4^{2-} (10%)、NH_4^+ (9%)、Mg^{2+} (8%)、Cl^- (6%)、Na^+ (5%) 和 NO_3^- (5%)。在尘暴、山谷风、原生气溶胶和次生气溶胶的共同作用下，表层雪中总的离子载量在春季达到最大，是冬季的三倍，同时所有离子在冬季达到它们的背景值。因此，Ca^{2+}的浓度在春季达到最大值，约是在秋季或冬季的 3 倍，随后迅速减小并在秋季和冬季达到背景值。表层雪中高浓度的 Ca^{2+}主要与来源于周围山体的风蚀粉尘有关，由于石灰化过程是干旱半干旱地区土壤形成的主要过程，并且产生大量的 $CaCO_3$ [29]。另外，

1 号冰川早期的气溶胶研究表明，由于局地亚洲粉尘的影响，化学成分在春末和夏初呈现出较高的浓度，而且指出 Ca^{2+}、Mg^{2+}、Na^{+}、Cl^{-} 和 SO_4^{2-}主要来源于中亚的沙漠和干涸的湖泊，而 K^{+}来自于人为源[26]。

4 结论

研究表明，表层雪中的 pH 值和电导率有着明显的季节变化特征。在春季和夏初由于尘暴频率增加，大气粉尘载量增大，可溶性离子的沉降作用增强，表层雪的 pH 值和电导率值较大；在夏末由于温度上升至最高，融水达到最大，可溶性离子随融水的径流而流失，表层雪的 pH 值和电导率较小。表层雪的 pH 值在春季呈现出较强的碱性，在冬季由于原生气溶胶向次生气溶胶的转化，大气中可溶性离子沉降作用的减弱呈现较弱的碱性。此外发现，NE 和 ENE 是控制表层雪中 pH 值和电导率的主导山谷风风向；Mg^{2+}、Ca^{2+} 和 Cl^{-}、SO_4^{2-}、Ca^{2+}、Na^{+}、K^{+} 分别是控制表层雪中 pH 值和电导率的主要离子，Ca^{2+}是最主要的离子。

在后沉积过程中，雪坑中的 pH 值和电导率在不同时期表现出不同的季节变化特征和淋溶过程。在 2003 年 10 月 4 日－2004 年 1 月 25 日，电导率具有稳定的波动趋势，值均小于 10 μs/cm（除 P1、P2 和 P3 外）；pH 值和电导率在一定程度上可以代表它们在大气中的初始水平。在 2004 年 3 月 20 日－2004 年 5 月 28 日，少量融水产生，部分可溶性离子发生迁移，在某些雪坑顶部出现大于 20 μs/cm 的电导率峰值（除 P1、P2 和 P3 外），融水对可溶性离子的作用较强。在 2004 年 6 月 11 日－2004 年 6 月 30 日，较多的融水产生，在雪坑上部和中部出现较多较大的峰值；在 2004 年 7 月 7 日－2004 年 9 月 8 日，大量融水产生，可溶性离子随融水径流而流失，融水对可溶性离子的作用较弱，电导率的峰值（除 P1, P2 和 P3 外）呈现稳定的波动趋势，在 10-20 μs/cm 范围内变动。此外，电导率峰值 P1 进入粒雪冰的时间比与它相对应的大粒经微粒浓度的峰值提前约 40 天。大多数雪坑中 pH 值和电导率的峰值一般出现在污化层附近，而且在有的雪坑中与污化层的位置有较好的一致性，这意为着污化层对可溶性离子的淋溶过程可能有一定的影响。另外，pH 值和电导率在雪坑中的淋溶过程受温度的影响较大，受降水的影响较小。

致谢：本项研究是天山冰川观测试验站开展的雪冰现代过程研究项目的一部分，是在全体观测和研究人员集体努力下完成的。在此对参加本项研究的每一个观测人员以及项目组人员焦克勤，韩添丁，杨惠安，王飞腾，李传金，张坤，李慧林，钱军，张明军等表示衷心感谢。

参考文献（References）：

[1] Wolff E. W., Peel D. A. The record of global pollution in polar snow and ice. *Nature*, 1985,313: 535-540.

[2] Barnola J M, Raynaud D, Korotkevich Y S, et al. Vostok ice core provides 160000 year record of atmospheric CO_2 [J]. *Nature*,1987,329:408-414.

[3] Gu Juan, HeYuanqing, Zhang Zhonglin, et al. The response of pH Value in Ice Core to Precipitation in the Mt. Yulong [J]. *Journal of Glaciology and Geocryology*, 2005, 4 (27): 509-514. [顾娟,何元庆,张忠林,等. 玉龙雪山浅冰芯 pH 值对冰川作用区降水量变化的响应. 冰川冻土,2005,4(27):509－514.]

[4] De Angelis, M., Barkov, N.I., Petrov, V. N. Aerosol concentrations over the last Climate Cycle (160kyr)

from an Antarctic Ice Core. *Nature*,1987,325:318-321.

5] Jouzel, J., Petit, J. R., Raynaud, D. Palaeoclimatic Information from Ice Cores: The Vostok Records.*Earth Sciences*,1990,81:349-355.

6] Mayewski, P. A., Meeker, L.D., Morrison, M. C., et al. Greenland Ice Core "Signal" aracteristics: An Expand View of Climate Change. *Journal of Geophysical Research*,1993, 98:12839-12847.

[7] Mayewski, P. A., Twiker, M. S., Whitlow, S. L., et al. Climate Change during the Last Deglaciation in Antarctica.*Science*,1996,272:1636-1638.

[8] Taylor K C, Hammer C U, Alley R B, et al. Electrical conductivity measurements from the ISP2 and GRIP Greenland ice cores[J].*Nature*,1993,366:549-552.

[9] Wolff E W, Moore J C, Clausen H B, et al. Long-term changes in the acid and salt concentrations of the GRIP Greenland ice core from electrical stratigraphy [J].*Journal of Geophysical Research*,1995,100:16249-16264.

[10] Hammer, C. U,. Acidity of polar ice cores in relation to absolute dating, past volcanism, and radio-echoes.*Journal of Glaciology*,1980,25(93):359-372.

[11] Xiao Cunde, Qin Dahe, Ren Jiawen, et al. The difference of atmospheric chemical loadings shown by conductivity of and ice between Antarctic, Arctic and Qinghai-Tibetan Plateau [J]. *Chinese Journal of Polar Science*,1999,10(1):45-50.[效存德,秦大河,任贾文,等.雪冰电导率反映的南、北极和青藏高原大气环境差异.极地研究,1999,(1):45-50.]

[12] Yao Tandong, Sheng Wenkun, Yang Zhihong. A study on ice and snow chemistry in Qing-Zang (Tibet) Plateau [A]. Yao Tandong, Agrta Y et al. Glaciological climate and environment on Qing-Zang Plateau [C]. Beijing:Science Press,1993,8-15.[姚檀栋,盛文坤,杨志红.青藏高原的冰雪化学研究[A].青藏高原冰川气候与环境[C].北京:科学出版社,1993,8-15.]

[13] Sheng Wenkun, Yao Tandong, Xie Chao, et al. Analysis of pH and electrical conductivity in Guliya ice cores since Little Ice Age [J]. *Journal of Glaciology and Geocryology*,1995,17 (4):360-365.[盛文坤,姚檀栋,谢超,等.古里雅冰芯小冰期以来的 pH 值和电导率分析.冰川冻土 [J],1995,17(4):360－365.]

[14] Sheng Wenkun, Yao Tandong. Acidity variation in the Guliya Ice Cap region approached by pH and electrical conductivity in ice core[A]. Proceedings of the Fifth Chinese Conference on Glaciology and Geocryology (Vol. 1)[C]. Lanzhou:Gansu Culture Press,1996,219-226.[盛文坤,姚檀栋.用冰芯的 pH 值及电导率探讨古里雅冰川作用区的干湿变化[A].第五界全国冰川冻土学大会论文集（上）[C].兰州:甘肃文化出版社,1996,219－226.]

[15] Hou Shugui, Qin Dahe, Ren Jiawen, et al. The present environmental processes of Ice Core pH and conductivity records: a case study at the Headwaters of the of the Urumqi River [J]. *Journal of Glaciology and Geocryology*, 1999, 21(3):225-232.[侯书贵,秦大河,任贾文,等. 天山乌鲁木齐河源 1 号冰川 pH 和电导率记录的现代环境过程. 冰川冻土,1999,21(3):225-232.]

[16] Li Xinqing, Qin Dahe, Jiang Guibin, et al. Atmospheric pollution of a remote area of Tianshan Mountain: Ice core record.*Journal of Geophysical Research*,2003, 108(D14):4,1-4,10.

[17] Luo Hongzhen. Hydrochemical features of the Glacier No.1 in the source region of Urumqi River, Tianshan. *Journal of Glaciology and Geocryology*,1983,5(2):55-64.[骆鸿珍. 天山乌鲁木齐河源 1 号冰川的水化学特征.冰川冻土,1983,5(2):55－64.]

[18] Zhang Yinsheng, Kang Ersi, Liu Chaohai. Mountain climate analysis in Urumqi River valley,

Tianshan.*Journal of Glaciology and Geocryology*,1994,16(4):333-341.[张寅生, 康尔泗, 刘潮海. 天山乌鲁木齐河流域山区气候特征分析.冰川冻土,1994,16(4):333-341.]

[19] Williams, M. W., Tonnessen K. A., Melack J. M., et al. Sources and spatial variation of the chemical composition of snow in the Tien Shan, China.*Annals of Glaciology*,1992,16:25-32.

[20] Li Zhongqin, Han Tianding, Jing Zhefan, et al. A summary of 40-year observed variation cts of climate and Glacier No.1 at the headwaters of Urumqi River, Tianshan, China [J]. *Journal of Glaciology and Geocryology*,2003,25(2):117-123.[李忠勤,韩添丁,井哲帆,等.乌鲁木齐河源区气候变化和 1 号冰川 40a 观测事实[J].冰川冻土,2003,25(2):117-123.]

[21] Han Tianding, Liu Shiyin, Ding Yongjian, et al. A characteristics mass balance of Glacier No.1 at the headwaters of the Urumqui river,Tianshan mountains. *Advances of Earth Science*, 2005, 20(3): 298-303.[韩添丁,刘时银,丁永建,等. 天山乌鲁木齐河源 1 号冰川物质平衡特征研究.地球科学进展,2005,20(3):298-303.]

[22] Liu Shiyin,Wang Ninglian,Ding Yongjian,et al. On the characteristics of glacier fluctuations during the last 30 years in Urumqi river basin and the estimation of temperature rise in the high mountain area[J]. *Advances in Earth Science*,1999,14(3):279-285.[刘时银,王宁练,丁永建,等.近 30 年来乌鲁木齐河流域冰川波动特征与流域高山带升温幅度地估算[J].地球科学进展,1999,14(3):279-285.]

[23] Li Xiangying, Li Zhongqin, You Xiaoni,et al. Study of the ice formation zones and stratigraphy profiles of snow pits on the Glacier No.1 at the headwaters of Urumqi river. *Journal of Glaciology and Geocryology*, 2006,28(1),37-44.[李向应,李忠勤,尤晓妮,等.天山乌鲁木齐河源 1 号冰川成冰带及雪层剖面特征研究.冰川冻土,2006,28(1),37-44.]

[24] Su Zhen,Liu Zongxiang,Wang Wenti,et al.Glacier fluctuations responding to climate change and forecast of its tendency over the Qinghai-Tibet Plateau[J].*Advances in Earth Science*,1999,14(6):607-612.[苏珍,刘宗香,王文悌,等.青藏高原冰川对气候变化地响应及趋势预测[J].地球科学进展,1999,14(6):607-612.]

[25] Li Zhongqin, Ross Edwards, E. Mosley-Thompson, et al. Seasonal Variabilities of Ionic Concentration in Surface Snow and Elution Process in Snow-firn Packs at PGPI Site on Glacier No.1 in Eastern Tianshan, China.*Annals of Glaciology*,2006.[In press]

[26] Sun Junying, Qin Dahe, Paul A. Mayewski, et al. Soluble species in aerosol and snow and their relationship at Glacier 1, Tien Shan, China.*Journal of Geophysical Research*,1998, 103(D21):28022-28027.

[27] Wang Feiteng, Li Zhongqin, You Xiaoni,et al. Seasonal evolution of aerosol stratigraphy in Glacier No. 1 percolation zone, eastern Tianshan, China.*Annals of Glaciology*,2006.[In press].

[28] Smart, C. C,. Temperature compensation of electrical conductivity in glacial meltwaters. *Journal of Glaciology*,1992,128(38):9-12.

[29] He Dixin. Forming and improving of pickled soil. Lanzhou: Gansu people press, 1980.[贺涤新.盐碱土的形成和改良.兰州:甘肃人民出版社,1980.]

SEASONAL VARIATIONS AND ELUTION PROCESSES OF PH AND ELECTRICAL CONDUCTIVITY IN SNOWPITS ON GLACIER NO.1 AT THE URUMQI RIVER HEAD, TIANSHAN MOUNTAINS

LI Xiang-ying[1], LI Zhong-qin[1], CHEN Zheng-hua[2], ZHAO Zhong-ping[1], YOU Xiao-ni[1], ZHU Yu-man[1]

(1. Tianshan Glaciological Station/Key Laboratory of Ice Core and Cold Regions Environment, Cold and Arid Regions Environmental and Engineering Research Institute, CAS, Lanzhou 730000, China; 2. College of Resources and Environment, Lanzhou University, Lanzhou 730000, China)

Abstract: Analyses of pH and electrical conductivity in surface snow and snowpit samples collected successively in a weekly basis during September 14, 2002 to September 28, 2004 on the east branch of Glacier No.1 at the Urumqi river head, Tianshan is presented. pH and electrical conductivity in surface snow show obvious seasonal variations, which to some extent are associated with the dominant NE and ENE valley wind. pH in surface snow is more alkaline and electrical conductivity in surface snow reachs maximum in spring because of the Asian dust storm increases and primary aerosols contribution; pH in surface snow is less alkaline and electrical conductivity in surface snow reachs minimum in winter due to the transformation of primary aerosol to secondary aerosol. During the post-depositional processes (October 4, 2003–September 8, 2004), pH and electrical conductivity in snowpits duing different periods show visible seasonal characteristics and elution processes. The date that the peak value P1 of electrical conductivity in snowpit merges into firn ice is about 40 days prior to that of large particles (Diameter>10 μ m) merging into firn ice. To some extent, the peak values of pH and electrical conductivity in some snowpits occur near dust layers and their peak values also correspond to the dust layers in snowpits, which imply that dust layers probably had an influence on elution processes of soluble ions. Electrical conductivity observations indicate different elution of some of ions in snowpits, the elution of soluble ions is more likely and easier to happen than that of insoluble ions in snowpits. Furthermore, correlation analysis shows that Ca^{2+} is the key ion determining pH and electrical conductivity in surface snow.

Key words: Glacier No.1; Snowpits; pH; Electrical conductivity; Seasonal variations; Elution processes.

利用雪层层位跟踪法研究暖型成冰作用的年限问题—以乌鲁木齐河源 1 号冰川为例

尤晓妮，李忠勤，王飞腾

（中国科学院 寒区旱区环境与工程研究所天山冰川站/冰芯与寒区环境实验室，甘肃 兰州 730000）

摘　要：降雪通过冷型或暖型成冰作用转化成为冰川冰．中国冰川以暖型成冰作用为主．然而，有关暖型成冰作用的年限，文献中却少有准确的报道．原因是缺少完整的野外观测作为依据．本文利用在雪层中插置竹板，通过竹板进行层位跟踪的方法，和历时 24 个月的连续观测，研究了 1 号冰川积累区（海拔 4130 m）降雪演化为粒雪冰的时间问题．结果表明，在夏季，新雪转化为细粒雪大约需要 7 天，细粒雪转化为粗粒雪约 20 天～3 个月；同样的转化在冬季分别需要大约 2.5 个月和 2～4.5 个月．粗粒雪转化成粒雪冰的时间大约 40 个月，转化主要发生在夏季消融季节．由此得到 1 号冰川 4130 m 处新雪演化为粒雪冰历时大约 41～47 个月．本文还研究了雪层层位下移速度的季节变化特征，随深度的变化和与密度的关系以及成冰量等．指出，夏末 8～9 月为主要成冰期．不同层位雪层的密实成冰速率由于其粒雪性质和密度的不同而有很大差别，融水是影响成冰时间及成冰量的重要因素．

关键词：1 号冰川；成冰年限；层位跟踪

1　引言

成冰年限是指降雪演化成冰川冰这一过程所需的时间，是冰川学研究的基本内容之一，同时对于目前冰芯记录的形成恢复研究意义重大．其因成冰作用类型的不同而不同．成冰作用有暖型和冷型两种[1]．冷型成冰是负温下的一种成冰方式，极地冰川多以此方式成冰[2]．Robert L.Hawley 利用垂直挤压速率和密度得出雪层的垂直速度，以此计算出南极 Taylor Dome 冰川稳定状态下的深度—时间范围[3]．暖型成冰作用则是在温度较高，有融水参与下的一种成冰方式。除了达索普[4-5]等少数冰川外，中国山地冰川多以暖型成冰为主．

我国对成冰年限的研究始于 1962 年，谢自楚等利用雪层剖面和年层特征得出 1 号冰川新雪转化为粒雪冰需要 3～5 年[6]．此后谢自楚对珠穆朗玛峰北坡、祁连山地区以相同的方法进行层位定年，分别得出两年、两年以上的成冰时间[7-10]．王晓军等人对 1 号冰川进行了多次观测[11-13]，根据冰板和污化面推测 1 号冰川成冰历时不少于 10 年，不同之处在于王晓军是通过冰芯资料对经过动力变质的冰川冰定年，而对降雪转化为粒雪冰的时间未进行论述[13]．1994 年，李忠勤等对古里雅冰帽 6400m 高度的积累区进行了雪冰转化机制研究，认为该处温度很低，夏季融水渗浸冻结速度快，在当年的雪层内即可冻结成为粒雪冰[14]

事实上，成冰年限除了受成冰作用影响外，与海拔等诸多因素有关．同一条冰川，成冰年限因海拔高度的不同有很大差异．如在消融区，附加冰的形成和破坏在一个夏季就可以完成[15]．这主要是因为不同的海拔高度其剖面厚度，水热条件及下伏冰的特性明显不同．本项研究所挖雪坑位于附加冰带上部的渗浸带内（海拔 4130m）[15]，完整的雪层组成自上而下依次为：表层新雪，细粒雪，粗粒雪，粒雪冰，冰川冰．新雪降落到冰川表面，在重力和表面微融水的作用下朝着自由能减小的方向密实化，逐步演化为细粒雪，粗粒雪，粒雪冰，冰川冰．融水在这一过程中起到了重要作用．一方面融水的参与加速了上述过程，另一方面融水冻结产生的相变潜热加剧了对雪层的改造．当融水下渗到粗粒雪下部，对该层粒雪进行改造并与之胶结形成粒雪冰，粒雪冰的平均密度约 0.8g/cm^3，颜色为微白色，冰体中充满大量圆形细密气泡[16-17]．粒雪成冰后继续压缩气泡内的气体使得冰密度进一步上升，并在拉伸、挤压作用下逐步具备动力变质的特征，此时的冰为冰川冰，密度约 0.9 g/cm^3．当雪—粒雪层吸收的热量增加，产生的融水一部分下渗到冰川冰面，依附其上形成附加冰，一部分沿着冰川冰表面流失．

本文所指的冰为粒雪冰，成冰年限即新雪转化为粒雪冰的时间[18]．

本项研究基于对多种方法的比较分析，确定利用竹板对雪层质点进行跟踪，首次比较准确的揭示了 1 号冰川成冰年限问题．较之前人的研究，雪层层位跟踪法可以对雪层准确定位，并通过速度计算将成冰过程定量化，使得成冰年限的研究更具有准确性．本文重点对成冰年限、雪层密实成冰速度及其影响因素、夏季成冰量等问题进行专题讨论．

2 研究方法

根据竹板研究成冰过程，可以对特定雪层进行稳定的跟踪观测，并将粒雪成冰过程通过下移速度定量化．依据的原理是：当某一根竹板的初始位置是新降雪，经过时间 $T_{新-冰}$ 之后被粒雪冰包裹，时间 $T_{新-冰}$即为新雪演化为粒雪冰的时间，在 $T_{新-冰}$内整个雪层物质刷新一遍.转化过程的中间阶段（细粒雪、粗粒雪）所需时间亦可结合剖面观测得到．而直接得到 $T_{新-冰}$至少需要四年的竹板变化资料．基于现有 24 个月的观测资料，可由上述方法得到新雪→细粒雪、细粒雪→粗粒雪的演化时间 $T_{新-细}$、$T_{细-粗}$，而粗粒雪→粒雪冰的转化时间尚不能直接观测到．我们利用相同雪层深度代表相似变质程度的原理及粗粒雪层的稳定性，对竹板变化进行叠加累计．具体方法是：选取位于较上层粗粒雪的竹板，记录其下移时间 ΔT_1，依据该竹板所处的末端位置找到与之具有相同层位深度的竹板，并记录下移时间 ΔT_2．依此类推，直到有一根竹板的末端位置位于粒雪冰．其间每根竹板所经历的时间依次记做 ΔT_1、ΔT_2、ΔT_3 $\cdots$ ΔT_n．对其求和即可得到粗粒成冰的时间：

$$T_{粗-冰}=\Delta T_1+\Delta T_2+\Delta T_3+\cdots+\Delta T_n \qquad ①$$

由此得到新雪转化为粒雪冰的时间：

$$T_{新-冰}=T_{新-细}+T_{细-粗}+T_{粗-冰} \qquad ②$$

基于上述原理，我们在乌鲁木齐河源 1 号冰川粒雪盆附近开挖雪坑，将竹板等距离（10cm）水平插至选定的雪坑中．定期对竹板到冰面的距离进行跟踪观测，从 2002 年 12 月 5 日至今，已有两年的竹板变化资料．为了防止小环境造成的观测差异，使进一步的剖面化学变化过程研究与竹板变化研究具有一致性，雪坑的位置选取在常年取样雪坑附近．将

竹板按照插入雪坑的先后次序进行标号，依次为 L1,L2,L3 …，并相间涂上红，蓝两色，以便于辨认．当有新雪覆盖或者竹板下移，在雪坑上部继续以 10cm 的起始间距插入竹板．随着雪层厚度的增加，竹板数量也不断增加，最多的时候曾经达到 27 根．夏季消融强烈，部分竹板因出露雪表层，或与下方竹板发生重叠而被撤去．观测时间因季节而不同．夏季雪层变化剧烈，观测为一周一次；冬季较稳定，观测间隔期是 2—3 周．为减少观测造成的扰动，每次观测结束后将雪坑填平．

3 结果与讨论

3.1 成冰年限

3.1.1 新雪到细粒雪的演化时间

新雪密实化程度低，转化为细粒雪的时间序列短，在现有竹板变化资料的基础上结合雪层剖面记录即得到演化时间．图 1 显示了新雪到细粒雪的变化情况，黑色加粗直线在剖面中的位置表示竹板所代表的雪层层位．由图 a 可得，竹板 L18 在 03 年 12 月 5 日位于新雪层，04 年 1 月 31 日位于风板，到 04 年 2 月 28 日即位于细粒雪，说明竹板 L18 所在雪层到此已经完成了新雪到细粒雪的演变．图 b 给出了夏季该阶段的变化情况：竹板 L14、L16 分别于 03 年 5 月 8 日和 03 年 5 月 16 日位于新雪层，经过一周之后其所在层位变成细粒雪．表 1 为新雪转化为细粒雪的时间．

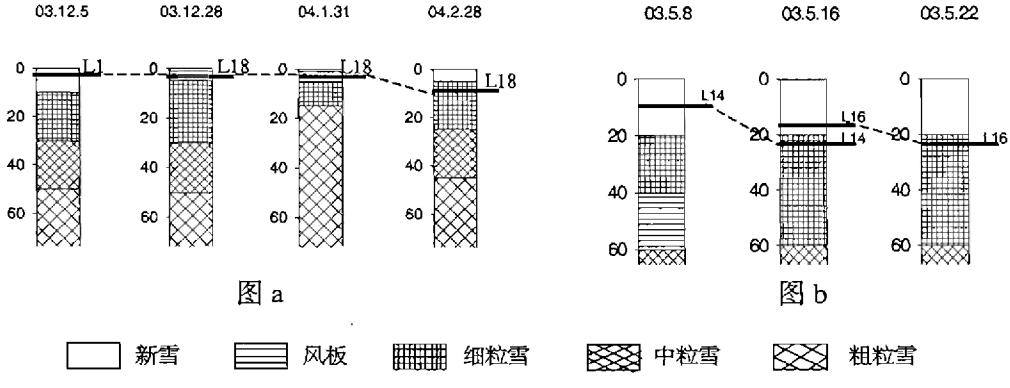

图 1 新雪到细粒雪演化示意图

Fig. 1 Sketch map of evolution process from snow to fine firn

表 1 新雪到细粒雪的转化时间

table 1 Evolution time from snow to fine firn

	新雪	细粒雪	$T_{新-细}$
L18	03 年 12 月 5 日	04 年 2 月 28 日	约 2.5 个月
L23	04 年 3 月 27 日	04 年 5 月 7 日	约 1.5 个月
L14	03 年 5 月 8 日	03 年 5 月 16 日	约 8 天
L16	03 年 5 月 16 日	03 年 5 月 22 日	约 6 天

由表 1 得出，新雪转化为细粒雪的时间 $T_{新\to细}$约 1 周～2.5 个月．表明：新雪到细粒雪的转化时间具有明显的季节差异，夏、冬所需时间比约为 1：11．这是因为夏季气温较高，雪层因接收来自大气中的热量而迅速升温，产生的表面融水垂直下渗，使得粒雪化过程加剧．冬季整个雪层处于稳定的负温状态，主要依靠雪层自身的压力作用,以重结晶的方式成冰，成冰时间较长；其次，新雪密度较小，空隙度大，其垂直压应力大于水分量，因此在重力作用下易发生沉陷．据谢自楚的研究，新雪降落至冰川表面即发生雪的圆化．晶粒的圆化有利于沉陷，其结果可使粒雪的密度增加到 550（或 580）kg．m^{-3}左右[19]．夏季融水的出现使晶粒被水膜包裹，从而增加晶粒活动的自由度，促发雪的沉陷[6]．

3.1.2 细粒雪到粗粒雪的演化时间

本阶段的演化依然可以通过雪层剖面记录得到．如图 2 所示：03 年 9 月 13 日竹板 L15 处于较新的细粒雪层，10 月 31 日该层细粒雪已转化为中粒雪，04 年 1 月 31 日观测发现竹板 L15 为粗粒所包裹（图 a），其间经历了大约 4.5 个月．03 年 3 月 13 日竹板 L5 位于细粒雪，约一个月之后完成了细粒雪到粗粒雪的改造（图 b）．表 2 给出了不同竹板细粒雪到粗粒雪的演化时间．

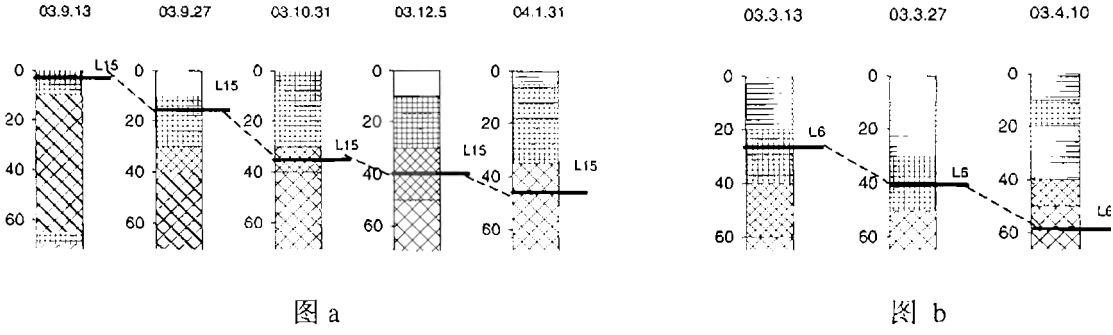

图 a 图 b

图 2 细粒雪到粗粒雪演化示意图

Fig. 2 Sketch map of evolution process from fine firn to coarse firn

表 2 细粒雪到粗粒雪的转化时间

table 2 Evolution time from fine firn to coarse firn

	细粒雪	粗粒雪	$T_{细\to粗}$
L4	03 年 2 月 13 日	03 年 3 月 20 日	约 1 个月零 1 周
L6	03 年 3 月 13 日	03 年 4 月 10 日	约 1 个月
L15	03 年 9 月 13 日	04 年 1 月 31 日	约 4.5 个月
L14	03 年 5 月 16 日	03 年 6 月 6 日	约 20 天

分析表明：细粒雪转化为粗粒雪的时间 $T_{细\to粗}$约 20 天～4.5 个月.该阶段的季节差异也很大，夏、冬转化时间比约 1：7．然而较之新雪转化为细粒雪，冬夏差异有所减小．这是由于较之新雪细粒雪孔隙度减小、密度增加，粒雪层在重力作用下的垂直向下运动受到制约．此外由于上覆新雪，夏季融水的作用程度也相对减弱．

3.1.3 粗粒雪到粒雪冰的演化时间

粗粒雪在晶粒性质上（硬度，密度，粒径等）与新雪和细粒雪有着较大差异，其密实

化程度高，转化时间序列长，雪层相对稳定．粗粒雪层中竹板的位置，基本反映了该雪层的变质程度．本阶段，我们根据前述原理，利用竹板叠加累计的方法计算转化时间．即将具有相同位置的竹板依次替换叠加，累计其变化时间．具体方法如下：

根据竹板位置资料，首先对竹板 L14 进行跟踪观测．L14 的初始位置位于最新形成的粗粒雪中，距冰面 149cm，经过约 11 个月的连续变化 2004 年 8 月 18 日到达距冰面 98cm 处．在 03 年 9 月 13 日的资料中找到具有相似雪层位置的竹板 L9（距冰面 99cm）．根据前述原理，此时的 L9 与 04 年 8 月 18 日的 L14 具有相近的变质程度．对 L9 跟踪观测得到其末端位置（04 年 8 月 18 日位置，下同）距冰面 55cm，历经约 11 个月．同理找到具有近似位置的竹板 L5（2003 年 9 月 21 日距冰面 55cm），经过约 11 个月得到其末端位置距冰面 20cm，具有相似高度的竹板为 L1（距冰面的初始距离为 18cm）．继续跟踪 L1，经过约 6.5 个月，于 2004 年 4 月 24 日发现其被粒雪冰包裹，表明这一层位的粗粒雪已经完成了到粒雪冰的改造．$T_{粗→冰}$表示粗粒雪成冰的时间，ΔT_1、ΔT_2、ΔT_3、ΔT_4分别表示每根竹板的演化时间（如图 3 所示），利用①式即可得到 $T_{粗→冰}$值．累计得到粗粒雪到粒雪冰的变化时间约 40 个月．利用同样方法依次叠加竹板 L15—L11—L7—L3，得到上述过程历时仍为 40 个月．

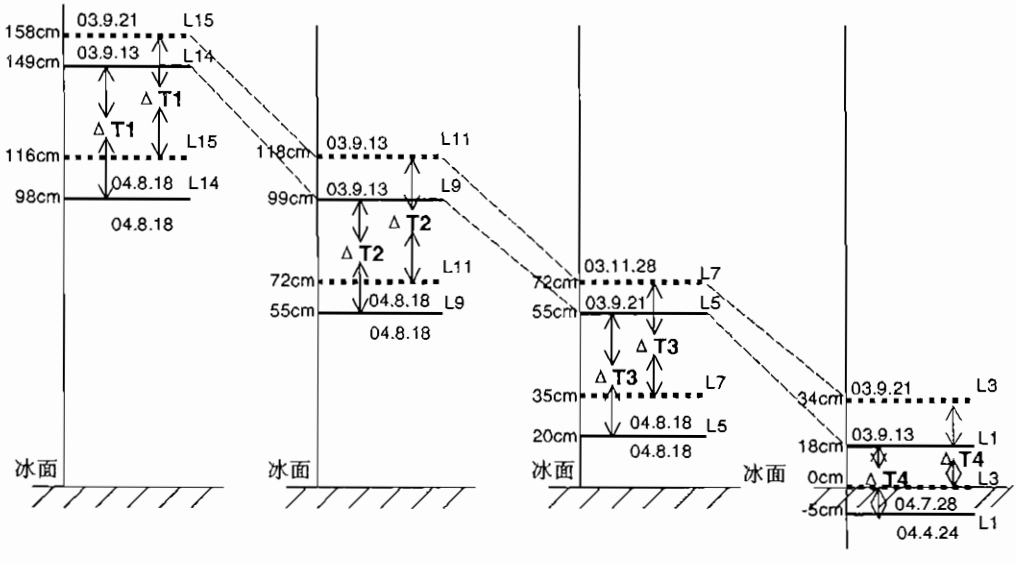

图 3　竹板累计叠加示意图

Fig. 3　Sketch map of bamboo stake's variation

上述过程中，粗粒雪转化为粒雪冰的时间是跨越季节的，其转化阶段主要发生在夏季消融期．早期研究通过在典型剖面撒人工污化模拟融水的下渗过程，得出融水影响的深度可达 20m[20]，因此融水依然是粗粒成冰的主要因素．夏季消融强烈，融水在密度较大、温度较低的粗粒雪层受阻发生冻结并释放潜热，释放的潜热又成为加热该冰层的主要热力来源[21]，进一步对该层位进行改造．冬季低温期，由于粗粒雪所处层位靠下，上覆新雪及细粒雪的压力作用较大，以冷型变质为主．

3.1.4　雪到粒雪冰的转化时间

根据各演化过程的研究，我们得到，新雪到细粒雪的转化时间 $T_{新→细}$约为 1 周～2.5 个

月，细粒雪到粗粒雪的转化时间 $T_{细\to粗}$约为 20 天～4.5 个月，粗粒雪转化为粒雪冰的时间 $T_{粗\to冰}$约为 40 个月.利用②式即可得到 1 号冰川 4130m 处成冰年限 $T_{新\to冰}$为 41～47 个月.浮动范围由新雪转化为粗粒雪的季节差异引起.而粗粒雪演化为粒雪冰的时间则跨越了季节，在整个成冰历时中占到 85%～97%．这与本项研究中用污化层定年得到的结果（3～4 年）十分吻合[15]．此外，该结果与谢自楚所指的成冰时间（3～5 年）亦相似．表 3 列出了雪—粒雪—粒雪冰各阶段的转化时间.

表 3 雪—粒雪—粒雪冰演化时间

table 3 Evoluation time of snow—firn—granula ice

	夏半年（5～9 月）	冬半年（10～4 月）
新降雪→细粒雪 $T_{新\to细}$	大约 1 周	约 2.5 个月
细粒雪→粗粒雪 $T_{细\to粗}$	约 20 天～3 个月	约 2～4.5 个月
新降雪→粗粒雪 $T_{新\to粗}$	约 1～5 个月	——
粗粒雪→粒雪冰 $T_{粗\to冰}$	约 40 个月	
新降雪→粒雪冰 $T_{新\to冰}$	大约 41～47 个月	

3.2 层密实成冰速度及其影响因素

为使本研究适用于更大范围并对不同季节成冰特点进行具体分析，以下我们对密实成冰速度进行讨论.由于竹板位置始终代表其所在雪层，竹板向下移动就是雪层向下移动，下移速度是雪层密实化快慢的表征．对竹板下移速度进行分析，即得到雪层的成冰速度特征.

3.2.1 季节变化

竹板在雪坑中的移动是一个由时间、深度和速度构成的三维轨迹．将竹板到冰面的距离与观测时间间隔做一个简单的速度运算，得出竹板下移的速度值并加上深度维和时间维便得到一幅竹板移动的三维图（见图 4）．根据本项研究对成冰期的划分[22]，将图所示的时段划分为冬季稳定期 wi（11 月中旬～次年 3 月下旬）、春季波动期 sp（4 月初～5 月底）、夏季剧变期 su（6 月初～9 月底）、秋季波动期 au（10 月初～11 月中旬），如虚线所示.

依据下图，我们对不同成冰期内雪层密实成冰特点进行总结如下：

①冬季稳定期（11 月中旬～次年 3 月中旬）．由图可得，这段时期竹板下移速度极为缓慢，有时连续几次观测到冰面距离均没有变化．速度随深度变化趋势不明显．原因是冬季风力较大，降雪少，表面或形成密度较大的风板，或细粒直接出露表层．冬季粒雪成冰速度有以下特点：（1）雪层处于稳定状态，成冰速度缓慢．成冰作用以冷型为主（2）随深度增加，不同性质粒雪成冰速度没有明显变化.

②春季波动期（3 月中旬～5 月底）．如图，在雪坑上部接近表面位置竹板下移速度出现明显的峰值，且随深度增加，速度递减显著．这是由于本时期内雪坑表面温度昼夜变化剧烈，融化再冻结作用频繁．降水开始增加，新雪在表层积累．这段时期成冰特征是：（1）雪层密实成冰速度开始增大，有随深度递减的趋势.（2）融水作用使得局部雪层成冰加速.

③夏季剧变期（6 月初～9 月底）．6、7 月份，表层竹板下移剧烈，但仍可以看到随深度递减的规律．到了 8、9 月，竹板出现剧烈波动，如图所示，03 年 8 月 23 和 04 年 8 月 18 的两次观测中发现，随着到冰面距离增加，竹板下移速度起初增大，接着开始变小，继

而又增大，两种趋势交替进行，表现出无规律性．速度极大值不是出现在表层新雪而以中部或中上部居多．这种现象与该时段内融水强烈参与有关．本期温度较高，消融量大，融水可以渗透几个年层的粒雪．夏季成冰速度有如下规律：（1）雪层在雪坑中的位置变化剧烈，成冰速度快．以融水的渗浸冻结成冰为主．（2）夏季初期成冰速度随深度减缓的趋势到末期变得无规律化．（3）8、9月是主要成冰期．

④秋季波动期（10月初～11月中旬）．是夏季成冰期向冬季过渡的时期．竹板下移速度转入低值，随深度的衰减趋势又开始明显起来．少量的降雪使得雪层表面竹板下移速度出现极大值．本阶段雪层密实成冰速度减小，开始趋于稳定．

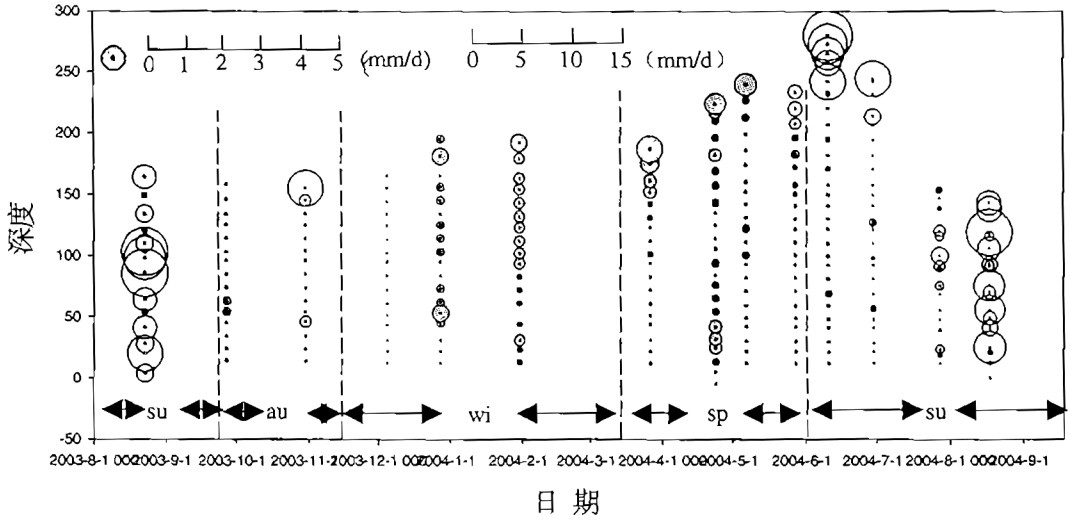

(图中横坐标表示日期，纵坐标表示雪坑深度，0刻度即指冰面．圆圈表示速度，单位mm/d，表示每天下移的毫米数．为了便于分析，图中灰色填充的部分经过放大处理，放大倍数为原值的4倍．左上方图例显示了圆的直径与速度的比例关系．虚线之间的区域代表不同的成冰期)

图4 竹板下移速度—深度—时间图

Fig.4 Bamboo stake's movement velocity vs depth and date

3.2.2 速度随深度变化

研究中，我们利用叠加的方法得到一套完整的新雪转化为粒雪冰的竹板速度图，基本反映了竹板下移速度随深度的变化趋势．将其与不同粒雪平均密度变化进行比较分析，发现二者具有相反的变化趋势（见图5）．

如图所示，实线代表竹板下移速度随深度的变化，虚线表示不同雪层（新雪，细粒雪，粗粒雪）的平均密度．总的说来，随竹板到冰面距离的减小，其下移速度呈波动状减小．密度则出现增大的趋势．由此可见，雪层的密度变化是影响竹板移动速度的一个重要原因．这是由于成冰过程其实就是雪密度不断趋于冰密度的过程[23]．

对速度—深度曲线分析发现，在新雪中速度随深度增加而减小．到细粒雪上部出现一个急剧的速度回升．结合剖面分析发现该处是一个类似深霜的松散层，孔隙度大、硬度低，一般位于粗粒雪上部认为其形成是由深霜在融水作用下体积减小，空隙增大所致．当细粒雪与粗粒雪发生临界变化时，速度开始急剧回落．竹板在粗粒雪中的变化相对平稳，这也

是本研究利用竹板叠加的方法探讨粗粒成冰的重要依据．分析表明，不同性质雪的密实化有如下特征：(1)雪层密实成冰速度在新雪和细粒雪阶段比较快，粗粒雪中则较为缓慢．(2)细粒雪到粗粒雪的转化阶段是成冰过程的转折点，在此之前雪层密实化速度快、波动大，之后则相对平稳．

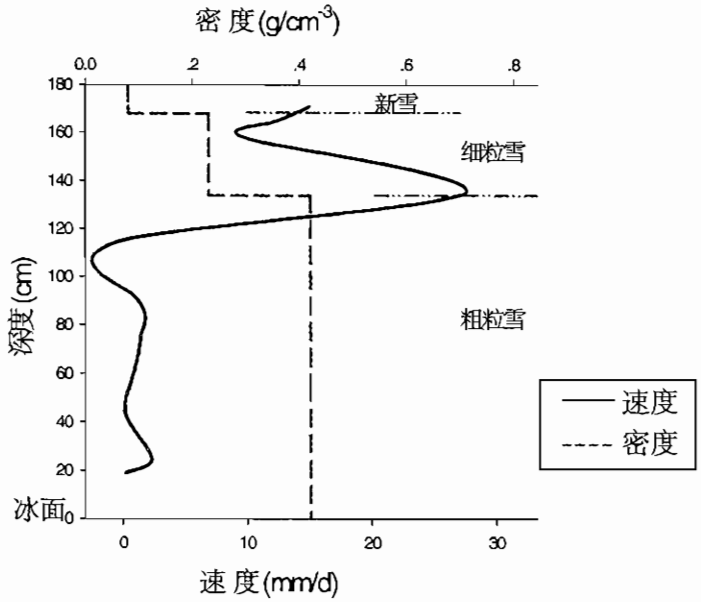

图 5 竹板下移速度及密度随深度变化曲线

Fig.5 the movement velocity of bamboo stake vs density and depth profiles

3.2.3 融水对成冰速度的影响

详细分析表明，融水是影响 1 号冰川成冰年限的重要原因,表现在三个方面．

首先，融水是雪层逐渐下移的原因之一．对于以暖型成冰作用为主的 1 号冰川来说，融水一方面通过加速雪的密实化过程使得雪层下移，另一方面由于物质损失而使雪层向下运动．该过程主要发生在暖季消融期．融水主要以两种方式在某层位消失：一是下渗．融水下渗是雪层中物质重新分配的重要方式，其对冰川内补给量的影响巨大[24]．二是冰面径流．当气温进一步升高，融水下渗至冰面一部分冻结成冰，而另一部分以冰面径流的形式消失．不同于融水渗浸再冻结的是，冰面径流造成了冰川物质的直接损失，而融水渗浸冻结只是物质的再分配．

其次，融水通过密度影响成冰速度．融水的渗浸再冻结对粒雪形态，密度，硬度等物理特性的改造是显著的．姚檀栋等对祁连山冰帽顶部的冰芯进行研究得出：融水是导致粒雪层密度加大的重要原因[23]．对 1 号冰川而言，融水造成雪层密度的增加主要表现在两个方面：一是融水对晶粒的包裹导致粒雪在沉陷过程中变紧密，从而使容重增加，孔隙率减少[6]．二是融水通过下渗再冻结作用填充于孔隙，使得发生冻结的层位（冰片层）密度值明显较大．有研究表明，融水区内的晶粒密实化所能得到的最大密度，要比干雪带内的高[26]．

最后，融水造成雪层成冰速度的季节变化．由于融水出现主要以温度较高的夏季为主，

使得粒雪的密实化速度具有显著的季节变化．主要表现在新雪到细粒雪，细粒雪到粗粒雪的演化过程中，夏、冬所需时间比分别达到 1：11 和 1：7．

在观测中我们发现，竹板除了按照理想状态向下移动外，还有间或的上移．该现象多发生在雪坑中部，以变化较剧烈的夏季出现最为频繁．对此认为可能由以下原因造成的：冰川连同其上部雪层是不断运动的[6]．由此导致的冰川的拉伸和挤压，造成竹板上下移动．此外，由于雪坑所处粒雪盆，雪层因重力作用向下运动、填充，亦有可能引起竹板上浮．同时，野外观测时人为导致的参照系误差也是在所难免的．除此而外，2003 年 5 月 16 日的一次观测资料中发现，前一周仍然相对独立的竹板 L5、L6、L7 在本周发生了重叠．这是由竹板间物质的流失引起．

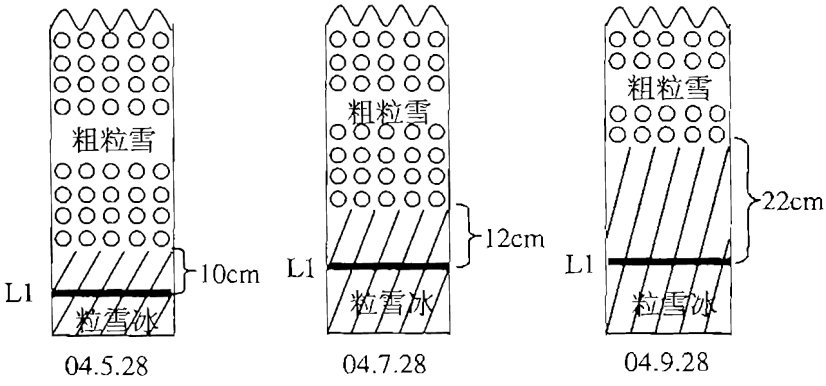

图 6 夏季成冰量示意图

Fig.6 Sketch map of ice formation volumn in summer

3.3 夏季成冰量

本研究区的夏季成冰量由融水下渗冻结形成，主要取决于冰川活动层中冰的冷储量、夏季降雪量、冰川表面热量平衡，融水渗浸特点及冰面排水条件等[9]，具有较大的年际变化和季节变化．本研究利用进入冰层的竹板距粒雪冰面的距离变化即可直接得到夏季成冰量．它包括融水下渗到粒雪冰面遇冷冻结形成的冰，亦包括粒雪冰本身融化再冻结形成的冰，而雪层上部或中部形成的渗浸冰片不在本研究的范畴.依据的原理是以竹板 L1 为参考，观测其距粒雪冰表面的距离.在一定时段内的距离变化值即这段时间的成冰厚度.对已进入冰层的竹板 L1 进行跟踪观测发现 04 年 5 月 28 日距冰面 10cm，7 月 28 日增至 12cm，表明在 6、7 两月约有 2cm 粗粒雪成冰；9 月底 L1 距冰面 22cm，表明 8、9 月约有 10cm 粗粒雪成冰（见图 6）．由此得到，1 号冰川夏季（6～9 月）成冰量约为 12cm，8、9 月为主要成冰期，占到夏季成冰量的 83%.这与根据雪层下移速度的变化特征得出的 8、9 月为主要成冰期的结果十分吻合．由于竹板进入冰层后，相对下移速度几乎为零，L1 在冰层中的下移可以忽略．

4 结论

本项研究基于两年的连续观测资料，利用雪层层位跟踪法对以暖型成冰作用为主的乌

鲁木齐河源 1 号冰川积累区（海拔 4130m）的成冰年限问题进行了专题研究，得出以下结论：

（1）新降雪转换为粒雪冰的时间．研究表明，1 号冰川新雪演化成粗粒雪的时间因季节不同而有很大差异．夏季，新雪转化为细粒雪仅需要 1 周的时间，细粒雪转化为粗粒雪约 20 天～3 个月．冬季，上述过程分别需要约 2.5 个月和 2～4.5 个月．粗粒雪演化成粒雪冰大约需要 40 个月，在整个成冰过程中占到 85%～97%．由此得到 1 号冰川新雪转化为粒雪冰历时约 41～47 个月．

（2）雪层层位下移速度特征．分析得到，雪层层位下移速度具有明显的季节和深度变化．夏季 8、9 月，下移迅速，纵向变化紊乱，是主要的成冰期．冬季则较为稳定，几乎不成冰．随深度增加，雪层下移速度有减小趋势，与密度呈相反变化．

（3）初步认为融水是影响成冰时间的重要原因．

（4）夏季（6～9 月）约有 12cm 粗粒雪成冰．

总体上看，成冰年限是一个诸多要素综合作用的结果，包括温度，海拔高度及融水对粒雪的改造等．本文仅对 1 号冰川 4130m 处的成冰年限进行了分析讨论．事实上，雪层下移速度 V 是一个关于雪层密度 P，温度 T 及融水 M 的函数 V=f(P,T,M)，进一步的研究可将这些参数定量化，建立这 4 者的函数关系，这样便可利用公式 dT=dh/v（其中 h 为雪层厚度，T 为成冰年限）计算出不同地区，不同海拔高度的冰川成冰年限．进一步的研究正在开展，我们已开始在不同高度利用此方法进行成冰历时的观测，并进行密度和温度的连续记录，融水在成冰过程中的作用研究也在试验中，相信这项研究将具有更大推广意义．

致谢：本项研究是天山冰川观测试验站开展的雪冰现代过程研究项目的一部分。是在全体观测和研究人员集体努力下完成的。没有观测人员长期全年度在冰川积累区的辛勤观测，便不会有本研究所需的第一手观测资料。谨此对参加本项研究的每一个观测人员以及项目组人员焦克勤，杨惠安，韩添丁，李向应，李传金，赵中平，钱军，张明军等表示衷心感谢。

参考文献(References):

[1] Shi Yafeng *et al.* An Introduction to the Glaciers in China Contents. Science Press: 55—65[中国冰川概论. 科学出版社 55—65.]

[2] Qing Dahe,desification process of snow firn in the surface layer of the Antartic ice. Journal of Glaciology and Geocryology 1987 [J]，9（3）:193—204[秦大河，南极冰盖表面层内雪的密度化过程，冰川冻土[J]1987，9（3），193—204]

[3] Robert L.Hawley, Edwin D.Waddington, Dating firn cores by vertical strain measurements. Journal of Glaciology [J], 2002, 48(162) 401~406.

[4] Yao Tandong, Pu Jianchen, Wang Ninglian et al., A new type of ice formation zone found in the Himalayas, Chinese Science Bulletin [J], 1999, Vol.44 No5: 467—473. [姚檀栋，薄健辰，王宁练，田立德，1998. 中国境内又一种新成冰作用的发现，科学通报[J]43（1）：94～97]

[5] Xu Baiqing, Yao Tandong,a study on the air-bubble formation process at altitude of 7100m

a.s.l.intheDasuopu glacier .Journal of Glaciology and Geocryology [J] 21（2）：120～124 [徐伯青，姚檀栋，1999.达索普冰川海拔 7100m 处气泡封闭过程研究.冰川冻土[J].21（2）：120～124]

[6] Xie Zichu,Huang Maohuan.A evolution of the snow-snowgrains layer and ice formation in the Glacier No.1 at the headwaters of the Urumqi River, Tianshan. An studies of glaciology and hydrology on the Urumqi River, Tianshan, Science Press[C],1965,1-14. [谢自楚,黄茂恒等. 天山乌鲁木齐河源 1 号冰川雪-粒雪层的演变及成冰作用.天山乌鲁木齐河冰川与水文研究,科学出版社[C],1965,1-14.]

[7] Xie Zichu, snow and ice formation process in northern xixiabangma peak. Investigtation reports in xixiabangma area.1982.science press[C].45～59 [谢自楚，1982a，希夏邦马峰北坡的积雪和成冰作用.见：希夏邦马峰地区科学考察报告[C].北京：科学出版社 45～59]

[8] Xie Zichu,*et al.*ice formation process in northern Everest area. Investigation reports in Everest area[C] 8～13[谢自楚，王宗太，1975a.珠穆朗玛峰地区北坡成冰作用.见：珠穆朗玛峰地区科学考察报告[C]（1966～1968）.8～13]

[9] Xie Zichu,*et al.*ice formation process in glacier of Qilan montain [谢自楚，伍光和等.祁连山冰川的成冰作用.中国科学院兰州冰川冻土所集刊，1984，5：27－40.]

[10] Xie Zichu. Snow Stratigraphy and Ice Formation on Law Dome, Antarctica. Journal of Glaciology and Geocryology [J]. 1984，6(1)：1－21.[谢自楚.南极洲洛多姆冰帽学的地层学及成冰作用研究.冰川冻土[J]，1984，6(1)：1－21.]

[11] Wang Xiaojun, Zhang Jinhua, *et al.*Obersavation on the stratification of snow and accumulation in the accumulation area of Glacier No.1 at the head of Ürümqi River. Annual Report on the Work At Tianshan Glaciological Station[M].1980-1981.11—15. [王晓军，张金华等.乌鲁木齐河源 1 号冰川积累区雪层剖面和积累量的观测.天山冰川观测实验站年报[M]. 1980-1981：11—15]

[12] Wang Xiaojun,Wu Guanghe,*et al.*Obersavation on accumulation and melt of Glacier No.1 at the head of Ürümqi River. Annual Report on the Work At Tianshan Glaciological Station[M]. 1984. [王晓军，伍光和等.乌鲁木齐河源 1 号冰川积累消融观测.天山冰川观测试验站年报[M]，1984.]

[13] Wang Xiaojun, Wang Zhongxiang, Wang Chunzu. Stratigraphic and Structural Analysis on An Ice Core to the Bedrock IN the Accumulation Area of Glacier No.1 at the Headwatgers of Ürümqi River. Journal of Glaciology and Geocryology[J]. 1996.18(4):337-346. [王晓军 王仲祥 王纯足.乌鲁木齐 1 号冰川的积消特征及成冰过程.冰川冻土[J].1996. 18(4):337-346.]

[14] Li Zhongqing, Yao Tandong, *etal.*Modern atmospheric environmenal records in Guliya Ice Cap of Qing-zang Plateau, Chinese Science Bulletin [J],Vol.40,No,10.874-875.[李忠勤，姚檀栋，皇翠兰，1994.青藏高原古里雅冰帽中的现代环境记录.科学通报[J]，40（10）：874-875]

[15] Wang Feiteng *etal.*Studying on ice formation process of surface snow layer in accumulation area of Glacier No.1 at the Ürümqi river head, Tianshan Mts. [王飞腾等.天山乌鲁木齐河源 1 号冰川积累区表面雪层演化成冰过程的观测研究.2004，待发.]

[16] Liu Chaohai, Xie Zichu, *et al.*A Research on the Mass Balance Processes of GlacierNo.1at the Headwaters of the Ürümqi River, Tianshan Mountains. Journal of Glaciology and Geocryology[J].1997,19(1): 17－24. [刘潮海，谢自楚等．天山乌鲁木齐河源 1 号冰川物质平衡研究[J]．冰川冻土.1997，19(1)：17－24.]

[17] С В КАЛСНИ, ОЧЕРКИ ГЛЯЦИИ[C].1982 [С В 卡列斯尼克，冰川学概论，中国科学院兰州冰川冻土研究所.1982]

[18] С В ÊÀËÑÍÈ, Î ÁÙ Àß ÄËß ÖÈÎ ÃÈß[C].1965 [С В 卡列斯尼克，普通冰川学，中国科学院地理研究所冰川冻土研究室.1965]

[19] Wang Xiaojun, Han Jiankang, Xie Zichu,*et al.*stratigraphic and structural analysis on an ice coretothebedrock in the accumulation area of glacier No.1 at the headwaters of Ürümqi River. Journal of Glaciology and Geocryology [J] 18（4）：337～346[王晓军，韩健康，谢自楚，Lluberas A,1996.乌鲁木齐河源 1 号冰川积累区透底冰芯底层及冰结构分析.冰川冻土[J]，18（4）：337～346]

[20] Shi Yafeng.Glaciers and their environments in China.Sciende Press [C].54-73[施雅风主编.中国冰川与环境.科学出版社[C]54-73.]

[21] Cai Baolin ,Xie Zizhu, Huang Maohuan.Mathimetical models fo the temperature and water-heat transfer in the percolation zone of a glacier.Cold Regions Sxience and Technology[J].12(1):39-47.

[22] Richard Kattelmann, Jeff Dozier , Observations of snowpack ripening in the Sierra Nevada, Califurnia, U.S.A. Journal of Glaciology[J],.1999, 45(151): 409~416.

[23] Yao Tandong, T hompson L G，1992. Densification process in filtration zone on the Dunde ice cap ,China. Proceedings of the fourth national conference on glaciology and geocryology.science press [C]. 34-40. [姚檀栋等.敦德冰帽冷渗浸带雪密实化过程研究.第四界全国冰川冻土学术会议论文集（冰川学），北京科学出版社[C]：34－40.]

[24] Zhang Jinhua *etal.* Obersavation on the stratification of snow in the accumulation area of Glacier No.1 at the head of Ürümqi River. Annual Report on the Work At Tianshan Glaciological Station[M]:19—27[张金华，王新中等，乌鲁木齐河源 1 号冰川积累区雪层剖面资料说明，天山川观测实验站年报第 2 期[M]，19—27]

[25] Li Zhongqin,Han Tianding,Jing Zhefan,et al.A summary of 40-year observed variation facts of climate and Glacier No.1 at the headwaters of Urumqi River,Tianshan,china[J].Journal of Glaciology and Geocryology,2003,**25**(2):117-123. [李忠勤,韩添丁,井哲帆,等.乌鲁木齐河源区气候变化和 1 号冰川 40a 观测事实[J].冰川冻土,2003,**25**(2):117-123.]

[26] W.S.B.Paterson. The Physics of Glaciers. Science Press [C]. 1987: 8.[W.S.B.佩特森.冰川物理学.科学出版社[C].1987：8.]

Study on Time Scale of Snow – Ice transformation through Snow Layer tracing method

—Take Glacier No.1 at the Headwaters of Ür ü mqi River as an Example

You Xiao-ni, Li Zhong-qin,Wang Fei-teng

(Tianshan Glaciological Station/Key Laboratory of Ice Core and Cold Regions Environment, CAREERI, CAS, Lanzhou Gansu 730000, China)

Abstract: Fresh Snow transforms to glacier ice through cold or warm type ice formation process. In China, the transformation on most glaciers takes place under a warm type ice formation process. However, the time scale of the transformation from snow to ice is poorly documented in literatures. The main reason for it is of lack of long-term field observation data. In this paper, an explicit transformation age from snow to granular ice at accumulation zone (4130m) of Glacier No.1 is given out based on our 24 months' continuous snow pits profile observation and the study by employing snow layer tracing method. Our study demonstrates that, in summer, the time for snow developing to fine firn is about 7 days, and the time for fine firn turning to coarse firn is about 20 days~3 months. The same transformation process takes about 2.5 months and 2~4.5 months respectively in winters. Thus, the snow to ice transformation age at this site is about 41~47 months in total. In addition, this paper also discussed the seasonal variability of snow layer's movement, the relationship between movement velocity with snow pit depth and density, and as well as the magnitude of ice formation volume in summer, etc. It concludes that the late summer (August-September) is a main time period for ice formation, and melting water greatly impacts on the snow to ice transformation process.

Key words: Tianshan; Glacier No.1; Ice formation age; Snow to ice transformation

天山乌鲁木齐河源 1 号冰川积累区表面雪层演化成冰过程的观测研究

王飞腾，李忠勤，尤晓妮

中国科学院 寒区旱区环境与工程研究所天山冰川站/冰芯与寒区环境重点实验室，甘肃 兰州 730000)

摘　要：冰川表面雪层演化成冰过程（亦称密实成冰过程）是冰川学重要的基础研究内容之一．由于这一过程的时间周期较长，需要长期的野外观测，因此前人的研究多侧重于雪层特征方面，对过程的研究则很有限．本文根据天山乌鲁木齐河源 1 号冰川（下简称 1 号冰川）积累区海拔 4130 m 处 28 个月，每周 1 次的连续雪层剖面观测，分析研究了雪层厚度、雪层中的污化层、冰片和各种粒雪随时间的演变过程．结果表明，雪层中各种要素的演变受水热条件的影响而呈现明显的季节特征．根据温度、融水渗浸程度及雪层剖面的变化程度，我们将其分成冬季稳定期，夏季剧变期和春秋波动期分别进行了论述．此外，本文还对雪层年限与年成冰量等基本问题进行了专门讨论．

关键词：1 号冰川；　过程研究；　雪层演变

1　引言

根据 IPCC 报告和世界冰川监测服务处（WGMS）报告，较小的山岳冰川对气候变化的响应极其敏感[1, 2]．近年来，随着全球气候的变化，我国西部自上个世纪 80 年代中期以来出现了强烈的气候由暖干向暖湿转型的信号[3]．就 1 号冰川所处的乌鲁木齐河河源区而言，90 年代中期以来气候变化最为明显[4]，气温升高给 1 号冰川带来了有观测记录以来最深刻的变化，这些变化不仅反映在冰川面积、厚度及末端上，也反映在冰川表面雪层特征及成冰带的变化上．如上个世纪 60 年代发现的冷渗浸带消失[5]，各成冰带谱的上限出现上移，雪层结构趋于简单、各层之间的界限变得模糊、东支顶部出现小冰面湖[6]等现象．在这种情况下，有必要对 1 号冰川的雪冰演化过程进行深入的研究．

冰川表面雪层演化成冰过程决定了冰川本身的许多特性，是冰川学重要的基础研究内容之一．然而，这一过程时间周期较长(3-5 年)，需要长期的野外观测，因此前人的研究多侧重于不同时段雪层特征方面，对演化过程的研究有限．2002 年 7 月起天山冰川观测试验站开展了冰雪物理、化学现代过程方面的研究，简称为 PGPI（the Program for Glacier Processes Investigation），为搞清 1 号冰川积累区雪层演化成冰过程创造了良好的机会．截止 2004 年 11 月，PGPI 项目共取得 111 个连续的雪坑剖面资料．本文系雪层剖面各组成要素的演变过程及季节变化特征的研究论述．

冰川表面雪层演化成冰过程因成冰作用类型不同而不同．成冰作用的类型主要有两种：即以极地为代表的冷型成冰作用和以大多数山地冰川为代表的暖型成冰作用．冷型成冰过程是指无融水参与、以重结晶方式成冰的过程．秦大河等[7,8]曾对南极地区雪层密实化过程

进行了研究，并将其化分为暖型、冷型及交替型三种类型．暖型成冰过程指有融水参与、以渗浸冻结等方式成冰的过程．我国大多数冰川的成冰作用以暖型为主．前人对此作了大量工作，主要集中在阿尔泰山、西昆仑山、喜马拉雅山、天山等地的冰川上[9~18]．其中，对 1 号冰川成冰作用的研究较为具体．上世纪 60 年代初谢自楚、黄茂桓首先对 1 号冰川雪层演变特征及成冰作用进行了研究[16]，80 年代王晓军、张金华、刘潮海也针对 1 号冰川积累区雪层剖面的一些特征进行了分析总结[17~19]．这些研究在雪层剖面特征、成冰年限、成冰带划分等方面取得了大量成果．遗憾的是，由于观测时间有限（最长的为 1 年），而且资料不连续，缺乏冬季观测资料，因而对雪层演化成冰这一重要的过程未能进行系统的分析描述．

2 研究概述

2.1 雪坑位置

研究雪层剖面变化特征及演变过程的基础是在野外开展对雪层内各组成要素演变过程的长期、连续的观测[3]．同时根据需要，对雪层温度、密度及物质平衡等各种参数进行测定．

PGPI 确定的定点观测雪坑位于 1 号冰川东支海拔 4130m 处的粒雪盆后壁．处在冰川渗浸冻结带内，坡向朝北，该位置属于日照时间最短的区域．特别是冬季，完全无直接的日照，而且风大寒冷，与高纬度极地的气候条件相似[16]．该处雪层剖面，年内与年际变化较小，内部的组成要素完整，是良好的过程研究位置．根据大西沟气象资料并进行降水量和温度的修订，得到该处多年平均降水量为 663.4mm，多年平均温度为－10.4℃[20~22]．

2.2 观测与记录

为了在长期的观测中使用统一的采样观测记录，我们制定了相应的操作规范．参照国内外常见的雪冰分类标准[23,24,25]和实际可操作性，对雪的类型按变质程度分为新雪、细粒雪（＜1mm）、中粒雪(1～2mm)与粗粒雪(2～4mm)四种，确定雪层下部的冰面为粒雪冰面．规定了如何记录雪层剖面的特征层位,包括污化层、深霜层、冰片等．

对参照面的选取亦进行了分析．在测量冰片的变化时，选取雪坑底部的冰面作为参照面，因为相对于雪面而言，冰面的变化较小．同样，在研究污化层的变化时，我们仍以该冰面作为参照面，对污化层进行编号，从冰面开始依次为 W_1、W_2、W_3…．在确定成冰量时，则选择了粗粒雪最下部的污化面作为参照面，通过观测污化层与冰面之间粒雪的厚度变化来研究成冰量．在主观测雪坑附近，挖取了另一个雪坑，插置了竹板，通过观察竹板的位置变化来揭示成冰过程的演变规律．

2.3 资料序列

对雪坑剖面进行观测的时间间隔为一周，全年度观测．自 2002 年 7 月—2004 年 11 月共获取了 28 个月共 111 个雪坑剖面的观测记录资料．

3 观测结果与讨论

观测结果表明，雪层剖面的季节变化十分明显．为探讨雪层在不同时间段的演变规律，我们根据如下指标将雪层演变成冰过程分为四个时期，表 1．

表 1 雪层演化过程中不同特征时段的划分指标

Table 1 The Index for different stages in snow to ice transformation process

指标 \ 演变期	冬季稳定期（WI）11 月中旬—3 月底	春季波动期（SP）4 月初—5 月底	夏季剧变期（SU）6 月初—9 月底	秋季波动期（AU）10 月初—11 月中旬
温度特征	<-10℃	-10℃～0℃	>0℃	-10℃～0℃
雪层剖面变化程度	稳定	波动	剧烈	波动
溶水渗浸程度	溶水极少，只能在雪层中形成薄冰片	上部产生溶水	雪层中溶水较多	上部产生溶水

以下我们对这四个时期的粒雪组成、冰片、污化面及雪层厚度等要素分别进行讨论，探索其变化规律.

3.1 雪层厚度变化

图 1 给出了观测雪坑 2002 年 9 月—2004 年 11 月的厚度与相应时段大西沟气象站的气温、降水变化情况. 从中看出，从冬季稳定期到秋季波动期的一个完整演变过程中，雪层厚度是一个由稳定到逐渐升高然后剧烈消融减薄最后又开始回升的过程.

冬季稳定期的主要特征是雪层厚度相对稳定. 原因是这段时间内降水量很少，温度较低，蒸发作用也很弱. 然而年际间的厚度变化可能是很大的. 2003 年的雪层厚度平均为 100cm，2004 年为 195cm，相差较大，其原因主要有 2 点：1）雪层厚度基数值不同. 2002 年是一个罕见的高温年，雪层大量消融，9 月初时雪坑厚度仅为 40cm 左右，2003 年气温正常，9 月初的雪层厚度在 180cm 左右. 2）降水量不同. 大西沟气象站的资料表明，2003 年 该时期降水量比 2002 年要大一些，前者为 15.3mm，后者为 10.3mm. 此外，在观测取样时为消除上次挖雪坑造成的局部小环境影响，会在观测时将雪坑壁挖进 20—30cm，这样也会对雪层厚度测量造成一定误差.

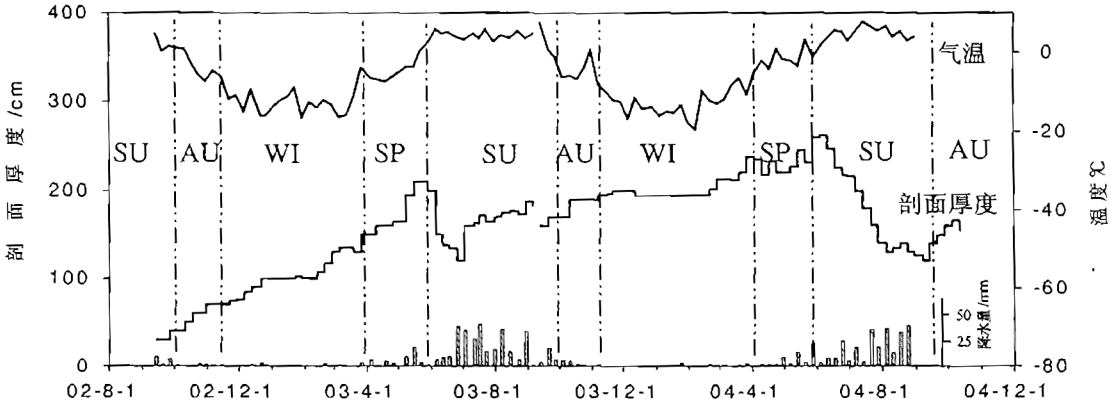

图 1 2002—2004 年雪层剖面厚度、气温、降水变化图

Fig.1 The variation of snowpit profile depth、temperature and precipitation at Daxigou Meteorologicaol station from 2002 to 2004

进入春季波动期后雪层厚度开始出现明显波动，但总的趋势是不断增加，到春末夏初，雪层厚度达到最大．成因主要有 2 个方面：1）此期间降水比冬季稳定期明显增加，同时温度出现波动，而且是在 0℃上下波动，造成消融程度不同．2）风吹雪造成的物质再分配对雪层厚度的影响．

到了夏季剧变期，降水开始增大，此期间集中了全年降水量的近 70%，是冰川得到补给最多的时期．但同期温度很高，消融量超过积累量，融水下渗有时可以穿过几个年层，甚至达到冰川冰表面．这种作用最直接的结果是雪层厚度减薄．从图中看出，6 月初的雪层厚度最大（2003 年为 210cm, 2004 年为 260cm），之后雪层开始剧烈消融，到 2003 年 7 月初时达到最薄值 120cm，之后又开始上升．2004 年的最薄值出现在 8 月 5 号（130cm），然后开始上升．

秋季波动期，降水量明显减小，气温相对于夏季剧变期已明显下降，同时也存在着波动，这也是秋季雪层厚度波动的主要原因．

从上面的分析看出，雪层厚度的变化总体上受气温和降水的共同作用，即厚度与气温呈反相关，与降水呈正相关．春季波动期间，雪层厚度受降水量的影响显著．进入夏季剧变期，随着气温的持续升高，尽管处于大降水量背景下也难阻挡雪层的强烈消融．这一现象说明，夏季剧变期时，气温是影响雪层厚度变化的主要因子．在秋季波动期，气温和降水量对雪层厚度的影响程度相当．进入冬季稳定期后温度较低，降水很少，雪层厚度相对稳定．一年之中，雪层最大厚度一般出现在 5 月底 6 月初，最小厚度一般出现在 7、8 月份．

3.2 粒雪的演化过程

3.2.1 粒雪化过程

完整的雪层剖面是由新雪、细粒雪、中粒雪、粗粒雪、污化层、冰片及冰透镜体等要素组成，其中粒雪是最主要的要素．

新雪降落在雪层表面，其形态不断的变化．首先表现在雪花六角表面上的微细构造（小沟、凹槽）消失，接着尖头部枝状缩短，孔隙减小，密度增大，随着时间的推移，逐渐演变成细粒雪.在融水和上部雪层的压力下，粒径进一步增大，密度增加，逐步向中粒雪和粗粒雪转化．最后，全部积雪层演变成粒径不同但层次分明的粒雪层剖面．粒雪化过程分为暖型和冷型两种作用．前者是在较低负温条件下进行的变质作用，后者是在温度接近或等于零度并有融水参与条件下进行的变质作用．已有的研究表明[16]，1 号冰川的粒雪化过程夏季以暖型变质作用为主，冬季以冷型变质作用为主．

在粒雪化研究过程中，我们利用竹板的层位跟踪功能，得到了图 2 所示的粒雪演变过程图．该图显示了粒雪密实化过程，黑色加粗直线在剖面中的位置表示竹板所代表的雪层层位．以 L_1 为例，竹板 L_1 在 03 年 9 月 13 日位于上部的细粒雪层，03 年 10 月 31 日位于中粒雪层，到 04 年 1 月 31 日即位于粗粒雪层，说明竹板 L_1 所在雪层到此已经完成了细粒雪到粗粒雪的演变，之后竹板 L1 处的粗粒雪继续向粒雪冰演化, 04 年 4 月 24 日、7 月 28 日竹板 L_1 分别到达距冰面 135cm、75cm 处．

从季节上说，夏季剧变期有融水参与，粒雪化过程以暖型为主，粒雪转化时间短，各层位下降的速率较快，尤其是雪层的上部．

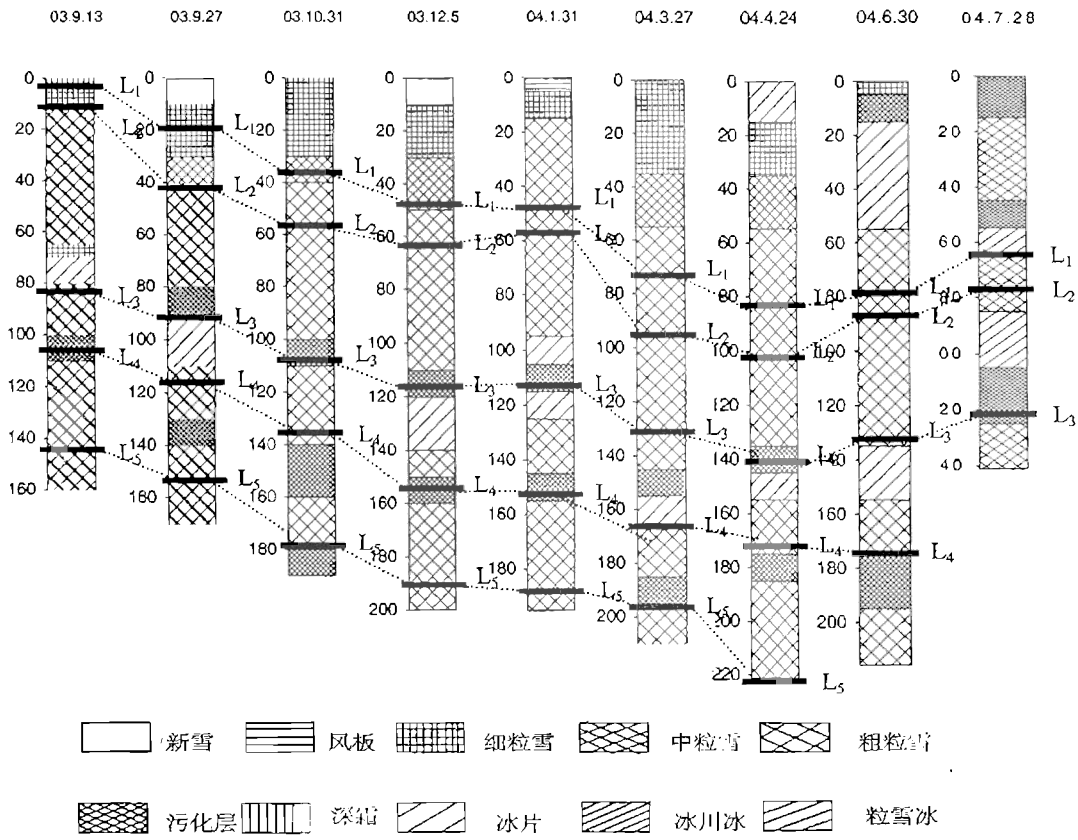

图 2 观测点雪坑剖面演变过程

Fig.2 Evolution of stratigraphic profiles of the snowpits at observation site

冬季稳定期温度较低，以 2003 年 2 月 6 号—3 月 6 号这段时间为例（表 2），在雪层 0cm 及 40cm 处气温较低，最高温也都在－10℃以下,粒雪化过程因此以冷型为主，粒雪转化过程慢，各层位下降速率慢.

表 2 冬季雪层温度变化情况

Table 2 Snow temperature variation in 2003 winter

项目 \ 时间		2003.2.6	2003.2.13	2003.2.20	2003.2.27	2003.3.6
0cm 温度	最高	-13.0	-12.5	-15.0	-10.4	-12.4
	最低	-29.5	-28.5	-25.5	-13.8	-31.3
40cm 温度	最高	-12.5	-11.0	-14.0	-14.1	-12.0
	最低	-17.0	-16.5	-22.3	-15.4	-15.4

春秋季波动期冷型变质作用与暖型变质作用相互交替，粒雪转化时间及各层位下降速

率介于二者之间．粒雪化类型的不同，造成粒雪转化时间具有明显的季节差异．研究发现（尤晓妮等，2004）：夏季剧变期时新雪转化为细粒雪的时间大约为 1 周，细粒雪到粗粒雪的时间为 2 个月；冬季稳定期时从“新雪”到细粒的演变时间大致为 2 个月左右的时间，从细粒雪到粗粒雪大致为 3～4 个月[26]．

3.2.2 粒雪组成的变化

过程研究中，我们十分感兴趣的是在粒雪化过程中，当雪坑剖面厚度发生变化时，粒雪组成是怎样变化的．下面我们定量讨论这一问题．图 2 给出了不同季节雪层各要素比例．从中看出，夏季剧变期粗粒雪所占的比例最大（70%），秋季波动期和冬季稳定期次之（65%，60%），春季波动期最小（55%）．新雪的情况则与粗粒雪相反，即春季波动期最大（9%），夏季最少（3%）．其它要素（冰片、深霜等）在夏季剧变期所占的比例最高（15%），秋春季波动期次之（12%，7%），冬季最小（3%）．其中，从春季波动期到夏季剧变期间，由于温度快速升高，雪层强烈消融，所以各要素发生的变化最大．其中，粗粒雪的比例增加了 15%，细粒雪和中粒雪由原来的 29%减少到 12%．表 1 给出了 2003 和 2004 年雪层厚度从最厚减到最薄这一过程中各要素的变化情况．从中看出，这两年雪层厚度减薄幅度分别为 90cm 和 132cm、其中新雪、细粒雪和中粒雪减少的幅度最大（2003 年共减少了 75cm，2004 年为 83cm），而粗粒雪变化的程度相对较小（2003 年为 15cm,2004 年为 33cm），归纳起来，雪层上部减少的程度最大，下部减少的程度相对较小．这一现象也表明,夏季消融主要发生在雪层上部的新雪、细粒雪中，而粗粒雪消融的比例较小．

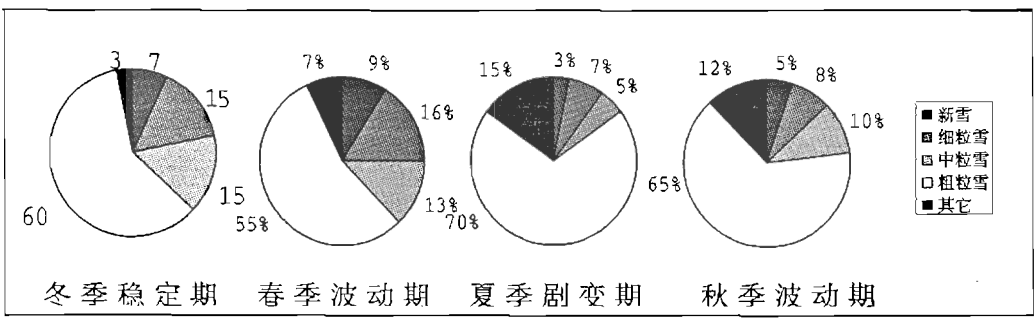

图 3 不同时期雪层中各要素的比例

Fig.3 The proportion of component at snow profile in different season

表 3 雪坑剖面厚度与雪坑内各组成成分厚度的关系

Table 3 The composition of snowpit with time

时间	雪层厚度	新雪	细粒雪	中粒雪	粗粒雪	其它成分
2003.5.16	210cm	20	40	40	105	5
2003.6.26	120cm	0	5	20	90	5
2004.6.4	262cm	0	45	40	160	17
2004.8.5	130cm	2	0	0	127	1

3.3 冰片变化

冰片是由表层积雪融水垂直下渗到一定深度时受阻而沿水平方向缓慢流动遇冷冻结而形成的. 在温度正常的年份，雪层中保存有不同时期形成的冰片. 2002 年是一个罕见的高温年，雪层消融十分强烈，因此上部的冰片几乎全部被消融掉. 图 4 显示出 2003 年 9 月 13 日—2004 年 10 月底这段时间内冰片的变化情况. 从中看出，从冬季稳定期到秋季波动期的演变过程中，冰片的数量先增加又急剧减少，其形成和分布具有明显规律性.

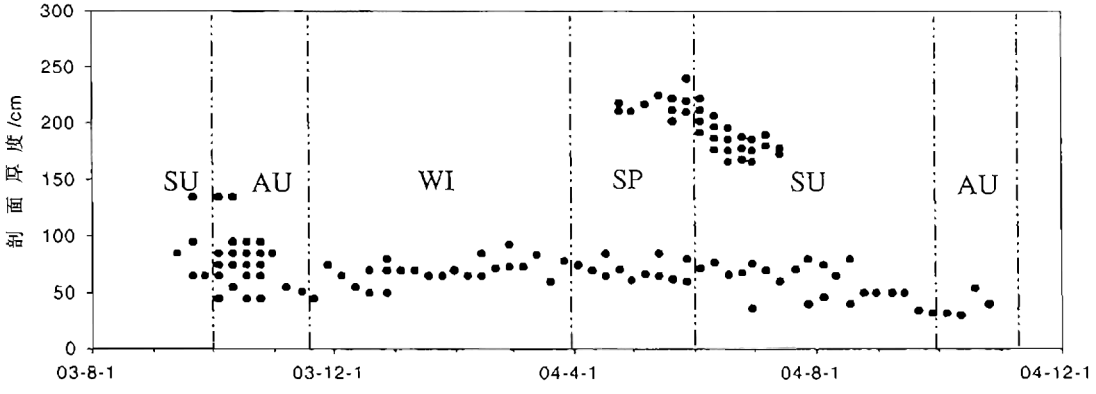

图 4 2003—2004 年观测雪坑内的冰片变化情况

Fig. 4 The variation of ice layer at observation site from 2003 to 2004

冬季稳定期的冰片相对稳定，主要集中在雪层下部的粗粒雪中. 春季波动期最显著特点是雪层上部出现了许多冰片，下部冰片的变化比较稳定. 上部冰片的出现是由这段时间的气温特点决定的，从图 5 中看出,2004 年春季气温的日较差大，且温度变化的范围在零摄氏度上下，这样便造成雪层表面白天有部分融化，夜晚这些融水被冻结成冰，在表面形成冰片. 下部冰片较稳定的原因主要有 2 点：1)春季雪层表面的温度不是很高，融水的影响程度仅限于表层，很难影响到下部的冰片. 2)上部新形成的冰片，密度较高、硬度较大，在雪层中相当于一个特殊的“隔板”，在一定程度上阻碍了上部热量、水分及其它物质向下部传输，保护了其下部的冰片. 进入 6、7 月份，温度开始升高，形成于春季的冰片随着雪层的消融，部分被消融掉，余下的则向下迁移. 与此同时，由于融水下渗程度的增加，再加上 6、7 月份的温度变化仍然具有春季波动期的特点（温度的日较差大、在零摄氏度上下波动），所以在雪层上部形成了更多的渗浸冰片，这些冰片与春季波动期相比不仅数量多而且厚度大. 进入 8、9 月份后，持续的高温造成雪层剧烈消融，存在于上部的冰片几乎全部被消融掉，下部冰片的位置也开始明显下移，随着上部融水的不断补充，其厚度也在不断增加. 夏季剧变期末保存下来的冰片到秋季波动期能否存在，主要取决于期间的温度及降水状况，2004 年这些冰片保存较好，2003 年则被大量消融. 所以每年保存下来的冰片数量是不确定的. 因此，在此若利用冰片对雪层及冰芯进行定年，缺乏科学性.

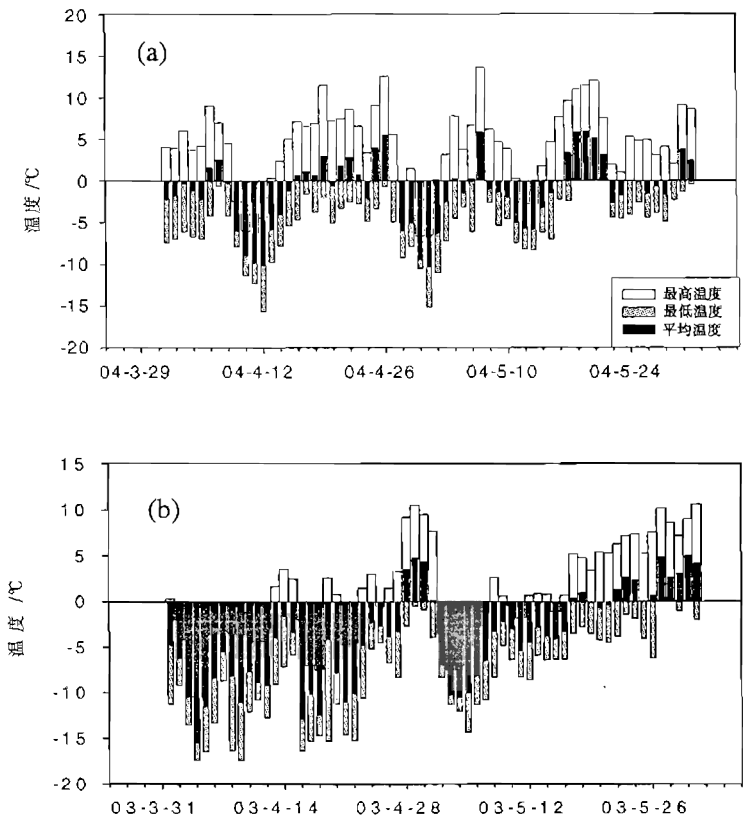

(其中 a 为 2003 年，b 为 2004 年)

图 5　春季温度变化情况

Fig .5　Temperature fluctuation in spring

3.4　污化层变化

3.4.1　污化层的形成

在许多山岳冰川中，污化层是颇为显著的标志，利用污化层进行年代确定是雪层乃至冰芯常用的定年方法之一.因此对污化层的形成及演化规律的研究具有重要的实际意义.前人按污化层形成季节将其分为冬春季污化和夏季污化[27]. 冬春季污化是由于冬季降雪很少，冰雪面长期暴露于空气中，在风力作用下，周围山体表面的风化碎屑物质迁移沉降于冰雪表面而形成，尤其是春季的沙尘天气将亚洲中部干旱-半干旱粉尘输送到冰川上来. 夏季污化是融水搬运污化物聚集于下部某一层位形成的，特别是在各特征层的交界面，例如细粒雪和粗粒雪之间. 研究发现，冬春季污化层由于污化程度很弱，有时并不能用肉眼观测到，如果有也会在春季甚至夏初的时候在雪层中有显现. 2003 年该污化层被观测到的时间为 4 月初，2004 年被观测到的时间为 6 月初，明显受到融水的加强. 夏季污化层的形成时间一般为 7、8 月份，污化程度重，颜色深.

3.4.2 污化层变化的影响因素

图 6 给出了 2002 年 9 月—2004 年 11 月的污化层变化情况. 从中看出，污化层具有明显的季节变化特征. 冬季稳定期污化层在位置和强度上相对稳定，春季波动期，随着气温的波动污化层也相应出现波动，夏季剧变期是一年中污化层变化最剧烈的时期，所有污化层急剧下移，既有新污化层形成，也有老污化层消失. 秋季波动期污化层继续下移后又趋于稳定.

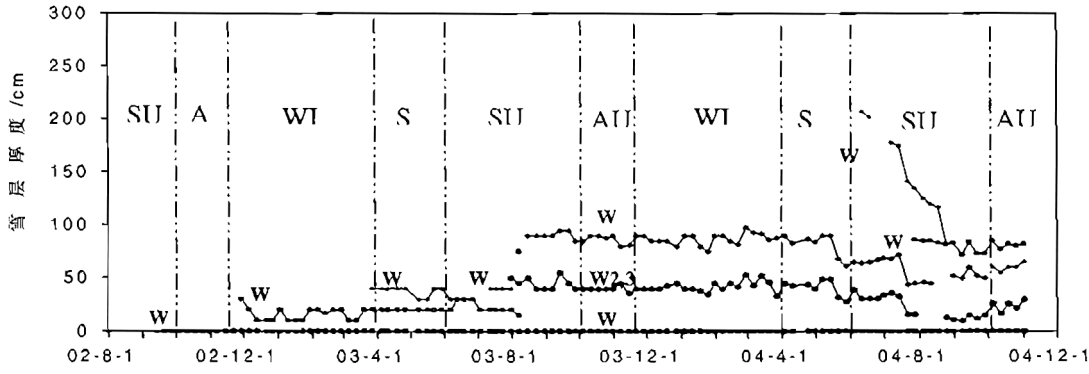

图 6 2002—2004 年污化层演变图

Fig.6 Evolution of dust layer from 2002 to 2004

影响污化层变化的因素很复杂，涉及到气温、降水、大气环流、冰川运动、太阳辐射及雪层自身压力等，在不同时段内各影响因素所起的作用不同. 冬季稳定期，整个雪层相对稳定，影响污化层变化的因素主要是雪层自身的压力及冰川的运动. 春季波动期，影响污化层的因素主要有 2 点，1）大气环流的强弱. 它决定着污化层的物质来源. 2）气温的高低. 这阶段气温开始升高，雪层上部产生了少量融水，融水会对新形成的污化层会有一定的影响. 夏季剧变期时，气温是影响污化层变化的最主要因素. 高温产生的大量融水，不仅造成了污化层的剧烈下移，同时也增加了下部污化层的强度. 在气温极高的年份，甚至会造成多条污化层的叠加，2002 年该现象最为显著. 秋季波动期，气温仍是影响污化层变化的主要因素.

3.4.3 污化层的演变过程

2002 年是一个罕见的高温年，雪层大幅度消融，最薄时仅为 30－40cm. 雪层处于积累的最初阶段，这为我们研究污化层的演变提供了很好的机会.

如图 6 所示，2002 年 9 月中旬时，雪层中只有一个污化层 W_1，该污化层是雪层强烈消融的产物，可能是 2002 年或 2001 年的多个污化层经消融后叠加形成的. 9 月份后，雪层仍有部分消融，物质经融水搬运后在 10 月底形成一个新的污化层 W_2，进入冬季稳定期后，雪面平均气温降至-10• 以下，整个雪层处于稳定的负温状态下，W_1 与 W_2 稳定. 2003 年 4 月时，冬季污化 W_3 在雪层中已明显的表现出来. 6 月份后雪层开始大量消融，新形成的污化层 W_3 与下部污化层 W_2 叠加在一起，并呈逐渐下移，8 月中旬 03 年的夏季污化层 W_4 也已形成. 9 月中旬后，雪层中的污化层稳定在 3 条，即 W_1、$W_{2,3}$、W_4. 此时观测雪坑的位置稍作调整，返回到 02 年 9 月 14 日时的最初位置，因此这三个污化层在雪层中的位置也相应的发生了变化. 自 2003 年 10 月到 2004 年 4 月这段时间，这三个污化层十分稳

定．04 年冬季污化因污化程度较弱，4、5 月份时在雪层中未被观测到，到 6 月中旬该污化层 W_5 才在雪层中显现，显然经过了夏季剧变期融水作用的改造，之后 W_5 与其它污化层一样在融水的作用下急剧下移，8 月初夏季污化层 W_6 形成，此后雪层急剧消融，8 月底污化层 W_5 叠加到 W_6 之上．10 月中旬后，雪层中的污化稳定在四个，即 $W_{1,}$、$W_{2,3}$、W_4、$W_{5,6}$．

3.4.4 污化层定年的基础

理想状态下，每年冬春季和夏季会有新污化层形成．经过夏季的强烈消融后，冬春季污化层一般会与下部的污化层相叠加，所以每年最终保存下来的污化层只有一个，即一个污化层代表一个年层．这种情况下，可以利用污化层对雪层乃至冰芯进行定年．

从现有的污化层资料看出，02 年雪层强烈消融，污化层正常的演变规律明显被打乱，夏末时雪层中只存在一个冰面污化 W_1．03、04 年污化层遵循正常的演变规律，这两年最终保存下来的污化层分别为 W_4 与 $W_{5,6}$．结合 02—04 年的污化层资料，可以对当前的雪层年限进行确定．在 2004 年 11 月初时，雪层中共有四个污化层（$W_{1,}$、$W_{2,3}$、W_4、$W_{5,6}$），根据 W_1 的形成时间为 2002 年或 2001 年，由此可以确定出雪层年限为 3～4 年．另外，通过竹板的方法（尤晓妮，2004），得到同期的雪层年限为 41～47 个月（3 年半～4 年）[26]，这与利用污化层定年的结果基本吻合，由此可以确定 1 号冰川积累区当前的雪层年限为 3～4 年．

从上面的分析中看出，污化层的形成和演变受多种因素的影响，其中气温的影响最大，因夏季（6-8 月）是一年中雪层消融最强烈的时期，故夏季平均气温在一定程度上能反映雪层消融的程度．从大西沟气象站 1959 年以来的气温资料看，2002 年的夏季平均气温（5.8℃）为近 45 年来的最高值，2003 与 2004 年的夏季平均气温（分别为 4.4℃，5.0℃）属于正常波动范围．所以在气温极高的年份（如 2002 年），污化层的数量和分布会受到强烈的干扰．

因此利用污化层对雪层及冰芯定年的方法具有一定的误差．若能解决气温—污化层变化模式，将会使该方法更具有科学性，这一模式的解决有待于进一步的观测研究．

4 对成冰量问题的讨论

夏季剧变期是 1 号冰川成冰的主要时期．成冰量的大小主要取决于两个因素：一是融水的渗浸程度，二是雪层的温度状况．由于这两个因素存在年际变化，所以成冰量也具有年际变化．下渗到雪层中的融水，大部分参与了对粒雪的改造，并冻结成冰，少部分沿冰面流失．

本项研究中，通过观测雪层下部粗粒雪的变化情况讨论夏季剧变期的成冰量问题．以 2004 年为例．选取污化层 W_3 作为参照面，从雪层剖面的柱状图中看出，2004 年 6 月 4 日时，W_3 下部的粗粒雪厚度为 27.0cm，6 月 25 日、7 月 28 日、8 月 31 日分别为 24.0cm、16.0cm、12.0cm.．进入到 9 月份后 W_3 下部的粗粒雪厚度稳定在 7.0cm 左右，即整个夏季剧变期 W_3 下部的粗粒雪共减少了 20.0cm，减少的这部分粗粒雪很可能绝大部分转变成粒雪冰．由于成冰量是一个诸多要素综合作用的结果，涉及到温度、冰川冷储及融水对粒雪的改造等因素．更准确的结果有待于进一步研究．

夏季剧变期形成后的粒雪冰经过一系列的动力变质作用，最后会转变成冰川冰，据王晓军等人的研究此过程大约需要 40—50 年的时间[11]．

5 结论

本项研究基于28个月的连续观测资料，对乌鲁木齐河源1号冰川积累区（海拔4130m）处的表面雪层演化成冰过程进行了专题研究，得出以下结论：

（1）雪层厚度的变化总体上受气温和降水的共同作用，即厚度与气温呈反相关，与降水呈正相关．雪层最大厚度一般出现在5月底6月初，最小厚度一般出现在7、8月．

（2）冰片是融水渗浸冻结的产物．春季波动期，雪层上部最容易形成冰片，到了夏季剧变期初，冰片在雪层大量形成．到夏季剧变期末时上部的冰片大多被融化掉，保存在下部的冰片相对稳定，这种状态一直持续到冬季．

（3）粒雪组成反映了粒雪化过程进行的情况，粗粒雪在夏季剧变期所占的比例最大，冬季稳定期次之，春季波动期最小．新雪的情况则与粗粒雪相反，即春季波动期最大，夏季最少．其它要素（冰片、深霜等）在夏季剧变期所占的比例最高，秋春季波动期次之，冬季最小．夏季雪层消融十分强烈，消融主要发生在雪层上部的新雪、细粒雪中，而粗粒雪消融的比例较小．

（4）污化层是雪层中颇为显著的标志层位，受气温的影响最显著．在一般年份，一年中最终只有一个污化层形成．在温度异常高的年份，污化层在雪层中的演变规律将会被打乱．

致谢：本项研究是天山冰川观测试验站开展的雪冰现代过程研究项目的一部分．是在全体观测和研究人员集体努力下完成的．没有观测人员长期全年度在冰川积累区的辛勤观测，便不会有本研究所需的第一手观测资料．谨此对参加本项研究的每一个观测人员以及项目组人员焦克勤，杨惠安，韩添丁，李向应，李传金，赵中平，钱军，张明军等表示衷心感谢．

参考文献

[1] Oerlemans.J,Anderson.B,Hubbard.A, *et al*. Modelling the response of glaciers to climate warming[J]. Climate Dynamics, 1998,**4**: 267-274.

[2] Meier, M.F. Contribution of small glaciers to global sea level[J]. Science, 1984,**226**, 1418-21.

[3] Shi Yafeng,Shen Yongping,Hu Ruji.Preliminary study on signal, impact and foreground of climate shift from warm-dry to warm-humid in the Northwest China[J].Journal of Glaciology and Geocryology,2002,**24**(3):220-226.[施雅风,沈永平,胡汝骥.西北气候由暖干向暖湿转型的信号、影响和前景初步探讨[J].冰川冻土,2002,**24**(3):220-226.]

[4] Li Zhongqin,Han Tianding,Jing Zhefan, *et al*. A summary of 40-year observed variation facts of climate and Glacier No.1 at the headwaters of Urumqi River,Tianshan,china[J].Journal of Glaciology and Geocryology,2003,**25**(2):117-123.[李忠勤,韩添丁,井哲帆,等.乌鲁木齐河源区气候变化和 1 号冰川 40a 观测事实[J].冰川冻土,2003,**25**(2):117-123.]

[5] Wang Xiaojun,Wang Zhongxiang,Xie Zichu.A Change trend of recent climatic on the Tianshan regions from the change of the past 28 years of the glacier No.1 at the Urumqi River headwater,Tianshan.Chinese[J] Science Bulletin,1988,**9**:693-696.[王晓军，王仲祥，谢自楚．从乌鲁木齐河源 1 号冰川二十八年来的变

化看天山地区近期气候变化趋势[J]，科学通报，1988，第 9 期. 693－696.]

[6] Li Zhongqin.A glacier melt water pool was discovered at summit of the east branch of the Glacier No.1 at Urumqi River head,Tianshan Mts.,Xinjiang[J]. Journal of Glaciology and Geocryology,2005,**27**(1),150-152. [李忠勤.天山乌鲁木齐河源 1 号冰川东支顶部出现冰面湖，冰川冻土[J]，2005，**27**（1）：150-152.]

[7] Qing Dahe.Desification process of snow firn in the surface layer of the Antartic ice. Journal of Glaciology and Geocryology 1987 [J]，9（3）:193-204.[秦大河.南极冰盖表面层内雪的密度化过程，冰川冻土[J]1987，9（3），193-204.]

[8] Xie Zichu. Snow Stratigraphy and Ice Formation on Law Dome, Antarctica. Journal of Glaciology and Geocryology[J]. 1984，**6**(1)：1-21.[谢自楚.南极洲洛多姆冰帽学的地层学及成冰作用研究[J].冰川冻土，1984，6(1)：1-21.]

[8] Shi Yafeng,Huang Maohuan,Ren Binghui.An introduction to the Glaciers in China Contents[M].Bingjing Science Press,1988,55-65.[施雅风,黄茂桓，任炳辉.中国冰川概论[M].科学出版社,1988, 55-65.]

[10] Huang Maohuan,Si Yafeng.Progress in the Study on Basic Features of Glaciers in China in the Last Thirty Years[J]. Journal of Glaciology and Geocryology, 1988,10(3):228-237.[黄茂桓,施雅风.三十年来我国冰川基本性质研究的进展[J].冰川冻土,1988,10(3):228-237.]

[11] Yao Tandong, Pu Jianchen, Wang Ninglian et al., A new type of ice formation zone found in the Himalayas. Chinese Science Bulletin [J], 1998, Vol.43 No1: 94-97.[姚檀栋，薄健辰，王宁练，田立德，1998.中国境内又一种新成冰作用的发现，科学通报[J]43（1）：94-97.]

[12] Xu Baiqing, Yao Tandong,a study on the air-bubble formation process at altitude of 7100m a.s.l.intheDasuopu glacier .Journal of Glaciology and Geocryology [J] 21（2）：120-124.[徐伯青，姚檀栋，1999.达索普冰川海拔 7100m 处气泡封闭过程研究.冰川冻土[J].21（2）：120-124.]

[13] Xie Zichu, snow and ice formation process in northern xixiabangma peak. Investigtation reports in xixiabangma area.1982.science press[C].45-59.[谢自楚，1982a，希夏邦马峰北坡的积雪和成冰作用.见：希夏邦马峰地区科学考察报告[C].北京：科学出版社 45-59.]

[14] Xie Zichu,Wang Zongtai.ice formation process in northern Everest area. Investigation reports in Everest area[C] 8-13.[谢自楚，王宗太.1975a.珠穆朗玛峰地区北坡成冰作用.见：珠穆朗玛峰地区科学考察报告[C]（1966～1968）.8-13.]

[15] Xie Zichu,*et al.*ice formation process in glacier of Qilan montain.[谢自楚，伍光和等.祁连山冰川的成冰作用中国科学院兰州冰川冻土所集刊，1984，5：27-40.]

[16] Xie Zichu,Huang Maohuan.A evolution of the snow-snowgrains layer and ice formation in the Glacier No.1 at the headwaters of the Urumqi River,Tianshan[A].An studies of glaciology and hydrology on the Urumqi River,Tianshan[C].Science Press,1965,1-14.[谢自楚,黄茂恒. 天山乌鲁木齐河源 1 号冰川雪-粒雪层的演变及成冰作用[A].天山乌鲁木齐河冰川与水文研究[C],科学出版社,1965,1-14.]

[17] Wang Xiaojun, Zhang Jinhua, *et al.*Obersavation on the stratification of snow and accumulation in the accumulation area of Glacier No.1 at the head of Ürümqi River[R]. Annual Report on the Work At Tianshan Glaciological Station.1980-1981.11-15.[王晓军，张金华等.乌鲁木齐河源 1 号冰川积累区雪层剖面和积累量的观测[R].天山川观测实验站年报. 1980-1981：11-15.]

18] Wang Xiaojun, Wang Zhongxiang, Wang Chanson. Stratigraphic and Structural Analysis on An Ice Core to the Bedrock in the Accumulation Area of Glacier No.1 at the Headwatgers of Ürümqi River. Journal of Glaciology and Geocryology[J]. 1996.**18**(4):337-346.[王晓军 王仲祥 王纯足.乌鲁木齐 1 号冰川的积消特征及成冰过程. 冰川冻土[J].1996. 18(4):337-346.]

19] Liu Chaohai, Xie Zichu,Wang Chunzu .A Research on the Mass Balance Processes of GlacierNo.1at the Headwaters of the Ürümqi River, Tianshan Mountains. Journal of Glaciology and Geocryology[J].1997,19(1): 17-24.[刘潮海,谢自楚,王纯足. 天山乌鲁木齐河源 1 号冰川物质平衡研究[J]. 冰川冻土.1997，**19**(1)：17-24.]

20] Jiao Keqin,Jing Zhefan,Han Yianding, *et al.* Variation of the Glacier No.1 at the headwaters Of the Urumqi River in the Tianshan mountains during the Past 42 Years and Its Trend Prediction[J].Journal of Glaciology and Geocryology,2004,**26**(3):253-259.[焦克勤，井哲帆，韩添丁，等. 2004，42 a 来天山乌鲁木齐河源 1 号冰川变化及趋势预测.冰川冻土，**26**(3)：253-259.]

21] Yang Daqing,Jiang Tong,Zhang Yinsheng, *et al.* Analysis and correction of errors in precipitation measurement at the heat of the Urumqi River,tianshan[J].Journal of Glaciology and Geocryology, 1988,**10**(4):384-399.[杨大庆,姜彤,张寅生,等.天山乌鲁木齐河源降水观测误差分析及其修正.冰川冻土,1988,**10**(4):384－399.]

[22] Wang Dehui,Zhang Paiyuan.On the valley climate of Urumqi River in the Tianshan Mountains [J]. Journal of Glaciology and Geocryology,1985,**7**(3):239-248.[王德辉，张怀远.天山乌鲁木齐河谷气候特征[J].冰川冻土,1985,**7**(3)239-248.]

[23] C•B• ÊÀËÑÍ È, Î ×ÅÐÊÈ ÃËß ÖÈÈ[C].1982.[C•B•卡列斯尼克，冰川学概论，中国科学院兰州冰川冻土研究所.1982.]

[24] C•B• ÊÀËÑÍ È, Î ÁÙ Àß ÃËß ÖÈÎ ÃÈß[C].1965.[C•B•卡列斯尼克，普通冰川学，中国科学院地理研究所冰川冻土研究室.1965.]

[25] W.S.B.Paterson. The Physics of Glaciers. Science Press. 1987:8.[W.S.B.佩特森.冰川物理学.科学出版社.1987：8.]

[26] You Xiaoni，Li Zhongqin,Wang Feiteng. Study on Time Scale of Snow - Ice transformation throughSnow Layer tracing method-Take Glacier No.1 at the Headwaters of Ürümqi River as an Example[J]. Journal of Glaciology and Geocryology,2004,**27**:In press.[尤晓妮，李忠勤，王飞腾.利用雪层层位跟踪法研究暖型成冰作用的年限问题-以乌鲁木齐河源 1 号冰川为例[J],冰川冻土，2005，**27**:待发.]

[27] Wang Xiaojun, Han Jiankang, Xie Zichu,*et al.*stratigraphic and structural analysis on an ice coretothebedrock in the accumulation area of glacier No.1 at the headwaters of Ürümqi River. Journal of Glaciology and Geocryology [J] **18**（4）：337-346.[王晓军，韩健康，谢自楚，Lluberas A,1996.乌鲁木齐河源 1 号冰川积累区透底冰芯底层及冰结构分析.冰川冻土[J]，**18**（4）：337-346.]

Snow to Ice Evolution Process Observation and Study at Percolation Zone on Glacier No.1 at Urumqi River Head, the East Tianshan, China

Wang Feiteng, Li Zhongqin,You Xiaoni

Tianshan Glaciological Station/Key Laboratory of Ice Core and Cold Regions Environment, CAREERI, CAS, Lanzhou Gansu 730000, China)

Abstract: Physical process of snow to ice transformation is one of important research contents in Glaciology. However, most previous studies on Glacier No.1 focused mainly on properties of the snow profiles, rather than the process due to lack of long-term field observation archive. The currently launched PGPI (the Program for Process Investigation) provides a unique opportunity to observe this evolution process and to trace every change in snow-firn pack at PGPI observation and experimental site on Glacier No.1, which in turn made a great contribute to PGPI.

During PGPI field campaigns from 2002 through to 2004, about 110snow/firn stratigraphy profiles (in weekly interval) were obtained at PGPI site (4130m a.s.l., in the percolation zone), and from where various physical measurements or observations have been made simultaneously, which allows us to delicately analyze the evolution process. In our study, particular effort was contributed to those visible layers on snow-firn stratigraphy, such as different sized firn, dust layers ice layers, etc., by tracing their evolution process over time. The results have reveled enormous details of these processes over the two-year period. It is founded that percolation of meltwater has a definitive impact on the transformation process at the site. Ice formation process in a year can be divided into four periods depending on features of the process: winter steady period, spring fluctuation periods, summer intense period and autumn fluctu- ation period. Different periods have been discussed respectively in the paper.

Key words: The east Tianshan; Glacier No.1; evolution process

离子色谱法测定大气气溶胶中的可溶性离子

赵中平，李忠勤

(中国科学院寒区旱区环境与工程研究所天山冰川观测试验站，兰州 730000)

E-mail:zhaozz902@yahoo.com.cn

摘　要：以新疆天山乌鲁木齐河源 1 号冰川上采集的大气气溶胶样品为例。主要就滤膜选取、样品采集、提取方法、分析技术、污染防范等方面进行了介绍，给出了离子色谱法分析中的检测限和不确定值。这种方法和技术同样适用于测定其它偏远高山地区和极地地区大气气溶胶中的可溶性成分。

关键词：离子色谱；气溶胶；可溶性离子

1　引言

大气气溶胶是指大气与悬浮在其中的固体和/或液体微粒共同组成的多相体系。由于它吸收或散射太阳辐射，并在云层中起重要的理化作用，因而在驱动气候环境变化中扮演着极为重要的角色。全球变化研究中，对气溶胶的研究主要通过采集不同区域，不同海拔高度大气层气溶胶样本，研究其物理化学特性，将所得信息代入各种气候环境模式，分析其对气候环境的影响。亦根据各种气溶胶的排放预测，通过相关模式研究对未来气候环境变化的贡献[1]。

离子色谱法广泛应用于冰雪和冰芯样品中各种阴、阳离子的测定[2-5]，但对含量极低、易污染的偏远高山地区和极地地区大气气溶胶中的可溶性离子的分析报道不多。本文以在海拔4100米的新疆天山乌鲁木齐河源1号冰川上采的气溶胶样品为例，主要就滤膜的选取、样品的采集、提取方法及污染的防范进行介绍，选用离子色谱法对大气气溶胶中的可溶性离子进行分析，得到了满意的结果。

2　滤膜的选取

由于滤膜在生产和运输过程中，往往带来一些可溶性的离子，因此在采样前需对各种滤膜进行空白值的测定，以选取本底值较低的滤膜作为采样滤膜。本次实验用 Pall Corporation 生产的 Zeflour Teflon 膜（直径 47mm,孔径 2 m）和 Whatman 公司生产的 glass microfiber filter(玻璃微纤维膜，直径 90mm)进行空白值的比较，两者均为刚开启的新膜，结果列于表 1。对 Zeflour Teflon 膜，首先用 200μl 色谱纯乙醇（或甲醇）完全润湿,之后用 25ml 去离子水提取，用超声波振荡 30 分钟，溶液直接用于离子色谱分析[6, 7]。而对 Whatman 膜，首先要用 25ml 氯仿饱和过的去离子水提取，之后在室温下放置 24 小时[8]。加入氯仿的目的是抑制潜在的细菌活动。溶液用 0.45μm 微孔过滤器过滤后才能用于分析。

表 1 Teflon 和 Whatman 膜空白值比较(μg/L)

table 1 Comparison of the blank values of Teflon and Whatman filters

Species	F^-	Cl^-	NO_2^-	Br^-	NO_3^-	SO_4^{2-}	Na^+	NH_4^+	K^+	Mg^{2+}	Ca^{2+}
Teflon	8.1	24.9	36.6	38.2	51.9	16.5	2.6	11.8	2.4	0.1	6.5
Whatman [1]	322	6190	40	479	56	68	7050	59.8	515	61	320
Whatman [2]	267	6032	39	387	38	59	6930	3.6	473	42.7	290

注： 1)用去离子水提取； 2)用氯仿饱和过的去离子水提取

考虑到 Whatman 滤膜的面积是 Teflon 滤膜的一倍多，Whatman 膜的空白值中 NO_2^-、NO_3^-、SO_4^{2-}和 NH_4^+与 Teflon 膜中的含量差不多，或稍小一些。而 K^+、Cl^-、Mg^{2+}和 Na^+的含量分别是 Teflon 膜的 200、250、400 和 2600 倍。造成 Whatman 滤膜中这些离子含量偏高的原因可能是滤膜需要进行前烘烧处理，或背景值本来就高，或者滤膜已经被污染，。从表 1 还可看出，Whatman 膜的空白值在加入氯仿之后得到不同程度的降低，说明细菌的活动还是有相当大的影响，不能忽视。因此，应选择背景浓度低的 Teflon 膜作为采样滤膜。

3 样品的采集

本次所用的采样器为美国 New Hampshire 大学设计生产的小流量采样器，包括采样头、直流抽气泵、体积流量计、太阳能电池板、蓄电池等。采样体积用在线体积流量计测量，采样期间每隔 1h 测量 1 次大气压和温度值，用以计算流经滤膜的空气的标准体积（标准状态，1 大气压，0℃）。

流速是气溶胶采样过程中最重要的一环。流速与气流入口的恰当匹配才能保证不同尺度、不同形状、不同化学成分的粒子能机会均等地到达相应的收集器，流速与收集器结构的恰当匹配才能保证各个收集器的收集效率大致相同。本次采样时的平均流速为 1.58m^3/h，线流速为 25.3cm/s。这种流速使得孔径为 2μm 的 Teflon 滤膜对粒径大于 0.035μm 的粒子的收集效率大于 97%[9]。气溶胶样品的抽气量在 5m^3到 10m^3不等，主要取决于天气状况[10]。在降雨/雪和浓雾天气下没有采集样品。

滤膜在净化实验室 100 级超净工作台上用外科手术专用的不锈钢镊子装入采样头，采样时采样膜离雪面 1.5m,面朝下；采样结束后，将采样头装入干净的塑料袋内，在超净工作台上将膜用不锈钢镊子从采样头中取出，采样面朝上置于预先用去离子水清洗干净的样品瓶中，拧紧并将样品瓶装入塑料袋中，分析前置于 4℃恒温避光保存。用色谱纯乙醇将采样头和不锈钢镊子冲洗干净，在超净工作台上晾干后装入新的滤膜。

尽管在取样和分析中采取了严格的污染控制措施，但由于样品制备、测试过程中不可避免地要与空气接触，其微量污染可能存在。也即很难保证测定结果中完全没有污染的影响。空白样品的测试可以定量地评估这种污染的种类和大小。野外空白 Teflon 滤膜的采集过程与样品完全一样，也是先装入采样头，拿到野外进行采样（不抽气），之后取出并置于干净的样品瓶中，4℃恒温避光保存。本次实验共取了 5 个野外空白样品和 2 个实验室空白样品，以估计样品采集和分析过程中所带来的污染物种类和大小。

已有研究表明，在气溶胶采集过程中，无论是使用多层滤器还是溶浊器都会产生后生现象[11,12]。根据后生现象对气溶胶浓度的贡献可分为正负两种。正的后生现象一般源于采

样过程中大气中的气体与滤膜或/和已收集的颗粒物反应；而负的后生现象一般源于所收集的颗粒物的挥发分解。在本次采样过程中，由于较低的温度（采样点常年在 0℃以下）和较短的采样时间（3-6 小时），样品中的后生现象可以忽略不计[13]。

4 污染的防范

为减少污染，采样时应迎风操作，附近有人为的活动（如观光、旅游等）时不能取样。在取样和分析过程中，操作人员应穿上特制的工作服，戴上面具和一次性塑料手套。所有的样品瓶、取样工具以及可能接触到样品的东西均用去离子水清洗干净。清洗过程包括三步，首先冲洗三遍，之后在去离子水中浸泡一周，使用前再清洗三遍[3]。洗完的器具要用离子色谱检查是否清洗干净

5 实验部分

5.1 仪器和试剂

Dionex-320 离子色谱仪，配有电导检测器和 PeakNet5.11 色谱工作站。超声波清洗器，用于样品溶解、流动相脱气和玻璃器皿清洗。

F^-，Cl^-，NO_2^-,Br^-,NO_3^-,SO_4^{2-},Na^+,NH_4^+,K^+,Mg^{2+}和 Ca^{2+}标准溶液均购自国家标准物质研究中心，$HCOO^-$标准采用由 Aldrich 化学公司生产的 AccuIon™ IC-FORM-1X-1 国际标样。甲醇为色谱纯，其它试剂均为国产优级纯。参考以前孙俊英等人的数据[6]分别配制成阴、阳离子混合标准储备液，分析时实行五点校正。NaOH 淋洗液首先由经超声真空脱气的去离子水配制成 50%NaOH 储备液，使用时再用吸液管从储备液中取其中间部分来作稀释，由此可减小空气中 CO_2 的影响[14]。所有的标准溶液和储备液均置于 4℃恒温保存。实验用水均使用电阻率为 18.2MΩ.cm 的去离子水。

5.2 色谱条件

阳离子：Dionex IonPac CS12A(4×250mm)分离柱，CG12A(4×50mm)保护柱；CAES 阳离子抑制器，抑制电流 65mA；15mmol/L MSA 淋洗液，流速为 1.0ml/min；进样量为 200μL；电导检测；以峰面积定量；室温条件下操作。

阴离子： AS11-HC (4×250mm)分离柱，AG11-HC(4×50mm)保护柱；ASRS-4mm 抑制器,抑制电流 52mA；15mmol/L NaOH 淋洗液，流速为 1.40ml/min；进样量 200μL；柱温为 30℃时操作。

5.3 样品的提取

气溶胶样品一般用去离子水和超声波提取。滤膜的表面积与需要的去离子水体积通常保持在 $1.5cm^2.ml^{-1}$ 左右[15]。Teflon 滤膜的提取首先要用甲醇（或乙醇）润湿，而对于 nylon 滤膜，用 PH 为 8.00 的 NaOH 溶液直接进行超声提取[16]。

Teflon 滤膜主要用于气溶胶中常见的无机阴、阳离子和简单的有机阴离子(如 $HCOO^-$、CH_3COO^-和 $C_2O_4^{2-}$)的分析,而石英滤膜常用于水溶性有机物的分析[17]。水溶性有机物主要包括：二元羧酸、酮酸、二羰基化合物、长碳链的脂肪酸和短链的一元羧酸等[18]。石英滤膜采用二氯甲烷做提取剂，冰水混合物和超声波提取，以减少挥发性有机物的损失[19]。

5.4 色谱条件的选择

5.4.1 色谱柱的选择

比较了 3 种阴离子交换色谱柱（IonPac AS4A-SC,AS16 和 AS11-HC)对 8 种阴离子（F^-

$HCOO^-$,Cl^-,NO_2^-，Br^-,NO_3^-,SO_4^{2-}和PO_4^{3-}）的分离情况。AS4A-SC 柱的离子交换容量较低，不宜作高浓度基体样品的分离，且 F^- 峰与死体积峰分离不满意。Br^- 和 NO_3^- 在亲水性强的 AS16 柱上的色谱行为相似，不能完全分离。AS11-HC 柱的离子交换功能基为烷醇基季铵，其离子交换容量较 AS4A-SC 和 AS16 大的多，亲水性较强，对 OH^- 选择性也强。OH^- 是一种非常易水合的离子，容易进入水合区，能有效地置换其它阴离子。因此在 AS11-HC 柱上用含有较低浓度 OH^- 的溶液作淋洗液，即可有效地洗脱各种阴离子，避免了使用高浓度 OH^- 的淋洗液和有机改进剂，自动抑制器也可以使用循环模式，使操作简单。

阳离子分离柱选用填充弱酸功能基的 CS12A 型柱，一次进样同时分析碱金属.碱土金属和铵[14]。

5.4.2 淋洗液洗脱条件的选择

采用 AS11-HC 分离柱，NaOH 做淋洗液，淋洗液浓度的变化对不同电荷的阴离子保留时间的影响是不同的，一价淋洗离子浓度的变化对两价溶质离子保留时间的影响比对一价溶质离子保留时间的影响大[20]。所以，不同的 NaOH 淋洗液浓度将会影响 NO_3^-和 SO_4^{2-} 的淋出顺序，使用 10mmol/L NaOH 淋洗时，NO_3^-先于 SO_4^{2-}流出分离柱，8 种阴离子均得到很好的分离，但 PO_4^{3-}的保留时间太长，色谱峰也会变宽。而使用浓度较大的 NaOH 做淋洗液时（如大于 20mmol/L），NO_3^-在 SO_4^{2-}后被淋出，且和 Br^-三个峰叠加在一起，分离不好。选用 15mmol/L NaOH 时，各种离子均能很好的分离，分析时间也比较短。另外可通过适当增加流速来缩短分析时间，但是流速的增加受分离柱最大操作压力的限制。候艳文等人[21]通过研究表明，随着淋洗液流速增加，不论用峰高还是峰面积定量，检测灵敏度都有不同程度的降低，尤其用峰面积定量时，峰面积随流速的增加而降低的现象更明显。本实验通过多次试验，最后选择 1.40ml/min 为最佳。这样，可在 12 min 内通过一次进样检测出 F^-,$HCOO^-$,Cl^-,NO_2^-，Br^-,NO_3^-,SO_4^{2-}和 PO_4^{3-}8 种阴离子，如图 1 所示。

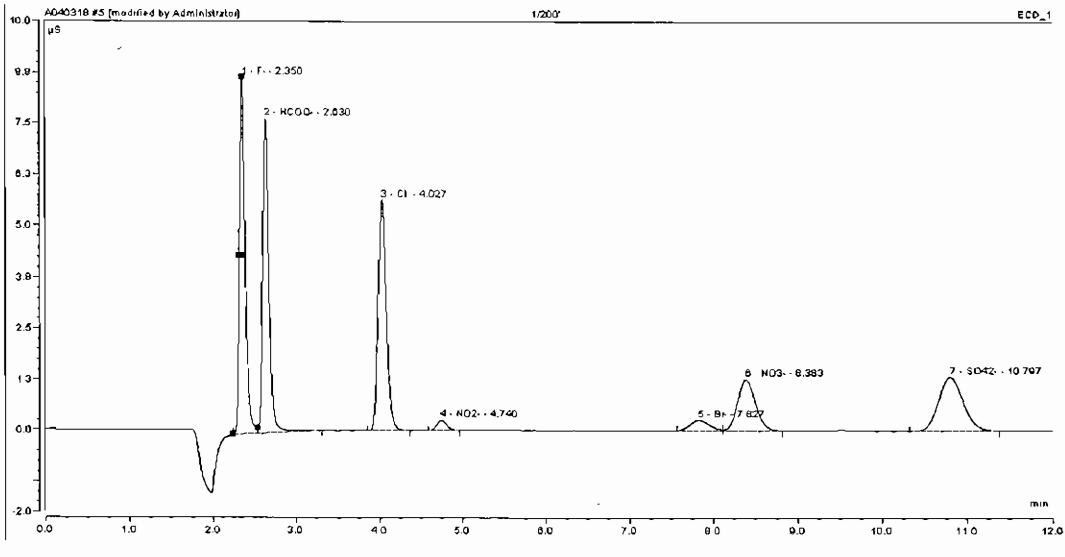

图 1 标准溶液的阴离子色谱图

Fig.1 Anion chromatogram of standard solution

用 15mmol/L MSA 做淋洗液，Na^+,NH_4^+,K^+,Mg^{2+}和 Ca^{2+}5 种阳离子在 15min 内得到很好的分离。在此淋洗强度下，互相干扰的 Na^+和 NH_4^+得到了解决，且使 Ca^{2+}和 Mg^{2+}之间有较小的峰间距，从而缩短分析时间，如图 2 所示。

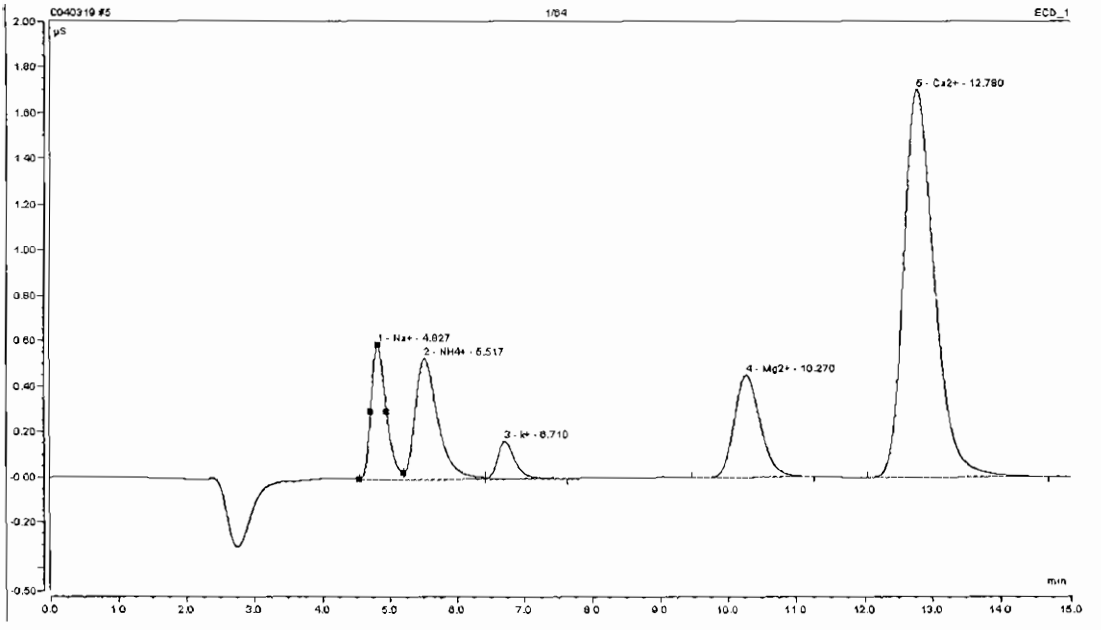

图 2 标准溶液的阳离子色谱图

Fig.2 Cation chromatogram of standard solution

5.5 实际样品的分析及各种离子的检测限和不确定性

实际样品的分析过程与标准液一样，表 2 为样品中各种离子的浓度、检测限和不确定值。样品中离子的检测限定义为所有空白样品中离子的标准偏差的两倍除以所采集的样品的平均抽气量(Talbot et al.1986)[22]。气溶胶中各种离子的检测限分别为（单位：neq/m^3）：Na^+(0.144), NH_4^+(0.030), K^+(0.032)，Mg^{2+}(0.003), Ca^{2+}(0.019), F^-(0.035), Cl^-(0.049), NO_2^-(0.043), Br^-(0.045), NO_3^-(0.027), SO_4^{2-}(0.036)。7 个空白样品中各种离子的空白值一直在变化（$HCOO^-$除外，它在 7 个空白样品中未能检测到），特别是 Na^+, NH_4^+, K^+, F^-和 Cl^-5 种离子的变化幅度更大，说明野外取样和实验分析过程中对这 5 种离子造成的污染程度最大。所有的样品浓度中均应扣除 7 个滤膜的平均空白值，由此导致一些样品中的 NH_4^+, F^-和 Br^-低于检测限。

表 2 实际样品中各种离子的浓度、检测限和不确定值的比较（neq/m^3）

table 2 Compasion of concentrations, detection limits and uncertainty of the soluble species in aerosols

	F^-	Cl^-	NO_2^-	Br^-	NO_3^-	SO_4^{2-}	Na^+	NH_4^+	K^+	Mg^{2+}	Ca^{2+}
样品浓度	1.2	4.0	2.99	1.2	2.84	12.2	4.51	10.46	0.79	1.1	14.48
检测限	0.035	0.049	0.043	0.045	0.027	0.036	0.144	0.030	0.032	0.003	0.019
不确定值	0.049	0.050	0.051	0.049	0.061	0.079	0.154	0.053	0.035	0.004	0.040

气溶胶中主要离子浓度的不确定性与离子在空白样品中的变化率和在色谱分析中的精密度有关（Miller and Miller,1988）[23]。本实验中样品平均的不确定值为（单位：neq/m^3）：Na^+(0.154), NH_4^+(0.053), K^+(0.035), Mg^{2+}(0.004), Ca^{2+}(0.040)，F^-(0.049), Cl^-(0.050), NO_2^-(0.051), Br^-(0.049), NO_3^-(0.061), SO_4^{2-}(0.079)。

采用标准加入法，平行测定 3 份样品中的各种离子浓度，计算所得的平均回收率在90%－106%。

6 结论

采用上述大气气溶胶样品的采集方法及实验分析技术，使得测定气溶胶中可溶性成分的检测限和不确定性问题得到很好的解决。南、北极和青藏高原等地区气溶胶中各离子的浓度是本实验中其离子的检测限或不确定值的十倍至上百倍[24]，但采用该套仪器和方法，在偏远地区进行大气气溶胶的采集和分析，仍可获得满意的分析结果。

参考文献：

[1] J.T.Houghton, Y.Ding, D.J.Griggs,et al. Intergovernmental Panel on Climate Change 2001,Climate Change 2001. The Pitt Building,Trumpington street,Cambridge,United Kingdom: The Press Syndicate of the university of Cambridge, 2001

[2] J.P.Steffensen. Analysis of the seasonal variation in dust ,Cl^-,NO_3^-,and SO_4^{2-},in two Central Greenland firn cores. Ann. Glaciol. ,1988,10: 171

[3] C.F.Buck,P.A.Mayewski,M.J.Spencer, et al. determination of major ions in snow and ice cores by ion chromatography. J. Chromatogr.,1992,594:225-228

[4] M.Legrand,M.De Angelis,F.Maupetit et al. Field investigation of major and minor ions along Summit(Central Greenland)ice cores by ion chromatography. J. Chromatogr.,1993,640:251

[5] A.Doscher, M.Schwikowski, H.W.Gaggeler. et al. Cation trace analysis of snow and firn samples from high alpine sites by ion chromatography. J. Chromatogr.A,1995, 706:249

[6] Junying Sun,Dahe Qin,Paul A.Mayewski,et al. Soluble species in aerosol and snowand their relationship at Glacier 1,Tien Shan,China. Journal of Geophysical Research,1998,103(D21):28022-28027

[7] Arun B. Shrestha, Cameron P.Wake and Jack E. Dibb, Chemical composition of aerosol and snow in the high Himalaya during the summer monsoon season. Atmospheric Environment., 1997,31(17):2815-2826

[8] Tarja Yli-Tuomi,Lisa Venditte,Philip K.Hopke,et al. Composition of the Finnish Arctic aerosol: collection and analysis of historic filter samples. Atmospheric Environment, 2003,37: 2358

[9] Liu,B.Y.H.,D.Y.H.Pui, and K.L. Rubow. Characteristics of air sampling filter media. In aerosols in the mining and industrial work environments, Vol. 3, Instrumentation(ed. By Marple V.A. and Liu B.Y.U.), Ann Arbor Science,MI, 1984:989-1037

[10] 候书贵. 乌鲁木齐河源区大气降水的化学特征. 冰川冻土，2001，23（1）：80-84

[11] Pierson, W.R., R.H. Hammerle and W.W. Brachaczek, Sulfate formed by interaction of sulfur dioxide with filters and aerosol deposits..Analytical Chemistry,1976,48:1808-1811

[12] Lipfert, F.W.,Filter artifacts associated with particulate measurements: recent evidence and effects on statistical relationships. Atmos. Environ., 1994, 28:3233-3249

[13] Arun B. Shrestha, Cameron P. Wake, Jack E. Dibb. et. al. Seasonal variations in aerosol concentrations and compositions in the Nepal Himalaya. Atmos. Environ. 2000, 34:3349-3363

[14] MOU Shi-fen,LIU Ke-na. The Principle and Application of Chromatography. Beijing: Chemical Industry Press,2000 .77～108〔牟世芬，刘克纳. 离子色谱方法及应用. 北京：化学工业出版社，2000. 77～108〕

[15] Cort Anastasio, Andrea L.Jordan. Photoformation of hydroxyl radical and hydrogen peroxide in aerosol prticles from Alert,Hunarut:implications for aerosol and snowpack chemistry in the Arctic. Atmos. Environ. 2004.,38:1153-1160

[16] Susanne Preunkert, Dietmar Wagenbach, Michel Legrand. Improvement and characterization of automtic aerosol sampler for remote(glacier)sites. Atmos. Environ.,2002,36:1221-1231

[17] Barbara J.Turpin, Pradeep Saxena, Elisabeth Andrews. Measuring and simulating particulate organics in the atmosphere: problems and prospects.Atmos. Environ.,2000,34:2983-3000

[18] 许士玉，胡敏. 气溶胶中的水溶性有机物研究进展. 环境科学研究，2000，13（1）：50-53

[19] Celia Alves, Casimiro Pio, Armando Duarte. Composition of extractable organic matter of air particles from rural and urban Portuguese areas. Atmos. Environ.,2001,35:5485-5496

[20] 崔鹤，牟志春，毛旭斌等. 离子色谱法测定碳酸盐的无机阴离子. 分析化学，2002，30（8）：1020

[21] 候艳文，牟世芬，候小平等. 阴离子交换色谱中淋洗液流速对测定灵敏度影响的讨论. 色谱，1998，16(4):348

[22] Talbot,R.W., Harris, R.C., Browell,E.V., Gregory, G.L., Sebacher, D.I. and Beck, S.M. Distribution and geochemistry of aerosols in the tropical North Atlantic troposphere: relationship to Saharan dust. J. Geophys. Res. 1986,91:5173-5182

[23] Miller, J.C. and Miller,J.N. Statistics for Analytical Chemistry. New York: Eltis Horwood,1988

[24] 孙俊英. 冰冻圈大气气溶胶和雪冰化学研究. 兰州：中国科学院寒区旱区环境与工程研究所博士论文. 2002

Determination of soluble ions in atmospheric aerosol by Ion Chromatography

ZHAO Zhong-ping, LI Zhong-qin

(Tianshan Glaciological Station,Cold and Arid Environmental and Engineering Research Institute,Chinese Academy of Sciences,Lanzhou 730000,China)

Abstract: Aerosol samples taking from Glacier No.1, at Urumqi river head, Tianshan Mountains, Xinjiang, Northwest China, as a example. Sampling and extracting methods, analyzing techniques,measures of avoiding contamination were introduced. Meanwhile, the detection limits and the uncertainty for atmospheric ion concertations were presented. These limits make the tecknique suitable in very remote atmospheres, such as other high elevation mountains and pole sites.

Key words: ion chromatography; aerosol; soluble ions

“AccuSizer 780A 光学粒径检测仪”在冰川微粒研究中的应用

朱宇漫，李忠勤，尤晓妮

（中国科学院寒区旱区环境与工程研究所/冰芯与寒区环境联合重点实验室/天山冰川站　兰州　730000）

摘　要：冰芯微粒的研究对反映大气粉尘变化具有重要意义。根据雪冰样品的特点，为寻求一种更便捷更适合的微粒检测方法，选择 AccuSizer 780A 光学粒径检测仪并尝试将其应用于冰川微粒的分析研究。通过对新疆天山 1 号冰川的大量雪冰样品微粒的检测分析，结果表明 AccuSizer 780A 光学粒径检测仪可满足冰川微粒研究的需要。

关键词：AccuSizer 780A；冰川微粒

1　引言

研究大气粉尘微粒和全球变化的关系，对直接或间接地揭示气候、环境变化规律有重要意义。大气中的粉尘是反映气候变化的一项重要指标，在全球变化中起着重要作用。而冰芯中的微粒是大气粉尘变化的最佳反映，不仅直接记录粉尘源区的气候和环境变化特征，还能反映不同地区和不同高度的大气粉尘变化差异。同时，微粒粒径的分布特征又与风力大小、传输距离和高度以及沉降机理等都有着密切关系，并存在着季节性变化。

我国西部山地冰芯是最靠近中亚粉尘源区的粉尘沉积介质，它是中亚粉尘传输过程中的必经之路，也是最基础的一个环节。作为研究大气粉尘演化和运动的理想观测点，它具有不同的沉积高度和搬运距离，是反映粉尘源区环境变化的显著代表。我们选择新疆乌鲁木齐河源天山 1 号冰川作为取样点，定期、连续采集不同深度的雪坑雪冰样品，对其粉尘记录及其微粒浓度和粒径分布变化进行测定分析。这里，我们选用 AccuSizer 780A 微粒粒径检测仪，首次并试验性地将其应用于冰川雪冰样品的微粒分析，分析结果符合研究需要。

2　测量仪器

2.1　仪器的选择

现代粒度测量技术中，较先进的、普遍采用的粒度分析仪器，以激光粒度仪和颗粒计数器为代表，如英国马尔文公司的 MasterSizer 系列激光粒度仪和美国贝克曼库尔特有限公司 Coulter Counter-Multisizer 系列颗粒计数器。而在冰川研究领域普遍使用 Coulter Counter 颗粒计数器来分析冰芯样品。

冰川雪冰样品，具有这几个方面的特点：一、由于受采样地点、环境及储存运输等条件的限制，取样体积很有限，而且对这有限的样品需要分析多个项目，往往是用于微粒检测的样品仅有几十毫升。二、冰川雪冰样品区别于乳剂、颜料等样品的特殊性是，颗粒物浓度相对较低，分散相比例＜分散剂。三、与工业化生产的油漆、药剂、染料等不同，冰

川雪冰样品中的颗粒是自然形成，颗粒大小分布不均，分布范围连续，粒径从纳米级至肉眼所见的几百微米都有覆盖，绝大多数颗粒集中在 20μm 以下，偶有几十、上百微米的少量颗粒出现。因有这些特点，使用先进的激光粒度仪和颗粒计数器因此受到某些限制。特别是应用 Coulter Counter 颗粒计数器时，检测的粒径范围受到小孔管直径的限制，使得测量范围的粒径很狭窄（小孔管直径的 2%～60%）。而山地冰芯中的微粒粒径范围很广，跨度达数个量级。所以，有必要探索新的仪器和测量方法。我们经过多方调研和送样试测，选用美国 PSS (Particle Sizing Systems)公司出产的新一代微粒粒径分析仪—AccuSizer 780A。其普遍应用于半导体工业、材料制造、制药业、生物技术、特殊化学制品、食品业……我们尝试将其应用于冰芯微粒研究，在国内尚属首次。希望寻求最适合的雪冰样品微粒测量仪器。

2.2 AccuSizer 780A 光学粒径检测仪介绍

AccuSizer 780A 采用的是单粒子光学传感（SPOS—Single Particle Optical Sensing）技术。其原理是：含有颗粒的悬浮液被充分稀释后（目的是避免粒子集中成一致的流动通路），通过一个小的、窄的、平板状的、由波长 630μm 的大功率红色激光二极管发光所产生的均匀亮度的一个“成像带”，通过的每个颗粒会引起此感应带通路上一个可测的脉冲，该值取决于粒子的平均粒径和被测的物理量—光散射（LS）和光消减（LE）的关系（如图 1）。在传感器中设计了脉冲高度随粒子直径增加而单调地增加的光亮/检测系统，通过比较检测的脉冲高度和由一组均质的已知粒径的标准粒子获得的一条标准校正曲线，建立粒子在一个时间段的粒度分布。

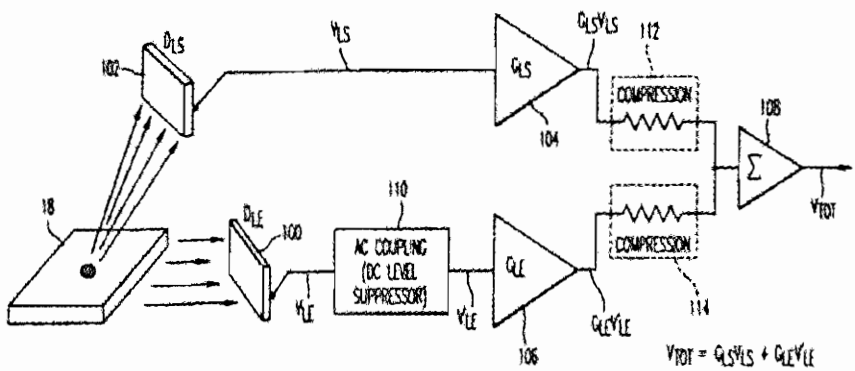

图 1 AccuSizer 780A 光学粒径检测仪原理图

如此的结构特点决定了其性能方面存在的优势：一、模块化设计结构便于故障检修和部件更换；二、应用单粒子光学传感（SPOS）原理，将两种物理作用—光消减和光散射技术(LE+LS)有机结合，通过光消减获得较大的动态粒径检测范围(高分辨率)(0.5～400μm)，通过光散射为小粒子提供了高灵敏度,测量结果呈现粒径的连续分布，得到的是真实的粒径“尾部”分布图，而不是近似的粒径分布图，其颗粒数是一颗一颗数出的，检测结果即是真实情况的描述。三、仪器的流体控制、传感器系统、自动稀释泵和大多数阀门仅同纯水相接触。不需要特殊的电解质溶液，仅用经过滤的去离子水做稀释剂，节省了分析和维持费用。四、传感器要求粒径在量程范围内的粒子浓度非常低，小于 9000 个/ml，因此对于绝大多数的样品，需经过稀释才能达到。有自动稀释系统可大大减少样品的取用量，有 1ml

样品即可满足分析；自动稀释功能还避免了在人工稀释操作过程中因部分污染物的侵入而导致检测误差的产生。五、由于集自动稀释、自动检测、数据处理及自动冲洗等自动检测功能于一身，所以分析时操作便捷、高效。测量时间只需 1～2 分种。8～512 个测量通道便于灵活选取。六、定期用已知粒径的标准颗粒进行校正，保证结果准确。正是这些与众不同的设计特点满足了雪冰样品分析的要求。

3 实验方法

3.1 实验条件

雪冰样品的采集、运输至室内分析全过程均采取了严格的防止污染措施。样品存贮于干净、密封的容器内，至分析前始终保持在摄氏零度以下，以保证其原始状态。样品从冰柜中取出，在洁净等级为百级的超净工作台和恒定室温下自然融化。分析时我们设置的操作参数如表 1：

表 1 微粒分析过程操作参数设置

传感器文件	保持稀释液体积	液体流速	稀释极限	测量时间	通道数	取样量
光散射范围	30ml	60ml/min	≤8000 个/ml	60Sec	128 个	1ml

每个样品检测完毕自动冲洗系统一次（必要时可冲洗多次），每次 60 秒。

3.2 实验过程

实验操作在超净工作台中进行。首先反复冲洗管路和系统，直至洗到颗粒 50 个/ml 以下即为干净（此指标是仪器设计规定）。在首次分析及更换稀释液后，先测定稀释液中颗粒的背景浓度（测量结果将自动扣除背景浓度）。将完全融化的样品摇动均匀，用移液器从中吸取 1ml 样品注入仪器，然后操作软件，仪器开始自动搅拌、稀释及分析。

3.3 测量的误差来源与不确定性及其消除

雪冰样品直接在密闭的采样容器中融化成为水，即可注入仪器测量，不需经过其他的前处理过程，避免了样品的二次污染。能造成样品污染或者引起测量误差及给测量结果带来不确定性的因素有稀释液（既超纯水）、取样定量、取样部位、实验环境和人为带入以及样品停放时间。

稀释液即超纯水，首先要经仪器内部的 MILLIPORE φ0.22μm 的 MILLIPAK®100 过滤器过滤后流入稀释杯。而仪器的设计测量范围＞0.5μm，因此来源于稀释液的污染影响可以排除。经测量，这种超纯水中微粒的背景值为 430 个/ml（多次测量的平均值），粒径范围集中在 10μm 内，这可能源自储水容器本身或空气中微粒的进入和水中的微小气泡。这一背景低于被分析的山地冰川雪冰样的最低浓度 200 倍以上。此结果对测量造成的误差可忽略，可在样品分析结果中加以扣除。

取样时定量的准确与否也会造成误差。我们用 Eppendorf（1000～5000μl）的移液器定在 1000μl 固定刻度来吸取样品。经测定，移液器 1ml 定量误差为 0.49%，此误差相对于天山冰川雪冰样的微粒浓度在 10^5 数量级及其以上来说，完全可以忽略不计。

测量取样时，样品中微粒的分散程度和取样部位会直接影响被测部分的真实性和代表

性。雪冰融化后，其中的较大颗粒受重力影响沉降在容器底部，造成微粒分散不完全均匀。若取样的移液管从容器中部和底部取样，会使测量结果偏高几倍甚至几十倍。移液管从容器上部和接近瓶壁处取样又会使测量结果偏低。取样方法引起的误差是不可避免的,关键是选择最合理的取样位置，尽可能减小因取样给结果带来的不确定性。我们的经验是：先摇晃样品容器，使融化过程中沉降在底部的较大颗粒和悬浮在上面的小颗粒混合均匀，并均匀分散在样液中，然后在临近底部、溶液的 1/3 处，半径 1 / 2 处吸样品，（中心及下部会因晃动产生涡流而聚集大部分较大微粒），才能保证取样基本真实，测量精度在 5%以内。同时注意尽量保证所有样品在相同的部位取样。

实验环境和人为污染所造成的系统误差是不可避免和始终存在的。所以我们从融化、取样、注样到分析整个实验过程都在洁净等级设计标准为 100 级的超净工作台内完成，以尽可能减小这一系统误差。

雪冰样品测量前融化、停放时间的长短也是影响到测量结果真实性和准确性的一个重要因素。因为随着时间的改变，样品微粒也发生着化学和物理的变化。如雪冰样品中部分 Ca 盐和 Mg 盐型微粒，本是不易溶解在融化的水中，若融化停放时间过长，可能会发生少量分解和溶解；相反水中可溶性离子又有结合成不溶性盐而沉淀下来的机会；同时，随着停放时间的延长，水中分散的微粒可能会发生聚集或重新结团变成大颗粒；水中溶解的气体会逐渐集结成大气泡等。这些变化会改变微粒的数量和粒径，使测量失去真实性，更不能保证结果的准确性。我们取了五个不同样品，每个样品约 20ml，延长停放时间后测量与刚融化时测量结果比较（表 2）：

表 2 延长融化停放时间后与刚融化时微粒测量表征量的变化结果比较

融化停放时间	数量浓度变化	平均粒径变化	相对表面积变化
4 小时	＋（0.81%～3.60%）	－（1.32%～5.08%）	0.5～15μm 间稍有升高 15～70μm 间稍有下降
16 小时	－（4.22%～11.89%） ＋（15.58%～19.28%）	＋(4.18%～9.30%)	0.5～20μm 间降低 20～100μm 间升高
24 小时	－(13.20%～21.33%) ＋(17.23%～38.23%)	＋(1.25%～9.02%)	0.5～10μm 间稍有下降 10～50μm 间升高不显著

经多次试验，我们建议雪冰样品（对于体积 20ml 左右）融化时间不宜超过 4 小时，停放 3 小时内测量偏差小于 4.3% 。

4 结果与讨论

4.1 结果的表达

AccuSizer 780A 为每一个样品提供了丰富的原始数据报告形式，包括粒径分布图（柱状图和对应的曲线图）以及粒径分布表。以 030410.3 号样品测量结果为例，图 2(a)～图 为各项目的分布柱状图，每图还有对应的曲线图，例如图 2(b)（其它略）。

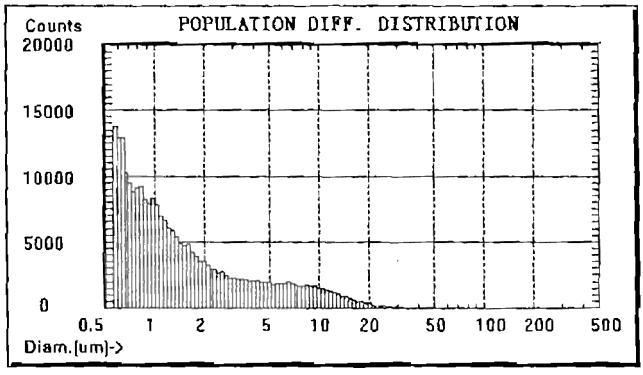

图 2(a) 总数微分分布（柱状图）

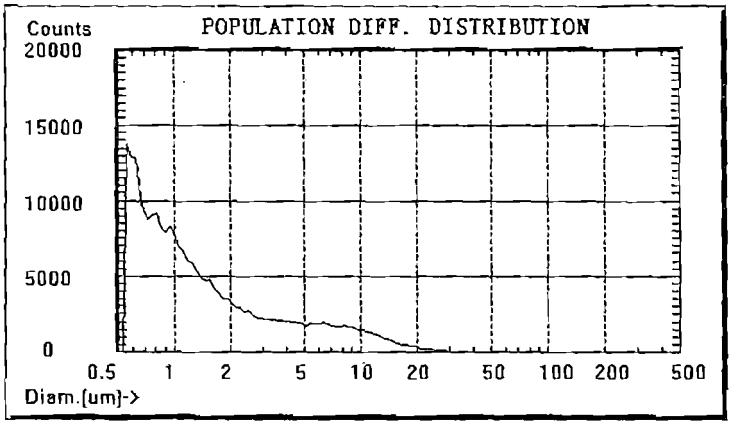

图 2(b) 总数微分分布（曲线图）

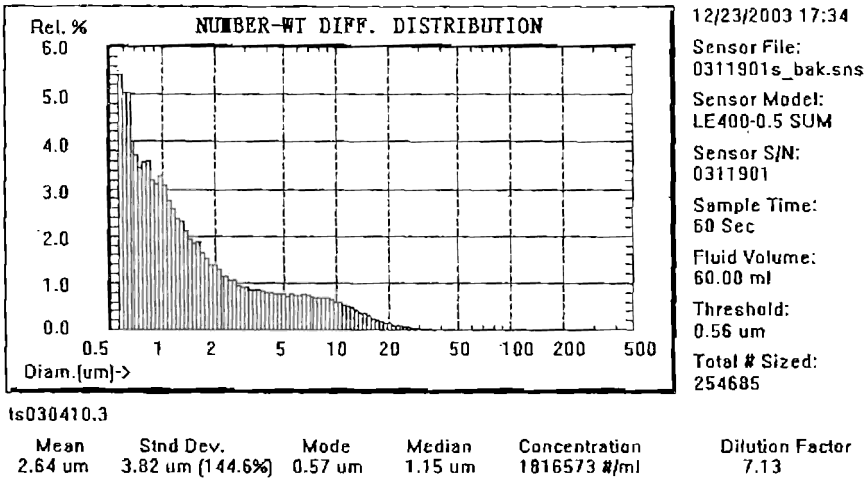

图 3 数量百分比微分分布

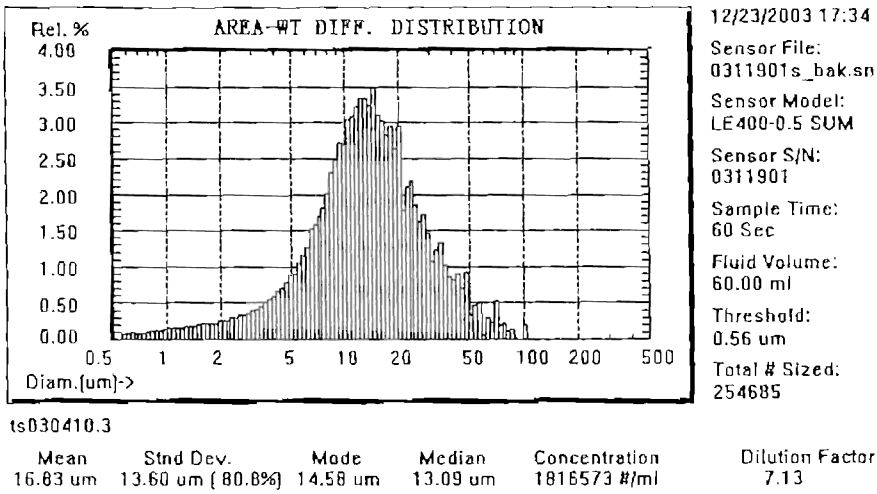

图 4 表面积百分比微分分布

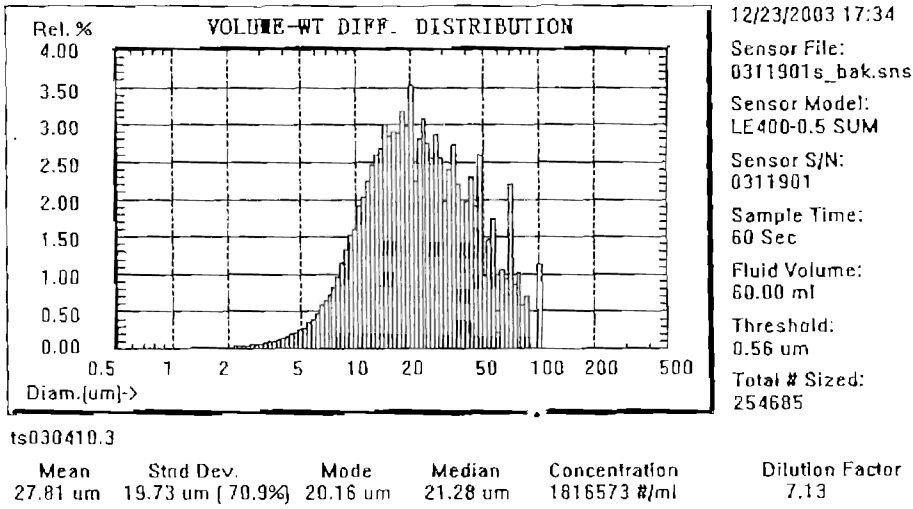

图 5 体积百分比微分分布

对于各通道微粒粒经详细分布和累计分布分别见表 3（截取部分分布，其余略）和表 4：

表 3 详细分布一览表

Summary of Detailed Distribution, Weightings Page

Diameter Range (microns)	# Part. Sized	Cum Num >=Diam.	Num %	Vol %	Cum Num % >=Diam.	Cum Vol % >=Diam.
0.56 — 0.59	13778	254685	5.410	0.003	100.000	100.000
0.59 — 0.62	12829	240907	5.037	0.003	94.590	99.997
0.62 — 0.65	12831	228078	5.038	0.004	89.553	99.994
0.65 — 0.69	10235	215247	4.019	0.003	84.515	99.991
0.69 — 0.73	9445	205012	3.709	0.004	80.496	99.987
0.73 — 0.77	8790	195567	3.451	0.004	76.788	99.983
0.77 — 0.81	9079	186777	3.565	0.005	73.336	99.979
0.81 — 0.86	9177	177698	3.603	0.006	69.772	99.975
0.86 — 0.91	8153	168521	3.201	0.006	66.168	99.969
0.91 — 0.96	7904	160368	3.103	0.007	62.967	99.963
0.96 — 1.01	8327	152464	3.270	0.009	59.864	99.956

……略

表 4 累计表

Cumulative Summary Table Page 1

Diameter (microns)	# Part. Sized	Cum Num >=Diam.	# Part./ml	Cum Num % >=Diam.	Cum Vol % >=Diam.	Max.#/ml	P/F
0.56	155289	254685	1816573	100.000	100.000	0	F
1.49	59003	99396	708955	39.027	99.858	0	F
4.51	25132	40393	288108	15.860	98.496	0	F
9.47	11747	15261	108851	5.992	89.510	0	F
16.46	2732	3514	25064	1.380	65.157	0	F
25.35	589	782	5578	0.307	41.739	0	F
36.50	149	193	1377	0.076	24.839	0	F
49.78	28	44	314	0.017	12.776	0	F
64.32	14	16	114	0.006	7.516	0	F
82.00	1	2	14	0.001	1.956	0	F
100.39	1	1	7	0.000	1.211	0	F
121.26	0	0	0	0.000	0.000	0	P
144.51	0	0	0	0.000	0.000	0	P
169.91	0	0	0	0.000	0.000	0	P
197.09	0	0	0	0.000	0.000	0	P
225.56	0	0	0	0.000	0.000	0	P

4.2 结果评价

因微粒测量测出的基本结果是粒度分布，它是一组数而不是单独一个数，这是粒度仪的重复误差特殊性所在。经过对第 516 号样品进行连续八次同等条件下测量，叠加 AccuSizer 780A 给出的八次测量的总数分布图结果（如图 6），得到一条重叠性非常好的曲线。

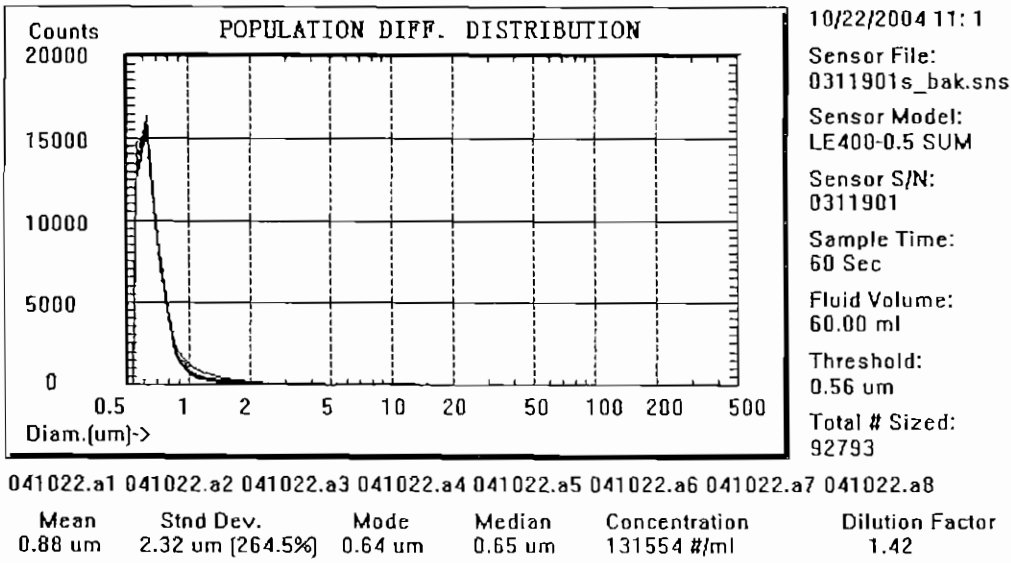

图 6 八次测量总数分布叠加图

微粒总计数多次测量的平均值为 94275.5，标准偏差为 4017.4，精度是 4.26%，其重复性误差＜5%，仪器测量重现性很好。

4.3 结论

利用 AccuSizer780A 光学粒径检测仪对取自天山乌鲁木齐河源 1 号冰川的近两千个微粒样品进行分析，测定结果表现出明显的规律性：微粒浓度在雪层中的变化具有明显的季节性，冬季是浓度曲线较稳定的时期，进入春季，可以观察到离子曲线的下移和减弱趋势。春末夏初，表层雪微粒含量出现明显峰值。根据仪器检测结果，夏末微粒浓度急剧减小。此外，微粒浓度是冰面污化的重要表征。通过仪器输出的粒径分布曲线发现，1 号冰川微粒粒径以 0.7～2μm 为主。测定结果与山地冰川微粒的分布变化规律一致。实验表明用 AccuSizer 780A 测量微粒是可行的、适合的，结果的重复性也是符合要求的并且其分析过程简便、快捷；0.5～400μm 的测量范围满足需要。采用该仪器和方法同样适用于测定其它地区雪冰样品中的微粒分布。

使用过程中发现此仪器也存在一定的局限性，表现在针对特殊样品（如极地冰芯）测量范围下限不够小、进样系统还未达到自动化，这还有待于进一步开发完善。

参考文献

[1] 邬光剑.幕士塔格和古里雅冰芯中微粒记录研究.[博士后研究工作报告] 兰州:中国科学院寒区旱区环境与工程研究所冰芯与寒区环境重点实验室.2004

[2] 李忠勤,孙俊英,侯书贵等.冰雪化学及其环境指示意义.中国冰川与环境——现在 过去和未来.施雅风主编,科学出版社,2000

[3] 陈培榕,邓勃主编.现代仪器分析实验与技术.清华大学出版社,1999.12

[4] AccuSizer AD User Manual. Release Date:02/03, [美国 PSS 公司]

[5] 徐剑青.使用 AccuSizer™ 仪的 CMP—slurry 的粒径检测, [美国 PSS 公司资料]

Application In Glacier by "AccuSizer 780A Optical Particle Sizer"

Zhu Yuman, Li Zhongqin, You Xiaoni

(Tianshan Glaciological Station/Key Laboratory of Ice Core and Cold Regions Environment, CAREERI, CAS, Lanzhou 730000, China)

Abstract: Study on microparticle in ice cores is very important because it can reflect the change of the atmospheric dust loading. Based on the characteristics of snow-ice samples, the "AccuSizer 780A Optical Particle Sizer" apparatus is choosed, and is used for the first time to analyze the microparticle in snow-ice samples retrieved from Glacier No.1 at the Urumqi river head,Tianshan Mountains,Xinjiang, in order to obtain a convenient and helpful analytical method of microparticle in ice cores. The experimental results show that the apparatus can satisfy the need of the microparticle research in ice cores.

Key words: AccuSizer 780A; microparticle in glacier

The Urumqi River source Glacier No. 1, Tianshan, China: Changes over the past 45 years

Baisheng Ye
Cold and Arid Regions Environmental and Engineering Research Institute, Chinese Academy of Sciences, Lanzhou, China
Daqing Yang
Water and Environmental Research Center, University of Alaska Fairbanks, Fairbanks, Alaska, USA
Keqin Jiao, Tianding Han, Zhefan Jing, Huian Yang, and Zhongqin Li
Cold and Arid Regions Environmental and Engineering Research Institute, Chinese Academy of Sciences, Lanzhou, China

This study analyzes long-term climate and glacier records to examine climate change and glacier response over the past 45 years in Urumqi River source region, the Tianshan Mountains of China. The results show that summer temperature and annual precipitation near the glacier increased by 0.8℃ and 87 mm (19%), respectively, during the study period. The glacier continuously retreated from 1962 to 2003, with the cumulated mass balance being -10,032 mm, or 20% of the glacier volume. Annual basin runoff has significantly increased by 413 mm or 62% during 1980-2003 due to precipitation increase and enhanced glacier melt caused by summer climate warming. Both summer precipitation and temperate are negatively correlated with mass balance and positively associated with runoff. Relative to precipitation-mass balance relation, the regression between temperature and mass balance is much stronger, indicating that summer temperature controls glacier mass balance and runoff changes.

1 Introduction

Global warming has caused shrinking of most glaciers and ice caps in the world over the last century,especially in recent decades [Dyurgerov and Meier, 2000].Small glaciers are highly sensitive to changes in temperature and precipitation making them important indicators of climate change [Meier, 1984; Oerlemans and Fortuin,1992]. The small, mountain glaciers make up less than 3% of the earth's ice cover, they account for approximately 20-50% of the 10-15 centimeter rise in sea level over the last century [Kuhn, 1993; Meier, 1984], and the total glacier and ice cap volume is equivalent to 0.24-0.7 m sea level rise [Meier and Bahr, 1996; Dyurgerov, 2002; Raper and Braithwaite, 2005]. Changes in the mass of these glaciers affect the volume and timing of stream flow that provides water for hydroelectric power production, irrigation, and domestic water supplies [Ostrem, 1991; Yao et al., 2004].

Glacier runoff is an important water resource in the arid northwest China [Yang, 1991].

Mountain glaciers in western China have experienced losses of mass and volume over the last several decades [Yao et al., 2004]. The Glacier No.1 located in the Urumqi River source has the longest monitoring records during 1958-2003 in China. Jiao et al. [2004] summarized the glacier mass balance results. This study systematically analyzes the long-term glacier, climate and hydrology records.

2 Site Description, Data Sets, and Method of Analyses

The Glacier No. 1 is located in the headwaters of the Urumqi River, Tianshan, China (43° 05'N, 86° 49'E) (Figure 1). It is a small valley glacier with two branches, the east and west branches. These two branches became separated into two small dependent glaciers in 1994 due to continued glacier shrinkage. The glacier is about 1.84 km^2 and 2.23 km long with elevation between 3740 and 4486 m a.s.l., the average ice thickness determined in early 1980's from the radar measurement is about 55 m [Zhang et al., 1985].

The glacier observation program at the Tianshan glacier station started in 1959 [Xie and Ge, 1965] and continued up to now with interruptions during 1967-1979. Field observations include glacier accumulation and ablation, equilibrium line altitude (ELA), changes in glacier length and area, and meteorological and hydrological data collections. Glacier data have been internally published in annual reports of the Tianshan Glacier Station from 1980-2004, and in the Glacier Mass Balance Bulletin (every two years) compiled by the World Glacier Monitoring Service of the International Commission on Snow and Ice [World Glacier Monitoring Service, 2003].

Glacier mass balance is calculated by contour maps of accumulation and ablation, using data measured at the permanent stake network (about 45-80 stakes in 8-9 rows on the glacier) and additional snow pits. Comparisons of methods for mass balance calculations show that the stake network generally provides accurate estimates of glacier mass balance [Elder et al., 1992]. The annual net accumulation, ablation and ELA also have been determined. The mass balance data are available from 1959 to 2003, except for 1967-1979. The missing data during 1967-1979 have been reconstructed, using the meteorological data [Zhang,1981], based on the relationship between summer air temperature and mass balance during 1958-1966. The glacier length and areas have been determined using glacier maps made in 1962, 1964, 1986, 1992, 1994, 2000 and 2001. The retreat of the glacier snout is directly measured every year. The glacier ice thickness or glacier bed altitude was measured by radar and verified by borehole data in 1981 [Zhang et al., 1985].

The meteorological data during 1958-2003 have been collected at the Daxigou meteorological station located at 3539 m a.s.l., about 3 km downstream of the glacier (Figure 1). The mean annual temperature and precipitation there are -5.1℃, and 450 mm, respectively.A hydrologic station, the Glacier No. 1 Station with a contributing drainage area of 3.34 km^2, has been set up 200 m downstream of the glacier terminus at 3689 m a.s.l. The glacier coverage of the basin is about 53% (various from 55.6% in 1980 to 51.1% in 2001). Discharge has been observed there during the melt period (May-Sept.) from 1980 to 2003.

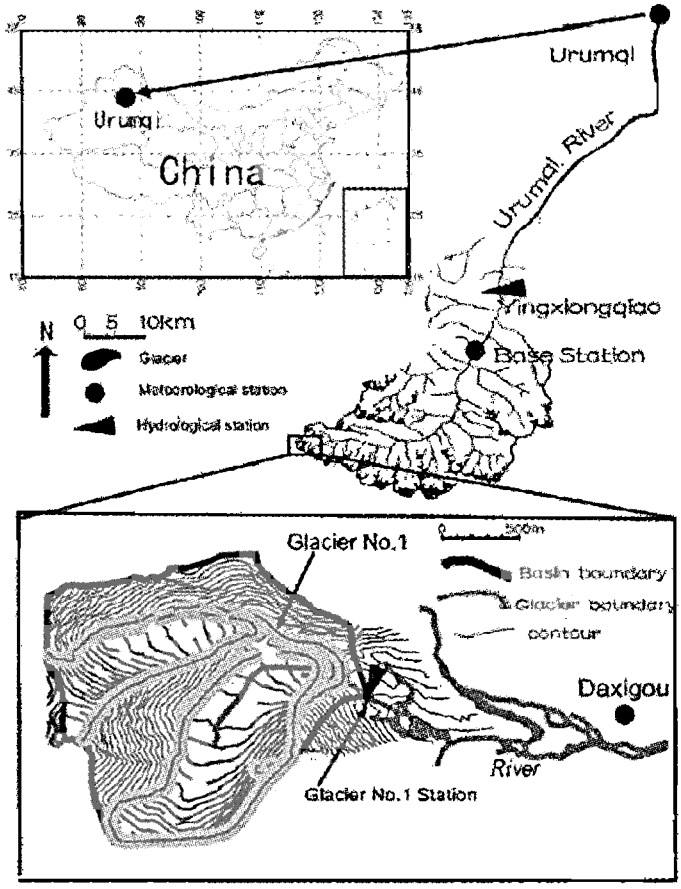

Figure 1. Locations of the Glacier No.1, and hydrologic and meteorological stations in the headwaters of the Urumqi River.

We carried out trend analyses by the linear regression for the long-term meteorological, hydrological and glacier data collected at or near the Glacier No.1, and used the standard t-test to determine the statistical significance of the trends. We also analyze the relationship among summer temperature, precipitation, and glacier mass balance and runoff to quantify the impact of climate change to glacier change.

3 Climate Change and Glacier Response

The seasonal regime of monthly temperature, precipitation and their trends is shown in Figure 2 (see auxiliary material[1])for the period 1958-2003. Monthly mean temperatures are -13~-16℃ in winter months (Dec-Feb) and 3~5℃ in summer months (Jun-Aug). Monthly temperatures during May to February have increased by 0.4-1.4℃ over the last five decades, and the increases in June, July,September and November were statistically significant at 95% confidence. However, March and April became slightly cooler by about 0.3-0.9℃ over the study period. As the result of the warming in most months, annual mean temperature has increased by

about 0.8℃ (95% significance level) over the last five decades. Temperature changes are particularly strong since 1997. For example, the summer (Jun-Aug) mean temperatures range from 3.0-4.6℃ during 1958-1996,and vary from 4.4 to 5.8℃ since 1997, indicating a step increase of 1.0℃ since 1997 (Figure 3a).

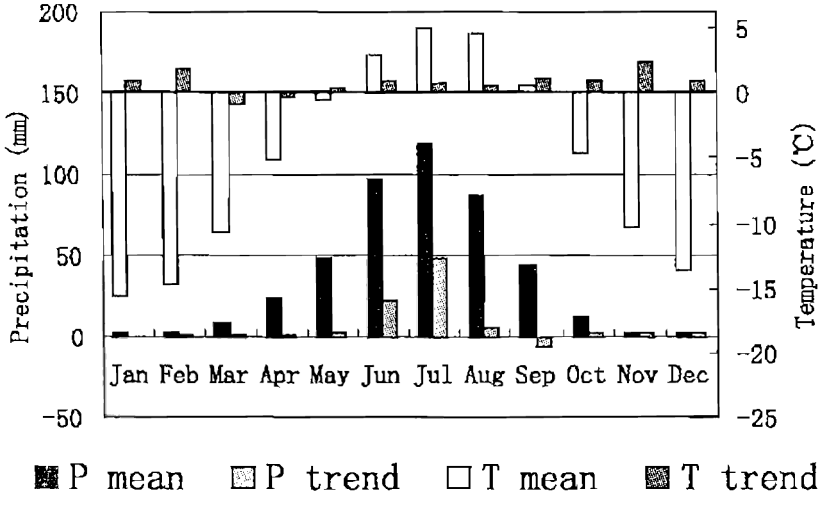

Figure 2. Long-term mean monthly temperature and precipitation, and their total trend at the Daxigou station during 1958-2003. Trends are in ℃ $(46a)^{-1}$ for temperature and mm $(46a)^{-1}$ for precipitation. See Table S1 of auxiliary material for data.

Monthly precipitation regime and its trend over the study period are also depicted in Figure 2. It shows that the monthly precipitation varies from 2-50 mm during September to May, and the summer months are relatively wet, with the peak amounts being 97-118 mm in July and August. Snowfall dominates in monthly precipitation, with only 17% rainfall in the warmest month of July. An upward trend was found in all months, except for September with a decrease of 6 mm. The increases are particularly significant (over 22 mm) in June and July, while trends in other months are 1-5 mm. Statistically, precipitation changes in July, November and December are significant at 95% confidence. The total trend of precipitation in summer reached 77 mm (25%) (above 95% significance level) during the study period. Annual total precipitation significantly increased by about 87 mm (19%) over the last several decades.Annual precipitation increases are very strong since 1987.The difference of mean annual precipitation between 1959-1987 and 1988-2003 is 76 mm or 17% of mean annual precipitation during the study period (Figure 3b).

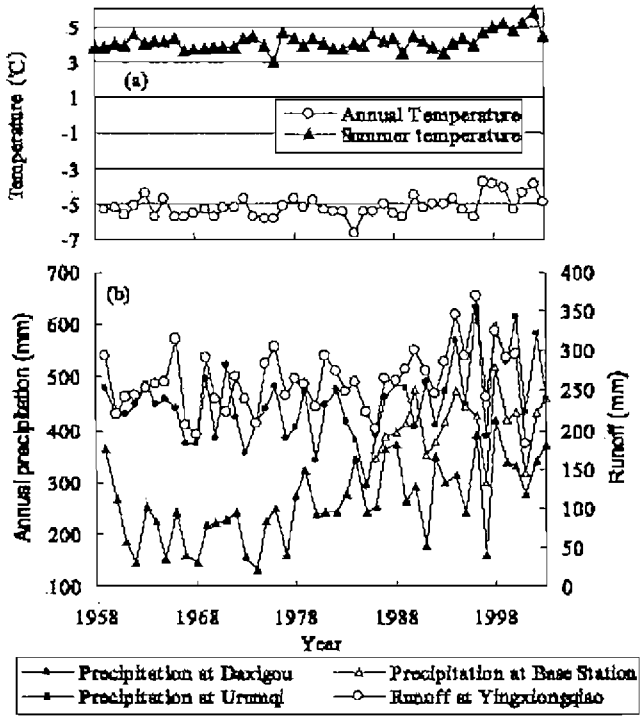

Figure 3. (a) Annual and summer (Jun-Aug) air temperature and (b) annual precipitation/runoff in the Urumqi River basin during 1958-2003. See Table S2 of auxiliary material for data.

Yearly precipitation increase in the upper basin is very strong. To confirm this change, we examined precipitation data at two stations further downstream and found that the precipitation increase has occurred not only in upstream basin, but also in middle stream and even in downstream of the river basin. Furthermore, yearly runoff at the Yingxiongqiao station that controls the mountain portion of the basin also increased by 44 mm (or 1 I%) during 1959-2001, indicating consistency in precipitation and runoff change over the mountain regions of the basin. Temperature and precipitation changes reported here seem to suggest a regime shift from warm-dry to warm-wet pattern over northwest China [Shi et al., 2003].

Annual mass balance varies between 375 and 860mm during 1958-2003. Glacier mass balance has been decreasing almost monotonically in the last 45 years, especially in the most recent 10 years. The 5 years of most negative mass balance (over 790 ram) all appeared after 1997 (Figure 4). Cumulative mass balance reached 10,032 mm over the study period, equivalent to glacier thinning of 11.1 m (20% of average glacier thickness).Precipitation and temperature changes affect glacier mass balance differently. Precipitation increases enhance accumulation, and temperature warming enhances ablation.The negative mass balance, caused by higher ablation than the accumulation, is associated with precipitation increase and temperature warming over the study area. This result implies that the effect of warming may overcome the influence of precipitation increase.

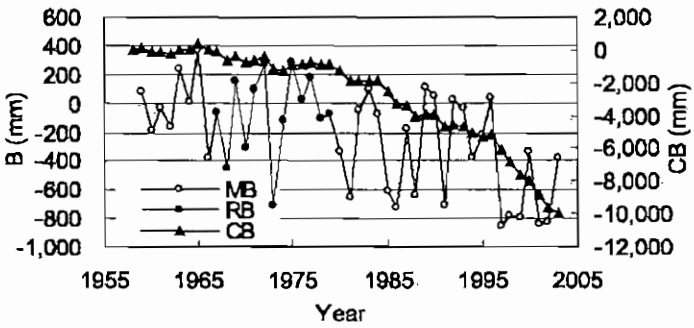

Figure 4. Annual and cumulative mass balance of the Glacier No.1 during 1959-2003. MB: measured mass balance, RB: reconstructed mass balance, CB: cumulative mass balance. See Table S3 of auxiliary material for data.

The mean ELA of the glacier is about 4056 m a.s.l.over 1959-2003. The ELA has moved up 37 m due to the climate wanning. The ELA rise is strong since 1997 - it is above 4050 m a.s.l, with the mean of 4110 m a.s.l.Furthermore, the glacier length and area observations during 1962-2003 also show a steady retreat of the glacier over the observation period. The glacier length and area decreased by 175 m (7.3%), and 0.24 km2 (12.4%) during 1962-2003. Yearly runoff at the hydrologic station below the glacier ranges from 350-1030 mm, and has significantly increased by 413 mm (or 62%) during 1980-2003 (Figure 5). This increase is mostly from the glacier mass loss - total of 404 mm during the same period.

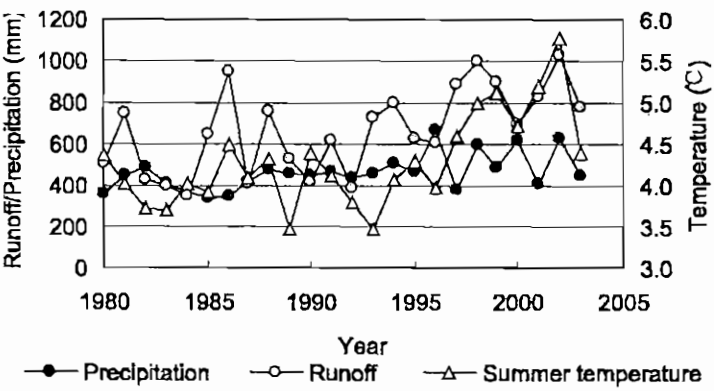

Figure 5. Summer (Jun-Aug) temperature, annual precipitation and runoff in the upper Urumqi River during 1980-2003. See Table S4 of auxiliary material for data.

To quantify the effect of climatic change on the glacier, we examine the relationships among summer temperature, precipitation and glacier mass balance and runoff.Figure 6a shows the relation between summer precipitation and mass balance/runoff. Summer precipitation is negatively correlated with mass balance and positively associated with runoff. These relationships, although very weak statistically, are reasonable, as higher precipitation leads to

higher runoff and lower glacier melt [Liu et al., 1998]. Similarly,summer temperature is negatively correlated with mass balance and positively associated with runoff (Figure 6b);These relationships, statistically significant at 99%, are expected for glacier basins, because higher temperatures lead to higher glacier melt (negative mass balance) and thus higher runoff. Regression results in Figure 6b suggest that the 1℃ summer temperature change leads to 486 mm glacier mass loss and 250 mm runoff change over the basin. This result shows that mass balance of this small glacier (53% of the basin) is more sensitive than basin runoff to temperature variation.

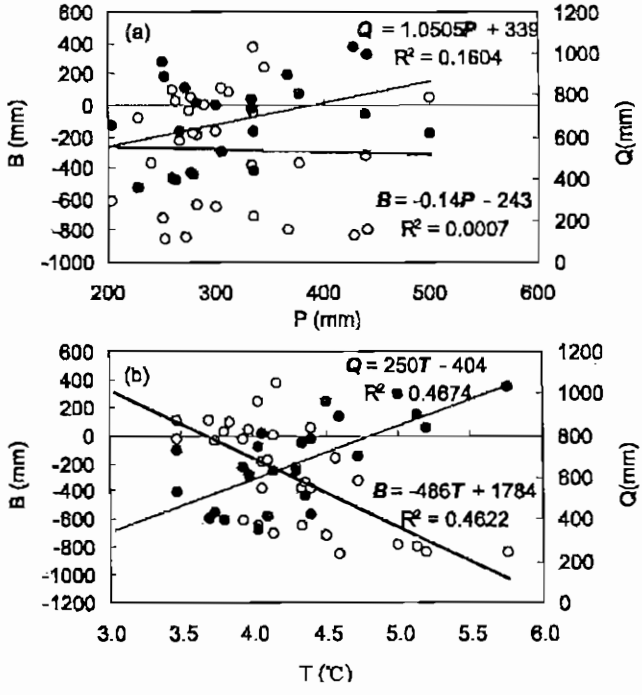

Figure 6. Regression relationships of summer temperature (T) and precipitation (P) vs. mass balance 03) and runoff (Q) during 1959-1966 and 1980-2003.

4 Summary

This study analyzes long-term climate and glacier records to examine climate change and glacier response over the past 45 years in the Urumqi River source area, the Tianshan Mountains of China. Trend analyses show the summer temperature, summer and annual precipitation near the glacier increased by 0.8℃, 77 mm (25%) and 87 mm (19%), respectively, during 1958 to 2003, with very significant changes over the most recent 8 years.

The glacier has continuously retreated from 1962 to 2003. Its length and area have shortened by about 175 m (7.3%) and reduced by 0.24 km^2 (12%), respectively, during 1962-2003. The cumulative mass balance is -10,032 mm, equivalent to 11.1 m of glacier ice, or 20% of the glacier volume. Basin annual runoff has significantly increased by 413 mm or 62% during 1980-2003 due to precipitation increase and enhanced glacier melt caused by regional

climate warming particularly in the summer season.

Regression analyses show that summer precipitation is negatively correlated with mass balance and positively associated with runoff. These relationships are reasonable, as higher precipitation leads to higher runoff and lower glacier melt. On the other hand, summer temperature is negatively correlated with mass balance and positively associated with runoff. Relative to precipitation-mass balance relation, the regression between temperature and mass balance is much stronger. A 1℃ increase in summer temperature leads to an increase of 486 mm glacier mass loss. This indicates that summer temperature controls glacier mass balance and runoff changes. It is important to note that, over the last 45 years, the negative mass balance, caused by higher ablation than accumulation, is associated with precipitation increase and temperature warming over the study area. This result suggests that the impact of warming (enhanced ablation) overcomes the effect of precipitation increase (enhanced accumulation) on glacier mass/runoff changes over the last 45 years.

Acknowledgments. This study was supported by the Innovation Project of CAS (KZCX3-SW-345), the project of CAREER/(2004116). We also thank all those colleagues who worked on hydrological and glacial observations at the Tianshan Glacier Station during 1958-2003.

References

[1] Dyurgerov, M. B. (2002), Glacier Mass Balance and Regime: Data of Measurements and Analysis, Occas. Pap. 55, edited by M. Meier and R. Armstrong, 268 pp., Inst. of Arct. and Alp. Res., Univ. of Colo.,Boulder.

[2] Dyurgerov, M. B., and M. F. Meier (2000), Twentieth century climate change: Evidence from small glacier, Proc. Natl. Acad. Sci., 97, 1406-1411.

[3] Elder, K., R. Kattelmann, D. Yang, S. Ushnurtev, and A. Chichagov (1992),Differences in mass balance estimation resulting from three alternative measurement techniques, Glacier Number 1, Tian Shan, Xinjiang Province, China, Ann. Glaciol., 16, 198-206.

[4] Jiao, K., Z. Jing, T. Han, B. Ye, H. Yang, and Z. Li (2004), Variation of Glacier No. 1 at the headwaters of the Urumqi River in Tianshan Mountains during the past 42 years and its trend prediction (in Chinese), Glaciol. Geocryol., 26, 253-260.

[5] Kuhn, M. (1993), Possible future contributions to sea level change from small glaciers, in Climate and Sea Level Change, Observations, Projec-tions, and Implications, edited by R. A. Warrick, E. H. Barrow, and T. M. Wigley, pp. 134-143, Cambridge Univ. Press, New York.

[6] Liu, C., Z. Xie, and M. B. Dyurgerov (1998), Tianshan Glacier, 227 pp., Science, Beijing.

[7] Meier, M. E (1984), Contribution of small glaciers to global sea level, Science, 51, 49-62.

[8] Meier, M. F., and D. B. Bahr (1996), Counting glaciers: Use of scaling methods to estimate the number and size distribution of the glaciers of the world, in Glaciers, Ice Sheets, and Volcanoes: A Tribute to Mark E Meier, Spec. Rep. 96-27, pp. 89-94, edited by S. C. Colbeck, Cold Reg. Res. and Eng. Lab., Hanover, N. H.

[9] Oerlemans, J., and J. P. E Fortuin (1992), Sensitivity of glaciers and small ice caps to greenhouse wanning, Science, 258, 115-117.

[10] Ostrcrn, G. (1991), Runoff forecasts for highly glacierized basins, in Runoff forecasts for highly glacierized basins: The role of snow and ice in hydrology, paper presented at Banff Symposium, September 1991, 1111-1123.

[11] Raper, S. C. B., and R. J. Bmithwalte (2005), The potential for sea level rise: New estimates from glacier and ice cap area and volume distribu-tion, Geophys. Res. Lett., 32, L05502, doi:10.1029/2004GL021981.

[12] Shi, Y., Y. Sben, D. Li, G. Zhang, Y. Ding, and E. Kang (2003), An Assessment of the Issues of Climatic Shift From Warm-Dry to Warm- Wet in Northwest China, 124 pp. Meteorological Press, Beijing, China.

[13] World Glacier Monitoring Service (2003), Glacier Mass Balance Bulletin 7 (200-2001), edited by W. Haebedi, M. Hoelzle, and R. Fmuenfelder, 87 pp., Zurich.

[14] Xie, Z., and G. Ge (1965), Study of accumulation, ablation and mass balance of glacier no. 1 at the headwater of Urumqi River, Tianshan, in Study of Glaciology and Hydrology on the Urumqi River, Tianshan, pp. 14-24, Science Press, Beijing, China.

[15] Yang, Z. (1991), Glacier Water Resources in China, 158 pp., Gansu Sci. and Technol., Lanzhou, China.

[16] Yan, T., S. Liu, J. Pu, Y. Shen, and A. Lu (2004), The recent retreat of glacier in High Asia and its effect on water resources, Sci. China, Set D, 34, 535-543.

[17] Zhang, J. (1981), Mass balance studies on Glacier No. 1 in Urumqi River, Tianshan, J. Glaciol. Geocryol., 3, 32-40.

[18] Zhang, X., G. Zhu, S. Qian, J. Cben, and Y. Sben (1985), Radar measuring ice thicknes of no. 1 glaicer at the source of Urumqi river, Tianshan, J. Glaciol. Geocryol., 7, 153-162.

Characteristics of mass balance of Glacier No.1 at the Headwaters of the Urumqi River, Tianshan Mountains

Han Tianding, Ding Yongjian, Ye Baisheng, Liu Shiyin, Jiao Keqin

(Cold and Arid Regions Environmental and Engineering Research Institute, CAS, Lanzhou, 730000, China)

Abstract: The temporal and spatial variations of mass balance on different time scales were analyzed to identify their response to climate change using long-term observed mass balance data during 1959-2002 in Glacier No.1 at the Headwaters of the Urumqi River, Tianshan Mountains, China. The results show that the accumulated mass balance of Glacier No.1 has decreased by -9599 mm water equivalent during 1959-2002 which is equivalent to about 10m mean thickness reduction for the glacier. The negative mass balance has been further enhanced in recent years and the mean mass balance was -739.6 mm a^{-1} during 1997-2002. The mass balance of the glacier shows a clear periodicity with positive and negative alternation of 7 and 15 years during the past several decades. Annual mass balance is significantly negatively correlated with summer air temperature from June to August. Annual air temperature shows stronger influences on the mass balance than annual precipitation. The influence of a temperature increase on the mass balance preceded the precipitation increase. Furthermore, monthly mass balance exhibits a negative correlation with monthly air temperature, significant at the 99% confidence level in July and August. Monthly mass balance is also negatively correlated with precipitation in May and August at the 95% confidence level, but positively and insignificantly correlated with precipitation in June and July. The negative relationship between mass balance and precipitation might be related to concurrent increases of precipitation and temperature.

Key words: mass balance, temperature, precipitation, Glacier No.1, Tianshan Mountains

1 Introduction

Glacier mass balance is directly linked to glacier fluctuations and climate change and alsc directly reflects changes of glacier volume, melting and runoff. As a result, glacier mass balance has been the focus of many researchers during the past several decades (Yang, 1992; Fountain and others, 1999; Chinn, 1999; Oerlemans and Reichert, 2000; Fricker and Roland, 2000 Hoelzle and others, 2003; Schneider and Jansson, 2004). Recent studies show that considerable climatic change has occurred in many regions of western China since the mid-1980s (Shi and others, 2002). Glacier No.1 and other high-altitude Asian glaciers are good indicators to

demonstrate climatic changes (Liu and others, 1998; 2000). Therefore, an intensive program with emphasis on mass balance studies on Glacier No.1 has been conducted since the late 1950s (Xie and Ge, 1965; Zhang, 1981; Zhang and others, 1984a; Zhang and others, 1984b) and continued up to now (Kang and others, 1994; Liu and others, 1997; Jiao and others, 2000; Yang and others, 2005; Han and others, 2005). This paper is intended to analyze the spatial and temporal variations of the mass balance of Glacier No.1 and to identify its response to the changes in temperature and precipitation.

2 Studied site description, datasets and methods

The Glacier No.1 (43.05°N; 86.49°E) is located at the headwaters of the Urumqi River, Tianshan Mountains, China (Fig. 1). Glacier No.1 is a small continental cirque-valley glacier, and comprises two parts of east and west branches with a total area of 1.95 km^2 in 1962 (Xie and Ge, 1965) These two branches became separated into two small glaciers in 1994 due to continued glacier shrinkage (Jiao and others, 2000). The area of the glacier measured in 1994 was 1.742 km^2, and had decreased to 1.708 km^2 in August of 2001 (Tianshan Glaciological Station, 2002). The horizontal distance between the tongues of the two branches was 45 m in 2001 (Yang and others, 2005).

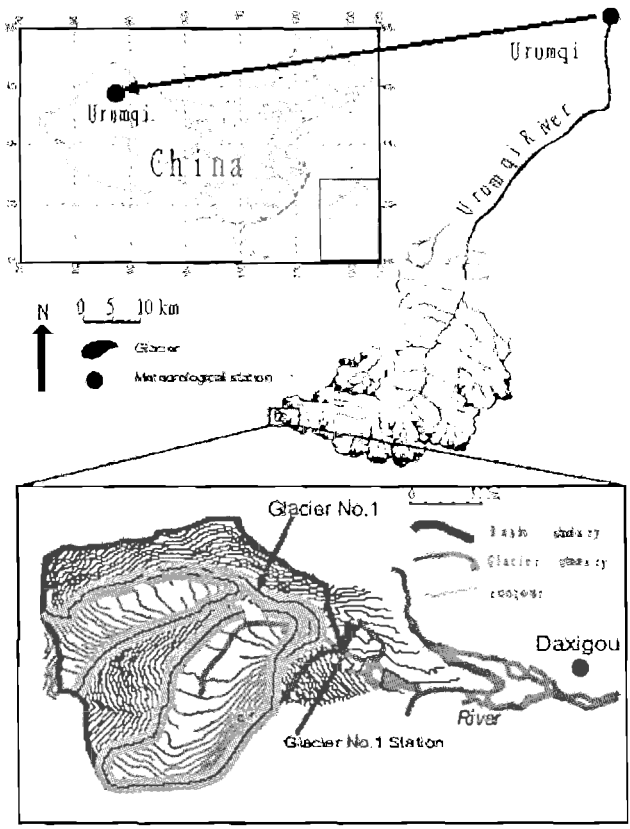

Fig. 1 Map showing the Location of Glacier No.1.

The mass balance observation on Glacier No. 1 started in 1959 using a permanent stake network on the glacier surface, and continued up to now with an interruption during 1967-1979. The glacier mass balance data has been published in annual reports of the Tianshan Glacier Station from 1980-2004, and in the Glacier mass balance bulletin every two years and fluctuations of glaciers every 5 years compiled by the Global Glacier Monitoring Service of the International Communication on Snow and Ice (ICSI). The annual mass balance data are available during 1959-2002 while monthly mass balance data are only available during 1980-2002. Daily ablation measurements have been conducted during June 29 through September 5 in 1989 using four stakes on the west branch of Glacier No.1 between 3815-3860 m a. s. l. (Tianshan Glaciological Station, 2002). Meteorological data has been collected from two Meteorological stations located downstream of the glacier. One is the Daxigou Meteorological station located at the elevation of 3539 m a. s. l. about 3km downstream from the glacier tongue, and another is Glacier No.1 Meteorological station located at the elevation of 3659 m a. s. l about 300 m downstream from the tongue of Glacier No.1 (Fig.1). The temperature and precipitation data are available during 1958-2002 at Daxigou station and during 1980-2002 at Glacier No.1 station. The spatial and temporal variations of mass balance were analyzed by statistical measures, such as trend and spectral analysis, correlation and partial correlation methods.

3 Characteristics of mass balance variations

3. 1 Annual mass balance

3.1.1 Characteristics of mass balance

The techniques of glacier mass balance measurements using a standardized method have been described by Meier (1962). The method of accumulation and ablation measurements has been applied in the observation of mass balance by using 51 stakes over Glacier No.1 (Fig. 1). The method can be expressed as the following equation:

$$bn=bi+bs+bsi \tag{1}$$

Where, bn, bi, bs and bsi are the mass balance, glacier ice, snow cover and superimposed ice mass balance for each stake, respectively. The total mass balance of the glacier (Bn) can be obtained by the area-weighted method for all altitude zones:

$$B_n = \sum_{j=1}^{m} b_j S_j \tag{2}$$

Where, S_j and b_j is area of altitude zone j and corresponding mass balance, respectively; n is the numbers of the glacier altitude intervals. The altitude interval used here is about 50 m. Figure 2 shows the annual mass balance, cumulative mass balance, and 5-year running mean mass balance of Glacier No.1 during 1959-2002. The cumulative mass balance reached -9599 mm water equivalent, and there were 29 negative balance years during the period. Moreover,

there were only 5 years with weak positive mass balance after 1980. A strong negative annual mass balance with -425.6 mm a-1 occurred during 1985-2002, 351.1 mm a-1 more negative than the mean mass balance of -74.5 mm a-1 during 1959-1984. Particularly the annual mean value of 739.6 mm a-1 during 1997-2002 points to a strong climatic warming in the recent 5 years.

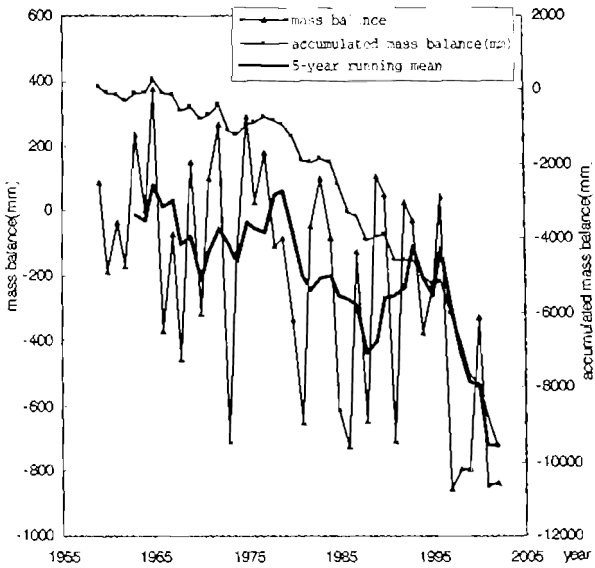

Fig. 2 Mass balance variations of Glacier No.1 during 1959-2002

The results of the spectral analysis (not shown) indicate that the mass balance of Glacier No.1 has a significant periodicity of both 7 and 15 years. Yang and others (2005) also report a periodicity of 3, 5, and 7 years of negative mass balance on the glacier.

3.1.2 Relationship between mass balance and air temperature and precipitation

Situated in the interior of the Tianshan Mountains, the Glacier No.1 is mainly affected by westerly airflow. The climate from October to March is very cold with little precipitation, and precipitation mainly concentrates in summer from June to August, a period of both strong ablation and accumulation. Both temperature and precipitation are important factors affecting the mass balance. Partial correlation analyses show that the mass balance is mainly influenced by summer mean air temperature from June to August, when the correlation coefficient is -0.62, significant at the 99%-level. However, the correlation coefficient between annual mass balance and precipitation in the same period is as low as 0.19 without statistical significance.

Air temperature has been rising in the late 1970s, and particularly so in winter (Liu and others, 1999; Han and others., 2002). The continuous increase of air temperature has led to enhanced glacier shrinkage (Li and others, 2003). Even though precipitation has also increased during this period, the mass balance still exhibits an unprecedented record negative balance. Obviously, the warming affected the glacier mass balance much more than the precipitation increase. The strong melting is mainly responsible for the significantly negative mass balance after 1997.

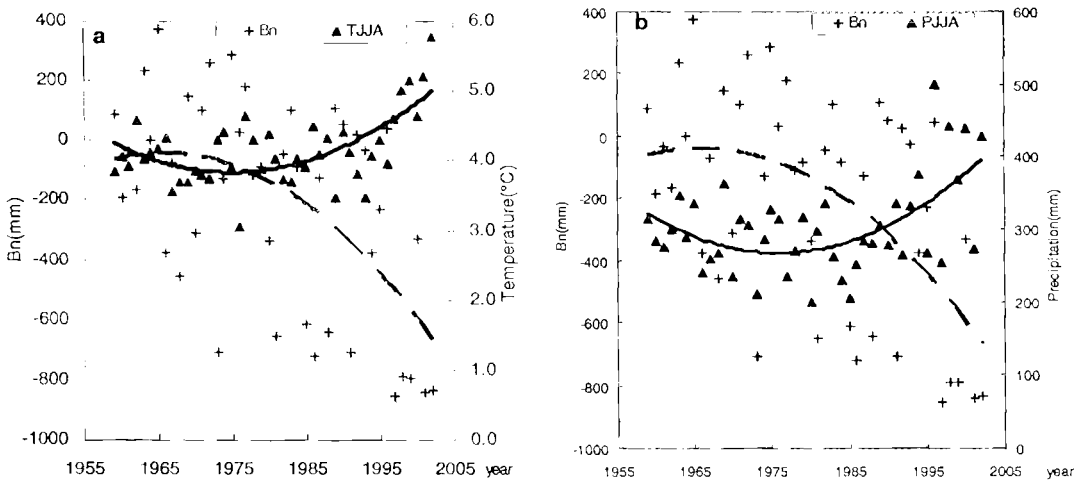

Fig. 3. Relationship between mass balance of Glacier No.1, and temperature (a) and precipitation (b) in summer during 1959-2002.

In addition, the air temperature increase preceded the precipitation increase (Fig. 3). Figure 3 shows the relationship between annual mass balance, mean air temperature and precipitation from June to August (JJA). It is evident that the glacial ablation increase coincides with the temperature increase, which had started in the late 1970s and has exacerbated in the middle to late 1990s. Meanwhile, the precipitation increase started only in the late 1980s.

3.1.3 Spatial variations of mass balance

The mass balance data (1980-2002) measured with the stake network on the surface of the glacier was used to identify the spatial patterns of mass balance variations. The mass balance was negative over the whole glacier during 1997-2002. This meant that the strong warming influenced not only the ablation rate but also the ablation area.

The spatial pattern of mass balance shows a clear seasonality. When glacial ablation strengthens, the accumulation rate is also high; as a result, the mass balance gradient is increased (Liu and others, 1997). The spatial pattern of mass balance also exhibits a marked interannual variation (Fig. 4). The amplitudes of annual mass balance variation are -2526.6 mm and -2095.2 mm in the ablation zones of the east and west branches, respectively, while amplitudes of annual mass balance in the accumulation zone were 1210.4 mm and 1209.2 mm for east and west branches, respectively (see Table 1). The amplitudes of ablation rate show an evident difference between the east and west glacier branches, while amplitudes of accumulation rate are close between the east and west glacier branches. The amplitudes of ablation rate in the ablation zones are greater than the amplitudes of accumulation rate in the accumulation zone. The glacier ablation in the accumulation zone is considerable when the glacier shows a strong negative annual mass balance.

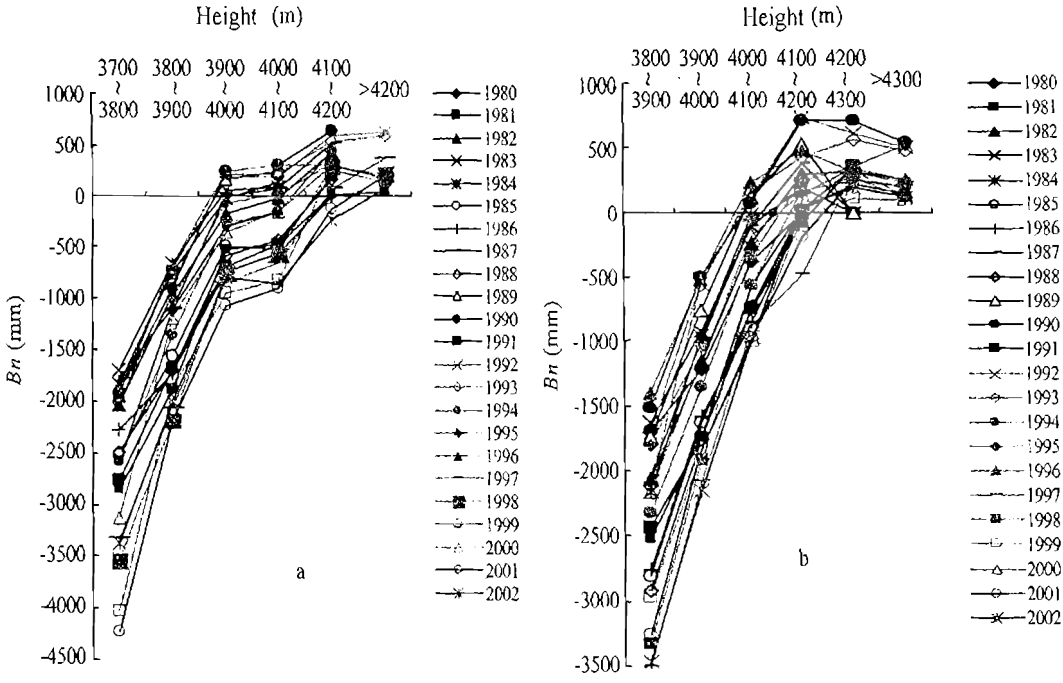

Fig. 4. Annual mass balance of Glacier No.1 at different altitudes for

(a) east and (b) west branches during 1980-2002.

Table 1.The amplitudes of maximum and minimum mass balance in the ablation and accumulation areas during 1980-2002

	ablation area				accumulation area			
	elevation (m)	year	mass balance (mm)	difference (mm)	elevation (m)	year	mass balance (mm)	difference (mm)
West branch	3800-3900	1996	-1398.9		4100-4200	1992	736.4	
		1997	-3494.1	-2095.2		1997	-472.8	1209.2
East branch	3700-3800	1983	-1692.4		4000-4100	1990	304.7	
		2001	-4219.5	-2526.6		2001	-905.7	1210.4

3. 2 Monthly mass balance

3.2.1 Characteristics of mass balance

The monthly mass balance of Glacier No.1 shows a clear seasonality. Weak accumulation and ablation occurs in winter from October to March, and mean accumulation rates are less than 1.5 mm per day. Moderate accumulation and ablation occurs in spring from April to May with a mean accumulation rate of more than 2mm per day, and ablation occasionally occurs through

melting of fresh snow. Strong accumulation and ablation exists in summer from June to August with the greatest ablation rate in July. The daily mean ablation rate ranges from 5 to 11 mm per day in the ablation area of the glacier, whereas the accumulation continuously increases in the accumulation area with a daily rate of 3-6 mm. Moderate ablation also occurs in autumn, especially in September. The ablation rate is generally lower than 3 mm per day, while the accumulation rate in the accumulation area varies between 1.5-2.0 mm per day (Liu and others, 1997).

3.2.2. Relationship between mass balance and air temperature and precipitation

Due to low air temperature from May to June the glacier mass balance is mostly slightly positive (Fig. 5), but a strong ablation period occurs from July to August and its mass balance variation is similar to that of the annual mass balance. This probably implies that July and August are very pronounced periods affecting the yearly variation of mass balance.

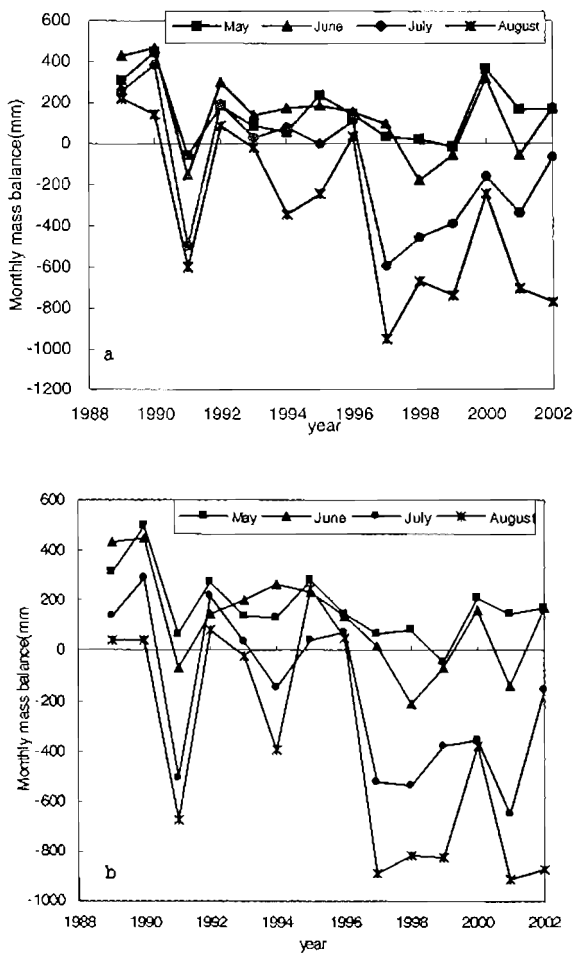

Fig. 5. Monthly mass balance for the west branch

(a) and the east branch (b) of Glacier No.1 from May to August during 1989-2002.

As precipitation and melting are both strong in the summer season, the variation of glacier mass balance depends on the both factors. Precipitation and air temperature impose varying controls on the glacier mass balance in different months. Partial correlation analyses are used to detect the effect between mass balance, air temperature and precipitation in different months. Results show that the relationship between monthly mass balance and monthly mean air temperature from May to August is negative, significant at the 99% confidence-level in July and August and at the 90% confidence-level in May and June. This means that higher temperature indicates stronger ablation from May to August, and vice versa. In addition, the correlation coefficient between monthly mass balance and monthly precipitation is negative in May and August, significant at the 95% confidence-level. This might be caused by concurrent air temperature changes. The monthly precipitation and mass balance in June and July exhibit a weak positive correlation. The results reveal that the glacier mass balance is influenced mainly by air temperature.

3.2.3 Spatial variations of mass balance

The spatial pattern of the glacier mass balance varies from season to season. The variation of the spatial pattern of the glacier mass balance throughout the year can help to understand the response of the glacier to seasonal climatic transitions. The monthly mass balance in 1993 and 2001 were used to represent the general characteristics before and after the glacier separated into two branches (Fig. 6).

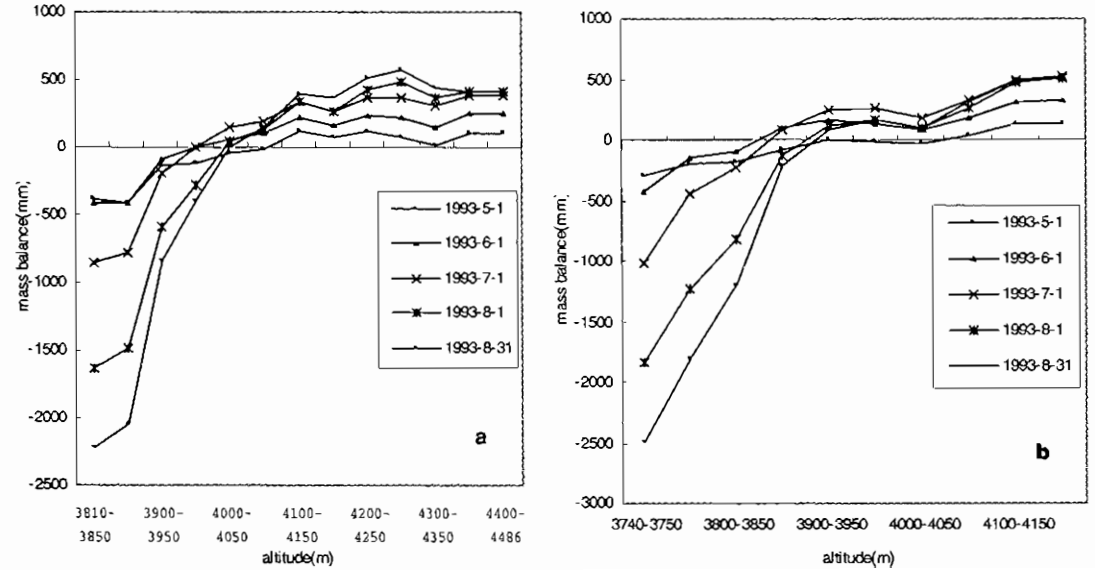

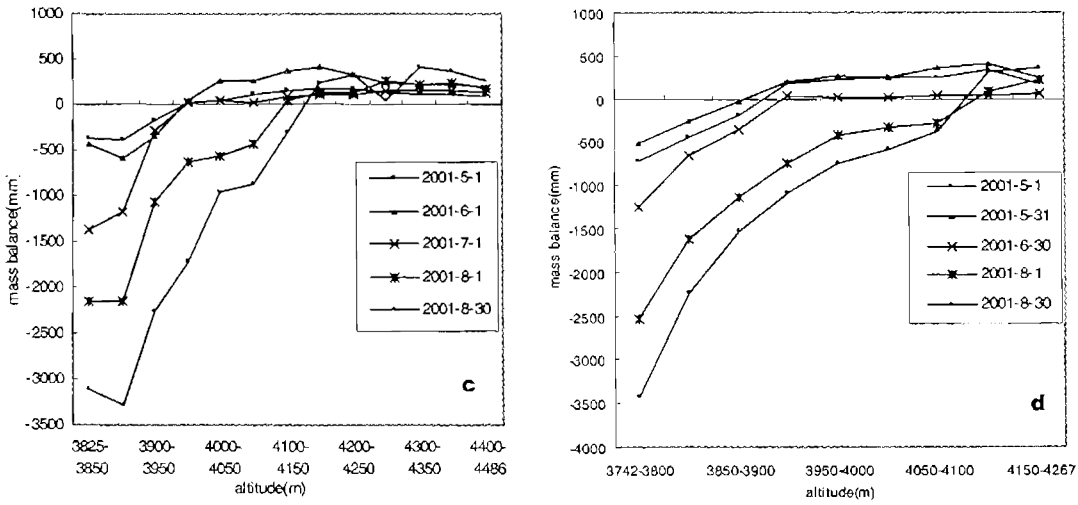

Fig. 6 Monthly mass balance of Glacier No.1 in

(a) 1993 and (b) 2001 for the west branch (left) and the east branch (right).

The spatial patterns of mass balance variations in May and June are much smaller than those in July and August (Fig. 6). The accumulation rate is small in the accumulation zone, so the strong ablation leads to a considerably decrease in the accumulation area. The accumulation zone area was 1.27 km2 and 0.65 km2 (total of west and east branches of Glacier No.1) in 1993 and 2001 respectively (Tianshan Glaciological Station, 2002). In addition, the equilibrium line of the glacier has been rising since 1996 (Han and others, 2005). The altitudes of the equilibrium line of Glacier No.1 were 3980 m a. s. l. and 4137 m a. s. l. in 1993 and 2001, respectively.

3. 3 Daily characteristics of ablation

The variation of daily ablation of the glacier shows a negatively correlation with daily mean air temperature (r = -0.41) but a positively correlation with daily precipitation (r = 0.46) (Fig.7), both of which were statistically significant at the 99% confidence-level. This shows that daily ablation is affected both by air temperature and precipitation. Furthermore, the correlation analysis indicates that the accumulated ablation (Bt) is significantly and positively correlated with accumulated positive temperature (T) at the 99% significance-level (Fig. 8); a relationship which can be expressed as:

$$Bt = -6.1202\ T + 46.649 \quad (3)$$

The observational and statistical analyses reveal that air temperature is mostly above average when the glacier is free of snow on the surface, and glacier ablation is then more severe, with a maximum daily ablation rate of 50-60 mm. The decreased albedo of the glacial surface leads to stronger ablation due to more heat input from solar radiation.

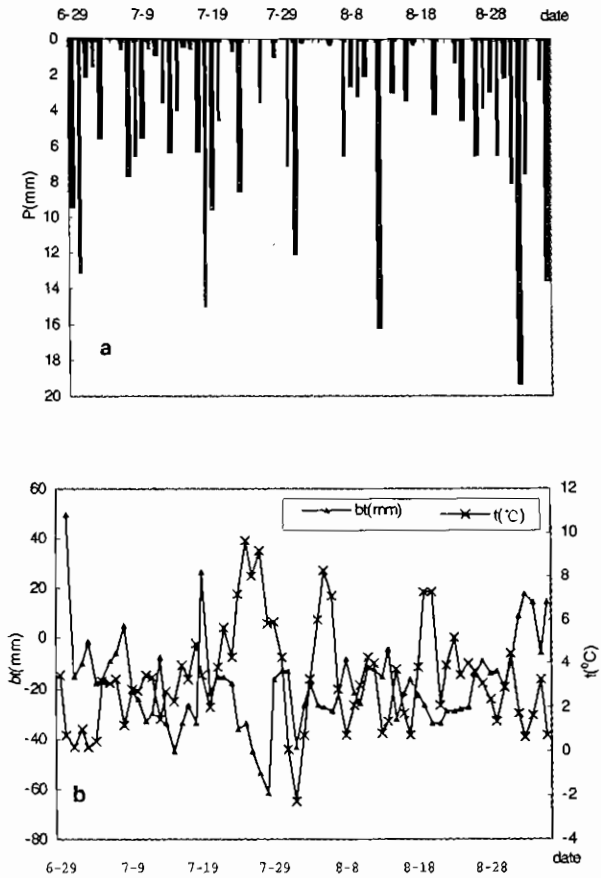

Fig. 7. (**a**) Daily precipitation and (**b**) daily temperature and mass balance of Glacier No.1 from Jun. 29 to Sept. 5 in 1989.

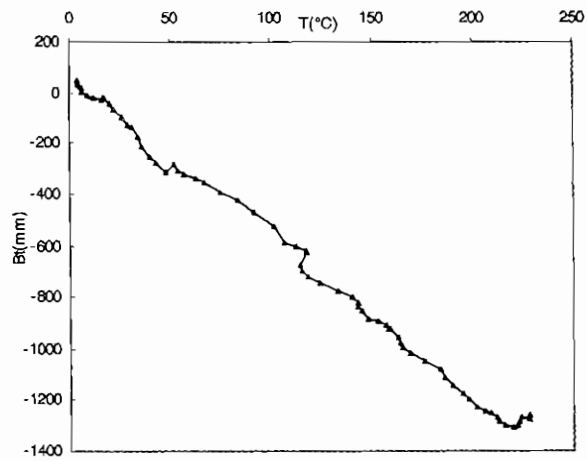

Fig. 8.Cumulative daily mass balance vs. cumulative positive daily temperature from Jun. 29 to Sept. 5 in 1989.

4 Discussion and Conclusions

Variations of glacier mass balance are affected by annual precipitation and summer mean temperature. There are several additional important factors that may influence the glacier mass balance, such as shortwave and long wave radiation (especially related to cloud cover), albedo, wind speed, ice temperature, evaporation, sublimation, and so on. Calculating the heat budget of the glacier will require considering these factors including precipitation and ice volume, in particular if melting and runoff are considered. This research emphasized the characteristics of different temporal and spatial variations of mass balance on Glacier No.1.

Results show that the correlation between monthly mass balance and monthly precipitation is negative in May and August. The negative correlation is probably due to the fact that heavy precipitation occurred contemporaneously with high temperatures in May and August.

The observed data show that the accumulated mass balance of Glacier No.1 was -9599 mm water equivalent during 1959-2002. The mass balance of Glacier No.1 has shown an accelerated negative trend since 1985, and the mean negative mass balance was -739.6 mm a-1 during 1997-2002. Weak mass gain occurred only in 5 years during 1980-2002. The climate warming not only enhanced the ablation, but also increased the ablation area. The mass balance of the glacier shows a clear periodicity with alternating 7 and 15 year cycles over the past several decades.

Annual mass balance has a significant correlation with mean air temperature in summer ($r = -0.62$ and $\alpha = 0.01$). However, it also shows a weak correlation or even no correlation with precipitation from June to August. This implies that the influence of increasing temperature on the mass balance overcame that of increasing precipitation. Furthermore, annual air temperature shows a greater influence on the mass balance than precipitation does.

Monthly mass balance exhibits a negative correlation with monthly mean air temperature; particularly the correlation coefficient in July and August exceeds the 99% confidence-level. Strong ablation of the glacier began in the late 1970s, while a significant increase of precipitation occurred in the late 1980s. As for the correlation between monthly mass balance and precipitation, it shows a weak negative correlation in May and August ($\alpha = 0.05$), but a positive correlation in June and July. The rising trend of the equilibrium line altitude of Glacier No.1 is very evidently due to climate warming.

The correlation between the daily accumulated ablation and the positive daily accumulated temperature was very remarkable with a correlation coefficient of -0.995 ($\alpha = 0.01$).

Acknowledgments

This work was supported by the Knowledge-Innovation Program of the Chinese Academy of Sciences (KZCX3-SW-345), the Key Open Laboratory of Atmospheric Chemistry of China Meteorological Bureau (project CCSF2005-3-DH17) and the National Natural Science Foundation of China (project 40371026, 40371028).

References:

[1] Chinn T. J. 1999. New Zealand glacier response to climate change of the past 2 decades. Global and Planetary Change, 22, 155–168.

[2] Fountain A. G., K. J. Lewis and P. T. Doran. 1999. Spatial climatic variation and its control on glacier equilibrium line altitude in Taylor Valley, Antarctica. Global and Planetary Change, 22, 1–10.

[3] Fricker, H. A. and C.W. Roland. 2000. Mass balance of the Lambert Glacier—Amery Ice Shelf system, East Antarctica: a comparison of computed balance fluxes and measured fluxes. Journal of Glaciology, 46(155), 561-570.

[4] Han T., B. Ye and K. Jiao. 2002. Temperature variations in the southern and northern slopes of Mt. Tianger in the Tianshan Mountains. Journal of Glaciology and Geocryology, 24(5), 567-570. [In Chinese with English abstract.]

[5] Han T., S. Liu, Y. Ding and K. Jiao. 2005. Characteristics of mass balance of Glacier No.1 at the Headwater of the Urumqi River, Tianshan Mountains. Advance in Earth Sciences, 20(3), 298-303. [In Chinese with English abstract.]

[6] Hoelzle M., W. Haeberli, M. Dischl and W. Peschke. 2003. Secular glacier mass balances derived from cumulative glacier length changes. Global and Planetary Change, 36(4), 219-310.

[7] Jiao K., C. Wang and T. Han. 2000. A Strong Negative Mass Balance Appeared in the Headwater of the Urumqi River. Journal of Glaciology and Geocryology, 22(1), 62-64. [In Chinese with English abstract.]

[8] Kang E., C. Liu, C. Wang, T. Han and W. Zhang. 1994. Seasonal variation of mass balance and altitude dependency of total melt in the glacierized source area of the Urumqi River. Journal of Glaciology and Geocryology, 16(2), 119-127. [In Chinese with English abstract.]

[9] Liu C., Z. Xie and C. Wang. 1997. A research on mass balance processes of Glacier No.1 at the Headwaters of the Urumqi River, Tianshan Mountains. Journal of Glaciology and Geocryology, 19(1), 17-24. [In Chinese with English abstract.]

[10] Liu S., N. Wang and Y. Ding. 1999. The characteristics of glacier fluctuations during the last 30 years in Urumqi River basin and the estimation of temperature rise in the high mountain area. Advance in Earth Sciences, 14(3), 279-285. [In Chinese with English abstract.]

[11] Liu S., Y. Ding, B. Ye, L. Wang and Z. Xie. 2000. Regional characteristics of glacier mass balance variations in High Asia. Journal of Glaciology and Geocryology, 22(2), 98-105. [In Chinese with English abstract.]

[12] Liu S., Y. Ding, L. Wang and Z. Xie. 1998. Mass balance sensitivity to climate change of the Glacier No.1 at the Urumqi River Head, Tianshan Mts. Journal of Glaciology and Geocryology, 20(1), 9-13. [In Chinese with English abstract.]

[13] Li Z., T. Han, Z. Jing, H. Yang, and K. Jiao. 2003. A summary of 40-Year observed variation facts of climate and Glacier No.1 at the Headwater of Urumqi River Tianshan Mountains, China. Journal of Glaciology and Geocryology, 25(2), 117-123. [In Chinese with English abstract.]

[14] Meier, M. F. 1962. Proposed definitions for glacier mass budget terms. Journal of Glaciology, 4(33),

252-263

[15] Oerlemans J. and B. K. Reichert. 2000. Relating glacier mass balance to meteorological data by using a seasonal sensitivity characteristic. Journal of Glaciology, 46(152), 1-6.

[16] Shi Y., Y. Shen and R. Hu. 2002. Preliminary study on signal, impact and foreground of climate shift from warm-dry to warm-humid in northwest China. Journal of Glaciology and Geocryology, 24(3), 220-226. [In Chinese with English abstract.]

[17] Schneider T. and P. Jansson. 2004. Internal accumulation in firn and its significance for the mass balance of Storglaciären, Sweden. Journal of Glaciology, 50(168), 25-34.

[18] Tianshan Glaciological Station. 2002. Annual Report of Tianshan Glaciological Station, Lanzhou: Lanzhou Institute of Glaciology and Geocryology, CAS, 1-16. [In Chinese.]

[19] Xie Z.and G. Ge. 1965. Accumulation, ablation and mass balance of the Glacier No.1 at the Urumqi River Head, Tianshan Mts. Study on glaciers and hydrology at the Urumqi River Head, Tianshan Mts. Beijing, Science Press, 24-34. [In Chinese.]

[20] Yang D. 1992. On the Mass Balance of 50 Mountain Glaciers in the Northern Hemisphere. Advances in Water Science, 3(3), 161-165. [In Chinese with English abstract.]

[21] Yang H., Z. Li, B. Ye, K. Jiao, Z. Jing and Z. Zhao. 2005. Study on mass balance and processes of Glacier No.1 at the Headwaters of the Urumqi River in the past 44 years. Arid Land Geography, 28(1), 76-80. [In Chinese with English abstract.]

[22] Zhang J. 1981. Mass balance studies on the No.1 Glacier of Urumqi River, Tianshan. Journal of Glaciology and Geocryology, 3(2), 32-40. [In Chinese with English abstract.]

[23] Zhang J., X. Wang and J. Li. 1984a. Study of the relationship between Mass balance change of Glacier No.1 and climate at the headwater of Urumqi River, Tianshan. Journal of Glaciology and Geocryology, 6(4), 25-36. [In Chinese with English abstract.]

[24] Zhang X., Z. Sun, J. Zhang and X. Kang. 1984b. Some relationships of the fluctuation of Glacier No.1 with climatic change at the source of Urumqi River, Tianshan. Journal of Glaciology and Geocryology, 6(4), 1-12. [In Chinese with English abstract.]

Mass balance and recession of Glacier No.1 at the Headwaters of the Urumqi River, Tianshan Mountains, China over the last 45 years

JING Zhefan[1,2], JIAO Keqin[1], YAO Tandong[1,2], WANG Ninglian[1,2], Li Zhongqin[1]

1. Key Laboratory Cryosphere and Environment, CAS, Lanzhou Gansu 730000, China

E-mail: jingzf@lzb.ac.cn

2. Institute of Tibetan Plateau Research, CAS, Beijing 100085, China.

ABSTRACT. Observations from 1959-2003 of Glacier No. 1 at the headwaters of the Urumqi River in the Tianshan Mountains show remarkable changes. The cumulative mass balance of the glacier is -10,032 mm, equivalent to 11.1 m of glacier ice, or 20% of the glacier volume, showing particular sensitivity to temperature change. The speed of glacier flow has gradually declined, especially since the 1980s. The flow speed of the east and west branches of the glacier have decreased from 1980 to 2003 by about 21% and 43%, respectively. The glacier has continuously retreated from 1962 to 2003. Its length has decreased by about 180m (7.5%) and its area has diminished by 0.23 km^2 (11.8%). Analyses show that summer precipitation is negatively correlated with mass balance and positively associated with runoff. These relationships are reasonable, as higher precipitation leads to higher runoff and lower glacier melt. On the other hand, summer temperature is negatively correlated with mass balance and positively associated with runoff, as higher temperatures lead to higher glacier melt and thus higher runoff-summer temperatures controlling mass balance variation. It is important to note that over the past 45 years the negative mass balance, caused by higher ablation than accumulation, is associated with precipitation increase and temperature warming over the study area.

INTRODUCTION

Annual or periodic changes in temperature and precipitation in glacial regions can be detected from mass balance and snow line measurements. If there is a change in the trend of regional climate then evidence from glaciers may directly reflect adaptations to such climate changes. Previous research has shown that not only is such a small glacier sensitive to climate change but easy to observe and study also.Glacier No.1 is located in the headwaters of the Urumqi River (43°05′ N, 86°49′ E), Tianshan, about 120 km southeast of Urumqi, China (Figure 1). It has the longest monitoring records of any glacier in China, covering the period 1958-2003. It is a small valley glacier with two branches, east and west. Due to glacier retreat, these two branches became separated into two, small independent glaciers in 1993. The length and area of the glacier has respectively decreased from 2.40km and 1.95km^2 in 1962 to

radar and verified by borehole data in 1981 (Zhang and others, 1985). Annual mass balance varies between 375 and 860mm during 1958-2003. Glacier mass balance has been decreasing in the last 45 years, especially in the most recent 25 years (Figure 2). During the last 45 years, a negative mass balance has existed in 30 years and a positive mass balance record existed in 15 years. Especially in the 25 year period since 1978, a positive mass balance appears in only five years, while the years of negative record existed in 80% of the years. During the last 25 years the mass loss of the Glacier No.1 represents 86% of the total of the past 45 years and 52% of the last decade. The five years of the most negative mass balance (over 790 mm) all appeared after 1997. The cumulative mass balance reached -10,032 mm over the study period, equivalent to a glacier

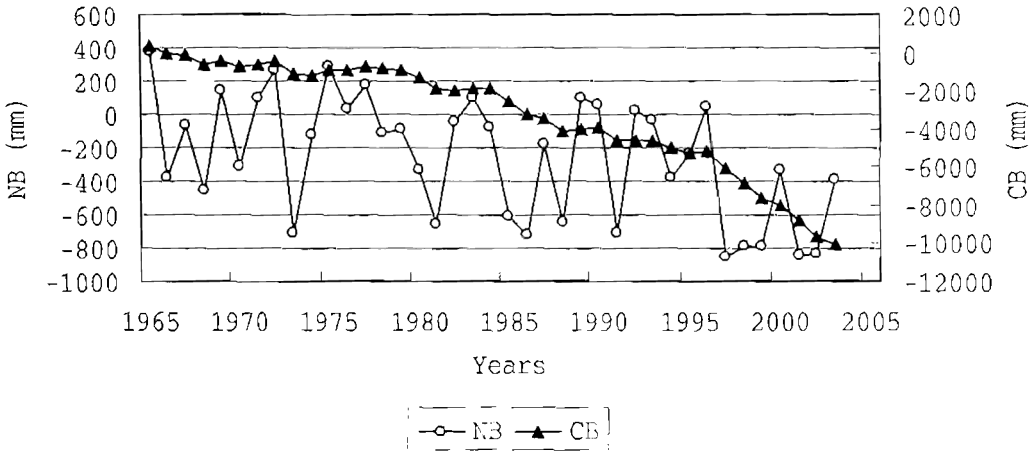

Figure 2 Annual and cumulative mass balance of the Glacier No.1

NB: net mass balance. CB: cumulative mass balance.

thinning of 11.1 m (20% of average glacier thickness). Measuring the flow speed of the glacier began in 1959. The triangular surveying method used was with a theodolite before 1985, a range finder was used during 1986-1995, and GPS was used from 1996. Data was also measured at the permanent stake network enabling mass balance calculations. The flow speed for 1960, 1961 and 1962, was 21.30m/a, 29.23m/a and 31.48m/a, respectively (Zhang Changqing, 1965). From August and September 1973 the flow speed of the glacier had been measured (Wang Wenying and others, 1976) and the flow speed of east and west branches was calculated to be 5.48 m/a and 10.32m/a (Huang Maohuan and others, 1982). Since 1980, continuous and systematic observations of glacier flow speed have been performed. Due to the terrain and surface slope of the glacier the flow speed of the west branch is larger than the east branch (Figure 3), and due to continued glacier shrinkage these two branches became separated into two small independent glaciers with a consequent sudden increase in flow speed in 1993. The speed of glacier flow is otherwise shown to be gradually decreasing, especially since 1994.. The flow speed of the east and west branches of the glacier have decreased over the period 1980 to 2003 by about 21% and 43%, respectively.

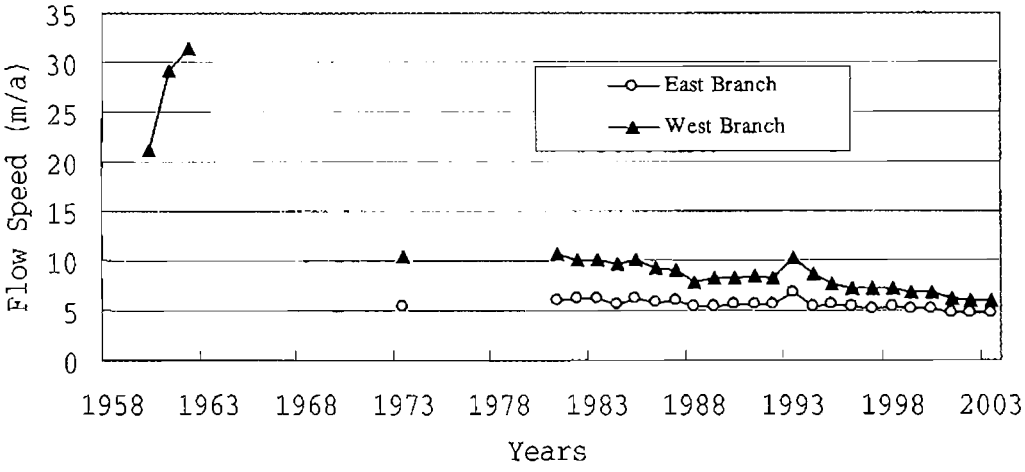

Figure 3 Flow speed of Glacier No.1

Such trends in glacier flow speed are completely consistent with trends in glacier mass balance. During 1958-2003, the mean thickness decreased by 11.1m (20% of average glacier thickness) of the glacier. As we know, the flow speed of the ice surface is directly proportional to the thickness of the glacier, and a change in thickness will have a strong influence upon flow speed, and therefore we can expect a corresponding decrease in glacier flow speed.

Since the 1960s, Glacier No.1 has been mapped nine times in Urumqi River basin using large scaled cartography, table topography (1962), ground photography (1973, 1980, 1986 and 1994), air-photography in 1964 and 1992 and GPS (2000, 2002). Additionally, since 1980 the location of the glacier terminus has been measured every year, providing reliable proof of dimensional changes in the glacier. During the period 1962-2003 the glacier terminus has retreated by 180.3m (7.5%), with an annual mean retreat of 4.4 m (Figure 4). The retreat speed was 5.96 m/a in 1963, 3.33 m/a in 1970s, 3.73 m/a in 1980s, and in 1990s was 4.61 m/a. Figure 4 shows that the glacier has always been in retreat and that the retreat speed increased in the 1980s and 1990s. Due to the retreat of the glacier terminus the east and west branches of the glacier separated completely to become two small glaciers in 1993. The retreat speed of the west branch terminus apparently quickens more than the east branch, the reason for the difference being the following: firstly, the dimensions of the west branch is less than the east branch, so the west branch is more sensitive to climate change; secondly, the area of the firn basin (accumulative area) of the west branch is smaller, that is, the glacier accumulation is less; thirdly, the underlying topography of the west branch terminus is an abrupt ice ridge, which not only makes the ice thickness decrease, but also break up more easily.

By using a series of large scale maps of glacier No.1, changes in glacier area can be calculated (Figure 5). The area of the glacier decreased by 0.23 km^2 (11.8% of the area in 1962) from 1962 to 2002. Furthermore, the mean ELA of the glacier is about 4056 m a.s.l. over the

period 1958-2003. The ELA has moved up 37 m due to climate warming. This rise is most noticeable since 1997, where it is above 4050m a.s.l. with a mean of 4110m a.s.l..

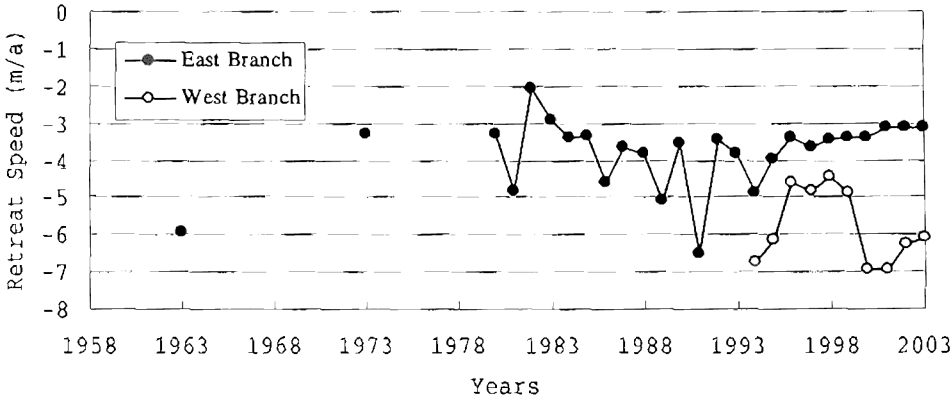

Figure 4 Rate of retreat for the Glacier No.1 terminus

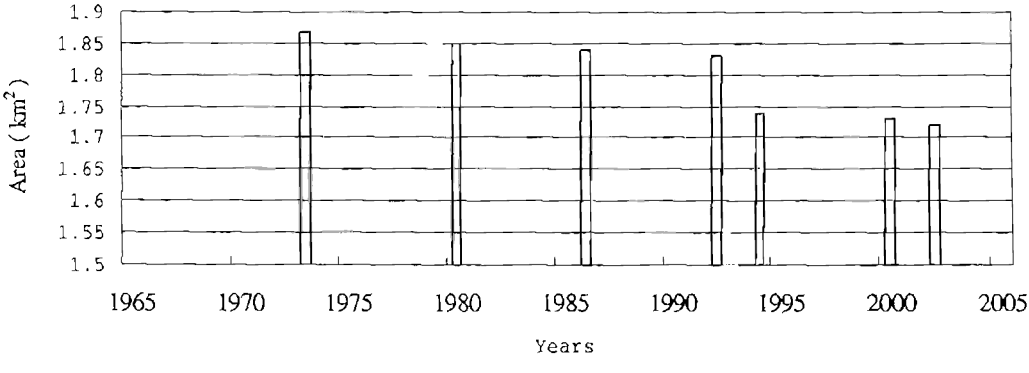

Figure 5 Variation in area of Glacier No.1

The seasonal regime of monthly temperature and precipitation is shown in Figure 6 for the period 1958-2003. Monthly mean temperatures are -13 to -16°C in winter months (Dec-Feb) and 3-5 °C in summer months (Jun-Aug). Trends in monthly temperature from February to May show an increase and the warming trend in the months in June, July, September and November is statistically significant at the 95% confidence level. However, March and April became slightly cooler by about 0.3-0.9 °C over the study period. As the result of the warming in most months, annual mean temperature has increased by about 0.8 °C over the last five decades. Temperature changes are particularly strong since 1997. For example, summer (Jun-Aug) mean temperatures range from 3.0-4.6 °C during 1958-1996, and from 4.4-5.8 °C since 1997, indicating a step increase of 1.0 °C since 1997 (Figure 7). This corresponds with a cumulative mass balance increase of more than 400 mm since 1997 (Figure 2) indicating that the mass balance of the glacier is sensitive to temperature change.

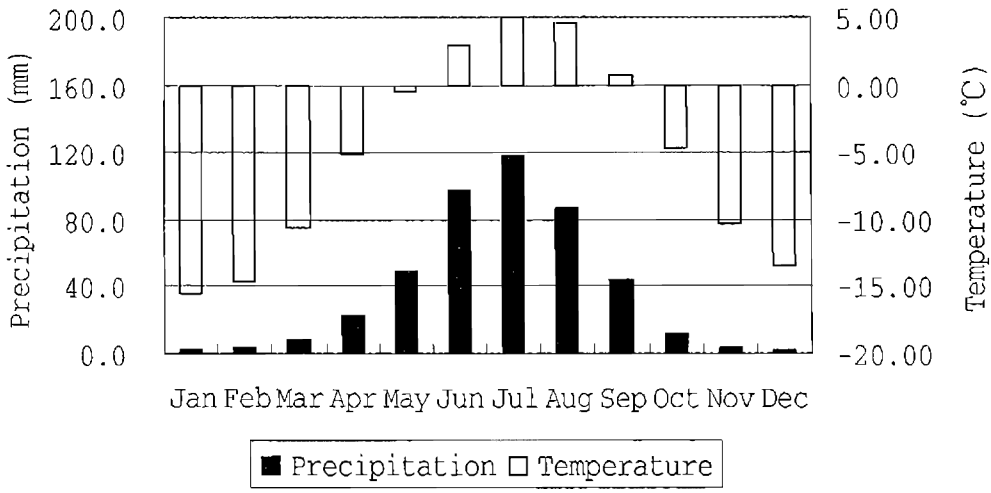

Figure 6 Mean monthly temperature and precipitation at Daxigou station from 1958 to 2003

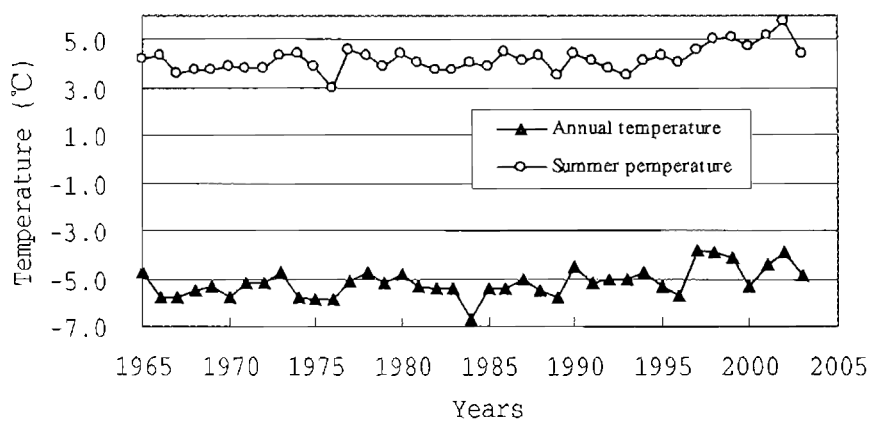

Figure 7 Annual and summer air temperature at Daxigou station during 1958-2003

The monthly precipitation regime is also depicted in Figure 6. It shows that the monthly precipitation varies from 2-50 mm during the winter half of the year (September to May), whereas the summer months are relatively wet, with peak amounts of 97 and 118 mm in July and August, respectively. Snowfall dominates the type of precipitation, with only 17% of the warmest month of July being rainfall. Statistically, annual total precipitation has increased significantly by 19% (87mm) over the last few decades. Annual precipitation has increased since 1987 along with the year-to-year variability. The difference between the mean annual precipitation from 1959-1987 to that of 1988-2003 is 76 mm or 17% of the entire record. (Figure 8). Summer precipitation is negatively correlated with mass balance and positively associated with runoff. These relationships, although very weak statistically, are reasonable, as higher precipitation leads to higher runoff and lower glacier melt (Liu Chaohai and others, 1998).

Similarly, summer temperature is negatively correlated with mass balance and positively associated with runoff, as higher temperatures lead to higher glacier melt and thus higher runoff.

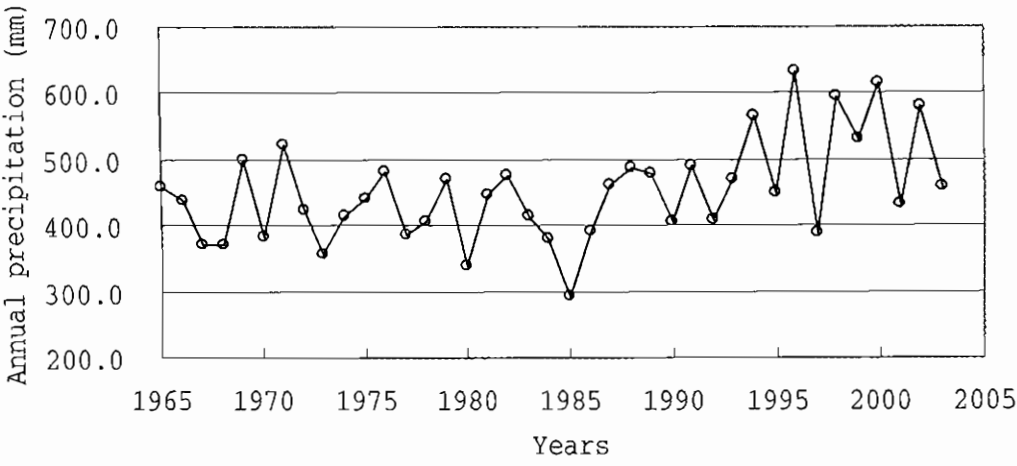

Figure 8 Annual precipitation at Daxigou station during 1958-2003

CONCLUSION

This study has analyzed long-term climate and glacier records to determine glacier response to climate change over the past 45 years in the Urumqi River, Tianshan Mountains, China. The cumulative mass balance is -10,032 mm, equivalent to 11.1 m of glacier ice, or 20% of the glacier volume. The mass balance of glacier No.1 has been shown to be sensitive to temperature change. The glacier flow speed has gradually decreased, especially since the 1980s, after which the decrease in glacier flow is even more evident. The flow speed of the east and west branches of the glacier decrease by about 21% and 43%, respectively, from 1980 to 2003. The glacier has continuously retreated from 1962 to 2003. Its length and area have decreased by about 180 m (7.5%) and 0.23 km^2 (11.8%), respectively.

Summer precipitation is negatively correlated with mass balance and positively associated with runoff. These relationships are reasonable, as higher precipitation leads to higher runoff and lower glacier melt. On the other hand, summer temperature is negatively correlated with mass balance and positively associated with runoff, as higher temperatures lead to higher glacier melt and thus higher runoff. The summer temperature controls glacier mass balance variation. It is important to note that, over the past 45 years, the negative mass balance, caused by higher ablation than accumulation, is associated with both a precipitation increase and temperature warming over the study area.

ACKNOWLEDGEMENTS

This research is supported by the Centurial Program (2004401) and the National Nature

Science Foundation of China (90202013), the Innovation Research Project (KZCX3-SW-339-3) of Chinese Academy of Sciences, and the National Basic Research Program of China (2005CB422003). This manuscript was improved by suggestions from two anonymous reviewers We thank Professor Peter Mayes for editing our English.

REFERENCES

[1] Chen, J., C. Liu, and M. Jin. 1996. Application of the repeated aerial photogrammetry to monitoring glacier variation in the drainage area of the Urumqi River. *J. Glaciol. and Geocryol.*, 18(4), 331-336.

[2] Huang, M., and Z. Sun. 1982. Some Flow Characteristics of Continental-type Glaciers in China. *J. Glaciol. and Geocryol.*, 4(2), 35-45.

[3] Jiao, K., C. Wang, and T. Han. 2000. A strong negative mass balance recently appeared in the Glacier No.1 at the headwaters of the Urumqi River. *J. Glaciol. and Geocryol.*, 22(1), 62—64.

[4] Li, Z., T. Han, Z. Jing, H. Yang, and K. Jiao. 2003. A summary of 40-year observed variation facts of climate and Glacier No.1 at headwaters of Urumqi River, Tianshan China. *J. Glaciol. and Geocryol.*, 25 (2) 117-123.

[5] Liu, C., Z. Xie, and M. B. Dyurgerov. 1998. Tianshan Glacier. Science Press, Beijing. 227-229.

[6] Sun, Z., Y. Chen, G. You and J. Han. 1985. Flow Characteristics of Glacier No.1 at the Headwater of Urumqi River, Tianshan. *J. Glaciol. and Geocryol.*, 7(1), 27-40.

[7] Tianshan Glaciological Station Annual Report of Tianshan Glaciological Station. 1980-2002. Lanzhou Institute of Glaciology and Geocryology, CAS. Vol.1-16.

[8] Wang, W., J. Liu, X. Luo and G. You. 1976. An retreat in the Glacier No.1 at the headwaters of the Urumqi River,Tianshan,at the 1962-1973 year and contrast survey of the movement. Collected Papers by Lanzhou Institute of Glaciology, Geocryology and desert. No.1. Science Press, 32-35.

[9] Xie, Z., and G. Ge. 1965. A accumulation, melt and mass balance of Glacier No.1 at the headwater of Urumqi River,Tianshan.An studies of glaciology and hydrology on the Urumqi River, Tianshan. Science Press, 14-24.

[10] Yang, D., T. Jiang, Y. Zhang and E. Kang. 1988. Analysis and correction of errors in precipitation measurement at the heat of Urumqi River, Tianshan. *J. Glaciol. and Geocryol.*, 10(4), 384-399.

[11] You, G. 1988. Map of Glacier No.1 and Glacier No.2 at the source of Urumqi River, Tianshan. Xian Cartographic Publishing House.

[12] Zhang, C. 1965. Calculated for the flow speed and thickness of Glacier No.1 at the Headwater of the Urumqi River in the Tianshan Mountains. A study of glaciology and hydrology on the Urumqi River, Tianshan. Science Press, 38-51.

[13] Zhang, J. 1981. Mass balance studies on the No.1 Glacier of Urumqi River, Tianshan. *J. Glaciol. and Geocryol.*, 3(2), 32—40.

[14] Zhang, J., X. Wang, and J. Li. 1984. Study of the relationship between Mass balance change of Glacier No.1 at the headwater of Urumqi River, Tianshan and climate. *J. Glaciol. and Geocryol.*, 6(4), 25—36.

[15] Zhang, J., G. Zhu, S. Qian, J. Chen and Y. Shen. 1985. Radar measuring ice thickness of glacier No.1 at the source of Urumqi river, Tianshan. *J. Glaciol. and Geocryol.*, 7(2), 153—162.

天山乌鲁木齐河源 1 号冰川东支顶部出现冰面湖

李忠勤

（中国科学院 寒区旱区环境与工程研究所天山冰川站/冰芯与寒区环境重点实验室，甘肃 兰州 730000）

天山乌鲁木齐河源 1 号冰川（下简称 1 号冰川）是天山冰川观测试验站进行长期观测试验的冰川之一。是国际冰川监测网中亚洲中部干旱—半干旱区冰川的代表，一直为世界冰川监测服务处(WGMS)选定的全球十条代表性冰川之一。其基本观测资料被定期刊登在由国际水文协会雪冰委员会、联合国环境规划署以及教科文组织（IAHS(ICSI)-UNEP-UNSCO）主办的数种资料报告上，被广泛推介于环境与全球变化研究，并曾为 IPCC 报告所引用。近年天山冰川站加强了对雪冰转化物理化学过程的研究，在积累区开展全年度的观测取样工作。

1　1 号冰川东支顶部冰面湖的发现

2004 年 11 月 16 日，天山冰川站过程研究组沿 1 号冰川东支冰川主流线自下而上挖取雪坑取样，攀登上海拔 4225m 冰川顶部源头区，惊异的发现，在冰川源头的西北方向呈显一个长约 15 m，高约 4 m，面朝南的裸露冰壁，冰壁下竟是一个约 30 m^2 的封闭水域，由于是冬季，水面已结冰，人可在上边行走（见照片 1，2），根据观察，其深度至少在 1.5m 以上。可以推断这在夏季是一个小的冰面湖。

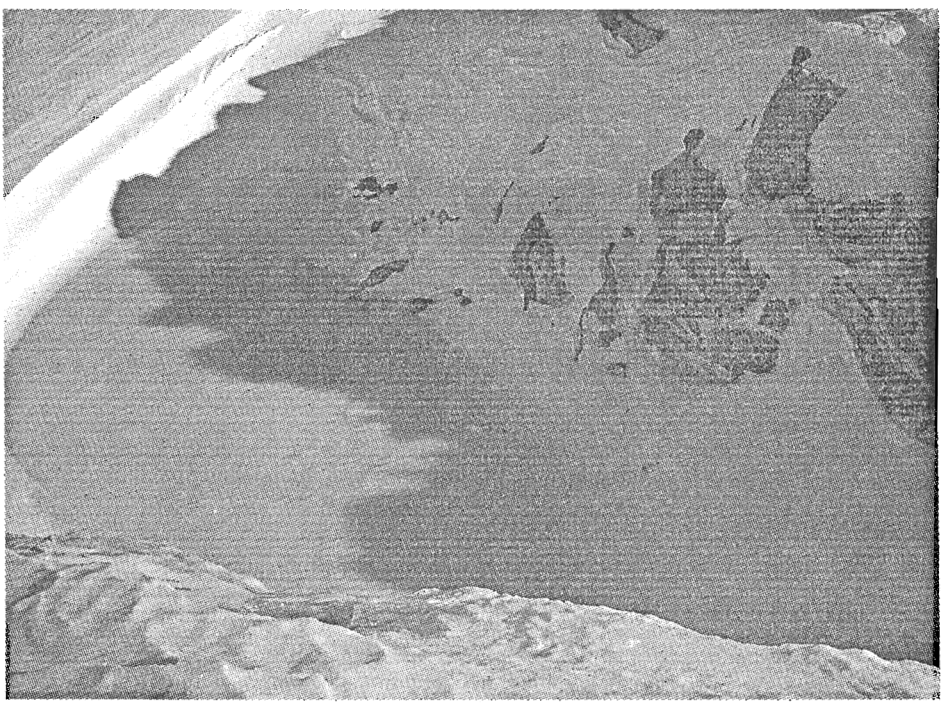

照片 1

照片 2

随后我们对冰源处雪层特征进行了观测，发现该区雪层最大厚度仅为 40 cm 左右，雪层下的冰面上存在一个强污化层，颜色较深（照片 3），推断是由夏季融水作用后形成的。另外，在冰壁上部冰川表面存在一个大约 15 m^2 完全无雪层的区域，冰川冰裸露表面（照片 4），有强烈消融的痕迹。所有这些现象表明，东支顶部冰源区目前已成为具有消融带特征的局部消融区。其量化的消融退缩情况目前尚不清楚。

2 相关研究回顾

有关 1 号冰川成冰作用和成冰带的研究始于上世纪 60 年代初。谢自楚、黄茂桓等将 1 号冰川自下而上划分为 4 个成冰带：消融带，渗浸—冻结带，渗浸带和冷渗浸—重结晶带[1]。1988 年，王晓军等发现[2]，由于气候变暖，冰川上部的冷渗浸—重结晶带特征消失，被渗浸带所取代。因而，在刘潮海等 1989 年的研究中，将 1 号冰川划分为 3 个成冰带，即消融带，渗浸—冻结带，渗浸带[3]。在上述研究中，均将东支顶部划为冷渗浸—重结晶带或渗浸带，但未做具体的描述。近年来我们在开展雪冰演化过程的研究中发现，由于温度上升，成冰带谱有由冷向暖转化，雪层剖面特征趋于简化的现象出现[4、5]。我们对 1 号冰川西支顶部也同时进行了考察，发现此处雪层仍具有渗浸带特征。

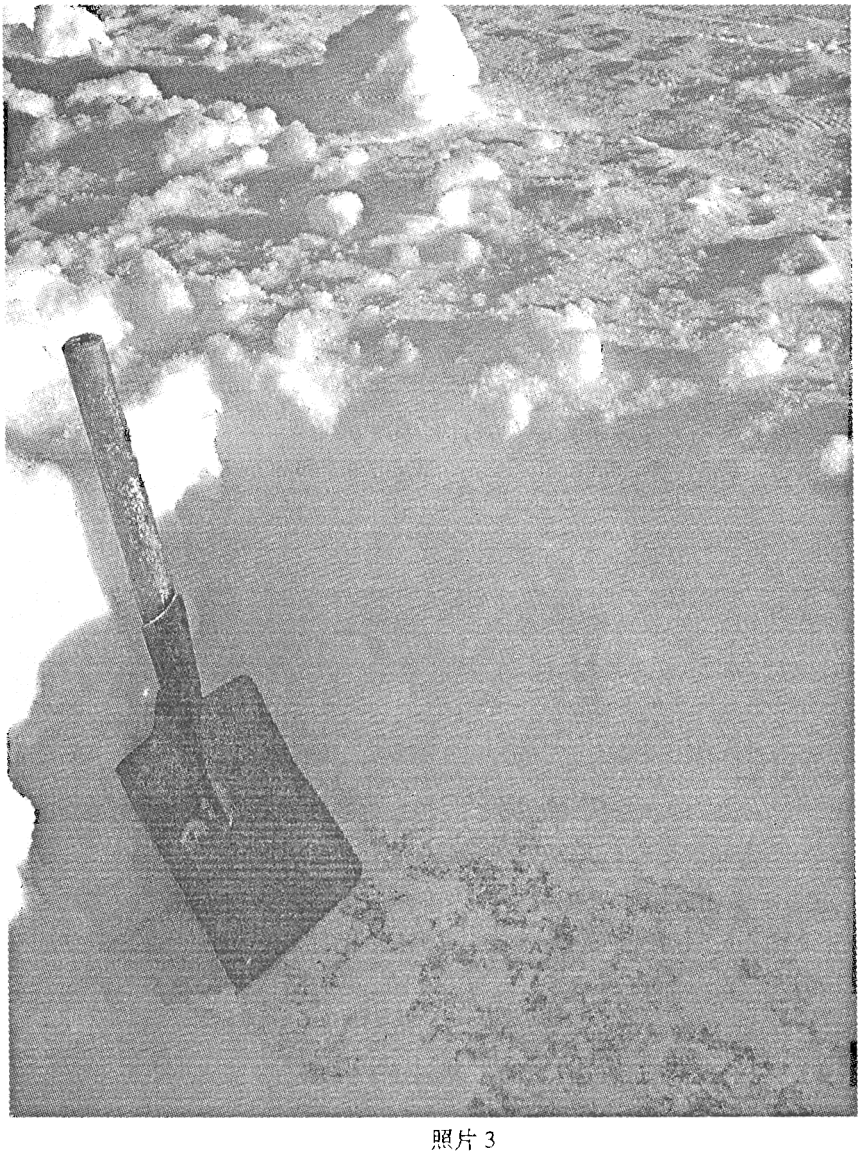

照片 3

3 近期气候变化是导致冰面湖形成的原因

根据最新研究[6, 7]，二十世纪 90 年代中期以来，河源区处于一个最为显著的暖湿阶段。1997—2002 年（2000 年除外）均出现了物质平衡大亏损。其中 2002 年的年均气温是有记录以来的最高值。气温升高给 1 号冰川带来深刻的变化，1958-2003 年这 45 年间，1 号冰川年平均物质平衡量为 –222.0 mm (约 –40.8×104m^3)，累积物质平衡量达到–9991.5 mm，亦即这期间冰川减薄了 11 m 多. 累积亏损量达 1838×104m^3 . 1 号冰川面积在 1962-2000 这 38 年间减少 0.22 km^2，为 11%，并呈加速减小趋势。1962 年至今，1 号冰川东支末端共退缩 175.2m，西支共退缩 197.6m。冰川表面运动速度减缓。1986 以来，冰川年均径流深较之以前翻了近一番。冰川消融的加剧与气温持续升高，冰川冷储减少有很大关系[6]。

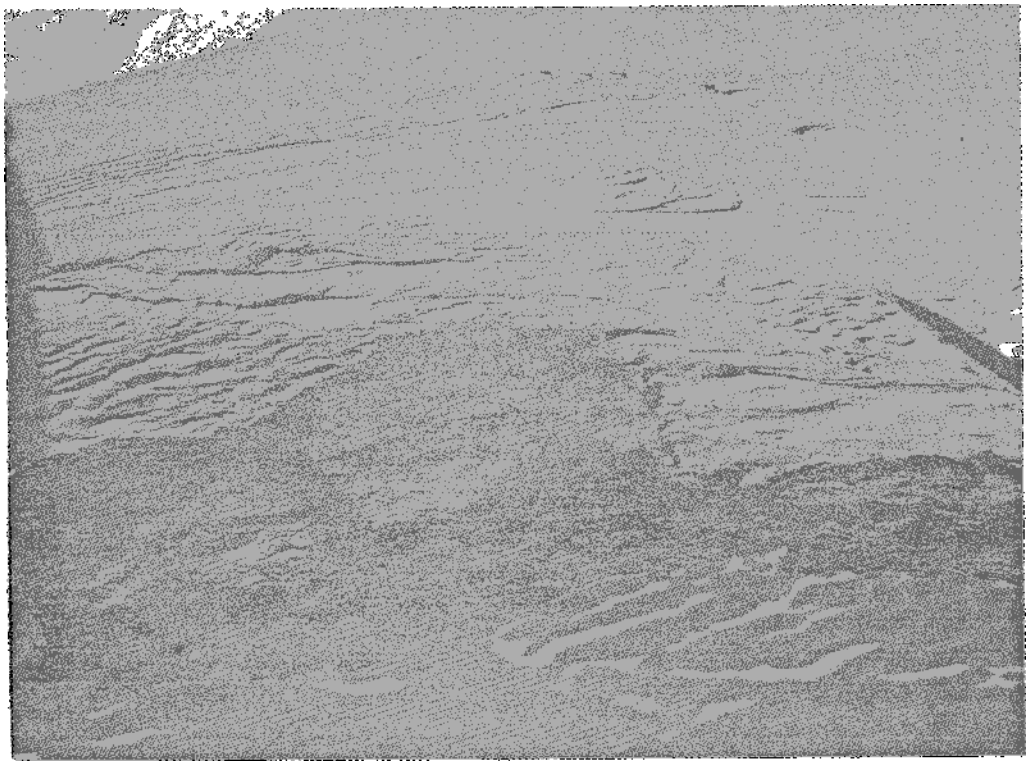

照片 4

气候持续转暖，加之东支顶部冰川末端朝南，周围不远处存在裸露岩石，大量接受日辐射，可能是此小冰面湖产生的直接原因。这一发现表明，在目前气候条件下，对冰川进退变化的监测不仅要在冰川末端进行，而且应该对冰川各个部位进行全方位的监测。冰川顶部出现强烈消融，表明冰川有可能在比较短的时期内大量消融而消失，这是各种冰川变化预测模式中应给予充分考虑的。

参考文献

[1] Xie Zi-chu,Huang Mao-huan. A evolution of the snow-snowgrains layer and ice formation in the Glacier No.1 at the headwaters of the Urumqi River,Tianshan,An studies of glaciology and hydrology on the Urumqi River,Tianshan,Science Press,1965,1-14. [谢自楚,黄茂恒等. 天山乌鲁木齐河源 1 号冰川雪-粒雪层的演变及成冰作用,天山乌鲁木齐河冰川与水文研究,科学出版社,1965,1-14.]

[2] Wang Xiao-jun,Wang Zhong-xiang,Xie Zi-chu. A Change trend of recent climatic on the Tianshan regions from the change of the past 28 years of the glacier No.1 at the Urumqi River headwater,Tianshan.Chinese[J] Science Bulletin,1988,9:693-696. [王晓军，王仲祥，谢自楚。从乌鲁木齐河源 1 号冰川二十八年来的变化看天山地区近期气候变化趋势，科学通报，1988，第 9 期，693－696.]

[3] Liu Chao-hai, Xie Zi-chu,Wang Chun-zu .A Research on the Mass Balance Processes of GlacierNo.1at the Headwaters of the Ürümqi River, Tianshan Mountains. Journal of Glaciology and Geocryology[J].1997,19(1): 17～24. [刘潮海，谢自楚,王纯足. 天山乌鲁木齐河源 1 号冰川物质平衡研究[J]. 冰川冻土.1997，**19**(1): 17～24.]

[4] 李传金,李忠勤,尤晓妮,等. 天山乌鲁木齐河源 1 号冰川不同时期雪层剖面、成冰带特征及成冰年限对比(待发)

[5] 王飞腾,李忠勤,尤晓妮,等. 天山乌鲁木齐河源 1 号冰川积累区表面雪层演化成冰过程的观测研究(待发)

[6] Li Zhongqin, Ellen Mosley-Thompson etc., Observed Facts of Glacier and Climate Change at Headwater Region of Urumqi River, China,(待发)

[7] Li Zhongqin,Han Tianding,Jing Zhefan, *et al.* A summary of 40-year observed variation facts of climate and Glacier No.1 at the headwaters of Urumqi River,Tianshan,china[J].Journal of Glaciology and Geocryology,2003,**25**(2):117-123. [李忠勤,韩添丁,井哲帆,等.乌鲁木齐河源区气候变化和 1 号冰川 40a 观测事实[J].冰川冻土,2003,**25**(2):117-123.]

[8] Jiao Ke-qin,Jing Zhe-fan,Han Yian-ding, *et al.* Variation of the Glacier No.1 at the headwaters Of the Urumqi River in the Tianshan mountains during the Past 42 Years and Its Trend Prediction[J].Journal of Glaciology and Geocryology,2004,**26**(3):253-259. 焦克勤，井哲帆，韩添丁，等. 2004，42 a 来天山乌鲁木齐河源 1 号冰川变化及趋势预测.冰川冻土，**26**（3）：253—259.

42 a 来天山乌鲁木齐河源 1 号冰川变化及趋势预测

焦克勤[1]，成 鹏[2]，井哲帆[1]，韩添丁[1]，杨惠安[1]，叶柏生[1]，李忠勤[1]

(1．中国科学院寒区旱区环境与工程研究所，甘肃　兰州　730000；
(2．乌鲁木齐市气象局，新疆　乌鲁木齐　830000)

摘　要：1959－2000 年间天山乌鲁木齐河源 1 号冰川发生了显著变化，冰川物质平衡累计达-7 976.0 mm，冰川末端退缩 171.06 m，冰川面积缩小 0.217 km^2，冰川厚度平均减薄 8.86 m。冰储量减小 21.9×10^6 m^3，冰川运动速度平均减小 39.3%，冰川成冰带谱上移，冷渗浸—重结晶带消失．从冰川物质平衡反映的气候变化趋势推测，1 号冰川要扭亏为盈，改变已有的巨大的物质亏损(-7 976.0 m)，除非要连续 21 a 出现 42 a 来最大正平衡(+374.0 mm)．已有的观测研究表明。这种情况不大可能出现，1 号冰川目前的退缩趋势还将持续相当一段时间，至少在未来 20~30 a 内不会出现明显的前进．从树木年轮反映的冷暖气候变化周期性推测，目前正处小冰期以来第三个温暖期．若这次温暖期重现 62～67 a 周期的情况，则温暖气候还将持续 20~30a 左右．可见 1 号冰川至少还将持续退缩 20~30 a．

关键词：1 号冰川变化；趋势预测；乌鲁木齐河；天山

1　引言

现代冰川发育地区气温和降水的年际或周期变化，直接影响着冰川物质平衡的增减和雪线的升降．如果气候波动具有某一变化趋势，则冰川就将通过自身速度的调整，改变冰川的规模以适应改变了的气候环境．已有观测研究结果表明。较小的冰川对气候变化的响应敏感，且易于观测研究．因此。在全球性或区域性气候变化研究的国际计划中把冰川作为监测气候变化的重要对象．

天山乌鲁木齐河源 1 号冰川(以下简称 1 号冰川)原为一条双冰斗—山谷冰川．由于全球气候变暖引起的冰川退缩．1 号冰川末端汇合的东、西支于 1993 年完全分离，并成为各自独立的冰川．冰川长度和面积由 1962 年的 2.40 km 和 1.950 km^2 分别减小到 2000 年的 2.20 km 和 1.733 km^2．

自 1959 年建立天山冰川观测试验站(以下简称天山冰川站)并有观测、试验和研究记录以来，1 号冰川的物质平衡、冰川规模(冰川长度、面积和体积)、冰川厚度和运动速度以及成冰类型均发生了明显的变化，反映了 1 号冰川乃至天山冰川 42 a 来对气候变化的响应．42 a 来的观测研究结果表明。对反映气候变化的冰川监测应引起人们的高度重视．

2　气候的基本特征

天山冰川站和大西沟气象站(海拔 3 539 m)1959－2000 年的气象记录统计结果表明，乌鲁木齐河源区年平均气温-5.2℃．负温月长达 7～8 个月，最冷月(1 月)平均气温-15.6 ℃，最热月(7 月)为 4.9 ℃．年平均降水量 441.1 mm．杨大庆等[1]对乌鲁木齐河

源区不同雨量计观测降水对比，以及普通雨量计动力损失、湿润损失和蒸发损失的观测实验表明，普通雨量计观测降水中的动力、湿润和蒸发损失3项之和为26.0%．从而得到天山冰川站和大西沟气象站修正后的多年平均降水量为524.2mm．以22.0 mm (100m)$^{-1}$的年降水梯度，推算出1号冰川零平衡线(海拔4 050 m)处的多年平均降水量为645.8 mm．王德辉等[2]对乌鲁木齐河谷气候特征研究表明，温度梯度最大出现在海拔3 500 m到山顶，为0.56～1.24 ℃ (100m)$^{-1}$，取其平均值0.88℃.(100m)$^{-1}$，按此推算1号冰川零平衡线处年平均气温为-9.7 ℃．

气候的季节变化，按月平均气温是否处于0℃可划分为冬、夏两个季节．冬季自10月至翌年4月．月平均气温均在0 ℃以下，消融很微弱，河水断流．冬季降水量仅占年降水量的10%左右，基本上为纯积累期．5月和9月为夏、冬季节的更替时期，它们是决定夏半年消融期长短的关键月份．5～9月的降水量约占年降水量的90%，降水量最多的时候也是消融最强的时期．因此，夏季月气温的高低和降水量的多寡直接关系到冰川的物质平衡，进而导致冰川发生一系列复杂的变化．

3 1号冰川的近期变化

3.1 物质平衡变化

冰川物质平衡是联系冰川与气候变化过程的一个重要环节，表1给出了1号冰川1958／1959—1999／2000年间的物质平衡值．42 a中有27 a为负平衡年份，负物质平衡量达-1 839.6×10^4 m(-10 002 mm水当量)；15 a为正平衡年份，正物质平衡量仅为+387.3×10^4 m^3 (2 026 mm)，累计物质平衡差额为-1 452.3×10^4 m^3(-7 976 mm)．尤其在1980年以后的20 a间，仅有5 a为正平衡年份，正物质平衡量只有58.9×104 m^3(320 mm)，而负平衡年份占到75%，负物质平衡量达-1 267.7×10^4 m^3(-7 039 mm)．物质平衡差额为-1 208.8×10^4 m^3 (-6 719 mm)．20世纪60年代，1号冰川负物质平衡量为-147．3×10^4 m^3(-756 mm)；70年代为-96.2×10^4 m^3(-501 mm)；80年代为-492．7×10^{4}m^3(-2 679 mm)；90年代猛增至-716.1×10^4 m^3(-4 040 mm)．最近20 a来1号冰川物质亏损量占总冰川物质亏损量的85%，而最近10 a则占到51%．可见1号冰川的物质亏损不仅持续进行，而且不断加剧．在本属积累区的粒雪盆内，不仅当年的积累物质被全部融化，而且原有下伏粒雪或冰层也在不断的被融蚀，整个冰川处于吃老本的状态．

3.2 冰川规模变化

自20世纪60年代以来，首先，应用平板仪(1962年)和地面立体摄影(1973、1980、1986、1994年)以及GPS(2001年)测量方法对1号冰川共进行过6次较正规的大比例尺(1：10 000和1.5 000)地形测量制图．另外，在1964年、1992年和2002年对乌鲁木齐河流域冰川进行了重复航空摄影测量．冰川末端位置和运动速度测量除1962年和1973年的两次外．从1980年开始，每年进行测量，这都为1号冰川规模变化研究提供了可靠依据．在1962－2000年期间。1号冰川末端位置累计退缩了171.06 m，年平均退缩量为4.07 m(表2)．由表2结果表明，20世纪60年代1号冰川后退速度为5.96 m.a^{-1}，70年代为3.28 m a^{-1}，80年代为3.63 m a^{-1}，90年代为4.61 m a^{-1}．可见1号冰川不仅持续处于退缩状态．而且从70年代以来，其退缩速度逐渐加大，并以90年代最为明显．故使原来在末端汇合的东、西支。于1993年已分离为两条各自独立的冰川．1号冰川分离解体后，西支的退缩速率明显大于东支．造成这种差异的原因有：1)西支小于东支，冰川变化对气候变化的响应更敏感；2)西

支粒雪盆(积累区)较小，即冰川补给少；3)西支冰舌末端下伏地形为一陡峻冰坎，不但冰川厚度变小，而且亦造成冰体崩解，从而使冰面高低起伏，接受太阳照射面积增大．进而促使冰川消融强烈和退缩速率加大．

表 1　1 号冰川物质平衡记录

Table 1　Mass balance record of the Glacier No.1

年度	零平衡线海拔 / m	积累区面积 / km^2	消融区面积 / km^2	纯积累量 / $10^4 m^3$	纯消融量 / $10^4 m^3$	纯物质平衡 总量 / $10^4 m^3$	纯物质平衡 平衡值 / mm	资料来源
1958/1959	4 005	1.17	0.78	63.9	47.0	+16.9	+87	文献[4]
1959/1960	4 060	0.86	1.09	49.6	86.2	-36.6	-188	
1960/1961	4 060	0.91	1.04	53.9	60.3	-6.4	-33	
1961/1962	4 075	0.86	1.09	51.6	84.2	-32.6	-167	
1962/1963	3 971	1.35	0.60	85.2	39.5	+45.7	+234	文献[5]
1963/1964	4 055	0.93	1.02	55.9	55.5	+0.4	+2	
1964/1965	3 948	1.53	0.42	99.8	26.8	+73.0	+374	
1965/1966	4 110	0.71	1.24	34.6	107.5	-72.9	-374	
1966/1967	4 063	0.89	1.06	58.4	72.0	-13.6	-70	
1967/1968	4 121	0.68	1.27	38.0	127.0	-89.0	-456	
1968/1969	4 008	1.15	0.80	77.4	48.6	+28.8	+148	
1969/1970	4 106	0.73	1.22	41.0	102.0	-61.0	-313	
1970/1971	4 015	1.11	0.84	71.1	51.2	+19.9	+102	
1971/1972	3 981	1.31	0.64	90.1	39.0	+51.1	+262	
1972/1973	4 146	0.60	1.35	27.0	165.0	-138.0	-708	
1973/1974	4 075	0.84	1.11	55.7	80.0	-24.3	-125	
1974/1975	3 982	1.27	0.60	89.8	36.0	+53.8	+288	文献[6]
1975/1976	4 066	0.85	1.02	48.4	43.0	+5.4	+29	
1976/1977	4 001	1.20	0.67	70.4	37.0	+33.4	+180	
1977/1978	4 155	0.52	1.35	28.1	48.4	-20.3	-110	
1978/1979	4 120	0.61	1.26	31.2	46.7	-15.5	-84	
1979/1980	4 038	0.88	0.96	20.7	82.4	-61.7	-335	
1980/1981	4 122	0.54	1.30	15.2	135.1	-119.9	-652	
1981/1982	4 025	0.88	0.96	62.1	70.3	-8.2	-45	
1982/1983	4 005	1.04	0.80	65.2	46.8	+18.4	+100	
1983/1984	4 007	1.07	0.77	30.8	46.0	-15.2	-83	文献[7]
1984/1985	4 097	0.56	1.28	19.6	132.2	-112.6	-611	
1985/1986	4 130	0.50	1.34	1.3	134.3	-133.0	-723	
1986/1987	4 025	0.91	0.93	36.5	68.8	-32.3	-176	文献[7]
1987/1988	4 080	0.66	1.18	10.8	129.2	-118.4	-644	文献[7]
1988/1989	3 980	1.29	0.55	59.8	40.8	+19.0	+103	文献[7]
1989/1990	3 959	1.30	0.54	54.0	44.5	+9.5	+52	文献[7]
1990/1991	4 130	0.57	1.27	5.5	135.4	-129.9	-706	
1991/1992	3 975	1.26	0.58	49.7	45.5	+4.2	+23	文献[7]
1992/1993	3 980	1.27	0.57	46.1	51.5	-5.4	-29	文献[7]
1993/1994	4 058	0.74	1.10	25.7	95.2	-69.5	-378	
1994/1995	4 035	0.92	0.92	19.1	61.1	-42.0	-228	
1995/1996	3 986	1.23	0.61	24.6	16.8	+7.8	+42	文献[7]
1996/1997	4 160	0.426	1.316	10.1	158.7	-148.6	-853	文献[8]
1997/1998	4 096	0.570	1.172	9.9	147.5	-137.6	-790	
1998/1999	4 122	0.539	1.203	8.2	145.9	-137.7	-791	文献[7]
1999/2000	4 063	0.867	0.875	17.2	74.6	-57.4	-330	

注：计算冰川物质平衡使用的冰川面积以 5 次测图为基础。但由于 1973 和 1994 年的成图滞后，故有 3 年（1973/1974 年、1994/1995 和 1995/1996 年）使用前一次测图的冰川面积。

表 2 1号冰川末端退缩速度

Table 2 Record of retreat speed at the terminus of the Glacier No.1

年度	平均退缩速度 /(m a⁻¹)			累计退缩距离 /m	资料来源
1962-09 —1973-08	- 5.96			- 65.60	文献[9]
1973-09 —1980-08	- 3.28			- 88.59	文献[7]
1980-09 —1981-08	- 4.83			- 93.42	
1981-09 —1982-08	- 2.06			- 95.48	
1982-09 1983-08	- 2.94			- 98.42	
1983-09 —1984-08	- 3.39			- 101.81	文献[7]
1984-09 —1985-08	- 3.35			- 105.16	
1985-09 —1986-08	- 3.58			- 108.74	
1986-09 1987-08	- 3.68			- 112.42	文献[7]
1987-09 1988-08	- 3.80			- 116.22	文献[7]
1988-09 —1989-08	- 5.13			- 121.35	
1989-09 —1990-08	- 3.57			- 124.92	
1990-09 —1991-08	- 6.51			- 131.43	
1991-09 1992-08	- 3.44			- 134.87	
1992-09 —1993-08	- 3.84			- 138.71	
	东支		西支		
1993-09 —1994-08	- 4.85	- 5.80	- 6.75	- 144.51	
1994-09 1995-08	- 3.95	- 5.06	- 6.17	- 149.57	文献[7]
1995-09 —1996-08	- 3.40	- 4.00	- 4.60	- 153.57	
1996-09 —1997-08	- 3.65	- 4.23	- 4.80	- 157.80	
1997-09 —1998-08	- 3.47	- 3.97	- 4.47	- 161.77	
1998-09 —1999-08	- 3.41	- 4.13	- 4.85	- 165.90	
1999-09 —2000-08	- 3.40	- 5.16	- 6.92	- 171.06	
平均	- 3.73	- 4.17	- 5.51	- 4.07	—

注：1993 年 1 号冰川完全分离成为 2 条独立的冰川，故列出了东、西支平均后退速度值。

表 3 1号冰川面积变化

Table 3 Variation in area of the Glacier No.1

时间	面积 /km²	面积缩小量 /km²	面积缩小率 /%	备注	时间	面积 /km²	面积缩小量 /km²	面积缩小率 /%	备注
1962-08	1.950	0.000	0.0	文献[9]	1986-08	1.840	0.110	5.6	文献[10]
1964-09	1.941	0.009	0.5	陈建明等[1)]	1992-08	1.833	0.117	6.0	陈建明等[4)]
1973-08	1.870	0.080	4.1	陈建明等[2)]	1994-08	1.742	0.208	10.7	焦克勤等[5)]
1980-08	1.840	0.110	5.6	孙作哲等[3)]	2000-08	1.733	0.217	11.1	井哲帆等[6)]

注：1）和 4）据航测地形图量算；2）、3）、5）据地面立体摄影图量算冰川变化图量算。

根据历次大比例尺地形测量制图，可量算出 1 号冰川面积的变化(表 3). 由表 3 可以看出，1962—2000 年间 1 号冰川面积缩小了 0.217 km^2，平均缩小率为 11.1%，与陈建明等[3]通过两次(1964 年和 1992 年)航空摄影测量成图对比获取的冰川变化值基本一致. 此外，据 1 号冰川物质平衡值估算，冰川厚度平均减薄 8.86 m，相应的冰川储量减小量达 17.3×10^6 m^3。减小的冰川储量占 1964 年相应冰川储量的 16.2%.

3.3 冰川厚度和运动速度变化

1962—2000 年间，1 号冰川厚度平均减薄 8. 86m. 由于冰川运动速度与冰川厚度变化成指数变化，因此. 厚度的变化必然引起速度的急剧变化(表 4). 从表 4 可以看出，近 42a 来冰川表面运动速度不断衰减。特别是进入 80 年代后，其衰减趋势更加明显. 1980—2000 年冰川运动速度仅是 1959—1973 年的 46.7%. 可以推测，今后一段时间内 1 号冰川平均运动速度不会超过 5.0 $m.a^{-1}$.

表 4　1 号冰川不同高度平均运动速度

Table 4　Average flow speed changing with time of the Glacier No.1

1959 —1962 年		1973 年		1980 —1990 年		1991 —2000 年	
断面海拔 /m	运动速度 /(m a^{-1})	断面海拔 /m	运动速度 /(m a^{-1})	断面海拔 /m	运动速度 /(m a^{-1})	断面海拔 /m	运动速度 /(m a^{-1})
3 800(6)	7.09	3 800(2)	4.39	3 797(6)	3.83	3 803(4)	3.87
3 870(3)	7.13	3 870(2)	10.92	3 867(3)	5.26	3 860(2)	5.04
3 990(4)	11.41	3 990(3)	11.63	3 991(5)	6.55	3 986(5)	5.92
4 055(4)	22.15	4 050(2)	11.12	4 061(5)	5.45	4 056(5)	3.96
平均	11.95		9.52		5.27		4.70

注：1）表中断面高度为平均高度；2）表中带括号的数为测点数.

3.4 冰川成冰带谱变化

冰川成冰带谱是根据冰雪融水参与的程度与由此而引起的积雪晶体的变化情况划分的. 在 20 世纪 60 年代，1 号冰川自下而上依次为消融带、渗浸冻结带、渗浸带、冷渗浸—重结晶带. 粒雪盆后壁广泛发育着冷渗浸—重结晶带，其特点为融水不能完全浸入年积雪层而使粒雪得以生存[11]. 但到 80 年代，由于融水的大量渗浸，粒雪在融水作用下发生再冻结，原来的粒雪层已为密实冻结粒雪和渗浸冰所取代[12]. 而到了 90 年代，除新近降雪(一般厚度在 40～50 cm)外，原来的密实冻结粒雪和渗浸冰已变成冰川冰. 成冰带谱的显著变化，也反映了冰川水热状况的改变.

4 冰川对气候变化的响应

根据乌鲁木齐河河源 42 a 来的气温和降水记录(表 5)，90 年代夏季、冬季和年平均温度比前 3 个 10 a(1959—1970 年、1971—1980 年和 1981—1990 年)分别高出 0.5～0.6 ℃、0.6～1.0℃和 0.6～0.8℃；而夏季和年平均降水量分别高出 68.2～93.9mm 和 61.5～79.1 mm. 显然。河源区处于一个最为明显的暖湿阶段，其结果使 1 号冰川物质负平衡、冰川面积和体积、冰川厚度和运动速度以及冰川末端退缩速度的变化量出现 42 a 来的最大值(表 1～4). 这与新疆以天山西部地区为主，乃至西北地区出现的气候转向暖湿，降水量、冰川

消融量和河流径流量连续多年增加，导致湖泊水位显著上升、洪水灾害猛烈增加、植被改善和沙尘暴减少相一致[13-17]. 80 年代的夏季、年平均温度和降水量差别甚小，而冬季温度却比前 2 个 10 a(1959—1970 年和 1971—1980 年)分别高出 0.2 ℃和 0. 4℃，这对于反映 1 号冰川变化的冰川负物质平衡、面积和体积、厚度和运动速度、末端位置，从 80 年代就已开始逐渐增大(表 1～4). 60－70 年代，冰川变化总体受气温和降水量的共同作用，即在变化上与气温呈反相关，与降水呈正相关[18].

表 5 乌鲁木齐河河源区的气温和降水

Table 5 Air temperature and precipitation at the headwaters of the muqi River changing with time

时间	平均气温/ C			平均降水量/ mm		
	5～8 月	12 月至翌年 2 月	年均	5～8 月	12 月至翌年 2 月	年均
1959 1970	2.8	- 14.9	- 5.2	343.3	2.3	436.9
1971 1980	2.9	- 15.1	- 5.3	323.0	3.1	424.4
1981 1990	2.9	- 14.7	- 5.4	317.6	3.3	419.3
1991 —2000	3.4	- 14.1	- 4.6	411.5	3.5	498.4

乌鲁木齐河河源区自 80 年代中期以来气温(尤其是冬季气温)持续升高，造成了冰川冷储的减少，致使冰川对气候变暖的敏感性大大增强. 在这一背景下，气温的稍许增加，亦造成冰川消融的非线性加速增加. 根据这一推断. 在目前全球气候持续变暖的大背景下，1 号冰川可能正经历着一种超出我们估算的速度消融. 因此，有必要对 1 号冰川重新进行基本的雪冰物理(冰川温度、冰川结构和成冰过程等)特征的观测研究，有助于对中国西部乃至世界许多地区自 80 年代中期以后，冰川消融速度加快. 冰川径流量增大的合理解释.

5 冰川变化的趋势预测

5.1 从物质平衡的变化趋势预测

从冰川物质平衡角度出发，冰川末端可以说是冰川的另一条零平衡线. 冰川末端位置变化，取决于冰川运动向下移动的冰量与当年消融量引起冰川后退之间的对比关系. 若前者大于后者则冰川前进，反之则退缩. 因此，在讨论冰川未来发展趋势时，不仅要考虑冰川年际平衡值的正负和大小. 更应考虑多年累积的物质平衡值. 42 a 来 1 号冰川负的累计平衡值高达 7 976.0 mm. 若要扭亏为盈，改变已有巨大的物质亏损，除非要连续 21 a 出现 42 a 来最大正平衡(+374.0 rmm). 根据已有的观测研究以及目前的气候变化趋势，这种情况不大可能出现. 因此，推测 1 号冰川目前的退缩趋势还将持续相当一段时间，至少在 20～30 a.

5.2 从树木年轮反映的冷暖周期性预测

康兴成[19]对乌鲁木齐河流域上树线附近树木年轮的周期分析计算，获得了反映该流域气温冷暖变化 456 a 序列的方差分析有 55、62~67 a 的主要周期. 在谱密度分析中存在 2~3 a 的短周期和 100 a、150 a 和 302 a 的长周期. 目前正处于小冰期以来第三个温暖时期，其周期约为 62~67 a. 1955~2000 年已经历 45 a. 若这次温暖期重现 1650~1710 年的情况，则目前的温暖气候还将持续 20 a 左右. 而冰川进退变化反映气候变化存在着滞后现象，一般山谷冰川进退变化滞后气候变化的时间约 10 a 左右. 由此推测 1 号冰川至少还将持续退

缩 20～30 a.

5.3 应用不同方法的计算值预测

王文悌等[20]按 J. F. Nye 扰动方程的频率解. 把 1959~1981 年作为 1 号冰川扰动的一个周期. 计算得出 1 号冰川最终要退缩 338 m，若以平均 4.0 $m.a^{-1}$ 的速度后退，则需要后退 80 a 左右. 由此可见. 1 号冰川还将继续退缩 30～40 a.

曹梅盛等[21]对稳定状态下冰川纵向断面计算得出，1 号冰川达到稳定状态，总面积比 1980 年减少 0.304 km^2. 实际上 1 号冰川面积比 1980 年减少 0.107 km^2. 可见 1 号冰川面积还要继续减少 0.197km^2，方能达到稳定状态.

综合上述，认为 1 号冰川在 2030 年前不会出现稳定或前进，不仅继以持续退缩，而且很可能出现消融和退缩的加速. 在中国冰川对 21 世纪全球变暖响应的预估中，施雅风等[22]引用 HadCM2 Gsal 模拟数值结合中国 3 类冰川分布区，提出了 2030、2070 和 2100 年 3 个时段的升温估计值. 其中. 2030 年亚大陆型冰川区(包括天山)升温 0.9℃的情况下，冰川面积或体积还要减少 15%. 可见. 在全球气候变暖的大环境下，1 号冰川的持续后退趋势是毫无疑问的.

参考文献(Riferences):

[1] Yang Daqing, Jiang Tong, Zhang Yinsheng, et al. Analysis and correction of errors in precipitation measurement at the head of Urümqi River, Tianshan [J]. Journal of Glaciology and Geocryology, 1988, 10(4): 384-399. [杨大庆，姜彤，张寅生，等. 天山乌鲁木齐河源降水观测误差分析及其修正 [J]. 冰川冻土，1988，10(4)：384-399.]

[2] Wang Dehui, Zhang Peiyuan. On the valley climate of Urümqi River in the Tianshan Mountains [J]. Journal of Glaciology and Geocryology, 1985, 7(3): 239—248. [王德辉，张丕远. 天山乌鲁木齐河谷气候特征 [J]. 冰川冻土，1985，7(3)：239. 248.]

[3] Chen Jianming, Liu Chaohai, Jin Mingxie. Application of the repeated aerial photogrammetry to monitoring glacier variation in the drainage area of the Urümqi River [J]. Journal of Glaciology and Geocryology, 1996, 18(4): 331-336. [陈建明，刘潮海，金明燮. 重复航空摄影测量方法在乌鲁木齐河流域冰川变化检测中的应用 [J]. 冰川冻土，1996，18(4)：331-336.]

[4] Xie Zichu, Ge Guangwen. Study of accumulation, ablation and mass balance of Glacier No.1 at the headwater of Urümqi River, Tianshan [A]. Studies of Glaciology and Hydrology on the Urümqi River, Tianshan [C]. Beijing: Science Press, 1965. 14-24. [谢自楚，葛光文. 天山乌鲁木齐河源 1 号冰川的积累、消融及物质平衡 [A]. 天山乌鲁木齐河冰川与水文研究 [C]. 北京：科学出版社，1965. 14-24.]

[5] Zhang Jinhua. Mass balance studies on the No. 1 Gacier of Urümqi River, Tianshan [J]. Journal of Glacioiogy and Geocryology, 1981, 3(2): 32-40. [张金华. 天山乌鲁木齐河源 1 号冰川物质平衡研究 [J]. 冰川冻土，1981，3(2)：32-40.]

[6] Zhang Jinhua, Wang Xiaojun, Li Jun. Study of the relationship between Mass balance change of Glacier No.1 at the headwater of Urümqi River, Tianshan and climate [J]. Journal of Glaciology and Geocryology, 1984, 6(4): 25. 36. [张金华，王晓军，李军. 天山乌鲁木齐河源 1 号冰川物质平衡变化与气候相互关系的研究 [J]. 冰川冻土，1984，6(4)：25. 36.]

[7] Tianshan Glaciological station. Annual Report of Titanshan Glaciological station, Vol. 1-16 [R].

Lanzhou Institute of Glaciology and Geocryology, CAS, 1980-2002. [天山冰川观测试验站. 天山冰川站年报, 1-16卷 [R]. 兰州: 中国科学院兰州冰川冻土研究所, 1980. 2002.]

8] Jiao Keqin, Wang Chunzu, Han Tianding. A strong negative mass belance recently appeared in the Glaeier No.1 at the headwaters of the Urümqi River [J]. Journal of Glaciology and Geocyology, 2000, 22 (1): 62-64. [焦克勤, 王纯足, 韩添丁. 天山乌鲁木齐河源1号冰川新近出现大的物质负平衡 [J]. 冰川冻土, 2000, 22 (1): 62—64.]

9] Wang wenying, Liu Jinghuang, Luo Xiangrui, et al, An retreat in thc Glacier No.1 at the headwaters of the Urümqi River, Tianshan, at the 1962-1973 year and coutrast survey of the movement [A]. Memoirs of Lanzhau Institute of Glaciology, Geocryology and Desert Research, No.1 [C]. Beijing: Science Press, 1976. 32-35. [王文颖, 刘景璜, 罗祥瑞, 等. 1962-1973年天山乌鲁小齐河1号冰川的后退和运动对比测量 [A]. 中国科学院兰州冰川冻土沙漠研究所集刊, 第1号 [C]. 北京: 科学出版社, 1976. 32-35.]

[10] You Genxiang. Map of Glacier No.1 and Glacier No.2 at the Source of the Urümqi River, Tianshan Mountains [M]. Xi'an: Xi'an Cartographic Publishing House,1988. [尤根祥. 乌鲁木齐河源1号和2号冰川图 [M]. 西安: 西安地图出版社, 1988,]

[11] Xie Zichu, Huang Maohuan. An evolution of the snow-firn layer and ice formation in the Glacier No.1 at the headwaters of the Urümqi River, Tianshan [A]. Studies of Gaciology and Hydrology on the Urümqi River, Tianshan [C]. Beijing: Science Press, 1965, 1-14. [谢自楚, 黄茂桓. 天山乌鲁木齐河源1号冰川雪-粒雪层的演变及成冰作川 [A]. 天山乌鲁木齐河源冰川和水文研究 [C]. 北京: 科学出版社, 1965. 1-14.]

[12] Wang Xiaojun, Wang Zhongxiang, Xie Zichu, Change trend of recent climatic on the Tianshan regions from the change of the past 28 years of the glacier No.1 at the Urümqi River Headwater, Tianshan [J]. Chinese Science Bulletin, 1988, 9: 693—696. [王晓军, 王仲祥, 谢自楚. 从乌鲁木齐河源1号冰川二十八年来的变化看天山地区近期气候变化趋势 [J]. 科学通报, 1988, 9: 693- 696、]

[13] Shi Yafeng,shen Yongping, Hu Ruji. Preliminary study on signal,impact and foreground of climatic shift from warm-dry to warm-humid in North west China [J]. Journal of Glaciology and Geocryology, 2002,24(3):219-226. [施雅风, 沈永平, 胡汝骥. 西北气候由暖干向暖湿转型的信号、影响和前景初步探讨 [J]. 冰川冻土, 2002, 24(3): 219-226.]

[14] Guo Ni, Zhangjie, Liang Yun. Climate change indicated by the recent change of inland lakes in Northwest China [J] Journal of Glaciology and Geocryology, 2003, 25(2): 211-214. [郭铌, 张杰, 梁芸. 西北地区近年米内陆湖泊变化反峡的气候问题 [J]. 冰川冻土, 2003, 25(2): 2ll-214.]

[15] Li Yuan, Tan Yuan, Jiang Fenqing, et al. Study on hydrological features of the Kaidu River and the Bosten Lake in the Second Half of 20th Century[J]. Journal of Glaciology and Geocryology, 2003,25 (2):215-218.[李宇安, 谭芫, 姜逢清, 等. 20世纪下半叶开都河与博斯腾湖的水文特征 [J]. 冰川冻土, 2003, 25(2): 215-218.]

[16] Su Hongchao, Wei Wenshou, Han Ping. Change in the air temperature and evaporation in Xinjiang during recent 50 year[J]. Journal of Glaciology and Geocryology, 2003, 25(2): 174-178. [苏宏超, 魏文寿, 韩萍. 新疆近50 a来的气温和蒸发变化[J]. 冰川冻土, 2003, 25(2): 174-178.]

[17] Zhang Guowei, Wu Sufen, Wang Zhijie. The signal of climatic shift in northwest China deduced form river runoff change in Xinjiang region [J]. Journal of Glaciology and Geocryology, 2003,25(2):183-187.[张国

威，吴素芬，王志杰．两北气候环境转型信号在新疆河川径流变化中的反映［J］．冰川冻土，2003，25(2)：183-187]

[18] Li Zhongqin, Han Tianding, Jing Zhenfan, et al. A summary of 40 year observed variation facts of climate and Glacier No.1 at headwaters of Urümqi River, Tianshan, China[J]. Journal of Glaciology and Geocryology, 2003, 25(2):117-123.[李忠勤，韩添丁，井哲帆．等．乌鲁木齐河源区气候变化和 I 号冰川 40 a 观测事实［J］．冰川冻土，2003，25(2)：117—123．]

[19] Kang Xingcheng. A preliminary analysis on the climatic changes in the drainage area of Urümqi River from tree ring[J]. Journal of Glaciology and Geocryology, 1985，7(2)：133-140．[康兴成，天山乌鲁木齐河流域年轮气候的初步分析［J］．冰川冻土，1985，7(2)：133-140．]

[20] Wang Wenti，Liu Zongxiang．Analysis of the frequency response behaviour of the G1acier No.1 at the Urümqi River Headwater，Tianshan [J]．Journal of Glaciology and Geocryology, 1984, 6(4):13-24.[王文悌，刘宗香．天山乌鲁木齐河源 1 号冰川频率响应特性的计算与分析［J］．冰川冻土，1984，6(4)：13-24.]

[21] Cao Meisheng, Meier M F. Calculation of glacial longitudinal sectionsunder stable conditions-Glacier No.1 at the headwater of the Urümqi River, Tianshan Mt. As an example[J]. Journal of Glaciology and Geocryology, 1987,9(2):131-138.[曹梅盛，迈耶 M F．稳定状态下冰川纵向断面计算－以天山乌鲁木齐河源 1 号冰川为例［J］．冰川冻土，1987，9(2)：131-138.]

[22] Shi Yafeng，Liu Shiyin. The calculation of Chinese glacier's response to the globe climatic warming in the 21th century[J]. Chinese Science Bulletin, 2000,45(4):434-438.[施雅风，刘时银．中国冰川对 21 世纪全球变暖响应的预估［J］．科学通报，2000，45(4)：434-438．]

Variation of the Glacier No. 1 at the Headwaters of the Urümqi River in the Tianshan Mountains during the Past 42 Years and Its Trend Prediction

JIAO Ke-qin, Cheng Peng, JING Zhe-fan, HAN Tian-ding,
YE Bai-sheng, YANG Hui-an, LI Zhong-qin

Abstract: The Glacier No. 1 at the headwaters of the Urümqi Rive in the Tianshan Mountains (thereafter called Glacier No.1) originally was a valley glacier with two cirques. Owing to glacial retreat caused by global warming, the east branch of the glacier separated from the west branch in 1993. The length and area of the glacier decreased from the 2.2 km and 1.950 km^2 in 1964 to 2.0km and 1. 733 km^2 in 2000, respectively.

The Glacier No.1 has remarkably changed during the past 42 years, which can be seen from the following factors : mass balance of - 7 976.0 mm, terminus retreat of 171.1 m, area decrease of 11.1%, mean thickness of 8.86m and flow speed decrease of 39. 3 %. In addition, owing to the upward shift of ice formation zones, cold percolation-recrystallization zone disappeared. These reflect the general trend of climate change during the past 42 years. The observation for 42 years shows that for those glaciers, through which climate change can be reflected, the observation should be greatly highlighted.

Based on the variation trend of glacial mass balance, it is predicted that the Glacier No. 1 would not make up the great mass deficits (-7 976.0 mm) and get surpluses unless it keeps continuous accumulation for 21 years with the extent of the biggest positive balance during the past 42 years (+374.0 mm). The previous researches show that the above condition hardly appears. Thus, it is conjectured that the retreating trend of the glacier will continuously go on for quite a long time, at least before the 2030s it is impossible to appear an apparent glacier advance.

Based on the periodic characteristics of cold-warm and dry-wet circles in climate change as derived from tree ring data, it is presumed that it is now in the third warm period since the Little Ice Age. From 1955 up to now, the period lasts 45 years. If the warm period recurs with a periodicity of 62~67 years, it will last about 20 years from now on. Thus, it is expected that the glacier will keep retreating for more scores of years.

Key words: variation of the Glacier No.1; trend prediction; Urümqi River; Tianshan Mountains

天山天格尔山南北坡降水特征研究

韩添丁[1]，丁永建[1]，叶柏生[1]，成　鹏[2]，谢昌卫[1]

(1. 中国科学院寒区旱区环境与工程研究所，甘肃 兰州，730000;
2.乌鲁木齐市气象局，新疆 乌鲁木齐，830000)

摘　要：对新疆天山天格尔山南北坡乌拉斯台河和乌鲁木齐河流域及其山前平原不同高度气象（水文）站近 40 年降水实测资料的统计分析，研究天山天格尔山南北坡不同坡向及高度的降水特征。结果表明：山区降水远大于山前平原，南北坡降水均主要呈现为增加趋势，冬季和夏季降水的增加趋势明显；山前平原区降水的年际变化幅度大于山区；冬、春季降水变率大于夏、秋季，南坡降水变率远大于北坡，冬、春季表现地尤为突出。年际降水的减少趋势出现在乌鲁木齐河流域中山峡谷地带的英雄桥水文站，其春季 3 月份的降水量减少趋势非常显著；乌鲁木齐河源大西沟气象站 4－5 月和 6－8 月月降水呈明显的反相关变化。

关键词：天山；南北坡；降水变化；趋势；相关

1　引言

近数十年来，全球气候温暖化趋势十分明显。气候变暖，水循环速度及频率加快，导致了全球降水量有明显的减少趋势[1]，降水时空变率增大；同时又明显表现出降水强度、月（日）等时段降水的差异[2-5]和区域降水的差异性变化。这种差异性在地处中国西北内陆干旱区的新疆却呈现了降水的明显增加趋势，尤其是 1987 年以后，上升趋势非常明显[6,7]。由于区内水汽来源和地形的差异特点，降水在平原区和山区差异较大，山区降水远大于平原区[6,8,9]。本文就新疆天山天格尔山南北坡降水变化的区域性特征进行研究，主要分析天格尔山南北坡降水的年（月）际变化及降水变率特点，分析其与全球降水变化、西北气候转型过程中降水效应的关系，及其降水在天山不同坡向及高度的响应特征。

2　资料

选取天山天格尔山南北两坡乌拉斯台河和乌鲁木齐河流域及山前平原不同海拔高度气象站（水文站）的降水实测资料，运用趋势和相关分析等方法，分析天山南北坡降水的高度变化及季节(年)变化特点，结合不同季节环流型式，探讨降水变化差异的原因。所选资料系列从 1950 年代至 2000 年不尽一致。南坡台站有：巴仑台（1958-2000 年）、黄水沟(1958-2001 年)、和静(1960-1995 年)和库尔勒(1959-2000 年)；北坡台站：英雄桥(1959-2001 年)，乌鲁木齐（1951-2000 年）、昌吉（1953-1996 年）、蔡家湖（1959-2000 年）和天山乌鲁木齐河源大西沟气象站（1958-2002 年）。所选台站资料系列均超过 20a 以上，其均值基本趋于稳定[10]，其趋势分析可以代表其长系列的变化趋势。

3 不同坡向及高度年降水特征

3.1 降水的年变化趋势

图 1 结果显示，天山南北坡各站降水基本表现为明显的增加趋势，尤以 20 世纪 80 年代中后期以来，年降水的增加趋势非常明显。其中蔡家湖、乌鲁木齐、大西沟、巴仑台及和静等站的降水增加趋势系数均达到了 0.05 的信度水平；南坡黄水沟站降水量增加的趋势系数为 0.48（达到了 0.01 的信度水平）；虽然天山北坡山前平原的昌吉和南坡的库尔勒等地降水量趋势系数未达到 0.05 的信度水平，但其降水仍呈现了明显的增加趋势。统计资料中，只有乌鲁木齐河流域英雄桥水文站的降水量呈现出明显的减少趋势（趋势系数为 -0.20），也未达到 0.05 信度水平；韩萍等[6]认为天山北坡乌鲁木齐—石河子一带的部分区域降水主要呈现减少的趋势，但从分析来看，山前平原区（包括乌鲁木齐）的降水减少趋势不甚明显，这种减少趋势仅出现在乌鲁木齐河峡谷地带的英雄桥，其可能与台站所在位置的地形特点有关。

由于西风环流是新疆降水的主要来源，天山北坡为迎西北来的湿润气流的迎风坡，南坡则为背风坡；因此，北坡乌鲁木齐河流域降水均大于南坡乌拉斯台河流域降水。

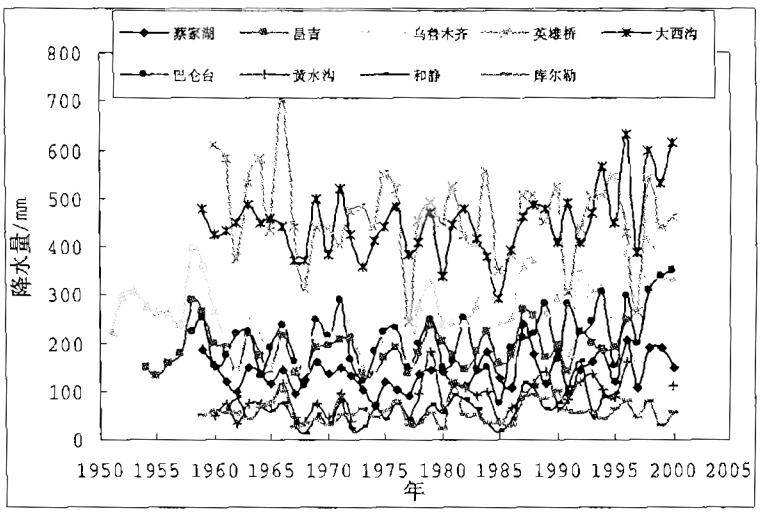

图 1 天山天格尔山南北坡降水量变化

Fig.1 Changes of annual precipitation in the southern and northern slopes of the Tianger Range in Tianshan Mountains

3.2 不同高度及坡向的年降水变率分析

表 1 为本文研究所选台站位置、海拔高度及年平均降水量，台站分布在天格尔山南北两坡不同高度区域及山前地带，降水的高度剃度变化及坡向差异明显，基本反映了天山乌垃斯台河和乌鲁木齐河流域降水随高度的变化特征。

降水随海拔高度的升高而递增的趋势非常明显（图 2），天山南坡的这种趋势更为突出，北坡在英雄桥附近呈现出最大降水量，其高度正好处在最大降水高度(1600-2100m)区域[11]，是北坡最大降水的第一高度带；中国科学院天山冰川站的野外观测数据表明，北坡的第二

大降水带存在于海拔 4000m 左右的乌鲁木齐河源高山冰雪带。

表 1 天山天格尔山南北坡各台站海拔及年平均降水量统计表

Table 1 Elevation and annual precipitation of the stations on the southern and northern slopes of the Tianger Range in Tianshan Mountains

坡 向	北坡					南坡			
台 站	蔡家湖	昌吉	乌鲁木齐	英雄桥	大西沟	巴仑台	黄水沟	和静	库尔勒
海拔/m	441	577	918	1920	3539	1739	1313	1102	934
年降水量/mm	139.4	186.7	259.9	468.5	449.4	210.0	86.3	62.7	55.9

年降水变率 *Cv* 与年降水量的大小呈明显的反相关关系，相关系数为-0.82 (达到了 0.01 的信度水平)；南坡降水变率明显大于北坡，中、低山带及平原区 *Cv* 值均明显大于高山区，乌鲁木齐河源大西沟气象站多年平均降水变率仅为 0.16，表明高山区年降水量变幅远小于其它区域。

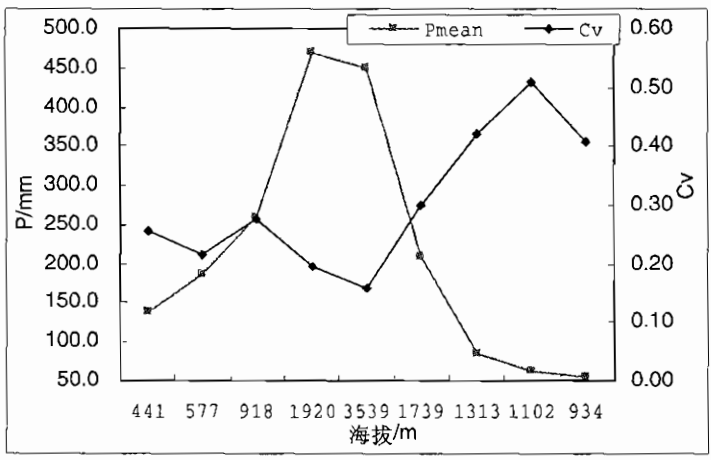

图 2 不同高度降水量和降水变率变化

Fig.2 Precipitation and variable coefficient in different elevations

3.3 不同坡向及高度台站年降水的相关性

从逐年降水实测资料的相关分析来看，南、北坡同一坡向山前平原的降水相关关系均较好；北坡中山带降水与高山带大西沟站降水及南坡不同高度的降水相关性不甚显著，南坡平原区降水与中山带巴仑台站降水相关性一般。初步分析认为：中山带降水的变化不完全同步于低山带和高山带，其局地对流降水的可能性较大，英雄桥站与其它台站（除库尔勒）的相关性较弱，表现为降水的独特变化，这也可能是造成英雄桥降水呈减少趋势和出现第一大降水带的原因；相反，南坡不同高度站的降水均与高山带北坡的大西沟站呈现非常好的相关关系，相似于同一坡向的降水相关性，其相关系数的显著水平一般均在 95% 以

上，基本反映了南北疆降水的同源性和变化的一致性。

表 2 南北坡各台站年平均降水量相关系数统计表

Table 2 The correlation coefficient of annual precipitation in the southern and northern slopes

台站	蔡家湖	昌吉	乌鲁木齐	英雄桥	大西沟	巴仑台	黄水沟	和静	库尔勒
蔡家湖	1								
昌吉	0.828**	1							
乌鲁木齐	0.832**	0.824**	1						
英雄桥	0.359*	0.463**	0.369*	1					
大西沟	0.456**	0.383*	0.526**	0.195	1				
巴仑台	0.367*	0.339*	0.464**	0.051	0.863**	1			
黄水沟	0.370*	0.494**	0.662**	0.292	0.584**	0.596**	1		
和静	0.234	0.353*	0.410*	0.147	0.485**	0.459**	0.457**	1	
库尔勒	0.241	0.270	0.272	0.467**	0.342*	0.151	0.441**	0.511**	1

注：*为 0.05 信度水平；**为 0.01 信度水平

4 月降水变化趋势分析

4.1 降水的月变化特征

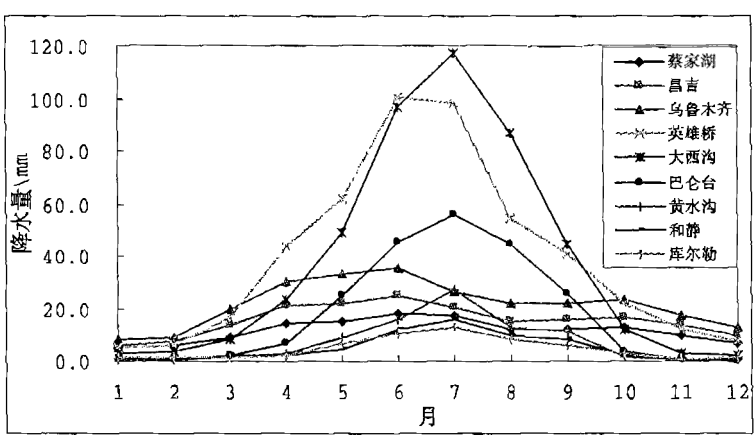

图 3 天山天格尔山南北坡月平均降水变化

Fig.3 Monthly precipitation changes in the southern and northern slopes of the Tianger Range in Tianshan Mountains

从图 3 中可以看出，天山南北坡月降水的区域性差异比较明显：大致相同的高度区域，北坡降水远大于南坡；高度效应同样显著；另外，季节的差异较大，天山北坡春、夏季降水量多于秋、冬季，最大月降水出现在 5-6 月。南坡降水的季节性特征更相似于高山区（乌鲁木齐河源大西沟气象站），最大降水均出现在 7 月份，尤其是大西沟和巴仑台的降水年

内变化过程完全一致；研究表明[12]，二者的气温年变化同样也有显著的相关性（相关系数达 0.63）,达到了 0.01 的信度水平，验证了南坡中山带和北坡高山带气候变化的相似性；秋季降水稍多于春季，冬季降水非常稀少。

由于北方寒流的天山阻隔加上下垫面沙漠戈壁的强冷却作用，北坡乌鲁木齐河流域冬季逆温层发育十分明显和稳定，逆温层上界可达海拔 2200m 以上[12]，逆温层的强烈发育导致了水汽凝结高度较低[12, 13]；从而在天山北坡形成了冬季（尤其是 11-12 月）山前降水多于中山带及高山区域的降水特征，这种降水的变化随着逆温层的消失而趋于正常，降水将再次呈现随高度的升高而递增的变化特点，冬季南坡降水则没有这种变化特征。

4.2 月降水变率的特征分析

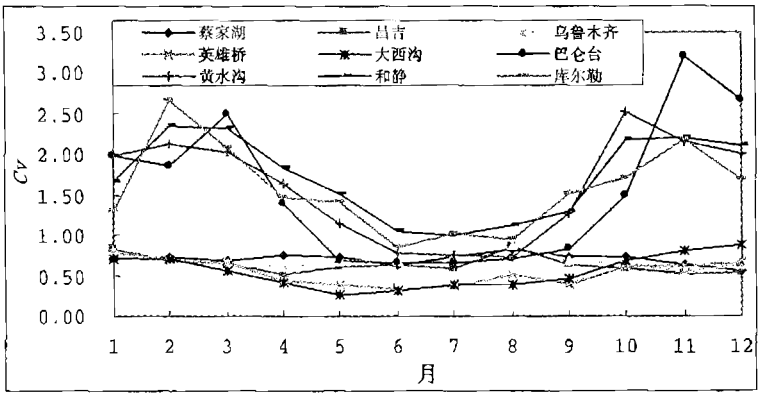

图 4 天山天格尔山南北坡月降水变率

Fig.4 Monthly precipitation variable coefficient in the southern and northern slopes of the Tianger Range in Tianshan Mountains

天山南北坡月降水变率的区域性差异明显(图 4)：同降水变率的年变化相似，南坡月降水变率远大于北坡，且季节差异性较大；北坡的降水变率相对值都较小，同样季节性差异也较小，中、高山带的英雄桥和大西沟夏季降水变率小于其它季节，冬季大西沟降水变率为北坡最大，且大于其余各站；南北坡夏季降水变率明显小于其余季节。

4.3 月降水变化的趋势分析

天山北坡英雄桥站降水量除了冬季（12-1 月）有轻微增加的趋势外，其余各月均显示为降水的减少趋势，春季(3 月)减少趋势明显（图 5），趋势系数为-0.325；蔡家湖站各月虽基本呈现为增加趋势，但同样存在 3 月份降水的明显减少趋势，趋势系数为-0.315,二者均达到了 0.05 的信度水平；同样，天山南坡的和静站逐月降水量基本上呈现为不显著的变化趋势，但冬季 11 月却表现出显著的减少特征，趋势系数为-0.335,同样也达到了 0.05 的信度水平。

不同台站月降水主要呈现为显著的增加趋势(图 6)，达到 0.05 信度水平以上的月降水有：夏季 6 月份的巴仑台；7 月份的蔡家湖、昌吉、乌鲁木齐、黄水沟；1 月份乌鲁木齐；11-12 月份的大西沟站及 12 月份的蔡家湖站。分析统计来看，月降水量增加的趋势主要集中在夏季和冬季，山前平原主要为夏季降水的增加，高山区冬季降水的增加趋势更为明显，乌鲁木齐河源大西沟站 12 月份降水的增加趋势系数为 0.40(达到了 0.01 的信度水平)，是年内月降水增加趋势最显著的台站，与天山乌鲁木齐河源明显的冬季升温过程相对应[12]。

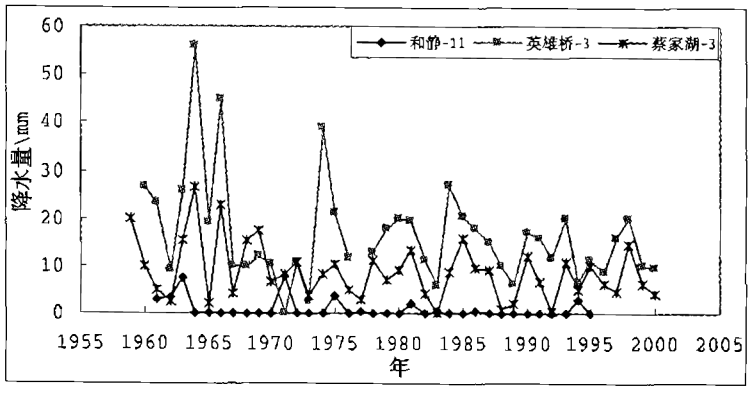

图 5 天山南北坡月降水量显著减少趋势

Fig.5 Decreasing trend of the monthly precipitation in the southern and northern slopes of the Tianger Range in Tianshan Mountains

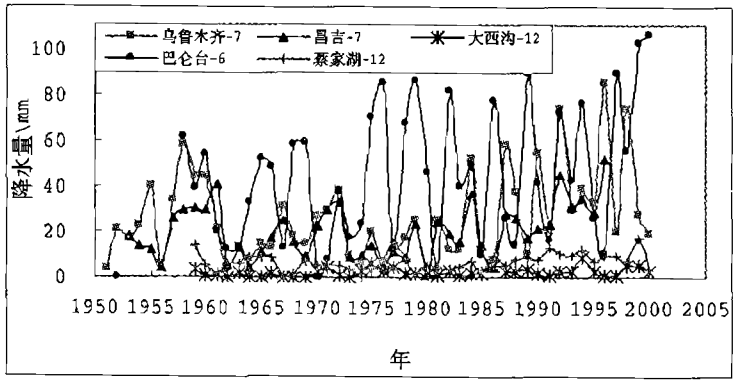

图 6 天山南北坡月降水量显著增加趋势

Fig.6 Increasing trend of the monthly precipitation in the southern and northern slopes of the Tianger Range in Tianshan Mountains

5 降水的月际变化相关分析

通常分析降水的年内变化多考虑月（季）降水量在年降水总量中的分配比例和差异，但较少对其之间的相关性进行分析。为此，我们对不同站点的逐月资料进行了相关性分析；结果显示：月降水在总体上基本呈现为年内各月的正相关关系，但同样存在着明显的负相关关系。由于天山南坡降水多集中在夏季，春季和冬季存在整月无降水的资料记录，从而使其月相关分析缺乏实质的气候意义，在此将不进行详细分析。相关分析主要针对北坡降水变化来进行。

天山北坡冬、春季降水与夏季降水的正相关关系相对比较明显，所选台站中，达到 0.01 信度水平的台站有：乌鲁木齐（4-7 月和 5-7 月），蔡家湖（1-7 月和 4-7 月）；达到 0.05 信度水平的台站是：蔡家湖（7-11 月和 7-12 月），昌吉（1-9 月），英雄桥（2-3 月和 6-12 月），大西沟（2-3 月和 6-12 月），可以看出，冬、春季月降水量的多少，可以部分地预示当年夏季（尤其是 7 月份）降水的多寡，山前平原的这种关系更为明显。

除了降水的这种正相关关系外，天山北坡高山区乌鲁木齐河源大西沟气象站降水存在4月和5月、6月和8月非常显著的负相关关系（图7），相关系数分别为-0.475和-0.376，分别达到了0.01和0.05的信度水平。

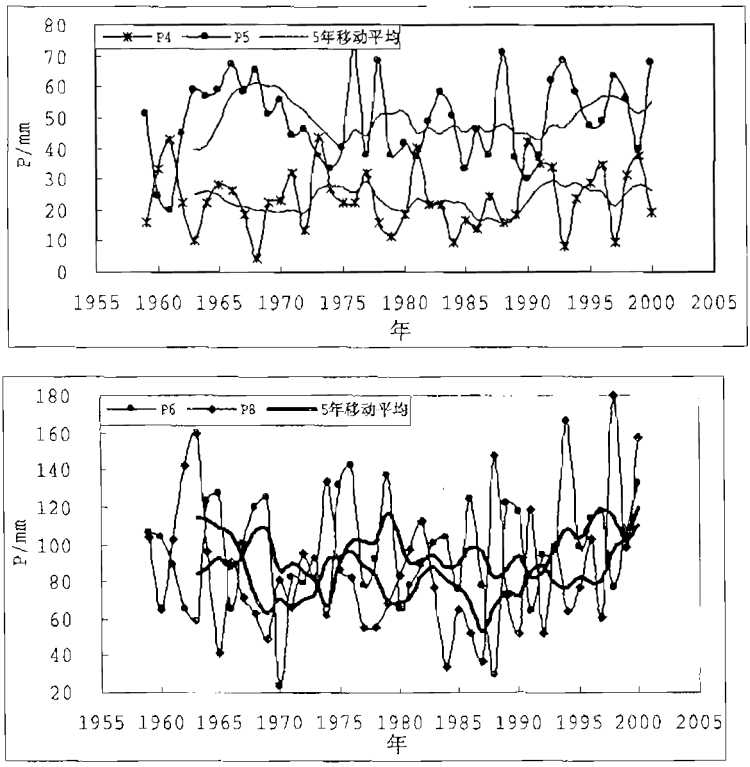

图7 天山乌鲁木齐河源大西沟站月降水的负相关关系

Fig.7 The inverse correlation of monthly precipitation at Da Xigou Weather Station in the headwaters of the Urumqi River

6 结论与讨论

天山南北坡各站年降水量基本表现为明显的增加趋势。北坡乌鲁木齐河流域降水均多于南坡乌垃斯台河流域。

英雄桥水文站年降水量呈现明显的减少趋势，春季(3月)减少趋势明显，趋势系数为-0.325（达到0.05的信度）。

不同坡向和高度的年降水变率Cv与年降水量呈反相关关系，南坡降水变率Cv明显大于北坡，季节性差异同样大于北坡，中、低山带及平原区明显大于高山区。

由于天山北坡冬季逆温层的强烈发育，形成了冬季（尤其是11-12月）山前降水多于中山带及高山区域的降水特征。北坡山前平原最大月降水一般出现在5-6月，中山带英雄桥出现在6月份；南坡降水的季节变化特征相似于高山区大西沟气象站，最大降水均出现在7月份。

天山乌鲁木齐河源大西沟站降水存在4月和5月、6月和8月非常显著的负相关关系，

其原因可能与环流型式的变化或局地小气候下的对流天气有关，这有待我们进一步的研究。

参考文献（References）

[1] Shi Neng, Chen Luwen , Precipitation fluctuation over globe land area in 1948-2000,Chinese Science Bulletin,2002, 47（21）, 1671-1674 [施能，陈绿文，全球陆地年降水场的长期变化（1948-2000 年）[J]，科学通报，2002, 47（21），1671-1674]

[2] Pavel Ya.Groisman , Richard W. Knight, and Thomas R. Karl ,2001,Heavy Precipitation and High Streamflow in the Contiguous United States: Trends in the twentieth Century ,Bulletin of the American Meteorological Society,Vol. 82 ,No. 2,219-246

[3] G. Kiely ,J.D. Albertson, and M.B. Parlange ,1998, Recent trends in diurnal variation of precipitation at Valentia on the west coast of Ireland ,J. of Hydrology ,207,270-279

[4] A.Serrano , V. L. Mateos and J. A. Garcia ,1999,Trend Analysis of Monthly precipitation Over the Iberian Peninsula for the Period 1921-1995 , Phys. Chem. Earth(B),Vol.24,N0.1-2.85-90

[5] HAIM KUTIEL, 1988 ,Rainfall variations in the Galilee(Israel), • .Variations ih the temporal distribution between 1931-1960 and 1951-1980, J. of Hydrology ,99,179-185

[6] Han ping, Xue Yan and Su Hongchao, Precipitation Signal of the Climatic Shift in Xinjiang Region [J], Journal of Glaciology and Geocryology,2003,25(2),179-182,[韩萍，薛燕，苏宏超，新疆降水在气候转型中的信号反应，冰川冻土，2003,25(2),179-182]

[7] Shi Ya-feng,Shen Yong-ping,Hu Ri-ji, Preliminary Study on Signal, Impact and Foreground of Climate Shift from Warm-Dry to Warm-Humid in Northwest China [J]. Journal of Glaciology and Geocryology, 2002,24（3），219-226 [施雅风，沈永平，胡汝骥，西北气候由暖干向暖湿转型的信号、影响和前景初步探讨[J]. 冰川冻土，2002，24（3），219-226]

[8] Yang Lianmei , Climate change of extreme precipitation in Xinjiang[J], Acta Geographica Sinica , 2003, 58(4), [杨莲梅，新疆极端降水的气候变化[J]，地理学报，2003,58(4)]

[9] Xue Yan ,Han ping, and Feng guohua, Change trend of the Precipitation and air temperature in Xinjiang since recent 50 years[J], Arid Zone Research,2003,20(2),127-130,[薛燕，韩萍，冯国华，半个世纪以来新疆降水和气温的变化趋势，干旱区研究，2003,20(2), 127-130]

[10] Li Shiming, Cheng Guodong, Li Yuanhong, et.al., Water resources rational utilization and entironment protect in the HEXI Corridor[M], Zhengzhou, Huanghe River Hydraulic publishing House, 2002,17-27 [李世明，程国栋，李元红等，河西走廊水资源合理利用与生态环境保护[M]，郑州，黄河水利出版社，2002,17-27]

[11] Ling Zhiguang, Climatology of Orograpic precipitation [M], Beijing,Science Press, 1995,26-32[林之光，地形降水气候学[M],北京，科学出版社，1995,26-32]

[12] Han Tianding. Ye Baisheng, Jiao Keqin. Temperature variations in the southern and northern slopes of Mt. Tianger in the Tianshan Mountains [J]. Journal of Glaciology and Geocryology, 2002, 24(5): 567-570. [韩添丁，叶柏生，焦克勤. 天山天格尔山南北坡气温变化特征研究[J]. 冰川冻土，2002, 24(5): 567-570.]

[13] Vladimir B. Aizen , Elena M. Aizen, John M, Melack, Pecipitation, melt and runoff in the northern Tien Shan [J]. Journal of Hydrology, 1996,186: 229-251.

Precipitation variations in the southern and northern slopes of the Tianger Range in Tianshan Mountains

Han Tianding, Ding Yongjian, Ye Baisheng, Cheng Peng, Xie Changwei

Abstract: Based on monthly and annual precipitation data of the southern and northern slopes of the Tianger Mt. in Tianshan Mountains , the spatial-temporal variations of precipitation and the major changing trend are analyzed.. Monthly precipitation is considered separately .The analyzed Precipitation series ranging from 1950s to 2002 are collected from nine meteorological and hydrological stations, which scatter all over the southern and northern slopes of the Tianger Range in Tianshan Mountains.

A statistical analysis shows that the increase trend of precipitation is obvious in the northern and southern slopes. The variable coefficient of precipitation is larger in the southern slope than in the northern slope, as such it is larger in winter and spring than in summer and autumn.

There is a decrease trend of the precipitation at Ying Xiongqiao hydrological station in the Urumqi River valley. The trend in March is more distinct ,with a trend coefficient of -0.325. There is a significant inverse correlation between April to May and June to August at the Da Xigou weather station in the headwaters of the Urumqi River, with correlation coefficients of -0.475 and -0.376 , respectively.

Key words: Tianshan Mountains; southern and northern slopes; precipitation variation; correlation

天山奎屯河哈希勒根 51 号冰川表面运动特征分析

井哲帆，叶柏生，焦克勤，杨惠安

(中国科学院寒区旱区环境与工程研究所，甘肃 兰州 730000)

摘　要：奎屯河哈希勒根 51 号冰川位于新疆奎屯市以南的天山依连哈比尔尕山北坡，奎屯河上游支沟哈希勒根河源区．1999 年 8 月，在该冰川上布设了用于冰川运动和冰川物质平衡观测研究的测杆 18 根，并进行了冰川表面运动、冰川物质平衡和冰川末端变化的首次观测．根据 2000 年 8 月和 2001 年 8 月的冰川运动观测资料，分析了奎屯河哈希勒根 51 号冰川的运动特征和冰舌末端的变化状况．结果表明：奎屯河 51 号冰川应属于亚大陆型冰川；1999 / 2000 年度和 2000 / 2001 年度的表面运动值不大，最大流速点的年运动速度为 3.15 m a^{-1}；运动速度垂直分量 U_Z 的变化规律同乌鲁木齐河源 1 号冰川的变化规律相同，即消融区的显出流作用和积累区的显入流作用．该冰川的冰舌末端处于相对稳定的退缩状态，1964—1999 年间平均退缩量约为 1.4 m· a^{-1}，而 1999—2001 年间的平均退缩量为 5.0 m· a^{-1}，反映出冰川退缩增大的趋势．

关键词：奎屯河哈希勒根；51 号冰川；GPS(全球定位系统)；运动；特征

1　简述

冰川运动特征分析是冰川变化研究的基础．运动是冰川区别于其它自然冰体的主要标志之一，运动使冰川具有生命力．冰川是气候的产物，它的存在与变化不仅对气候变化具有明显的反馈、调节和指示作用，而且对于生态环境、水资源变化等具有重要影响[1-3]。因此，对冰川运动特征的研究分析是尤其重要的．

天山冰川观测试验站在逐步规范、完善、巩固和提高观测试验基础研究项目的基础上，为了继续扩大和丰富我国冰川观测研究空间，充实和积累我国冰川观测研究基础，于 1998 年决定选择和开辟天山冰川站第二个冰川观测点，拟开展冰川的物质平衡、冰川表面运动、冰舌末端进退变化等方面的定期监测工作．

1999 年 8 月，经过选点考察，确定了天山奎屯河哈希勒根 51 号冰川为天山冰川站第二个冰川定位观测点．在该冰川上布设了用于冰川运动和冰川物质平衡观测研究的测杆 18 根，并进行了冰川表面运动、冰川物质平衡和冰川末端变化的首次观测．

2000 年 8 月，第二次对奎屯河哈希勒根 51 号冰川进行了上述项目的观测，获得了一个周年的冰川变化资料，标志着天山奎屯河哈希勒根 51 号冰川的表面运动速度、物质平衡和冰川末端变化研究项目正式实施．

2001 年 8 月，又进行了上述项目的观测。本文即根据 1999—2001 两个周年的冰川表面运动观测资料，对天山奎屯河哈希勒根 51 号冰川的运动特征进行分析．

2　奎屯河哈希勒根 51 号冰川概况

奎屯河哈希勒根 51 号冰川位于新疆奎屯市以南的天山依连哈比尔尕山北坡，奎屯河上

游支沟哈希勒根河源区．根据1964年9月航空摄影，1972年出版的1：5×10^4地形图量算获得的主要数据结果为：51号冰川的地理位置为84° 24′E；43° 43′N，其形态特征属于冰斗冰川，冰川朝向NE，最高海拔4 000 m，冰舌末端高度3 400 m，雪线高度3 610 m，冰川面积1．48 km^2，最大长度1．7 km．冰面较为平整、洁白，裂隙不甚发育．

3 观测资料

3.1 观测方法

使用GPS(全球卫星定位系统，SOKKIA GSSIA型)测量技术在冰川外围测定了2个基本控制点(K_1和K_2，以便于长期定位观测)和3个冰舌末端变化观测控制点，建立起观测控制网．冰川表面运动速度的观测是使用精密光学经纬仪，从控制点K_1、K_2上对布设在冰川表面的测杆进行重复前方交会，以坐标法计算出冰体单位时间内的空间位移．冰舌末端变化测量采用距离丈量法观测．

3.2 资料说明

坐标系的建立，由于是小区域的观测，所以选用独立坐标系，以K_1—K_2方向为横坐标Y轴，X轴为垂直于Y轴的纵坐标，Z为垂直于XY平面竖直向上的坐标轴．以K_1点坐标X=1000.00 m、Y=1000.00 m、Z=3435.00 m为起算点．

表1为1999／2000年度和2000／2001年度的冰川表面运动速度，表2是冰舌末端的年进退变化量，表1中U_X、U_Y、U_Z是分别平行于X、Y和Z轴的速度分量，U_{xy}为速度的水平分量．图1为天山奎屯河哈希勒根51号冰川表面运动点示意图．

表1　流速点运动速度

Table1　Surface velocities of surveying points

点名	1999年8月26日—2000年8月22日				2000年8月22日—2001年8月22日			
	U_x/m	U_y/m	U_z/m	U_{xy}/(m·a^{-1})	U_x/m	U_y/m	U_z/m	U_{xy}/(m·a^{-1})
A_1	-1.03	-2.52	-1.47	2.75	-1.02	-2.54	-1.48	2.74
A_2	-1.12	-2.56	-1.45	2.82	-1.16	-2.54	-1.46	2.79
A_3	-1.18	-2.45	-1.51	2.75	-1.22	-2.42	-1.50	2.71
B_1	-1.57	-1.66	-1.22	2.31	-1.52	-1.67	-1.20	2.26
B_2	-1.43	-1.48	-1.30	2.08	-1.45	-1.50	-1.28	2.09
B_3	-1.41	-1.53	-1.26	2.10	-1.41	-1.53	-1.27	2.08
C_1	-1.16	-1.34	-1.15	1.79	-1.18	-1.35	-1.16	1.79
C_2	-1.11	-1.27	-1.23	1.71	-1.14	-1.29	-1.21	1.72
C_3	-1.04	-1.18	-1.19	1.59	-1.08	-1.20	-1.17	1.61
C_4	-1.26	-1.09	-1.16	1.69	-1.28	-1.11	-1.15	1.69
D_1	-1.33	-1.46	-1.11	1.99	-1.36	-1.48	-1.09	2.01
D_2	-1.21	-1.52	-1.14	1.96	-1.26	-1.54	-1.12	1.99
D_3	-1.42	-1.23	-1.20	1.90	-1.47	-1.26	-1.17	1.94
D_4	-1.96	-1.17	-1.52	2.31	-1.98	-1.19	-1.53	2.31
E_1	-2.73	-1.22	-2.16	3.02	-2.87	-1.29	-2.19	3.15
E_2	-2.85	0.76	-1.10	2.98	-2.91	0.78	-1.11	3.01
E_3	-2.80	0.82	-1.34	2.95	-2.85	0.88	-1.33	2.98
F	-1.61	-0.62	-1.38	1.75	-1.64	-0.65	-1.36	1.76

根据上述观测方法求得速度的误差分析方法[4, 5]可知，水平分量 U_{xy} 最大误差为 ±0.06 m· a^{-1}，垂直分量 U_Z 最大误差为±0.08 m· a^{-1}.

4 运动特征分析

4.1 运动速度的年际变化

奎屯河 51 号冰川 1999 / 2000 年度和 2000 / 2001 年度的表面运动速度值 Uxy 不大.从表 1 中可以看出，该冰川 1999 / 2000 年度的最大流速点为 E1 点，高度在海拔 3 600 m 的平衡线处，其年流速为 3．02 m．2000 / 2001 年度的运动速度变化也不大，约有 50%的点(靠近雪线)，其运动速度略有增大，但是增幅较小，在 0．01～0.15 m a^{-1} 间，另有 30%的点(冰舌下部)，运动速度值略有减小．最大流速点仍为 E1 点，其速度值为 3．15 m a^{-1}，比 1999 / 2000 年度的最大速度增大了 0.13 m· a^{-1}.

该冰川运动速度的水平分布表现为：运动速度矢量基本向主流线幅合，或平行于主流线(图 1).

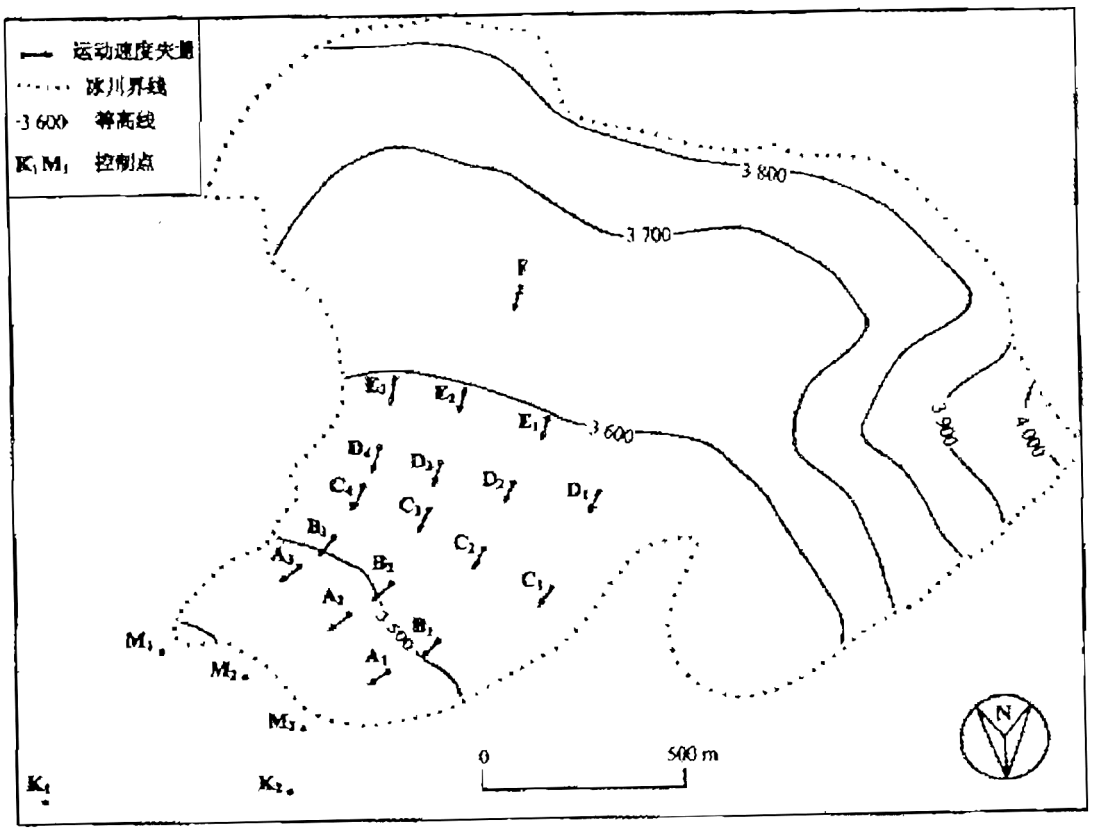

图 1 奎屯河 51 号冰川表面运动点示意图

Fig. 1 Points for surface velocity surveying

由图 2 可以看出，运动速度的纵向分布表现为： A 断面为第一个高速区，流速在这里加速的主要原因是该断面布设在冰舌末端的上沿，纵向坡度较陡． B—D 断面，冰面坡度较缓，为局布压缩区，流速必然减慢．E 断面正好位于平衡线高度处，其运动速度为最大区，完全符合冰川运动的一般规律.

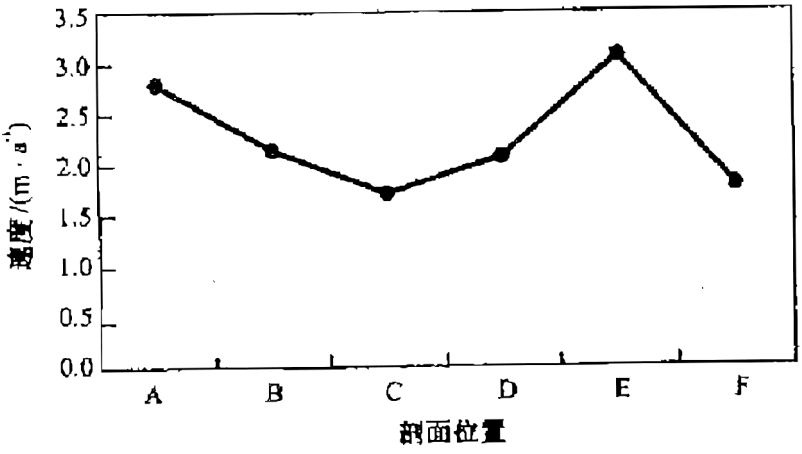

图 2　表面运动速度纵剖面图

Fig. 2　longitudinal profile of surface velocities

运动速度垂直分量 U_Z 的变化规律同乌鲁木齐河源一号冰川的变化规律完全相同[6~8]. 即消融区的显出流作用和积累区的显入流作用.

4.2　冰舌末端变化

冰川末端进退的观测方法是通过在 GPS 测定的控制观测点进行重复距离丈量得出的. 表 2 反映了 1964—2001 年的冰舌末端变化量，其中 1964—1999 年的变化量，是根据 GPS 测量结果与 1964 年地形图资料对比得出. 35 a 间该冰川末端仅退缩了 49 m，平均每年退缩量为 1. 4 m，说明在这期间，该冰川末端变化不大，处于相对稳定状态. 从表中可以看出，1999 / 2000 年度冰舌末端的平均退缩量为 4.83 m. 2000 / 2001 年度的平均退缩量为 5.20 m，反映出自 20 世纪 90 年代末期以来，冰川退缩增大的趋势. 这与 20 世纪以来气候的变化特征是密切相关的[9]，从 19 世纪 80~90 年代起，我国气温开始上升，到 20 世纪 40 年代达到最高，冰川消融增大，出现退缩. 此后转为降温，60～70 年代初达到低点，冰川积累并出现前进或处于稳定状态. 70 年代后又趋于转暖，至 90 年代，气温达到 20 世纪最高的阶段. 因此，冰川消融随气候的逐渐变暖而出现加剧的趋势.

表 2　冰舌末端变化(1964—2001)

Table 2　Variation of the glacier terminus

时　间	1964-09~1999-08	1999-08~2000-08	2000-08~2001-08
末端变化/m	-49	-4.83	-5.20
年平均变化/m	-1.40	-4.83	-5.20

注："－"表示为后退.

参考文献(References):

[1] Wang Nillglian, Ding Liangfu. Study onthe glacier variation in Bujiagangri Section of the East Tanggula Range since the Little Ice Age [J]. Journal of Glaciology and Geoeryology, 2002, 24(3): 234-244. [王宁练，丁良福. 唐古拉山东段布加岗日地区小冰期以来的冰川变化研究 [J]. 冰川冻土，2002，24(3)：234-244.]

[2] Liu Shiyin, Shen Yongping, Sun Wenxin, et al. Glacier variation since the maximum of the Little Ice Age in the Western Qilian Mountains, Northwest China [J]. Journal 0f Glaciology and Geocryology, 2002, 24(3): 227-233.[刘时银，沈永平，孙文新，等. 祁连山西段小冰期以来的冰川变化研究[J]. 冰川冻土，2002，24 (3)：227-233.]

[3] Shi Yafeng. Estimation of the water resources affected by climatic warming and gacier shrinkage before 2050 in west China [J]. Journal of Glaciology and Ceocryology, 2001, 23(4): 333-341. [施雅风. 2050年前气候变暖冰川萎缩对水资源影响情景预估[J]. 冰川冻土，2001，23(4)：333-341.]

[4] Sun Zuozhe, Chen Yaowu, You Genxiang, et al. Flow characteristics of Glacier No. 1 at the headwater of Urumqi River, Tianshan[J]. Journal of Glaciology and Geocryology, 1985, 7(1): 24-40. [孙作哲，陈要武，尤根祥，等. 天山乌鲁木齐河源1号冰川的运动特征 [J]. 冰川冻土，1985，7(1)：24-40.]

[5] Wuhan College of Surveying and Mapping. Surveying and Mapping [M]. Beijing. "Surveying and Mapping Publishing House, 1979. 198-204. [武汉测绘学院. 测量学[M]. 北京：测绘出版社，1979. 198-204.]

[6] Jing Zhefan. Surface velocity and the termini variations of Glacier No. 1 at the headwater of Urumqi River, Tianshan [R]. Annual Report of Tianshan Glaciological Station, 1997, 14: 76-79. [井哲帆. 乌鲁木齐河源1号冰川表面运动速度和冰舌进退变化(1995-1996)[R]. 中国科学院天山冰川观测试验站年报，1997，14： 76-79.]

[7] Jing Zhefan. Surface velocity and the termini variations of Glacier No.1 at the headwater of Urumqi River, Tianshan [R]. Annual Report of Tianshan Glaciological Station, 1999, 15: 154-159. [井哲帆. 乌鲁木齐河源1号冰川表面运动速度和冰舌末端变化(1996 / 1997 和 1997 / 1998 年度)[R]. 中国科学院天山冰川观测试验站年报，1999，15：154-159.]

[8] Jing Zhefan. Surface velocity and the termini variations of Glacier No.1 at the headwater of Urumqi River, Tianshan [R]. Annual Report of Tianshan Glaciological Station, 2001, 16: in press. [井哲帆. 乌鲁木齐河源1号冰川表面运动速度和冰舌末端变化(1998 / 1999 和 1999 / 2000 年度)[R]. 中国科学院天山冰川观测试验站年报，2001，16：待刊.]

[9] Pu Jianchen, Yao Tandong, Wang Ninglian, et al. Puruogangri ice field and its variations since the Littl Ice Age of the Northern Tibetan Plateau [J]. Journal of Glaciology and Geocryology, 2002, 24(1): 87-92. [蒲健辰，姚檀栋，王宁练，等. 普若岗日冰原及其小冰期以来的冰川变化[J]. 冰川冻土，2002，24(1)：87-92.]

Surface Velocity on the Glacier No.51 at Haxilegen of the Kuytun River, Tianshan Mountains

JING Zhe-fan, YE Bai-sheng, JIAO Ke-qin, YANG Hui-an

(Cold and Arid Regions Environmental and Engineering Research Institute, Chinese Academy of Sciences, Lanzhou Gansu 730000, China)

Abstract: The Glacier No.51 is located at the headwaters of the Kuyntun River in the Tianshan mountains, with an area of about 1.48 km^2 and the largest length of about 1.7 krn, of which the ELA ranges from 3 400 to 4 000 m a. s. 1. The flow velocities of the glacier have been surveyed sinee 1999 by using GPS and traditional technique. The surface velocities were determinate over a period of two years(1999—2001). The largest surface velocity was 3.15 m a^{-1}. Velocity vectors appear the flow charaeteristics of a valley glacier. Positional variation of glacier terminus was obtained by comparing maps of 1: 50 000 and field observations from 1964 to 1999. It Was found that the terminus of the glacier has retreated by about 49m, with an average rate of 1.4 m.a^{-1}, in the period. It retreated 10.03 m from Aug. 1999 to Aug. 2001, with an average rate of 5.0 m.a^{-1}, showing an intensified retreat

Key words: Haxilegen of Kuytun River; G1acier No.51; GPS; flow characteristics

过去 44 年乌鲁木齐河源一号冰川物质平衡及其过程研究

杨惠安，李忠勤，叶柏生，焦克勤，井哲帆，赵中平

（中国科学院寒区旱区环境与工程研究所天山冰川观测试验站，甘肃 兰州 730000）

摘　要：本文报告 1997－2003 年度天山乌鲁木齐河源一号冰川物质平衡的观测结果，分析比较了过去 44 年间一号冰川物质平衡、累积物质平衡的变化过程，以及反映气候－地形要素和冰川发育条件要素的平衡线高度和冰川积累区比率，认为一号冰川负平衡波动期随时间推移而递增，目前处于其观测历史上物质平衡亏损最为强烈的时期.

关键词：一号冰川；物质平衡；累积物质平衡；平衡线高度；冰川积累区比率.

新疆气候变化[1]反映在当地具有气候指示器的冰川变化方面是[2]必然的。天山乌鲁木齐河源一号冰川（简称一号冰川，后同）物质平衡观测研究结果在 1997 年出现监测历史上最大的负平衡[3]。近年来一号冰川物质平衡变化结果及其 44 年监测过程如何，亦为各方所关注。因为，物质平衡是直接观测获得的冰川变化结果之一，政府间气候变化问题研究小组（IPCC）的国际评估报告，明确认可冰川变化是很可靠的气候指示器和对气候变化早期察觉策略很有价值的气候要素[4]。本文论述一号冰川近期（1997－2003 年）物质平衡观测研究结果及其与过去 44 年结果进行比较，探索其变化规律。

1　冰川面积的变化

一号冰川自 1959 年建立长期定位观测站以来，至今已进行过 6 次大比例尺精确测绘制图，目前最新的一号冰川图完成于 2001 年末。一号冰川面积变化见表 1。

1993 年以前，一号冰川是由其东支和西支两条支冰川汇流而形成（图 1；照片 1）。1962 年首次实测冰川面积为 1.95 km^2[5]。进入 20 世纪 90 年代初期，由于一号冰川西支冰舌退缩所致，早先汇入东支的西支冰舌，因后继补给无力而于 1993 年彻底脱离东支，至此，一号冰川蜕变为两条各自完全独立的冰川，即目前的一号冰川东支和一号冰川西支，截止 2001 年 8 月底，一号冰川西支脱离一号冰川东支后的水平距离已达 45m（照片 2）。1994 年实测的一号冰川面积为 1.742km^2，即一号冰川东支和一号冰川西支面积分别为 1.115 km^2 和 0.627 km^2。2001 年 8 月底再一次实测，一号冰川面积为 1.708 km^2，即一号冰川东支和一号冰川西支面积分别为 1.101km^2 和 0.607 km^2。自 1994 年以来的 7 年间面积萎缩了 0.034 km^2，平均每年减少率为 2.8‰。

目前的一号冰川实际上是由两条冰川所构成的综合体，即原一号冰川的东支、西支及其面积之和。为了与历史资料衔接和比较，物质平衡结果即以此基础求得。以两条冰川面积加权平均获得一号冰川的平衡线高度。两条冰川积累区面积之和与其总面积之和之比的百分率即为一号冰川积累区比率（AAR）。

表 1 天山乌鲁木齐河源一号冰川历年物质平衡、平衡线、积累区比率一览表

年份	冰川面积 (km^2)	物质总量 (10^4m^3)	平衡值 (mm)	平衡线海拔 (m)	冰舌变化 (±m)	积累区比率 (%)	资料来源
1959/60	1.950	-36.6	-187.7	4060		44.1	谢自楚[5]
1960/61	1.950	-6.4	-32.8	4060		46.7	
1961/62	1.950	-32.6	-167.2	4075	0.0	44.1	
1962/63	1.950	+45.7	+234.4	3971		69.2	张金华[6]
1963/64	1.950	+0.4	+2.0	4055		47.7	
1964/65	1.950	+73.0	+374.4	3948		78.5	
1965/66	1.950	-72.9	-374.0	4110		36.4	
1966/67	1.950	-13.6	-69.7	4063		45.6	
1967/68	1.950	-89.0	-456.4	4121		34.9	
1968/69	1.950	+28.8	+147.7	4008		59.0	
1969/70	1.950	-61.0	-313.0	4106		37.4	
1970/71	1.950	+19.9	+102.0	4015		56.9	
1971/72	1.950	+51.1	+262.0	3981		67.2	
1972/73	1.950	-138.0	-707.7	4146	-65.6	30.8	
1973/74	1.950	-24.3	-124.6	4075		43.1	
1974/75	1.870	+53.8	+287.7	3982		67.9	张金华[6]
1975/76	1.870	+5.4	+29.0	4066		45.5	
1976/77	1.860	+33.4	+179.6	4001		64.5	
1977/78	1.860	-20.3	-109.1	4155		72.0	
1978/79	1.850	-15.5	-84.0	4120	-22.99	67.0	
1979/80	1.840	-61.7	-335.3	4029	-16.0	47.8	
1980/81	1.840	-119.9	-651.6	4107	-4.8	29.3	
1981/82	1.840	-8.2	-44.6	4006	-2.1	47.8	
1982/83	1.840	+18.4	+100.0	3987	-2.9	57.6	张金华[7]
1983/84	1.840	-15.2	-82.6	3992	-3.4	58.2	王晓军[4]
1984/85	1.840	-112.6	-612.0	4092	-3.4	30.4	
1985/86	1.840	-133.0	-722.8	4125	-3.5	27.2	
1986/87	1.840	-32.3	-175.5	4013	3.7	49.5	王纯足[7]
1987/88	1.840	-118.4	-643.7	4072	-3.8	35.9	刘潮海[7]
1988/89	1.840	+19.5	+105.9	3965	-5.1	33.6	
1989/90	1.840	+9.6	+52.0	3946	-3.6	70.4	王纯足[7]
1990/91	1.840	-129.9	-706.0	4125	-6.5	30.9	
1991/92	1.840	+4.2	+22.8	3960	-3.4	68.3	刘潮海[7]
1992/93	1.840	-5.3	-29.0	3967	-3.8	69.0	王纯足[7]
1993/94	1.840	-69.5	-377.7	4053	-4.9	40.4	
1994/95	1.840	-42.0	-228.3	4031	-4.0	50.1	
1995/96	1.840	+7.8	+42.4	3976	-3.4	66.8	刘时银[7]
1996/97	1.742	-148.6	-853.0	4137	-3.7	24.5	焦克勤[7]
1997/98	1.742	-137.6	-789.9	4085	-3.5	32.7	
1998/99	1.742	-137.7	-790.7	4122	-3.41	30.9	杨惠安[7]
1999/2000	1.742	-57.4	-329.7	4063	-3.40	49.8	
2000/01	1.708	-143.4	-839.6	4128	-3.10	38.1	
2001/02	1.708	-142.4	-833.9	4141	-3.10	34.8	
2002/03	1.708	-65.5	-383.5	4074		47.7	杨惠安[8]

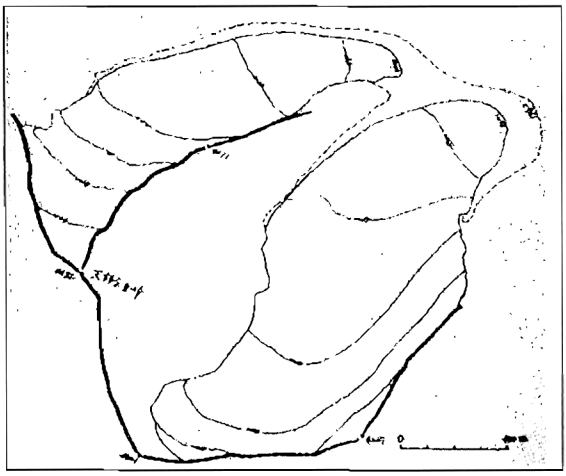

图 1 一号冰川 1962－2001 年变化图（根据井哲帆 2001 年 8 月测绘的 1/5000 图绘制）

2 1997－2003 年物质平衡

1997－2003 年，一号冰川 7 个观测年中物质平衡结果均为负平衡年（表 1），尽管没有出现新的超记录，但总体上仍处于数值很大的负平衡状态，其中除 2000 年（-329.7 mm）和 2003 年（-383.5 mm）的负平衡量较相邻年份有较大减少之外，2001 年（-839.6 mm）和 2002 年的负平衡量则与 1997 年出现的历史上最大负平衡记录（-853mm）相差无几。统计和比较以往谢自楚（1965）、张金华（1984）以及天山冰川站年报（1－16 卷，1978-2002 年）[7]可以看出，物质平衡过程存在阶段性波动变化，最近 7 年仍处于 1997 年以来的负平衡波动阶段，这个负平衡波动的波长已持续 7 年，至少 2003 平衡年末还看不出负平衡波动结束迹象。由此可见，1997－2003 年是一号冰川物质平衡观测历史上持续时间最长的还在持续延伸的负平衡波动，最近 7 年物质平衡负值和平衡线的居高不下，以及积累区比率的锐减，乃是负平衡阶段物质平衡出现的必然结果。

3 过去 44 年冰川物质平衡阶段性变化

我们把一号冰川积累和消融观测过程进行一个年度（或一周年）的结果称之为冰川物质平衡的正平衡年或负平衡年，一年或连续几年的物质平衡正负结果称之为正平衡阶段或负平衡阶段。过去 44 年间，一号冰川物质平衡变化有如下特点。

（1）一号冰川物质平衡结果随时间的变化是一个阶段性的波动过程。与一号冰川邻近的大西沟气象站 5－8 月主要降水季节的降水变化过程大体一致，但其变化趋势则是相反的（图 2），即从 20 世纪 80 年代中期以来，随着时间的推移，降水趋势在增大，而物质平衡的负平衡趋势也在加剧（本文不做讨论）。一号冰川物质平衡观测研究时间已有 44 年历程，负平衡年与正平衡年之比为 30：14，起止时间为 1960－2003 年，平均约两个以上负平衡年即有一个正平衡年相对应。但实际结果却是，负平衡阶段出现 9 次（图 3），其中 3 年期波长的频数出现 3 次，1 年期出现 2 次，5 年期为 2 次，2 年期为 1 次，而最近已达 7 年的负平衡波长还未结束。以 2 年以上主要波长作比较（可忽略 1 年期波长），则负平衡

总的变化趋势呈 3 年、5 年和超过 7 年期波长的渐进式发展，负平衡阶段性波长随时间在逐渐延长，目前已达 7 年（1997－2003 年）的负平衡波长还没有结束足以说明了这种趋势。与负平衡波动相对应的正平衡波动出现 8 次，起止时间在 1963－1996 年，其中 3 年期波长的频数出现 2 次，2 年期出现 2 次，1 年期的频数多达 4 次。正平衡波长随时间的变化则表现为 3 年、2 年和 1 年期的递减式发展趋势，其波长时间在逐渐缩短，出现频数减少，以至发展到最新的 7 年中没有出现正平衡波动的结果。应该说一号冰川物质平衡的这种变化结果是近年来全球变暖趋势在高山冰川上的具体反映。

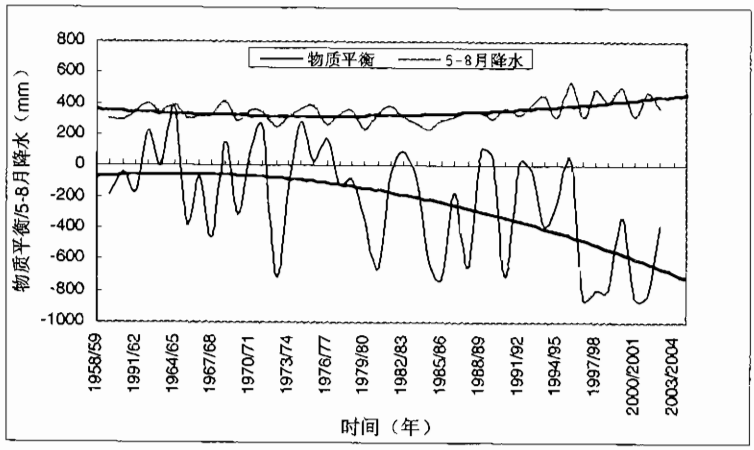

图 2　一号冰川物质平衡与降水变化过程及趋势

（2）依物质平衡波动过程比较一号冰川物质平衡结果，3 次 3 年期波长的负平衡年平均量分别为-129 mm、-300 mm和-212 mm，2 次 5 年期波长的负平衡年平均量分别为-245 mm和-447 mm，新近的负平衡波动还在发展而实测结果已持续达负平衡波长 7 年期（1997-2003 年）的年平均负平衡量则达到-689 mm，可见不同阶段的负平衡量各有高低，但总的趋势是明显在递增，现阶段是一号冰川物质平衡观测史上冰川物质亏损最为严重的时期。正平衡波动以及平衡量正好与负平衡相反，2 次 3 年期波长的正平衡年平均平衡量分别为+204 mm和+165 mm，2 次 2 年期年平均平衡量分别为+182 mm和+79 mm，4 次 1 年期则分别为+148 mm、+100 mm、+23 mm和+42 mm，正平衡量随着时间的推移而递减显著。

截止 2003 平衡年末，一号冰川由于负平衡波动期及其负平衡量的逐渐加剧，以及冰川面积的萎缩，44 年来一号冰川累积物质平衡达到了空前的-10114 mm，这相当于 44 年释放了总量达 $1821\times10^4m^3$ 的水，同时亦表明整个冰川表层厚度平均减薄了 11.2m（图 3）。

（3）气候－地形综合作用于冰川的指标是平衡线高度。1960 年以来，一号冰川平衡线介于海拔 3946－4155m 之间，44 年平均 4052m，负平衡年平衡线高于正平衡年平均 92m。30 个负平衡年的平衡线介于海拔 3967－4155m 之间，平均 4082m。14 个正平衡年平衡线介于海拔 3946－4066m，平均 3990m。大西沟气象站 5－8 月平均气温年变化与一号冰川平衡线高度变化趋势一致（图 4），平衡线升高趋势，加剧了物质平衡负平衡的趋势（图 5）。

（4）冰川积累区比率（AAR）的大小反映冰川补给条件的优劣变化，与物质平衡结果同步变化（图 5）。过去 44 年间，一号冰川 AAR 介于 25%－79%之间，AAR 平均 44%。所有正平衡年的 AAR 介于 32－79%之间，平均 58%。所有负平衡年的 AAR 介于 25－58%之间，平均约 38%。

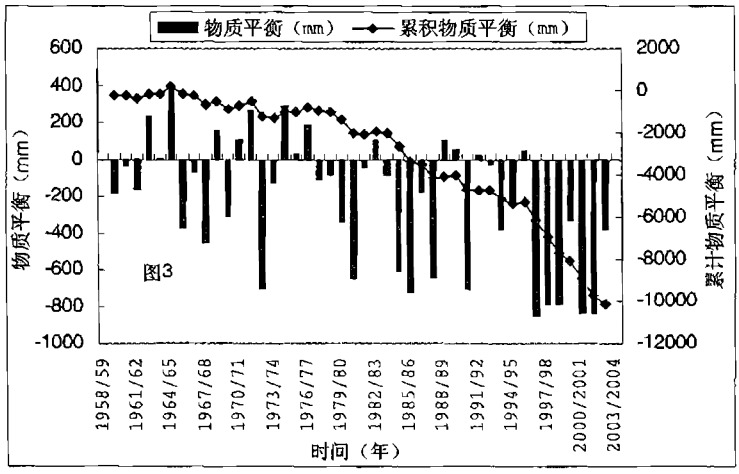

图 3 一号冰川物质平衡年变化及其累积变化过程

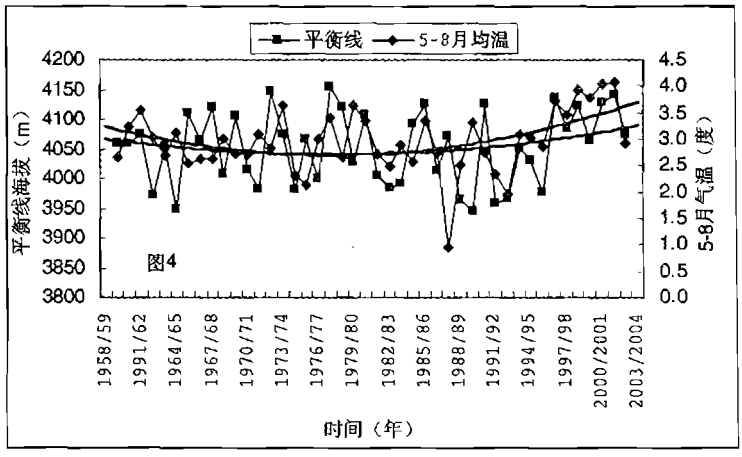

图 4 一号冰川平衡线与 5-8 月平均气温变化趋势

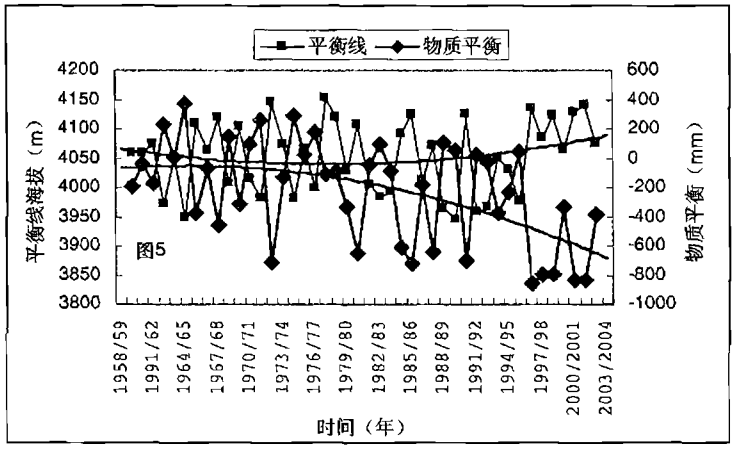

图 5 一号冰川平衡线与物质平衡变化过程及趋势

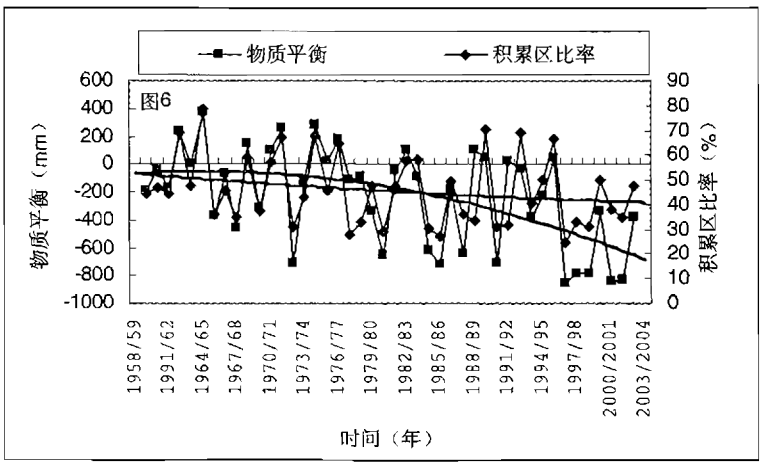

图 6　一号冰川物质平衡与积累区比率变化过程

4　结语

纵观过去 44 年观测结果，一号冰川物质平衡过程经历了 8 次正平衡波动和 9 次负平衡波动，2003 平衡年末仍处于还在持续延伸的第 9 个负平衡波动期内。正平衡波动期出现于 1963一1996 年间，并于 1975一1996 年间依时序出现由 3 年、2 年和 1 年波动期逐渐递减的趋势。负平衡波动期贯穿 1960一2003 年间的 44 年，几乎囊括 1一7 年之间 5 个自然数所能表示的波长年数（缺少 4 年期波长），总体上负平衡波动期依次由 3 年、5 年和 7 年（还在监测中，无结果不能肯定）时序的波动期波长是逐渐递增的。新近 7 年（1997一2003 年）是一号冰川监测史上负平衡波动期最长并且继续延伸的物质亏损最强烈的时期。这是气候变暖作用于冰川指示器的具体体现。因此，最新负平衡波动期继续延伸的可能性依然很大。

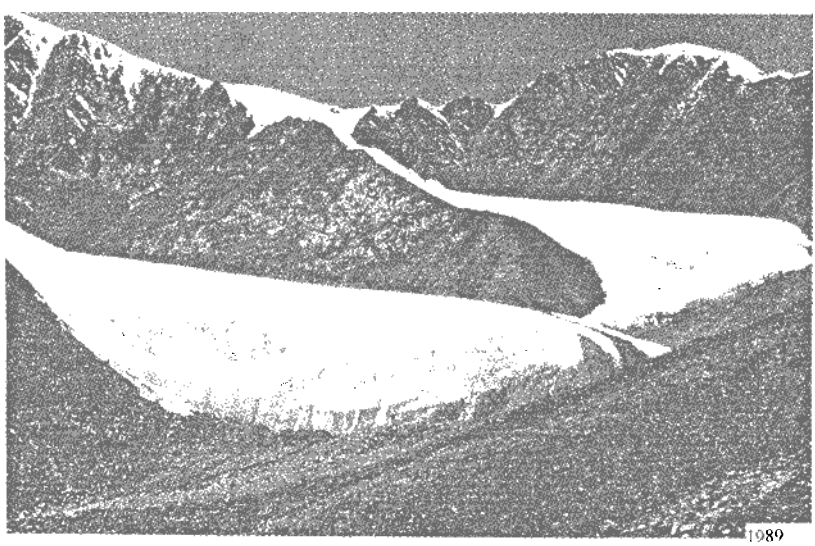

照片 1　1989 年的一号冰川，西支冰舌末端与东支冰舌连为一体，当时的一号冰川面积为 1.84km^2.

照片 2 2001 年 8 月的一号冰川，冰川面积为 1.708km^2，西支冰舌末端告别东支冰川的水平距离达到了 45m.

参考文献

[1] 胡汝骥，樊自立，王亚俊，杨 青，黄玉英. 近 50a 新疆气候变化对环境影响评估[J]. 干旱区地理. 2001. 24（2）：97～103.

[2] 李忠勤，韩添丁，井哲帆，杨惠安，焦克勤. 乌鲁木齐河源区气候变化和一号冰川 40a 观测事实. 冰川冻土. 2003. 25（2）：117～123.

[3] 焦克勤，王纯足，韩添丁. 天山乌鲁木齐河源一号冰川出现大的物质负平衡，冰川冻土，2000，**22**（1）：62~64.

[4] Yang Huai.The Extensive Information of mass Balance of Urumgihe Sources No.1 Glacier in Tianshan of China. Glacier Mass Balance Bulletin, Bulletin No.6（1998－1999）[R].Compiled by the World Glacier Monitoring Service, IAHS（ICSI）－UNEP－UNESCO－WMO, 2001.

[5] 谢自楚，葛光文. 天山乌鲁木齐河源一号冰川的积累、消融及物质平衡，天山乌鲁木齐河冰川与水文研究，北京，科学出版社，1965，24~24.

[6] 张金华，王晓军，李 军. 天山乌鲁木齐河源一号冰川物质平衡变化与气候相互关系的研究，冰川冻土，1984，**6**（4）：25~36.

[7] 天山冰川站. 天山冰川站年报，1～16 卷[R]. 兰州：中国科学院旱区旱区环境与工程研究所（中国科学院兰州冰川冻土研究所），1980～2002.

[8] Yang Huai.The Extensive Information of mass Balance of Urumgihe Sources No.1 Glacier in Tianshan of China.. Glacier Mass Balance Bulletin, Bulletin No.7-8（2000－2003）[R].Compiled by the World Glacier Monitoring Service, IAHS（ICSI）－UNEP－UNESCO－WMO, 2005.

A Study of Mass Balance and Process of Glacier No.1 at Headwater of Urumqi River In the past 44 years

Yang Hui-an, Li Zhong-qin, Ye Bai-sheng, Jiao Ke-qing,Jing Zhe-fan, Zhao Zhong-ping

(Tianshan Glaciological Station, Cold and Arid Regions Environmental and Engineering Research Institute, Chinese Academy of Sciences, Lanzhou Gansu 730000, China)

Abstract: The observed results of mass balance of Glacier No.1 at headwater of Urumqi River,Tianshan mountains, from1997 to 2003 were reported. Mass balance of Glacier No.1 in the past 44 years, the variety process of cumulative net balance,as well as equilibrium line altitude (ELA) and accumulation area ratio(AAR) which reflect topography and climate factor and glacier growth conditions were compared and analyzed. This paper thinks that the fluctuations cycle of negative balance extends as time goes on, at present it situated the most intensive deficit period from the observed histories.

Key words: Glacier No.1; Mass Balance; cumulative net balance; equilibrium line altitude (ELA) ; accumulation area ratio(AAR)

天山乌鲁木齐河源 1 号冰川 2002/03 年物质平衡

杨惠安，李忠勤，焦克勤

（中国科学院寒区旱区环境与工程研究所，甘肃 兰州 730000）

1 概况

一号冰川 2002/03 年度物质平衡测点布设是在上一年的基础上进行的，即分别在东支和西支冰川消融区表面，从冰舌开始自下而上布设 A—I 等 9 个横剖面，各横剖面一般在冰面上等距离布设 3 根测杆。近年来由于冰舌末端消融强烈以及退缩之故，使得东支 A 剖面和西支 A、B、C 剖面的冰面地形变得越来越陡峻，尤其西支东侧冰舌更是悬冰削壁，冰裂隙密布，行动非常危险，这些冰面上布设测杆和观测测杆的难度也越来越大，这些断面测杆布设的数量亦因此减少到 1 个点到 2 个点（西支 C 剖面）。积累区资料以雪坑观测结果获得。2002/03 年一号冰川物质平衡测点平均密度为 29 根/km^2。

本年度一号冰川物质平衡观测方法与上一年相同，即从 5 月初开始观测，每月底或月初观测一次，至 8 月底为最后一次结束年度观测。由于今年 4 月底至 5 月上旬连续为降雪天气，故本年度第一次观测较之往年推后了约一周时间，是在 5 月 8 日进行的。

一号冰川已解体为相互完全独立的一号冰川东支和一号冰川西支，为了便于与历史资料比较，一号冰川的零平衡线高度是利用面积加权法求得的。

2 物质平衡观测计算结果

在观测、统计和计算工作的基础上，2001－2002 年一号冰川和一号冰川东支、西支物质平衡获得如下若干结果：

⑴一号冰川西支 2002/03 年度单点物质平衡观测数据（表 1）；

⑵一号冰川东支 2002/03 年度单点物质平衡观测数据（表 2）；

⑶一号冰川 2002/03 年度冬平衡结果为+176.2 mm，其中一号冰川东支为+188.0 mm，一号冰川西支为+154.9 mm（表 3）；

⑷一号冰川 2002/03 年度物质纯平衡结果-383.5 mm，其中一号冰川东支为-386.9 mm，一号冰川西支为-377.3 mm（表 4）；

⑸一号冰川西支 2002/03 年度各高度带物质平衡（表 5）；

⑹一号冰川东支 2002/03 年度各高度带物质平衡（表 6）；

⑺一号冰川 2002/03 年度冬平衡等值线图（图 1）；

⑻一号冰川 2002/03 年度物质纯平衡等值线图（图 2）。

表 1 2002/03 年度 1 号冰川西支单点物质平衡观测数据统计表

剖面	测杆 (№)	海拔 (m)	纯积消量 (mm) 2003.5.8.	03.5.29.	03.6.26.	03.7.31.	03.8.30.	合计 (mm)
A	1	3830	-481.0	-607.0	-1495.0	-2403.0	-3063.0	-3063.0
B	1	3855	-425.3	-886.0	-1191.0	-1899.0	-2787.0	-2787.0
C	1	3900	193.1	79.0	-234.0	-658.5	-1360.0	-1360.0
	2	3902	-383.0	-414.0	-945.0	-1341.0	-2041.5	-2041.5
	平均	3901	-95.0	-167.5	-589.5	-999.8	-1700.8	-1700.8
D	1	3928	129.0	135.0	-558.0	-991.5	-1507.5	-1507.5
	2	3926	77.5	59.0	-423.0	-689.5	-1200.7	-1200.7
	3	3933	-301.0	-268.0	-1040.5	-1610.5	-2279.5	-2279.5
	平均	3929	-31.5	-24.7	-673.8	-1097.2	-1662.6	-1662.6
E	1	3974	-98.0	9.0	-231.0	-432.0	-976.5	-976.5
	2	3976	179.4	105.0	-205.4	-391.0	-1128.6	-1128.6
	3	3994	-1.1	85.5	-481.5	-883.5	-1453.5	-1453.5
	平均	3981	26.8	66.5	-306.0	-568.8	-1186.2	-1186.2
F	1	4013	477.0	603.0	-50.8	-24.1	-460.5	-460.5
	2	4021	105.0	84.0	-188.0	-214.1	-464.0	-464.0
	3	4027	31.2	57.0	-423.0	-529.5	-1019.0	-1019.0
	平均	4020	204.4	248	-220.6	-255.9	-647.8	-647.8
G	1	4045	408.2	648.0	15.0	54.6	-223.5	-223.5
	2	4055	154.0	82.3	-1.0	-20.2	-310.0	-310.0
	3	4048	181.0	129.0	-123.0	-105.4	-208.5	-208.5
	平均	4053	247.7	286.4	-36.3	-23.7	-247.3	-247.3
H	1	4077	12.0	30.0	50.0	98.2	-21.0	-21.0
	2	4073	157.3	155.5	-60.0	-30.5	-362.9	-362.9
	3	4070	153.0	158.6	30.0	66.0	70.4	70.4
	平均	4073	107.4	114.7	6.7	44.6	-104.5	-104.5
I	1	4087	193.7	192.0	65.0	127.5	-17.4	-17.4
L1	1	4125	144.5	249.0	360.6	477.2	150.0	150.0
L2	1	4175	218.9	260.0	371.6	488.2	356.0	356.0
L3	1	4225	229.9	271.0	382.6	499.2	362.6	362.6
L4	1	4300	246.4	287.5	399.1	515.7	372.5	372.5
L5	1	4375	262.9	304.0	415.6	532.2	382.4	382.4
L6	1	4450	279.4	320.5	432.1	548.7	392.1	392.1

表 2 2002/03 年度 1 号冰川东支单点物质平衡观测数据统计表

剖面	测杆 (№)	海拔 (m)	纯积消量 (mm) 2003.5.8.	2003.5.29.	2003.6.26.	2003.7.31.	2003.8.30.	合计 (mm)
A	1	3776	-86.5	-136.4	-885.0	-1666.5	-2529.0	-2529.0
B	1	3801	206.4	171.0	-516.0	-1189.5	-1962.0	-1962.0
	2	3801	80.0	-66.0	-647.0	-1189.5	-1752.0	-1752.0
	3	3801	51.0	-251.5	-1011.0	-1702.5	-2515.5	-2515.5
	平均	3801	62.7	-70.7	-764.8	-1437.0	-2189.6	-2189.6
C	1	3849	199.5	193.2	-217.5	-714.0	-1221.0	-1221.0
	2	3852	-126.0	-150.0	-459.0	-880.5	-1443.0	-1443.0
	3	3847	417.0	201.0	-265.0	-640.5	-1182.0	-1182.0
	平均	3849	163.5	81.4	-313.8	-745.0	-1282.0	-1282.0
D	1	3894	243.0	192.1	-144.0	-273.0	-864.0	-864.0
	2	3890	105.5	68.5	-471.0	-821.0	-1200.6	-1200.6
	3	3892	93.0	111.0	-282.0	-345.0	-436.0	-436.0
	平均	3892	147.2	123.9	-299.0	-479.7	-833.5	-833.5
E	1	3922	165.0	132.0	-90.5	-160.5	-376.0	-376.0
	2	3923	191.0	199.0	-118.2	83.0	-261.0	-261.0
	3	3923	144.0	142.6	-75.0	-96.0	-195.0	-195.0
	平均	3923	166.7	157.9	-94.6	-57.8	-277.3	-277.3
F	1	3971	229.0	202.4	65.5	-5.0	-137.0	-137.0
	2	3965	184.5	160.3	-66.0	-102.0	-206.5	-206.5
	3	3966	215.4	234.0	39.0	53.0	127.5	127.5
	平均	3967	209.6	198.9	12.8	-18.0	-72.0	-72.0
G	1	4008	136.1	153.0	-90.0	-139.0	-315.5	-315.5
	2	4004	85.8	72.5	-156.0	-174.2	-294.0	-294.0
	3	4003	291.5	243.0	120.6	99.0	159.0	159.0
	平均	4005	171.1	156.2	-41.8	-71.4	-150.2	-150.2
H	1	4058	286.5	300.0	75.1	66.5	-69.0	-69.0
	2	4043	231.0	204.6	68.0	67.8	28.5	28.5
	3	4058	179.5	127.6	21.0	69.0	126.0	126.0
	平均	4053	232.3	210.7	54.7	67.8	28.5	28.5
I	1	4075	196.9	238.0	349.6	466.2	285.7	285.7
J	1	4125	271.5	249.0	360.6	477.2	350.0	350.0
K	1	4170	217.8	258.9	370.5	487.1	355.4	355.4
L	1	4250	235.2	276.3	388.1	504.7	366.0	366.0

表 3　1 号冰川 2002/03 年度冬平衡观测计算结果

项　目	平衡线海拔（m）	纯　积　累			纯　消　融			物 质　平 衡	
		积累区面积（km^2）	积累量（10^4m^3）	积累深（mm）	消融区面积（km^2）	消融量（10^4m^3）	消融深（mm）	总 量（10^4m^3）	平衡值（mm）
1 号东支	3789	1.058	20.9	197.2	0.043	0.2	43.3	20.7	188.0
1 号西支	3994	0.538	11.1	206.0	0.069	1.7	252.3	9.4	154.9
1 号冰川	3862	1.596	32.0	200.5	0.112	1.9	169.6	30.1	176.2

表 4　1 号冰川 2002/03 年度物质平衡观测计算结果

项　目	平衡线海拔（m）	纯　积　累			纯　消　融			物 质　平 衡	
		积累区面积（km^2）	积累量（10^4m^3）	积累深（mm）	消融区面积（km^2）	消融量（10^4m^3）	消融深（mm）	总 量（10^4m^3）	平衡值（mm）
1 号东支	4066	0.498	11.4	228.9	0.603	54.0	895.5	-42.6	-386.9
1 号西支	4089	0.316	9.3	294.3	0.291	32.2	1106.5	-22.9	-377.3
1 号冰川	4074	0.814	20.7	254.3	0.894	86.2	964.2	-65.5	-383.5

表 5　1 号冰川西支 2002/03 年度各高度带物质平衡（mm）

海拔高度区间（m）	冰川面积（km^2）	观　测　时　间　（年/月/日）				
		2003/5/8	2003/5/29	2003/6/26	2003/7/31	2003/8/30
4400-4486	0.030	290	325	425	550	340
4350-4400	0.034	278	304	416	532	328
4300-4350	0.045	266	285	378	525	300
4250-4300	0.036	253	279	363	503	285
4200-4250	0.035	246	266	383	499	270
4150-4200	0.037	197	255	372	488	216
4100-4150	0.053	184	221	213	475	110
4050-4100	0.112	198	297	12	50	-133
4000-4050	0.088	175	267	-188	-283	-458
3950-4000	0.067	-2	21	-490	-833	-1434
3900-3950	0.041	-63	-96	-632	-1049	-1692
3850-3900	0.024	-260	-527	-890	-1449	-2254
3825-3850	0.005	-453	-747	-1343	-2151	-2925
3825-4486	0.607	150	183	-11	-44	-364

表 6 1 号冰川东支 2002/03 年度各高度带物质平衡（mm）

海拔高度	冰川面积	观测时间（年/月/日）				
区间（m）	(km^2)	2003/5/8	2003/5/29	2003/6/26	2003/7/31	2003/8/30
4150-4267	0.120	227	268	379	496	391
4100-4150	0.081	234	254	255	482	358
4050-4100	0.095	215	233	202	337	237
4000-4050	0.169	202	184	7	-2	-41
3950-4000	0.160	190	171	-41	-49	-107
3900-3950	0.205	177	141	-197	-268	-495
3850-3900	0.118	155	103	-306	-612	-998
3800-3850	0.088	113	5	-539	-1091	-1656
3742-3800	0.065	-12	-104	-825	-1552	-2259
3742-4267	1.101	177	153	-89	-183	-397

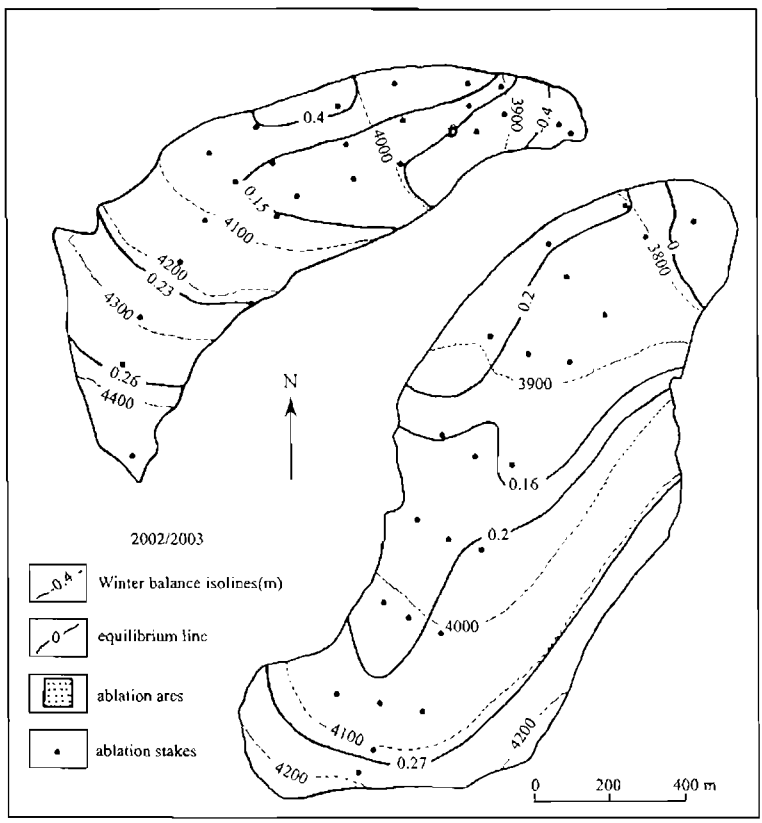

图 1 2002/03 年度一号冰川冬平衡等值线图

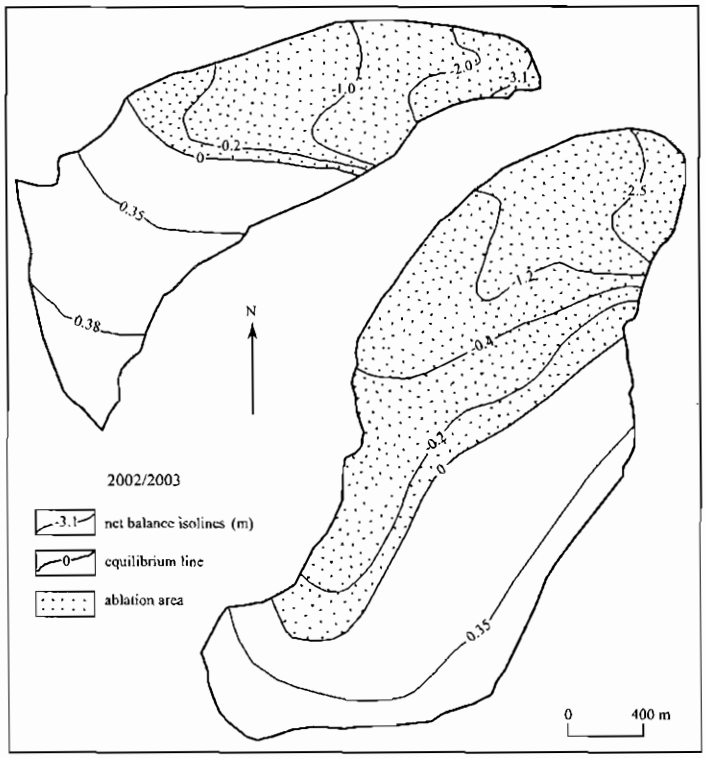

图 2　2002/03 年度一号冰川纯平衡等值线图

3　结果比较

2002/03 年度一号冰川物质平衡结果是-383.5 mm，仍为负平衡年，而且是自 1997 年以来的最新负平衡周期内连续出现的第 7 个负平衡年，这在一号冰川物质平衡观测历史上极为罕见（图 3）。但与上一年物质平衡结果（-833.9 mm）比较，本年度一号冰川物质平衡的负平衡量较上一年减少了 54%，比其最近 7 年的物质平衡平均值（-688.6 mm）减少了 44.3%，也是最近 7 年中两个负平衡值较低的年份之一。

大西沟气象站气象资料统计结果表明，本年度乌鲁木齐河源地区平均气温为-4.6℃，比上年下降 0.6℃，但仍高出多年平均值 0.6℃。年度内冷季（9~4 月）平均气温-8.3℃，比上年同期下降 0.2℃，仍高于同期多年平均值 1.0℃，本年度内 1 月的月均温不仅高于上年同期 1.2℃，尤其更高于多年同期平均值达 3.1℃；暖季（5~8 月）中的 4 个月内，除 6 月较上年升高 0.4℃外，其余 3 个月的的气温均较上年有所降低。暖季平均气温 2.9℃，比上年同期平均值下降 1.2℃，也低于同期多年平均气温 0.1℃。其中，11 月、2－5 月各月和 7、8 月的月均温低于上年同期 0.5－3.1℃之间，2 月和 8 月分别为降温幅度最小和最大月。年度降水总量为 453.5mm，比上年减少了 27.6%，总体上接近或略高于本区多年平均降水水平。年度内冷季（9~4 月）降水占年度总量的 17.4%，比上年同期减少 46.7%，也少于同期多年平均值 20%；暖季（5~8 月）降水占年度总量的 82.6%，比上年同期减少 21.8%，但

仍高于同期多年平均值 6.1%。

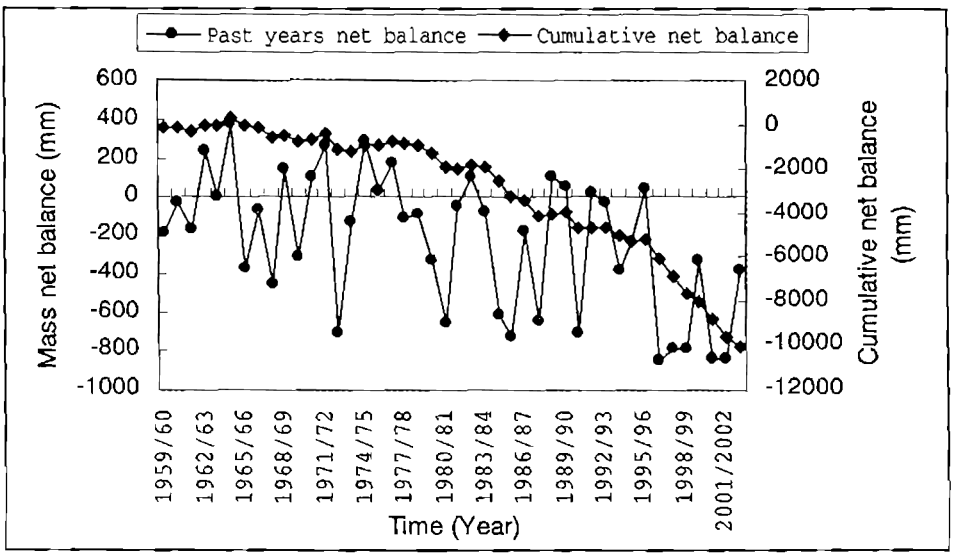

图 3 一号冰川 44 年间年净平衡与累计净平衡变化过程

冰川补给期与消融期同时同步，是大陆性冰川的主要特征。综合气温和降水资料可以看出，本年度气候状况相对于上年为低温少雨的干冷年份，但总体上年均温仍高于多年平均值 0.6℃，年内冷季气温则高于同期多年平均值 1.0℃，暖季平均气温（2.9℃）较同期多年平均值（3.0℃）略有下降（下降值为 0.1℃），而年度降水量亦与多年平均值（450.1mm）非常接近。

根据上述结果可以认为，本年度暖季（冰川补给期）气温的偏低抑制了冰川的强烈消融，导致本年度冰川物质负平衡量相对于近几年超常的巨额负平衡量而有所减少。本区本年度平均气温仍偏高多年平均值的情况，仍是本年度一号冰川物质平衡结果依然为负值的主要因素。

参考文献

[1] 焦克勤，王纯足. 天山乌鲁木齐河源一号冰川物质平衡观测研究（1996/97 和 1997/98 年度）.中国科学院天山冰川观测试验站年报.1996-1998 年报，1999 年 4 月，15：109-122.

[2] 杨惠安，王纯足，焦克勤，等.天山乌鲁木齐河源一号冰川 1998/99 年物质平衡.中国科学院天山冰川观测试验站年报.1999-2002 年报，2003 年 11 月，16：75-85.

[3] 杨惠安，叶柏生，焦克勤. 天山乌鲁木齐河源一号冰川 1999/2000 年物质平衡.中国科学院天山冰川观测试验站年报. 1999-2002 年报，2003 年 11 月，16：86-92.

[4] 杨惠安，李忠勤，焦克勤. 天山乌鲁木齐河源一号冰川 2000－2002 年物质平衡.中国科学院天山冰川观测试验站年报. 1999-2002 年报，2003 年 11 月，16：93-103.

[5] 杨惠安，李忠勤，焦克勤. 天山乌鲁木齐河源一号冰川 2002/03 年物质平衡.中国科学院天山冰川观测试验站年报.见本年报（第 17 卷）.

天山乌鲁木齐河源 1 号冰川 2003/04 年物质平衡

杨惠安，李忠勤

（中国科学院寒区旱区环境与工程研究所天山冰川站，甘肃 兰州 730000）

1 概况

2003/04 年度乌鲁木齐河源一号冰川物质平衡观测网点的布设是在上一年的基础上进行的，即分别在东支和西支冰川消融区表面，从冰舌开始自下而上布设 A—I 等 9 个横剖面，各横剖面一般在冰面上等距离布设 3 根测杆。近年来由于冰舌末端消融强烈以及退缩之故，使得东支 A 剖面和西支 A、B、C 剖面的冰面地形变得越来越陡峻，尤其西支东侧冰舌更是冰悬壁削，冰裂隙密布，涉及这些区域的冰面测杆的布设和观测行为都非常危险，尤其是西支 C 剖面东侧冰面裂隙密布，布设测杆和测杆观测的难度也越来越大，这些断面测杆布设的数量亦因此减少到 1 个点到 2 个点（西支 C 剖面）。积累区资料以雪坑观测结果获得。2003/04 年一号冰川物质平衡测点平均密度为 29 根/km^2。图 1 为 2003/04 年一号冰川物质平衡观测网点。

本年度一号冰川物质平衡观测方法与上一年相同，即从 4 月末开始观测，每月底或月初观测一次，至 8 月底为最后一次结束年度观测。

一号冰川已解体为相互完全独立的一号冰川东支和一号冰川西支，为了便于与历史资料比较，一号冰川的零平衡线高度是利用面积加权法求得的。

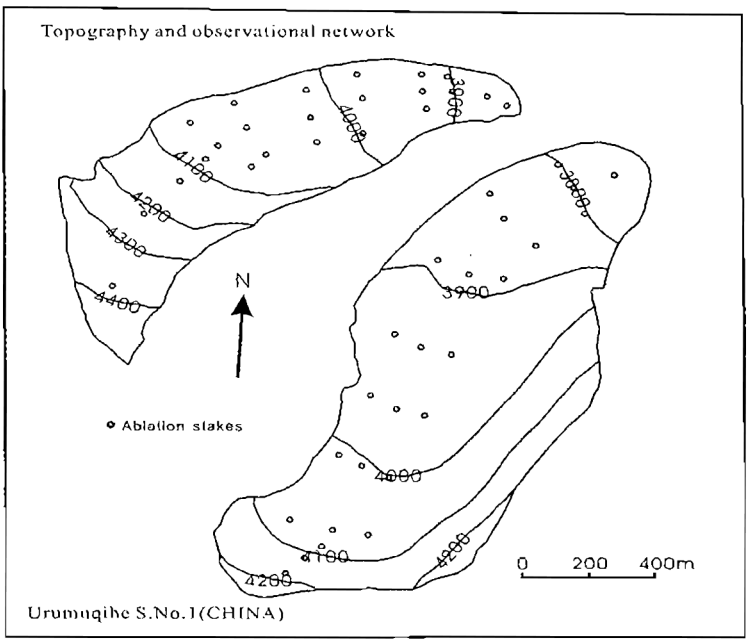

图 1　2003/04 年一号冰川物质平衡观测网点

2 物质平衡观测计算结果

在观测、统计和计算工作的基础上，2003/04 年一号冰川和一号冰川东支、西支物质平衡获得如下若干结果：

(1)一号冰川西支 2003/04 年度单点物质平衡观测数据（表 1）；

表 1 2003/04 年度 1 号冰川西支单点物质平衡观测数据统计表(2003/8/30-2004/8/31)

剖面	测杆	海拔	纯积消量（mm）					合计
	(№)	(m)	03.8.30-04.4.30.	2004.5.30.	2004.7.1.	2004.8.1.	2004.8.31.	(mm)
A	1	3830	-1022.0	-1473.4	-2478.0	-3151.4	-3315.0	-3315.0
B	1	3855	-631.0	-906.4	-1659.0	-2163.6	-2766.0	-2766.0
C	1	3900	-256.9	-270.4	-856.0	-1592.4	-2053.0	-2053.0
	2	3902	-613.5	-644.1	-1324.5	-2204.7	-3084.9	-3084.9
	平均	3901	-435.2	-457.3	-1090.3	-1898.6	-2569.0	-2569.0
D	1	3928	-263.5	-236.7	-895.5	-2034.9	-2245.5	-2245.5
	2	3926	-754	-745.3	-1238.3	-2091.7	-2396.3	-2396.3
	3	3933	-508.3	-554.4	-1174.5	-2189.9	-2542.5	-2542.5
	平均	3929	-508.6	-512.1	-1102.8	-2105.5	-2394.8	-2394.8
E	1	3974	-182	-84.9	-372	-1642	-1594	-1594
	2	3976	-490.9	-971.8	-1319.4	-1572.4	-1831.4	-1831.4
	3	3994	-255	-150.6	-726	-1689.2	-2212	-2212
	平均	3981	-309.3	-402.4	-805.8	-1634.5	-1879.1	-1879.1
F	1	4013	-158.1	-81.2	-725.6	-1118.2	-1481.2	-1481.2
	2	4021	102.5	-27	-250	-1026	-1224.6	-1224.6
	3	4027	86	131.2	-43	-979	-1265.8	-1265.8
	平均	4020	10.1	7.7	-339.5	-1041.1	-1323.9	-1323.9
G	1	4045	-229	-99.1	-340.5	-947.5	-1219.5	-1219.5
	2	4055	-258.5	-173.9	-440	-1304	-1489	-1489
	3	4048	-56.5	16.8	280.5	-547.5	-717.9	-717.9
	平均	4053	-181.3	-85.4	-166.7	-933.0	-1142.1	-1142.1
H	1	4077	220	327	129	-1050	-1199	-1199
	2	4073	-109	-71.4	-320.6	-1183.6	-1343.6	-1343.6
	3	4070	93.1	257.2	91.6	-274.4	-357.8	-357.8
	平均	4073	68.0	170.9	-33.3	-836.0	-966.8	-966.8
I	1	4087	-21.4	4.8	-125.1	-864.1	-450.0	-450.0
L1	1	4125	309.0	209.8	28.7	-525.9	-290.7	-290.7
L2	1	4175	299.5	208.3	220.4	-80.9	297.8	297.8
L3	1	4225	367.5	322.3	354.6	234.6	340.4	340.4
L4	1	4300	348.4	341.2	335.4	315.5	276.6	276.6
L5	1	4375	302.1	397.4	316.2	283.9	234	234
L6	1	4450	232.5	362.9	297.1	220.8	212.8	212.8

⑵—号冰川东支 2003/04 年度单点物质平衡观测数据（表 2）；

表 2　2003/04 年度 1 号冰川东支单点物质平衡观测数据统计表（2003.8.30—2004.8.31.）

剖面	测杆 (No.)	海拔 (m)	纯积消量（mm） 03.8.30-04.4.30.	2004.5.30.	2004.7.1.	2004.8.1.	2004.8.31.	合计 (mm)
A	1	3776	-975.0	-974.4	-1188.0	-2327.0	-2826.0	-2826.0
B	1	3801	-184.5	-220.2	-1035.0	-1955.8	-2385.0	-2385.0
	2	3801	-120.0	-107.6	-774.0	-1850.0	-2223.0	-2223.0
	3	3801	-409.9	-540.7	-1390.5	-2140.3	-2560.5	-2560.5
	平均	3801	-238.1	-289.5	-1066.5	-1982.0	-2389.5	-2389.5
C	1	3849	-144.5	-70.1	-454.5	-1505.5	-1905.5	-1905.5
	2	3852	-103.8	-159	-696.0	-1405.2	-1755.0	-1755.0
	3	3847	-58.5	24.0	-240.0	-974.0	-1201.5	-1201.5
	平均	3849	-102.3	-68.4	-463.5	-1294.9	-1620.7	-1620.7
D	1	3894	39.6	79.4	-15.0	-944.6	-1192.0	-1192.0
	2	3890	32.4	102.4	-401.4	-1378.4	-1643.4	-1643.4
	3	3892	58.5	-122.6	-23	-748.2	-864.5	-864.5
	平均	3892	43.3	19.7	-146.5	-1023.7	-1233.3	-1233.3
E	1	3922	12.5	129.2	-140.0	-952.0	-1275.7	-1275.7
	2	3923	183.5	-202.4	-475.5	-1654.2	-1870.6	-1870.6
	3	3923	12.5	1039.8	-70.5	-602.2	-694.8	-694.8
	平均	3923	69.3	322.2	-228.7	-1069.5	-1280.4	-1280.4
F	1	3971	-158	441.6	-15.5	143.2	-983.0	-983.0
	2	3965	102.5	36.7	140.8	-730.1	-860.9	-860.9
	3	3966	58.5	191.5	16.5	-499.5	-541.5	-541.5
	平均	3967	1.0	223.3	47.3	-362.1	-795.1	-795.1
G	1	4008	-128.7	-45.1	-659.5	-1306.7	-1442.2	-1442.2
	2	4004	-11	37.8	-189.0	-1398.0	-1545.4	-1545.4
	3	4003	190.5	765.0	-18.0	663.6	-237.0	-237.0
	平均	4005	16.9	252.6	-288.8	-680.4	-1074.9	-1074.9
H	1	4058	-84.0	-3.2	-753.0	-1086.0	-1194.0	-1194.0
	2	4043	15.5	-8.5	213.5	26.7	-26.5	-26.5
	3	4058	9.6	301.2	52.0	-356.4	-51.0	-51.0
	平均	4053	-19.6	96.5	-162.5	-471.9	-423.8	-423.8
I	1	4075	120.0	120.0	177.0	-207.0	-189.0	-189.0
J	1	4125	352.5	363.9	368.7	148.9	185.0	185.0
K	1	4170	435.5	499.2	560.4	319.1	251.1	251.1
L	1	4220	351.1	349.4	376.1	287.6	292.9	292.9

(3)—号冰川 2003/04 年度冬平衡结果为+21.7 mm，其中—号冰川东支为+46.4 mm，—号冰川西支为-22.5 mm（表 3）；

(4)—号冰川 2003/04 年度物质纯平衡结果-754.7 mm，其中—号冰川东支为-705.6 mm，—号冰川西支为-843.9 mm（表 4）；

(5)—号冰川西支 2003/04 年度各高度带物质平衡（表 5）；

(6)—号冰川东支 2003/04 年度各高度带物质平衡（表 6）；

(7)—号冰川 2003/04 年度冬平衡等值线图（图 2）；

(8)—号冰川 2003/04 年度物质纯平衡等值线图（图 3）。

表 3 1 号冰川 2003/04 年度物质平衡观测计算结果

项 目	平衡线海拔 (m)	纯积累 积累区面积 (km^2)	纯积累 积累量 (10^4m^3)	纯积累 积累深 (mm)	纯消融 消融区面积 (km^2)	纯消融 消融量 (10^4m^3)	纯消融 消融深 (mm)	物质平衡 总量 (10^4m^3)	物质平衡 平衡值 (mm)
1 号东支	4096	0.457	8.7	190.2	0.644	86.4	1341.3	-77.7	-705.6
1 号西支	4173	0.245	4.9	201.6	0.362	56.2	1551.5	-51.2	-843.9
1 号冰川	4123	0.702	13.6	193.7	1.006	142.6	1417.5	-128.9	-754.7

表 4 1 号冰川 2003/04 年度冬平衡观测计算结果

项 目	平衡线海拔 (m)	纯积累 积累区面积 (km^2)	纯积累 积累量 (10^4m^3)	纯积累 积累深 (mm)	纯消融 消融区面积 (km^2)	纯消融 消融量 (10^4m^3)	纯消融 消融深 (mm)	物质平衡 总量 (10^4m^3)	物质平衡 平衡值 (mm)
1 号东支	4039	0.893	12.9	144.7	0.208	7.8	374.9	+5.1	+46.4
1 号西支	4093	0.355	6.5	184.3	0.252	7.9	313.7	-1.4	-22.5
1 号冰川	4058	1.248	13.6	109	0.46	15.7	341.3	+3.7	+21.7

表 5 1 号冰川西支 2003/04 年度各高度带物质平衡（mm）

海拔高度区间（m）	冰川面积 (km^2)	观测时间（年/月/日） 2004.4.30.	2004.5.30.	2004.7.1.	2004.8.1.	2004.8.31.
4400-4486	0.030	320	350	221	224	380
4350-4400	0.034	377	352	284	234	370
4300-4350	0.045	435	367	300	261	350
4250-4300	0.036	467	344	319	275	330
4200-4250	0.035	455	319	300	169	275
4150-4200	0.037	345	244	231	-107	150
4100-4150	0.053	250	144	50	-519	-300
4050-4100	0.112	-160	6.5	-100	-838	-963
4000-4050	0.088	-280	-138	-350	-838	-1380
3950-4000	0.067	-410	-438	-775	-1638	-1920
3900-3950	0.041	-550	-463	-1037	-1913	-2765
3850-3900	0.024	-720	-725	-1425	-2125	-3120
3825-3850	0.005	-995	-1238	-2113	-2513	-3300
3825-4486	0.607	-23	-6.8	-195	-676	-844

表 6 1 号冰川东支 2003/04 年度各高度带物质平衡（mm）

海拔高度区间（m）	冰川面积 (km^2)	观测时间（年/月/日）				
		2004/4/30	2004/5/30	2004/7/1	2004/8/1	2004/8/31
4150-4267	0.120	375	443	450	288	270
4100-4150	0.081	309	337	363	100	135
4050-4100	0.095	192	194	50	-263	-220
4000-4050	0.169	45	182	-225	-575	-580
3950-4000	0.160	32	251	-175	-644	-750
3900-3950	0.205	38	142	-113	-832	-840
3850-3900	0.118	-32	-24	-307	-1160	-1170
3800-3850	0.088	-170	-179	-766	-1639	-1750
3742-3800	0.065	-607	-632	-1128	-2155	-2170
3742-4267	1.101	46	127	-162	-703	-706

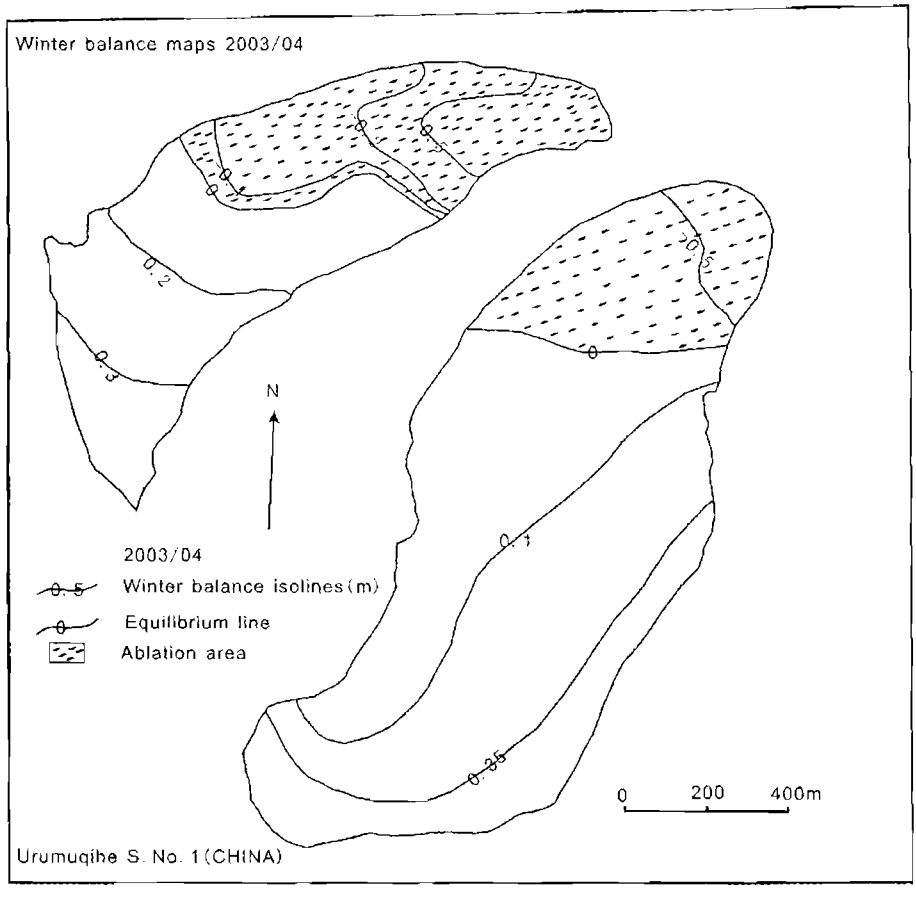

图 2 一号冰川 2003/04 年度冬平衡等值线图

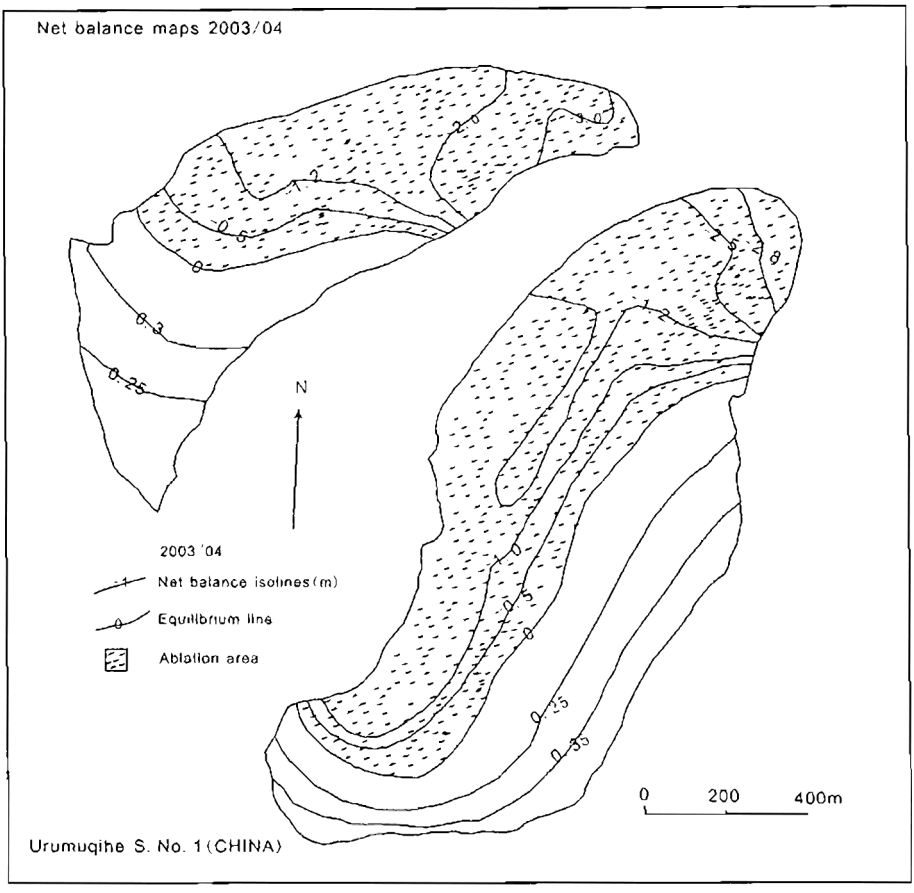

图 3 一号冰川 2003/04 年度纯平衡等值线图

3 气候状况

根据大西沟气象站气象资料统计，2003/04 年度（9－8 月）天山乌鲁木齐河源地区年平均气温为-4.4℃，比上年同期升高了 0.1℃，但仍高出多年平均值 0.8℃；本年度除 1 月、3-5 月、7-8 月的 6 个月月平均气温较上年有明显上升，上升幅度在 0.3℃（8 月）－4.6℃（4 月）之间，而 10-2 月和 6 月的 6 个月月平均气温则比上年同期有明显下降，下降幅度为 0.6℃（6 月）－2.9℃（1 月）。本年度冷季（9~4 月）平均气温-8.4℃，比上年同期下降 0.2℃，仍高于同期多年平均值 0.8℃；本年度暖季（5~8 月）4 个月内，除 6 月月均温较上年降低 0.6• 外，其余 3 个月的月气温均较上年同期有所升高，升高幅度介于 0.3℃（8 月）－2.1℃（7 月）之间。

天山乌鲁木齐河源地区本年度降水总量为 425.5mm，属于 2000 年以来降水量减少年份之一，降水量比上年同期减少了 6.2%，大体上接近且略少于本区多年降水平均水平。年度内冷季（9~4 月）降水占年度总量的 19.5%，但比上年同期减少 2.1%，也少于同期多年平均值 2.6%；暖季（5~8 月）降水占年度总量的 80.5%，虽比上年同期减少 2.1%，但仍高于同期多年平均值 2.5%。

4 结果比较

2003/04 年度一号冰川物质平衡结果是-754.7 mm，仍为负平衡年，而且是自 1996 年以来的最新负平衡周期内连续出现的第 8 个负平衡年。与过去 44 年来的物质平衡结果比较，连续延续出现 8 年负平衡年周期的现象（杨惠安等，2005），在一号冰川物质平衡观测历史上为首次出现（图 4）。

与上一年物质平衡结果（-383.5 mm）比较，本年度一号冰川物质平衡的负平衡量较上一年增加了 103.3%，比其最近 8 年物质平衡平均值（-697 mm）增加了-57.8mm 水层，也是最近 8 年中第六个负平衡值较高年份之一。

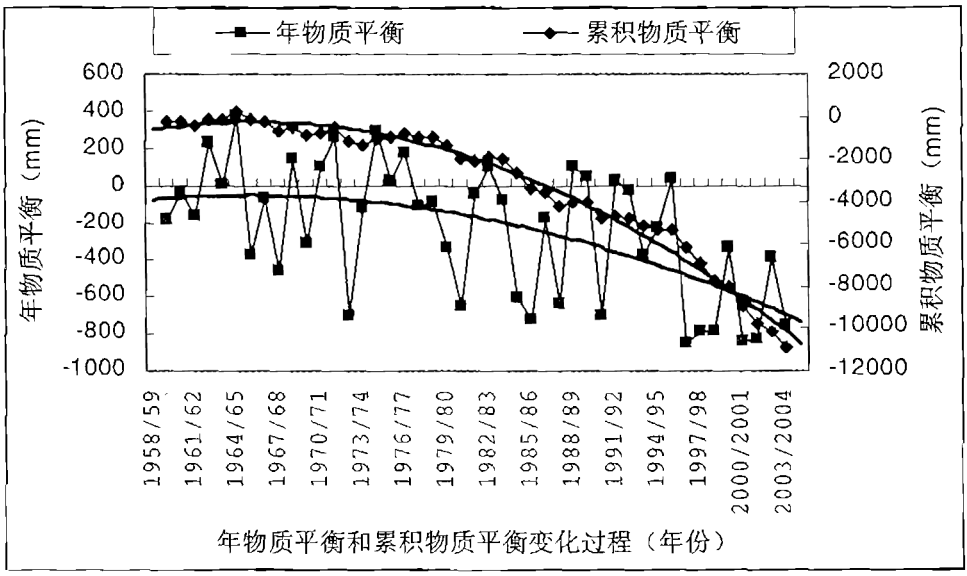

图 4　一号冰川年物质平衡和累积物质平衡年变化过程

冰川补给期与消融期同时同步，是大陆性冰川的主要特征。综合气温和降水资料可以看出，本年度气候状况相对于上年为低温少雨的干冷年份，但总体上年均温仍高于多年平均值 0.6℃，年内冷季气温则高于同期多年平均值 0.8℃，暖季平均气温（3.6℃）较同期多年平均值（3.0℃）略有升高（升高值为 0.6℃），而年度降水量亦与多年平均值（451.1 mm）较为接近。

可以认为，天山乌鲁木齐河源地区本年度平均气温持续偏高多年平均值的情况，仍是本年度一号冰川物质平衡结果依然出现负值的主要因素。

5 亟待新一轮测图

一号冰川整体自 1993 年末因其西支末端完全解体脱离东支以来至 2002 年间，一号冰川西支末端冰面部分工作还可以涉足，甚至不时有旅游者骑马在上盘桓，但近年来末端冰面陡峭（东支末端与此类似），已难以涉足冰面，联系到持续近 8 年来的负平衡状况和 2001 年 8 月的冰川面积测绘结果表明，其退缩速度似在逐年加速。一号冰川西支末端冰川退缩方式亦表现为两种不同的方式：即末端东侧以块状冰崩（照片 1-2，2003 年一号冰川西支

末端的块状冰崩和西侧自然消融冰厚度自然减薄退缩状况），这在小冰川中罕见；而末端西侧则以通常的表面自然消融冰厚度自然减薄退缩出现。目前冰川物质平衡观测和计算工作仍使用的是2001年8月测绘完成的一号冰川地形图，使用与冰川变化不同步的冰川图，难免影响其计算结果的精度。鉴于近年来冰川物质负平衡的持续性，测绘新的一号冰川图，将是进一步提高冰川变化长期监测的精确度的必不可少的基础工作。

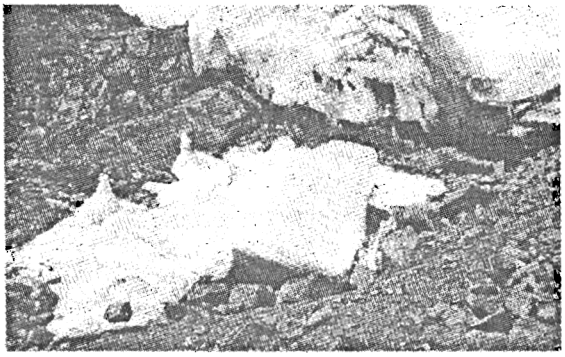

照片1 2003年一号冰川西支末端的块状冰崩

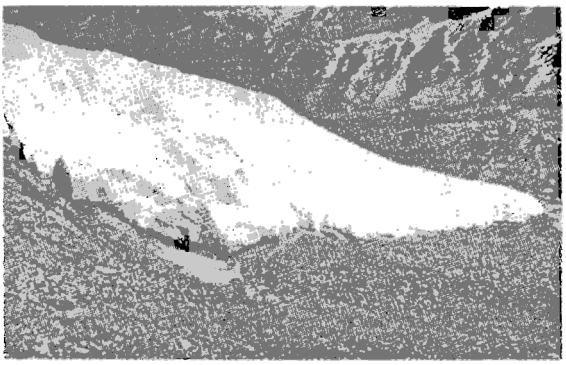

照片2 2003年一号冰川西支末端形态（右为东侧，左为西侧）

参考文献

[1] YANG Hui-an,LI Zhong-qin,YE Bai-sheng, et al.2005.Study on Mass Balance and Pprocess of Glaier NO.1 at the Urumqi River in the Past 44 Years. Arid Land Geography.Vol.28,No.1:p76-80. [杨惠安，李忠勤，叶佰生，等. 过去44年乌鲁木齐河源一号冰川物质平衡结果及其过程研究[J]. 干旱区地理，2005，28（1）：76-80.]

[2] 杨惠安，王纯足，焦克勤，等.天山乌鲁木齐河源一号冰川1998/99年物质平衡.中国科学院天山冰川观测试验站年报.1999-2002年报，2003年11月，16：75-85.

[3] 杨惠安，叶柏生，焦克勤. 天山乌鲁木齐河源一号冰川1999/2000年物质平衡.中国科学院天山冰川观测试验站年报. 1999-2002年报，2003年11月，16：86-92.

[4] 杨惠安，李忠勤，焦克勤. 天山乌鲁木齐河源一号冰川2000－2002年物质平衡.中国科学院天山冰川观测试验站年报. 1999-2002年报，2003年11月，16：93-103.

[5] 杨惠安，李忠勤，焦克勤. 天山乌鲁木齐河源一号冰川2002/03年物质平衡.中国科学院天山冰川观测试验站年报.见本年报（第17卷）.

天山冰川观测试验站水文气象资料整编说明（2003）

韩添丁，叶柏生

（中国科学院寒区旱区环境与工程研究所天山冰川站，甘肃 兰州 730000）

天山冰川观测试验站的常规水文、气象观测在乌鲁木齐河源区的 1 号冰川水文点、空冰斗水文点、总控制水文点以及后峡基本营地进行，本文为 2003 年度资料整编结果报告。

1 号冰川水文点设在离 1 号冰川末端 300m 的河道上，实施 1 号冰川冰雪径流的监测，断面海拔 3659m，流域面积 3.34km^2，其中冰川面积 1.708km^2。为混凝土矩形断面（高 1.0m，宽 1.6m），气象场设在断面左岸。

空冰斗水文点设在乌鲁木齐河源区左侧，斗口朝南，进行高山区积雪、多年冻土融水径流的观测，断面海拔 3805m，流域面积 1.68km^2，为混凝土矩形断面（高 1.0m，宽 1.0m），气象场设在断面右岸。

在乌鲁木齐河源区大西沟和罗布道沟汇合处，设有总控制水文点，控制监测乌鲁木齐河源区降水和 7 条冰川以及冰川周围高山积雪、多年冻土的总融水径流；该控制端面海拔 3408m，流域面积 28.9km^2;其中冰川面积 5.6km^2。为混凝土断面，设有工作桥，气象场设在断面左岸冰碛丘上。

三个水文断面均装有自计水位计，测流主要用流速仪法，即时流量由水位－流量关系线求得。气象观测项目主要为气温、降水、湿度、蒸发、地温、日照等。后峡基本营地气象观测场位于乌鲁木齐河谷，海拔 2130m，进行常规气象要素观测。所有观测资料均按规范进行整理（附表）。

表 1 乌鲁木齐河源 1 号冰川水文点逐日平均流量表（流量：m^3/s）

日\月	1	2	3	4	5	6	7	8	9	10	11	12
1					0.000	0.355	0.180	0.225				
2					0.000	0.310	0.225	0.290				
3					0.000	0.310	0.270	0.510				
4					0.000	0.420	0.225	0.580				
5					0.000	0.445	0.270	0.555				
6					0.000	0.335	0.245	0.290				
7					0.000	0.355	0.290	0.200				
8					0.000	0.445	0.400	0.155				
9					0.000	0.400	0.270	0.155				
10					0.000	0.270	0.270	0.225				
旬总数					0.000	3.645	2.645	3.185				
旬平均					0.000	0.365	0.265	0.319				
11					0.000	0.155	0.245	0.245				
12					0.000	0.135	0.270	0.225				
13					0.000	0.200	0.290	0.200				
14					0.000	0.200	0.225	0.225				
15					0.000	0.245	0.200	0.270				
16					0.000	0.155	0.290	0.375				
17					0.025	0.200	0.245	0.465				
18					0.045	0.465	0.290	0.245				
19					0.115	0.510	0.270	0.245				
20					0.155	0.335	0.310	0.200				
旬总数					0.340	2.600	2.635	2.695				
旬平均					0.034	0.260	0.264	0.270				
21					0.115	0.270	0.355	0.180				
22					0.045	0.335	0.425	0.245				
23					0.115	0.290	0.445	0.445				
24					0.135	0.180	0.245	0.510				
25					0.135	0.180	0.225	0.510				
26					0.225	0.200	0.245	0.420				
27					0.180	0.200	0.200	0.335				
28					0.200	0.245	0.245	0.225				
29					0.155	0.180	0.245	0.155				
30					0.155	0.155	0.200	0.135				
31					0.200		0.180	0.135				
旬总数					1.660	2.235	3.010	3.295				
旬平均					0.151	0.224	0.274	0.300				
月总数					2.000	8.480	8.290	9.175				
月平均					0.068	0.283	0.403	0.447				
月最大					0.465	1.060	0.780	1.290				
日期					26	18	23	4				
月最小					0.000	0.065	0.135	0.065				
日期					1	13	1	9				

表 2 乌鲁木齐河源 1 号冰川水文点逐日平均气温表（气温：℃）

日\月	1	2	3	4	5	6	7	8	9	10	11	12
1	-17.5	-16.9	-15.9	-7.0	-0.9	7.1	1.9	2.9	3.7	-8.5	-5.0	-18.1
2	-12.9	-15.4	-14.9	-8.2	-7.2	3.8	2.8	4.2	4.4	-6.6	-4.4	-16.4
3	-11.9	-13.7	-17.8	-12.3	-10.4	4.8	3.7	5.4	4.7	-5.4	-5.0	-17.6
4	-12.1	-14.3	-20.3	-16.0	-10.7	6.4	3.2	5.1	3.7	-5.4	-7.4	-20.2
5	-11.2	-12.1	-21.6	-13.1	-8.3	4.8	4.9	2.1	5.2	-2.8	-8.6	-16.4
6	-10.5	-12.9	-22.0	-10.4	-8.8	5.9	4.8	1.6	5.3	-3.5	-18.0	-15.6
7	-13.1	-13.0	-19.8	-7.4	-7.4	3.6	4.6	3.4	6.5	-4.1	-15.4	-15.1
8	-14.8	-16.3	-17.9	-10.7	-4.2	4.0	5.3	-0.6	9.7	-8.0	-17.3	-13.5
9	-15.2	-18.3	-14.9	-13.7	-3.8	3.4	2.9	1.8	10.1	-10.8	-14.4	-12.8
10	-13.5	-18.2	-18.8	-9.4	-4.7	3.3	3.6	3.2	6.8	-12.0	-15.9	-10.4
旬总数	-132.7	-151.1	-183.9	-108.2	-66.4	47.1	37.7	29.1	60.1	-67.1	-111.4	-156.1
旬平均	-13.3	-15.1	-18.4	-10.8	-6.6	4.7	3.8	2.9	6.0	-6.7	-11.1	-15.6
11	-12.2	-17.1	-18.3	-10.9	-6.3	2.7	2.1	3	5.1	-13.0	-11.7	-10.4
12	-14.6	-14.1	-17.9	-10.9	-6.9	4.8	3.2	3.7	5.8	-9.8	-7.3	-8.2
13	-16.4	-12.2	-16.3	-8.9	-4.4	5.7	3.3	2.2	5.0	-7.7	-11.0	-7.5
14	-11.3	-15.6	-16.6	-3.6	-4.9	5.7	-0.5	2.7	2.1	-6.1	-11.2	-18.2
15	-9.2	-18.3	-13.4	-5.3	-5.1	2.4	1.9	5.2	-0.4	-3.7	-5.9	-16.1
16	-9.1	-12.0	-14.8	-12.2	-3.5	2.7	4.5	6.1	-4.7	-4.5	-7.4	-16.5
17	-9.2	-8.8	-13.7	-12.1	-0.9	4.3	3.7	6.4	-4.7	-6.7	-10.2	-16.4
18	-6.7	-9.6	-11.1	-13.0	-0.1	5.1	6.0	3.6	-5.9	-10.9	-14.8	-15.8
19	-6.5	-10.7	-6.8	-4.6	-1.4	5.7	6.0	1.6	-1.2	-4.2	-18.6	-12.0
20	-10.7	-13.2	-10.8	-8.9	-1.7	4.2	3.3	2.9	2.4	-3.6	-13.9	-12.3
旬总数	-105.9	-131.6	-139.7	-90.4	-35.2	43.3	33.5	37.4	3.5	-70.2	-112.0	-133.4
旬平均	-10.6	-13.2	-14.0	-9.0	-3.5	4.3	3.4	3.7	0.4	-7.0	-11.2	-13.3
21	-9.9	-14.5	-8.6	-11.9	-0.9	3.9	5.1	3.3	2.0	-3.0	-10.0	-12.2
22	-10.0	-11.9	-7.0	-11.9	-0.1	4.3	5.4	4.7	3.1	-6.0	-11.2	-9.4
23	-13.7	-14.1	-3.2	-6.6	1.6	-0.1	4.0	7.3	-2.1	-7.1	-9.1	-15.1
24	-21.6	-15.1	-5.2	-3.0	1.4	1.2	2.6	8.1	-4.6	-6.4	-15.2	-14.7
25	-23.6	-14.6	-5.5	-3.2	-0.1	2.5	1.2	5.9	-4.5	-5.1	-12.1	-13.6
26	-19.6	-19.0	-7.8	-5.1	0.1	2.7	5.0	3.8	-1.0	-2.2	-13.9	-16.5
27	-16.9	-16.3	-4.1	-4.2	3.6	1.8	4.0	2.6	-6.8	-0.2	-21.4	-18.2
28	-14.7	-11.0	-1.6	2.2	1.6	2.3	3.5	1.0	-14.0	-1.1	-13.5	-14.9
29	-14.5		-5.6	2.6	1.7	2.2	-0.1	-0.4	-10.6	-0.8	-14.6	-15.4
30	-12.3		-8.0	1.8	3.6	0.9	-0.4	0.3	-8.3	-0.9	-20.8	-16.5
31	-14.9		-4.8		3.5		0.3	2.6		-4.0		-17.1
旬总数	-171.7	-116.5	-61.4	-39.3	16.0	21.7	30.6	39.2	-46.8	-36.8	-141.8	-163.6
旬平均	-15.6	-14.6	-5.6	-3.9	1.5	2.2	2.8	3.6	-4.7	-3.3	-14.2	-14.9
月总数	-410.3	-399.2	-385.0	-237.9	-85.6	112.1	101.8	105.7	16.8	-174.1	-365.2	-453.1
月平均	-13.2	-14.3	-12.4	-7.9	-2.8	3.7	3.3	3.4	0.6	-5.6	-12.2	-14.6
月最高	-2.5	-0.8	5.0	7.9	10.9	11.5	11.0	12.2	14.8	5.0	-2.0	-3.5
日期	19	19	28	28	31	3	19	16	9	27	1	12
月最低	-28.0	-22.0	-24.9	-19.2	-14.1	-5.0	-4.2	-4.3	-18.0	-16.2	-27.0	-23.0
日期	25	15	6	9	5	24	30	6	28	11	27	4
年统计	最高 14.8 9 月 9 日				最低-28 1 月 25 日				平均气温	-6.0		

表 3 乌鲁木齐河源 1 号冰川水文点逐日降水量表（降水量：mm）

日\月	1	2	3	4	5	6	7	8	9	10	11	12
1												
2												
3						2.4	1.4					
4								2.8				
5												
6						0.1	4.2	37.8				
7						1.4						
8					10.5							
9					0.5	1.0	10.2	1.3				
10					14.1	6.0	3.6			7.4		
11					0.5		3.4	2.2				
12					2.5			3.0				
13							1.7	0.6				
14					2.9		36.2	5.7			1.2	
15						0.2						
16						14.0	1.3					
17	0			3.0			2.0					
18					0.7		0.5	4.1	8.0			
19					0.8			2.5			0.9	
20						6.8	7.4		11.9			
21					0.8	1.2						
22					1.6	2.1	0.2	1.1				
23	0.1					15.5	5.6					
24						9.2						
25						1.1	7.8					
26												
27		1.2	2.9			0.2		12.4				
28						11.3	2.0	24.0	14.3			
29						9.2	2.8	3.1				
30						16.2						
31					1.5		1.8					
总量	0.1	1.2	2.9	3.0	36.4	97.9	92.1	100.6	34.2	7.4	2.1	0
降水日数	2	1	1	1	11	17	17	13	3	1	2	
最大日降水量					14.1	16.2	36.2	37.8	14.3			
日期					10	30	14	6	28			
年统计	降水量 377.9		降水日数 69									

表 4 乌鲁木齐河源 1 号冰川水文点逐日平均相对湿度表（相对湿度：%）

日\月	1	2	3	4	5	6	7	8	9	10	11	12
1						30	58	82				
2						69	62	77				
3						54	75	90				
4						50	72	83				
5						65	58	88				
6						54	68	63				
7						69	63	66				
8						78	58	89				
9						88	85	56				
10					81	78	71	61				
旬总数					81	635	670	755				
旬平均						64	67	76				
11					61	63	85	70				
12					66	30	68	76				
13					68	34	82	87				
14					79	46	86	54				
15					81	85	70	54				
16					42	65	58	61				
17					32	53	77	59				
18					42	56	48	71				
19					69	59	54	77				
20					71	59	70	50				
旬总数					611	550	698	659				
旬平均					61	55	70	66				
21					70	78	59	62				
22					54	73	70	65				
23					52	93	63	62				
24					72	54	61	52				
25					73	47	63	62				
26					20	47	44	79				
27					49	70	71	84				
28					68	66	62	88				
29					70	79	64	56				
30					52	79	68	48				
31					53		80	44				
旬总数					633	686	705	702				
旬平均					58	69	64	64				
月总数						1871	2073	2116				
月平均						62	67	68				
月最小					0	14	18	17				
日期					26	1	26	31				
附注	相对湿度只在 5-8 月冰川消融期观测											

表 5 乌鲁木齐河源空冰斗水文点逐日平均流量表（流量：m^3/s）

日\月	1	2	3	4	5	6	7	8	9	10	11	12
1					0.000	0.120	0.245	0.050				
2					0.000	0.080	0.280	0.050				
3					0.000	0.120	0.220	0.050				
4					0.000	0.064	0.080	0.050				
5					0.000	0.071	0.057	0.280				
6					0.000	0.057	0.064	0.220				
7					0.000	0.050	0.064	0.230				
8					0.000	0.050	0.057	0.120				
9					0.000	0.057	0.220	0.026				
10					0.000	0.071	0.230	0.071				
旬总数					0.000	0.740	1.517	1.147				
旬平均					0.000	0.074	0.152	0.115				
11					0.000	0.050	0.160	0.064				
12					0.000	0.034	0.220	0.080				
13					0.000	0.018	0.080	0.160				
14					0.000	0.042	0.120	0.220				
15					0.000	0.034	0.245	0.160				
16					0.018	0.057	0.280	0.080				
17					0.018	0.057	0.270	0.071				
18					0.026	0.050	0.245	0.064				
19					0.034	0.057	0.220	0.057				
20					0.064	0.071	0.245	0.057				
旬总数					0.160	0.470	2.085	1.013				
旬平均					0.016	0.047	0.209	0.101				
21					0.080	0.050	0.160	0.042				
22					0.160	0.057	0.120	0.042				
23					0.160	0.057	0.120	0.042				
24					0.160	0.160	0.071	0.050				
25					0.071	0.230	0.120	0.050				
26					0.080	0.071	0.120	0.050				
27					0.120	0.050	0.064	0.080				
28					0.071	0.270	0.057	0.160				
29					0.064	0.205	0.064	0.220				
30					0.064	0.064	0.050	0.230				
31					0.057		0.064	0.160				
旬总数					1.087	1.214	1.010	1.126				
旬平均					0.099	0.121	0.092	0.102				
月总数					1.423	3.755	8.574	5.662				
月平均					0.041	0.081	0.245	0.162				
月最大					0.280	0.500	0.480	0.520				
日期					24	24	18	6				
月最小					0.000	0.000	0.016	0.000				
日期					1	13	14	9				

表 6 乌鲁木齐河源空冰斗水文点逐日平均气温表（气温：℃）

日\月	1	2	3	4	5	6	7	8	9	10	11	12
1	-18.2	-16.8	-15.7	-6.5	-1.7	4.4	2.8	2.2	2.3	-8.8	-6.8	-19.2
2	-12.3	-14.6	-14.5	-8.0	-7.4	2.4	3.5	2.7	2.5	-6.9	-5.7	-17.0
3	-11.8	-13.7	-17.2	-11.5	-10.5	3.2	3.5	4.2	2.3	-5.5	-5.7	-17.7
4	-12.4	-13.9	-20.1	-15.8	-10.7	4.1	3.3	4.0	2.0	-4.9	-8.1	-20.5
5	-11.1	-11.9	-20.9	-12.7	-9.8	3.1	5.7	1.2	3.1	-3.4	-8.0	-16.0
6	-10.1	-13.1	-21.5	-10.0	-8.2	4.9	5.1	3.3	3.7	-3.1	-16.8	-14.7
7	-13.4	-12.9	-19.1	-6.9	-7.1	2.9	4.3	2.7	5.1	-4.7	-15.2	-15.7
8	-14.9	-16.7	-17.4	-10.7	-4.5	4.1	4.8	-0.9	7.4	-7.8	-16.9	-12.8
9	-15.6	-18.4	-14.5	-13.2	-3.4	4.1	3.0	1.4	7.3	-9.0	-13.7	-11.3
10	-13.1	-18.1	-18.0	-9.4	-4.6	3.9	3.9	2.9	4.9	-11.2	-15.7	-9.8
旬总数	-132.9	-150.1	-178.9	-104.7	-67.9	37.1	39.9	23.7	40.6	-65.3	-112.6	-154.7
旬平均	-13.3	-15.0	-17.9	-10.5	-6.8	3.7	4.0	2.4	4.1	-6.5	-11.3	-15.5
11	-12.9	-16.5	-17.2	-11.0	-6.7	3.4	2.8	2.3	4.3	-12.0	-11.4	-10.6
12	-15.1	-14.8	-17.8	-10.9	-6.2	4.9	3.8	2.9	5.4	-11.4	-7.5	-8.3
13	-16.3	-12.0	-16.7	-6.2	-4.2	5.4	4.0	1.8	4.8	-9.1	-11.0	-7.3
14	-11.5	-15.8	-16.9	-4.1	-4.1	3.8	0.8	1.8	2.1	-7.8	-11.0	-16.1
15	-10.8	-18.3	-15.1	-5.6	-5.4	1.3	2.5	4.3	1.0	-5.7	-6.1	-15.8
16	-9.2	-12.8	-14.8	-10.8	-6.6	1.5	3.9	4.9	-2.7	-6.3	-7.7	-16.3
17	-10.0	-9.4	-14.0	-12.1	-3.3	3.4	4.7	5.3	-2.1	-8.2	-10.1	-16.8
18	-7.8	-8.6	-11.3	-12.0	-2.7	4.7	6.2	2.6	-3.5	-11.3	-15.0	-14.7
19	-7.0	-7.7	-6.7	-3.7	-3.1	5.1	5.6	1.2	1.1	-4.6	-19.3	-11.1
20	-11.5	-12.3	-10.7	-8.4	-3.8	3.1	3.1	2.1	3.5	-3.9	-13.8	-14.4
旬总数	-112.1	-128.2	-141.2	-84.8	-46.1	36.6	37.4	29.2	13.9	-80.3	-112.9	-131.4
旬平均	-11.2	-12.8	-14.1	-8.5	-4.6	3.7	3.7	2.9	1.4	-8.0	-11.3	-13.1
21	-10.0	-14.4	-8.3	-11.7	-2.9	2.6	4.8	2.2	1.8	-3.9	-10.0	-14.4
22	-9.9	-12.1	-6.3	-11.5	-1.3	3.9	5.9	4.0	2.6	-7.4	-11.4	-12.2
23	-14.4	-13.7	-3.0	-6.5	-0.5	0.7	4.2	5.8	-2.4	-8.0	-9.4	-19.1
24	-21.8	-15.0	-5.4	-2.3	0.2	0.8	2.7	7.0	-4.6	-7.3	-15.0	-18.7
25	-24.3	-14.4	-6.3	-3.3	-1.8	2.0	0	4.6	-4.5	-5.5	-12.6	-17.8
26	-19.6	-18.5	-8.1	-4.9	-1.6	2.5	3.4	2.8	-3.0	-2.8	-14.3	-18.2
27	-16.6	-15.9	-4.5	-3.7	2.3	2.0	3.5	1.5	-6.1	-1.4	-21.0	-19.4
28	-14.4	-10.4	0.8	2.2	0.0	2.1	2.8	-0.4	-12.7	-1.8	-14.0	-16.5
29	-14.3		-5.7	2.7	0.3	2.6	-0.2	-0.5	-10.2	-1.5	-15.5	-16.8
30	-12.2		-7.4	2.4	1.8	1.8	0	-1.8	-8.4	-2.0	-21.9	-17.2
31	-14.1		-4.9		1.3		0.7	1.5		-5.2		-17.4
旬总数	-171.6	-114.4	-59.1	-36.6	-2.2	21.0	27.8	26.7	-47.5	-46.8	-145.1	-187.7
旬平均	-15.6	-14.3	-5.4	-3.7	-0.2	2.1	2.5	2.4	-4.8	-4.3	-14.5	-17.1
月总数	-416.6	-392.7	-379.2	-226.1	-116.2	94.7	105.1	79.6	7.0	-192.4	-370.6	-473.8
月平均	-13.4	-14.0	-12.2	-7.5	-3.7	3.2	3.4	2.6	0.2	-6.2	-12.4	-15.3
月最高	-3.2	0.0	5.0	7.2	7.8	9.9	11.2	11.0	12.4	3.7	-3	-4.5
日期	19	19	28	29	31	1	18	16	8	28	2	12
月最低	-28.8	-21.8	-24.0	-18.9	-14.0	-3.0	-4.4	-4.1	-15.7	-15.0	-26.5	-23.0
日期	25	15	6	9	5	28	29	29	28.0	11	27	1
年统计	最高	12.4	日期	9月8日	最低	-28.8	日期	1月25日	平均气温	-6.3		

表 7 乌鲁木齐河源空冰斗水文点逐日降水量表（降水量：mm）

日\月	1	2	3	4	5	6	7	8	9	10	11	12
1												
2												
3						2.8						
4								3.3				
5												
6						0.2	3.3	37.6				
7						1.3						
8					10.3	0.0						
9						0.8	8.6	0.8				
10						5.8	4.7			6.8		
11							3.4	2.9				
12							6.4	3.7				
13							1.4	0.8				
14							37.0	5.7				
15					17.8	0.2					0.8	
16						15.3	1.2					
17	0			3.2			1.3					
18							0.6	4.1				
19					1.2			2.9			1.2	
20						7.3	7.3		12.0			
21					0.2	1.3						
22					1.7	2.1	0.1	0.9				
23	0.1					15.0	5.6					
24						10.3						
25						1.2						
26							7.6					
27		1.0	1.7			0.3		11.8				
28						12.8	2.1	24.3	14.0			
29						8.5	2.3	2.9				
30						16.5						
31					1.2		2.4					
总量	0.1	1.0	1.7	3.2	32.4	101.7	95.3	101.7	26.0	6.8	2.0	0
降水日数	2	1	1	1	6	18	17	13	2.0	1	2	
最大降水量	0.1	1	1.7	3.2	17.8	16.5	37	37.6	14	6.8	1.2	
日期	23	27	27	17	15	30	14	6	28	10	19	
年统计	降水量	371.9	降水日数	64								

表 8 乌鲁木齐河源空冰斗水文点逐日平均相对湿度表（%）

日\月	1	2	3	4	5	6	7	8	9	10	11	12
1						40	74	56				
2						76	85	62				
3						68	84	79				
4						73	92	91				
5						75	73	100				
6						70	82	72				
7						84	77	87				
8						86	77	99				
9						96	98	72				
10						93	85	84				
旬总数						761	827	802				
旬平均						76	83	80				
11						72	92	86				
12						43	78	87				
13						50	92	94				
14						62	94	69				
15						93	87	70				
16						91	89	82				
17					52	75	91	72				
18					67	76	60	84				
19					82	79	71	91				
20					84	81	82	62				
旬总数						722	836	797				
旬平均						72	84	80				
21					80	90	83	78				
22					74	86	93	78				
23					75	100	82	71				
24					86	73	80	62				
25					88	65	81	72				
26					28	65	67	91				
27					44	85	85	88				
28					67	80	78	98				
29					72	93	59	82				
30					60	84	54	68				
31					63		64	63				
旬总数					737	821	826	851				
旬平均					67	82	75	77				
月总数						2304	2489	2450				
月平均						77	80	79				
最小					16	27	27	37				
日期					26	1	24	1				
附注	相对湿度只在 5-8 月冰川消融期观测											

表 9 乌鲁木齐河源总控水文点逐日平均流量表（m^3/s）

日\月	1	2	3	4	5	6	7	8	9	10	11	12
1					0.000	1.150	2.320	1.090				
2					0.000	1.150	1.940	1.280				
3					0.000	1.090	1.810	1.460				
4					0.000	1.350	1.570	1.940				
5					0.000	1.200	1.570	4.000				
6					0.000	1.200	1.810	3.570				
7					0.000	1.280	1.570	2.600				
8					0.530	1.150	1.810	1.940				
9					0.530	1.200	2.460	1.200				
10					0.530	1.280	2.460	0.980				
旬总数					1.590	12.050	19.320	20.060				
旬平均					0.159	1.205	1.932	2.006				
11					0.530	1.090	2.460	0.780				
12					0.530	1.090	2.460	0.740				
13					0.530	1.090	2.320	0.780				
14					0.740	1.150	2.900	0.740				
15					0.980	1.200	2.900	0.740				
16					1.280	1.350	2.900	0.780				
17					1.030	1.280	2.460	0.780				
18					0.880	1.350	2.200	0.980				
19					0.740	1.690	2.200	0.930				
20					0.740	1.570	2.200	0.820				
旬总数					0.798	1.286	2.500	0.807				
旬平均					0.798	1.286	2.500	0.807				
21					0.930	1.460	2.060	0.740				
22					1.030	1.940	2.320	0.780				
23					1.030	2.600	2.320	0.980				
24					0.930	2.200	1.940	1.030				
25					1.030	1.940	1.810	1.090				
26					0.980	1.280	1.690	1.200				
27					1.030	1.200	1.570	1.200				
28					1.090	1.810	1.570	1.570				
29					0.930	1.810	1.350	1.350				
30					0.980	2.460	1.150	1.150				
31					1.090		0.980	0.980				
旬总数					11.050	18.700	18.760	12.070				
旬平均					1.005	1.870	1.705	1.097				
月总数					23.965	59.437	89.332	63.880				
月平均					0.685	1.454	2.552	1.825				
月最大					1.940	4.200	4.860	7.160				
日期					16	23	14	6				
月最小					0.580	0.930	0.980	0.480				
日期					1	13	31	12				

表 10 [illegible]均气[illegible]（气温：℃）

日\月	1	2	3	4	5	6	7	8	9	10	11	12
1	-13.1	-17.5	-15.8	-0.6	-0.3	8.0	4.0	4.6	5.5	-5.9	-2.9	-14.7
2	-12.6	-16.1	-15.3	-2.3	-5.8	5.4	4.5	6.3	5.3	-3.6	-3.8	-14.6
3	-14.6	-12.2	-17.1	-7.2	-9.0	6.1	5.3	7.4	5.3	-3.2	-2.3	-13.9
4	-14.2	-13.9	-19.2	-12.2	-9.4	7.6	5.0	7.0	4.5	-2.9	-5.0	-17.0
5	-11.0	-12.7	-19.7	-9.3	-9.2	6.1	6.7	4.2	6.2	0.3	-7.1	-16.6
6	-11.9	-13.2	-19.8	-6.1	-7.8	6.0	5.4	3.3	5.9	-1.4	-15.8	-15.3
7	-12.6	-12.5	-16.0	-3.1	-5.9	5.3	5.5	5.2	6.5	-0.4	-14.6	-14.8
8	-15.0	-15.3	-13.4	-7.0	-2.6	6.5	5.0	1.8	9.3	-5.7	-17.1	-13.5
9	-15.4	-17.3	-9.6	-9.0	1.2	5.1	4.2	3.7	9.2	-10.0	-13.4	-11.7
10	-15.6	-17.8	-12.4	-6.6	-1.0	5.6	4.6	4.6	7.6	-9.6	-14.5	-10.1
旬总数	-136.0	-148.5	-158.3	-63.4	-49.8	61.7	50.2	48.1	65.3	-42.4	-96.5	-142.2
旬平均	-13.6	-14.8	-15.8	-6.4	-5.0	6.2	-5.0	4.8	6.5	-4.2	-9.6	-14.2
11	-14.7	-16.3	-12.9	-7.2	-3.3	5.4	3.7	4.8	6.6	-10.9	-9.8	-10.5
12	-15.5	-14.8	-13.1	-5.8	-2.9	5.9	4.1	5.3	8.3	-10.0	-4.1	-8.2
13	-16.3	-12.0	-12.0	-1.6	-1.3	6.1	4.2	4.0	6.3	-7.4	-8.1	-11.5
14	-11.5	-13.8	-15.3	1.8	-2.1	5.9	0.6	4.8	4.7	-5.2	-11.3	-17.6
15	-10.0	-16.3	-15.2	-0.2	-3.2	4.2	3.1	6.7	2.7	-3.0	-6.1	-17.1
16	-7.7	-10.7	-12.0	-10.4	-2.0	4.2	5.9	7.0	-1.4	-5.5	-7.9	-15.6
17	-9.5	-6.7	-10.4	-8.4	0.8	6.5	5.4	8.2	-0.9	-7.3	-11.2	-16.0
18	-7.0	-9.2	-8.1	-10.2	1.4	7.3	7.3	5.6	-2.8	-7.8	-13.2	-15.6
19	-6.3	-13.0	-4.6	-3.2	0.7	7.8	6.6	5.2	0.4	-3.2	-18.3	-13.9
20	-9.7	-12.5	-7.8	-6.7	0.1	5.9	5.2	4.7	4.9	-2.4	-14.9	-14.0
旬总数	-108.2	-125.3	-111.4	-51.9	-11.8	59.2	46.1	56.3	28.8	-62.7	-104.9	-140.0
旬平均	-10.8	-12.5	-11.1	-5.2	-1.2	5.9	4.6	5.6	2.9	-6.3	-10.5	-14.0
21	-11.6	-12.3	-4.7	-8.2	1.5	4.9	7.2	5.5	5.2	-1.0	-8.7	-14.2
22	-12.7	-10.2	-3.6	-10.1	1.6	4.9	7.3	6.8	5.5	-2.9	-10.2	-11.5
23	-13.8	-11.3	-0.2	-3.2	2.9	1.9	6.1	8.1	0.5	-3.8	-8.7	-14.9
24	-20.2	-12.2	-2.3	-1.3	3.0	2.0	4.1	8.9	-1	-3.0	-12.3	-15.7
25	-24.0	-13.4	-1.8	-2.9	0.1	4.3	2.9	7.5	-0.1	-1.5	-12.0	-11.2
26	-20.0	-17.3	-3.9	-3.5	1.8	4.7	6.6	4.5	0.6	-1.3	-10.2	-15.7
27	-18.8	-15.8	1.2	-2.9	5.4	6.7	6.4	2.6	-3.7	0.0	-20.7	-20.1
28	-16.3	-9.9	6.1	3.1	2.9	3.4	4.6	1.4	-11.1	-1.1	-12.7	-17.8
29	-14.2		0.6	4.8	4.0	4.1	0.9	2.1	-9.3	-0.5	-11.5	-17.3
30	-13.1		-0.6	2.8	5.5	2.7	-0.3	1.8	-6.9	0.0	-16.8	-19.6
31	-15.3		1.6		5.5		2.2	1.7		-0.4		-18.9
旬总数	-180.0	-102.4	-7.6	-21.4	34.2	39.6	48.0	50.9	-20.3	-15.5	-123.8	-176.9
旬平均	-16.4	-12.8	-0.7	-2.1	3.1	4.0	4.4	4.6	-2	-1.4	-12.4	-16.1
月总数	-424.2	-376.2	-277.3	-136.7	-27.4	160.5	144.3	155.3	73.8	-120.6	-325.2	-459.1
月平均	-13.7	-13.4	-8.9	-4.6	-0.9	5.4	4.7	5.0	2.5	-3.9	-10.8	-14.8
月最高	-1.2	-1.8	10.5	10.0	13.2	14.8	12.8	14.8	14.0	6.6	0.1	-2.0
日期	19	19	28	28	31	18	18	24	8	21	1	12
月最低	-29.9	-23.2	-24.3	-15.5	-15.0	-3.7	-5.1	-3.0	-18.5	-15.5	-24.9	-22.9
日期	25	27	6	5	5	24	29	31	28	9	27	27
年统计	最高	14.8	日期	6月18日	最低	-29.9	日期	1月25日	平均气温	-4.5		
				8月24日								

表 11 乌鲁木齐河源总控水文点逐日降水量表（降水量：mm）

日\月	1	2	3	4	5	6	7	8	9	10	11	12
1					1.1							
2				1.5	2.3	4.2						
3				0.6		0.4	2.1					
4				3.9	2.7			3.8			1.6	
5					0.2	0.2	0.1	28.5				
6					0.6		3.3	6.3			0.7	
7						1.4				1.2		
8										3.7		
9	0.2		0.1	1.2	2.2	1.1	11.5			0.2		
10					12.9	4.7	4.2	0.7		1.0		
11					1.5	0.6	8.3	2.5		0.8		
12				1.5			3.3					
13												
14		0.1					39.5	8.1				0.5
15		2.0			0.4	8.0	1.3		1.2		1.3	
16						1.9	0.8		0.4			
17							2.2					
18				4.2	1.5			3.2	13.2			
19		0.3				11.4	5.2	2.6				
20		0.4			0.9	2.3	3.3					
21				0.9	0.8	1.0	0.2				0.9	
22				0.6	1.3	13.1	6.1	0.9				
23						13.3	6.7					
24							2.9					
25		0.8	0.1			0.7						
26			4.2									
27			1.7	2.1		9.6	1.8	13.3				
28					1.1	6.7	4.4	24.2	13.8			
29					0.1	17.3						
30					0.2							
31					1.4		2.7					
总量	0.2	3.6	6.1	16.5	31.2	97.9	109.9	94.1	28.6	6.9	4.5	0.5
降水日数	1	5	4	9	17	18	20	11	4	5	4	1
最大降水量	0.2	2	4.2	4.2	12.9	17.3	39.5	28.5	13.8	3.7	1.6	0.5
日期	11	15	26	18	10	29	14	5	28	10	4	14
年统计	降水量	400	降水日数	99								

表 12 乌鲁木齐河源总控水文点逐日平均相对湿度表（相对湿度：%）

日\月	1	2	3	4	5	6	7	8	9	10	11	12
1						36	62	62				
2						67	77	56				
3						65	80	70				
4						62	73	83				
5						66	66	92				
6						71	75	74				
7						72	67	71				
8						76	81	89				
9						95	90	68				
10					72	81	78	76				
旬总数					72	691	749	741				
旬平均						69	75	74				
11					65	61	86	78				
12					73	43	82	76				
13					61	60	90	85				
14					83	58	99	55				
15					82	86	80	61				
16					49	67	75	72				
17					47	58	86	62				
18					65	67	56	87				
19					74	70	69	83				
20					79	68	72	62				
旬总数					678	638	795	721				
旬平均					68	64	80	72				
21					74	84	68	65				
22					60	83	75	66				
23					65	96	62	63				
24					76	62	82	65				
25					85	51	67	63				
26					21	66	58	85				
27					34	79	74	92				
28					65	74	89	87				
29					56	81	66	64				
30					51	79	76	72				
31					60		61	58				
旬总数					647	755	778	780				
旬平均					59	76	71	71				
月总数					1397	2084	2322	2242				
月平均						69	75	72				
最小					8	21	8	21				
日期					26	1	30	6				
附注	相对湿度只在 5-8 月冰川消融期观测											

表 13 乌鲁木齐河源后峡基本营地气象场逐日平均气温表（气温：℃）

日\月	1	2	3	4	5	6	7	8	9	10	11	12
1	-22.1	-11.2	-7.3	-0.2	4.5	13.1	10.8	10.9	11.1	2.4	1.3	-16.2
2	-15.2	-9.1	-10.1	-0.5	1.4	12.4	11.7	11.8	11.4	2.6	1.5	-13.8
3	-11.3	-9.4	-8.8	-3.9	-0.6	13.3	13.0	13.7	11.8	3.9	0.7	-12.8
4	-12.4	-9.5	-9.2	-5.5	-0.2	15.4	13.1	13.3	11.7	4.5	1.3	-11.8
5	-12.7	-8.7	-10.6	-3.9	1.6	15.5	14.2	11.3	12.0	4.5	-1.8	-14.3
6	-10.3	-6.8	-11.3	1.7	3.0	13.0	13.7	10.3	12.3	4.4	-9.5	-12.2
7	-7.9	-6.7	-11.5	2.7	4.2	12.0	13.0	10.7	12.7	4.5	-11.4	-12.4
8	-10.2	-9.2	-8.2	-3.0	5.6	13.4	14.1	9.6	13.9	2.1	-10.0	-11.8
9	-10.0	-12.3	-8.7	-2.3	5.5	12.7	13.0	11.4	15.0	0.9	-8.7	-10.9
10	-11.7	-12.7	-9.3	-0.5	2.2	13.5	14.0	10.9	15.2	-1.7	-7.2	-7.8
旬总数	-123.8	-95.6	-95.0	-15.4	27.2	134.3	130.6	113.9	127.1	28.1	-43.8	-124.0
旬平均	-12.3	-9.6	-9.5	-1.5	2.7	13.4	13.1	11.4	12.7	2.8	-4.4	-12.4
11	-11.8	-12.5	-9.3	-0.5	2.8	13.7	12.4	12.2	13.7	-2.2	-5.6	-8.3
12	-12.4	-9.4	-8.8	1.6	6.0	13.6	12.9	12.8	13.4	-2.1	1.8	-9.8
13	-14.3	-7.5	-11.3	3.2	6.5	14.4	11.7	11.6	11.2	-0.5	-6.8	-10.7
14	-10.9	-9.6	-10.5	4.8	6.0	14.4	9.1	12.6	9.8	0.0	-7.1	-13.0
15	-9.5	-8.8	-11.8	-2.6	6.8	13.0	11.1	13.2	7.1	1.1	-3.3	-17.1
16	-9.2	-9.0	-8.5	-10.7	6.9	12.5	11.5	13.5	6.5	-0.1	-2.9	-15.7
17	-7.4	-4.8	-4.7	-8.1	8.9	13.8	12.4	15.2	6.7	-1.0	-4.8	-16.0
18	-6.5	-6.5	-2.5	-8.1	9.0	15.8	13.4	11.3	4.7	0.3	-5.8	-15.6
19	-6.5	-9.4	-0.1	-4.4	7.2	14.9	12.2	11.4	7.4	2.0	-10.6	-12.9
20	-7.7	-9.5	-2.0	-4.5	7.6	12.1	11.9	12.0	9.3	3.5	-11.7	-14.1
旬总数	-96.2	-87.0	-69.5	-29.3	67.7	138.2	118.6	125.8	89.8	1.0	-56.8	-133.2
旬平均	-9.6	-8.7	-7.0	-2.9	6.8	13.8	11.9	12.6	9.0	0.1	-5.7	-13.3
21	-11.1	-7.4	0.0	-1.8	8.9	12.4	14.2	11.2	11.3	3.2	-6.9	-13.0
22	-7.7	-6.8	2.5	-0.5	6.6	13.0	13.9	12.5	8.2	1.4	-6.5	-11.9
23	-8.9	-7.5	3.8	3.2	9.9	9.8	12.4	14.1	6.0	2.9	-6.0	-10.7
24	-12.4	-9.9	1.1	3.3	8.5	8.8	10.6	14.1	3.7	2.2	-6.9	-15.4
25	-18.5	-9.2	3.6	4.0	8.2	10.4	10.5	12.6	4.0	2.6	-11.4	-14.5
26	-17.1	-9.8	1.5	3.7	7.4	11.6	11.3	11.1	5.1	3.9	-10.4	-11.8
27	-15.2	-10.6	3.2	5.8	10.4	11.1	11.0	11.3	1.7	4.2	-15.6	-13.9
28	-15.2	-6.0	6.3	9.8	10.1	12.0	9.8	9.3	-2.7	5.2	-10.6	-15.0
29	-11.4		2.7	11.7	9.5	11.3	5.9	9.9	-2.1	5.7	-12.4	-13.1
30	-11.1		1.6	10.8	11.5	10.3	6.6	11.0	0.4	7.0	-16.1	-12.8
31	-10.6		3.3		11.9		8.6	10.4		3.0		-12.8
旬总数	-139.2	-67.2	29.6	50.0	102.9	110.7	114.8	127.5	35.6	41.3	-102.8	-144.9
旬平均	-12.7	-8.4	2.7	5.0	9.4	11.1	10.4	11.6	3.6	3.8	-10.3	-13.2
月总数	-359.2	-249.8	-134.9	5.3	197.8	383.2	364.0	367.2	252.5	70.4	-203.4	-402.1
月平均	-11.6	-8.9	-4.4	0.2	6.4	12.8	11.7	11.8	8.4	2.3	-6.8	-13.0
月最高	8.0	8.3	17.5	24.0	20.3	25.5	22.1	24.1	25.7	19.5	13.0	-2.2
日期	21	17	28	29	23	5	5	17	9	29	2	11
月最低	-25.6	-20.0	-19.4	-17.5	-4.0	2.0	0.8	3.0	-9.5	-8.2	-21.1	-22.6
日期	1	27	7	8	5	24	31	31	29	12	30	20
年统计	最高	25.7	日期	9月9日	最低	-25.6	日期	1月1日	平均气温	0.7		

表 14 乌鲁木齐河源后峡[illegible]气象场逐日降水量表（降水量：mm）

日\月	1	2	3	4	5	6	7	8	9	10	11	12
1			0.2	0.1	4.4							
2				0.1	5.2	2.0	2.0					
3				0.3	3.4		0.4	1.7				
4			0.7	1.4	1.9		0.2	6				0.5
5			0.1		0.2		0.3	14.9			1.4	
6						3.8	3.0	7.7				
7						2.5	5.8	1.5		2.6		
8		0.5		0.3	0.5	0.7	2.4	2.6		2.2		
9				0.2	3.3	2.0	2.0	0.8				
10			0.2		20.9		12.6	0.3				
11				0.3	0.1		17.2					
12				0.7			1.2		6.0			
13					0.2		5.6	2.5	1.2			
14							39.0					
15		1.1				1.1	6.1					0.3
16				1.5		3.5	2.0	0.6				
17							0.4			0		
18				1.3	0.3			4.1	2.6		1.0	
19					0.4	3.0	9.0	6.9			1.1	
20	0.8	2.0		0	2.9	1.4	6.1					
21		2.8		0.7	4.9	1.4						
22				1.7	1.1	0.5	6.2	0.5				
23		0.8			2.4	13.8	5.0	0.6	5.7			
24	0.9					1.3	8.9				3.0	
25				3.3	0.7	6.3	13.2	9.1				
26		0.9	3.0	3.2		3.5		2.9			0.5	
27						3.8	4.9	6.6	5.2			0.5
28						0.9	3.4	20.5	11.0			
29			0.2		5.6	2.8			1.6			
30					0.6	20.3						
31					0.9							
总量	1.7	8.1	4.4	15.1	59.9	74.6	156.9	89.8	33.3	4.8	7.0	1.3
降水日数	2	6	6	15	20	19	24	18	7	3	5.0	3
最大日降水量	0.9	2.8	3	3.3	20.9	20.3	39	20.5	11	2.6	3.0	
日期	24	21	26	25	10	30	14	28	28	7	24.0	
年统计	降水量	456.9	降水日数	128								

表 15 乌鲁木齐河源后峡基本营地气象场逐日平均相对湿度表（相对湿度：%）

日\月	1	2	3	4	5	6	7	8	9	10	11	12
1	94	87	87	92	89	70	78	73	70	85	80	91
2	84	77	78	85	98	71	78	83	70	85	70	85
3	80	70	75	92	99	68	76	77	67	79	82	85
4	84	73	92	89	95	60	72	92	63	76	89	90
5	83	61	85	69	74	60	70	95	62	77	96	83
6	78	65	86	58	73	79	83	84	58	81	90	78
7	78	76	81	69	70	77	79	91	60	84	88	79
8	89	92	71	78	71	76	72	89	57	92	85	79
9	93	92	84	68	75	84	81	78	61	74	83	76
10	85	91	77	59	91	79	84	85	56	84	81	82
旬总数	848	784	816	759	835	724	773	847	624	817	844	828
旬平均	85	78	82	76	84	72	77	85	62	82	84	83
11	73	82	79	76	86	65	79	82	70	65	74	83
12	83	72	83	75	66	67	76	76	75	61	66	85
13	85	78	76	64	70	68	87	81	82	60	92	94
14	76	92	69	69	66	74	86	66	85	61	84	96
15	83	86	67	94	56	70	81	68	82	59	67	97
16	84	80	65	92	58	75	82	72	80	63	76	80
17	86	72	69	87	57	66	84	69	76	77	89	78
18	84	88	70	92	73	56	70	87	89	78	89	74
19	85	89	66	79	89	58	80	83	73	61	88	66
20	88	95	70	92	83	75	77	81	66	60	86	69
旬总数	827	834	714	820	704	674	802	765	778	645	811	822
旬平均	83	83	71	82	70	67	80	76	78	64	81	82
21	78	88	63	87	87	79	75	81	63	66	75	68
22	71	81	62	76	77	69	89	76	79	80	76	71
23	85	87	54	61	85	87	88	74	93	82	74	86
24	93	86	82	70	90	82	89	77	92	67	90	92
25	91	79	78	94	96	75	83	87	82	69	94	82
26	79	93	90	98	64	76	88	86	77	70	90	89
27	67	84	73	79	68	76	90	81	90	67	86	99
28	67	72	65	62	76	71	88	90	89	62	78	86
29	59		90	60	88	80	84	72	82	65	85	78
30	72		78	61	82	82	80	70	87	59	88	72
31	74		67		77		74	67		84		78
旬总数	836	670	802	748	890	777	928	861	834	771	836	901
旬平均	76	84	73	75	81	78	84	78	83	70	84	82
月总数	2511	2288	2332	2327	2429	2175	2503	2473	2236	2233	2491	2551
月平均	81	82	75	78	78	73	81	80	75	72	83	82
月最小	29	25	20	17	15	18	35	28	21	13	34	47
日期	28	4	28	23	8	13	18	31	4	24	15	11
附注												

固定客座人员一览表

经天山冰川观测试验站推荐，中国科学院寒区旱区环境与工程研究所批准，下列人员为天山冰川观测试验站固定客座人员。

姓　名	性别	出生日期	职称	工作单位
朱　城	男	1954	教　授	南京大学
何元庆	男	1956	研究员	中科院寒旱所
易朝路	男	1959	研究员	中科院青藏高原研究所
沈永平	男	1961	研究员	中科院寒旱所
刘耕年	男	1962	教　授	北京大学
安黎哲	男	1963	研究员	中科院寒旱所
谭敦炎	男	1963	教　授	新疆农业大学
李心清	男	1965	研究员	中科院贵阳地化所
孙　波	男	1965	教　授	国家海洋局极地研究所
效存德	男	1969	研究员	中国气象科学研究院
徐柏青	男	1969	研究员	中科院青藏高原研究所
侯书贵	男	1970	研究员	中科院寒旱所
陈　拓	男	1971	研究员	中科院寒旱所
任红旭	女	1972	教　授	新疆农业大学
周石硚	男	1963	副研究员	中科院青藏高原研究所
郭治龙	男	1970	副研究员	中科院寒旱所
邬光剑	男	1972	副研究员	中科院青藏高原研究所

天山冰川观测试验站水文气象资料整编说明（2004）

韩添丁，叶柏生

（中国科学院寒区旱区环境与工程研究所天山冰川站，甘肃 兰州 730000）

天山冰川观测试验站的常规水文、气象观测在乌鲁木齐河源区的 1 号冰川水文点、空冰斗水文点、总控制水文点以及后峡基本营地进行，本文为 2004 年度资料整编结果报告。

1 号冰川水文点设在离 1 号冰川末端 300m 的河道上，实施 1 号冰川冰雪径流的监测，断面海拔 3659m，流域面积 3.34km^2，其中冰川面积 1.708km^2。为混凝土矩形断面（高 1.0m，宽 1.6m），气象场设在断面左岸。

空冰斗水文点设在乌鲁木齐河源区左侧，斗口朝南，进行高山区积雪、多年冻土融水径流的观测，断面海拔 3805m，流域面积 1.68km^2，为混凝土矩形断面（高 1.0m，宽 1.0m），气象场设在断面右岸。

在乌鲁木齐河源区大西沟和罗布道沟汇合处，设有总控制水文点，控制监测乌鲁木齐河源区降水和 7 条冰川以及冰川周围高山积雪、多年冻土的总融水径流；该控制端面海拔 3408m，流域面积 28.9km^2;其中冰川面积 5.6km^2。为混凝土断面，设有工作桥，气象场设在断面左岸冰碛丘上。

三个水文断面均装有自计水位计，测流主要用流速仪法，即时流量由水位－流量关系线求得。气象观测项目主要为气温、降水、湿度、蒸发、地温、日照等。后峡基本营地气象观测场位于乌鲁木齐河谷，海拔 2130m，进行常规气象要素观测。所有观测资料均按规范进行整理（附表）。

表 1 乌鲁木齐河源 1 号冰川水文点逐日平均流量表（流量：m^3/s）

日 \ 月	1	2	3	4	5	6	7	8	9	10	11	12
1					0.000	0.000	0.375	0.270				
2					0.000	0.000	0.535	0.355				
3					0.000	0.025	0.445	0.445				
4					0.000	0.065	0.535	0.650				
5					0.000	0.065	0.605	0.465				
6					0.000	0.135	0.335	0.355				
7					0.000	0.310	0.375	0.225				
8					0.000	0.225	0.445	0.025				
9					0.000	0.135	0.420	0.025				
10					0.000	0.180	0.375	0.135				
旬总数					0.000	1.140	4.445	2.950				
旬平均					0.000	0.114	0.444	0.295				
11					0.000	0.155	0.420	0.135				
12					0.000	0.200	0.555	0.180				
13					0.000	0.225	0.490	0.155				
14					0.000	0.465	0.535	0.225				
15					0.000	0.335	0.760	0.270				
16					0.000	0.335	0.760	0.200				
17					0.000	0.420	0.760	0.200				
18					0.000	0.780	0.465	0.245				
19					0.000	0.780	0.400	0.200				
20					0.045	0.535	0.355	0.225				
旬总数					0.045	4.230	5.500	2.035				
旬平均					0.004	0.454	0.550	0.204				
21					0.045	0.535	0.200	0.200				
22					0.025	0.650	0.225	0.180				
23					0.000	0.555	0.375	0.180				
24					0.000	0.335	0.355	0.115				
25					0.000	0.245	0.420	0.115				
26					0.000	0.245	0.245	0.115				
27					0.000	0.180	0.245	0.115				
28					0.000	0.135	0.245	0.115				
29					0.000	0.180	0.310	0.115				
30					0.000	0.420	0.310	0.115				
31					0.000		0.200	0.115				
旬总数					0.070	3.480	3.130	1.480				
旬平均					0.006	0.348	0.285	0.135				
月总数					0.115	8.850	13.075	6.465				
月平均					0.004	0.295	0.422	0.209				
月最大					0.180	1.320	1.900	1.260				
日期					21	18	16	4				
月最小					0.000	0.000	0.090	0.000				
日期					1	1	13	9				
年统计	年总数	28.505	最大流量	1.900	7.16	最小流量	0	5.1	平均流量	0.232		
	径流量	246825	m^3	径流模数	69.54	$L/s.km^2$	径流深度	739	mm			

表 2 乌鲁木齐河源 1 号冰川水文点逐日平均气温表（气温：℃）

日\月	1	2	3	4	5	6	7	8	9	10	11	12
1	-15.6	-25.7	-17.1	-3.6	-11.9	-1	5.6	4.6	-0.5	-2.0	-7.3	-12.8
2	-16.5	-25.4	-13.4	-3.9	-8.0	-0.2	5.1	7.0	1.8	0.8	-7.8	-15.3
3	-17.8	-20.2	-10.5	-2.7	-4.3	-0.3	5.2	9.0	0.2	-0.8	-7.5	-11.0
4	-17.6	-18.7	-12.1	-2.8	-1.8	2.8	6.3	4.8	-0.9	-3.4	-6.7	-13.8
5	-16.8	-19.0	-10.2	-3.8	-2.4	3.8	7.5	5.1	2.2	-2.0	-3.6	-18.3
6	-16.0	-18.2	-11.0	0.1	-1.1	4.4	1.3	6.6	3.3	-0.6	-7.0	-13.1
7	-15.9	-16.6	-6.1	1.7	5.1	4.0	1.8	5.5	3.3	-0.5	-8.6	-11.5
8	-14.7	-11.1	0.8	-1.4	-0.3	3.4	5.5	1.4	2.4	-6.4	-12.2	-15.2
9	-15.2	-11.9	-8.4	-7.8	-2.9	2.0	5	2.6	-1.3	-5.4	-14.1	-12.9
10	-16.3	-12.1	-17.3	-11.1	-3.7	2.2	2.9	0.2	-0.9	-4.1	-12.5	-13.6
旬总数	-162.4	-178.9	-105.3	-35.3	-31.3	21.1	46.2	46.8	9.6	-24.4	-87.3	-137.5
旬平均	-16.2	-17.9	-10.5	-3.5	-3.1	2.1	4.6	4.7	1.0	-2.4	-8.7	-13.8
11	-11.7	-12.0	-14.4	-11.8	-6.5	0.7	6.1	2.0	-3.3	-2.3	-10.3	-9.5
12	-10.1	-8.3	-12.8	-12.6	-7.3	2.6	9.2	2.5	2.7	-1.3	-12.3	-8.5
13	-15.4	-5.2	-8.0	-7.2	-6.6	5.4	9.3	2.9	6.4	-1.9	-14.0	-8.7
14	-21.6	-11.9	-6.6	-6.2	-3.6	6.4	9.6	5.4	3.5	-3.0	-12.3	-8.0
15	-18.4	-13.4	-7.9	-2.8	-2.7	3.9	9.8	6.9	-2.0	-4.0	-9.8	-9.2
16	-13.5	-8.8	-8.3	-1.0	-1.2	4.2	9	4.0	-1.1	-7.3	-8.9	-12.1
17	-16.0	-6.6	-3.5	0.3	2.2	5.2	9.3	4.4	-1.8	-7.7	-7.8	-9.6
18	-15.3	-12.1	-8.0	-0.3	4.4	6.6	7.9	3.5	-3.9	-9.5	-8.8	-6.1
19	-18.4	-17.9	-8.7	2.0	5.0	6.3	5.0	3.7	-3.4	-13.3	-11.8	-10.0
20	-17.8	-16.5	-12.2	-0.7	4.3	4.8	2.4	3.2	-2.3	-11.9	-11	-18.1
旬总数	-158.2	-112.7	-90.4	-40.3	-12.0	46.1	77.6	38.5	-5.2	-62.2	-107.0	-99.8
旬平均	-15.8	-11.3	-9.0	-4.0	-1.2	4.6	7.8	3.8	-0.5	-6.2	-10.7	-10.0
21	-16.1	-15.4	-12.4	0.5	1.9	4.1	-1.7	0.2	0.5	-8.5	-9.5	-20.7
22	-13.9	-16.2	-11.2	1.3	-3.7	4.5	2.6	1.6	-3.9	-6.7	-11.1	-16.5
23	-10.9	-17.9	-12.9	-0.6	-3.0	5.2	5.8	1.2	-5.2	-5.6	-9.6	-17.4
24	-11.5	-14.3	-10.6	-3.7	-0.8	0.5	5.9	1.2	-4.7	-5.7	-10.5	-20.0
25	-11.5	-11.6	-11.0	2.0	-0.4	0.9	4.4	-0.3	-2.4	-4.9	-11.4	-21.6
26	-14.0	-8.8	-15.1	5.2	-1.5	1.4	2.1	0.4	-2.6	-4.7	-10.9	-23.8
27	-15.0	-12.8	-13.6	-0.6	-1.4	0.2	3.2	2.4	-1.6	-4.4	-9.1	-19.6
28	-15.9	-14.3	-12.9	-6.9	-2.1	-0.6	5.8	3.0	-5.6	-10.4	-6.7	-23.3
29	-19.5	-16.8	-8.8	-6.6	0.2	3.0	6.8	2.4	-7.8	-12.6	-4.7	-19.2
30	-24.1		-10.1	-10.8	2.3	5.9	4.2	3.5	-5.2	-11.5	-10.3	-14.7
31	-23.3		-5.2		1.0		1.3	3.1		-8.5		-12.8
旬总数	-175.7	-128.1	-123.8	-20.2	-7.5	25.1	40.4	18.7	-38.5	-83.5	-93.8	-209.6
旬平均	-16.0	-14.2	-11.3	-2.0	-0.7	2.5	3.7	1.7	-3.8	-7.6	-9.4	-19.1
月总数	-496.3	-419.7	-319.5	-95.8	-50.8	92.3	164.2	104.0	-34.1	-170.1	-288.1	-446.9
月平均	-16.0	-14.5	-10.3	-3.2	-1.6	3.1	5.3	3.4	-1.1	-5.5	-9.6	-14.4
最高	-6.0	-1.0	4.8	11.0	11.7	12.3	15.1	13.0	11.5	7.0	-1.5	-3.0
日期	12	17	8	26	7	19	15	15	13	2	29	18
最低	-26.0	-31.2	-20.0	-14.0	-15.8	-4.2	-3.2	-3.9	-9.5	-17.0	-17.5	-26.2
日期	30	1	1	10	1	1	21	25	29	30	9	26
年统计	最高	15.1	日期	7月15日	最低	-31.2	日期	2月1日	年平均	-5.4		

表 3 乌鲁木齐河源 1 号冰川水文点逐日降水量表（降水量：mm）

日\月	1	2	3	4	5	6	7	8	9	10	11	12
1					1.0	0.9		0				
2							0.0		10.3			
3							6.0					
4							0.4	8.2				
5								1.5		3.4		
6					1.8							
7							0.4	0				
8					0.1		0	7.3				
9					0.6						0.3	
10				3.7				7.2				
11					10.1	6.2	5.2	5.0				
12					3.5			2.5				
13					0.5	1.9		11.3				
14							0		7.2			
15					2.6							
16						9.3	0	0.8				
17					0.4		0.0	14.7				
18												
19							6.8	6.5				
20			0.3			1.0	14.7	9.2				
21		2.0			2.1	2.2	16.3	35.8	8.6			7.0
22					11.8		6.3					
23					2.2							
24				2.6	1.0	24.0	6.3	1.4				
25					0.0	0.3	3.3					
26					2.7		3.8					
27			1.2			5.9	4.1					
28		0.6										
29					3.6	0.2	0.5					
30						0.4	0.2	1.1				
31							27.2					
总量	0.0	2.6	1.5	6.3	44.0	52.3	101.5	112.5	26.1	3.4	0.3	7.0
降水日数		2	2	2	16	11	20	16	3	1	1	1
最大降水量		2	1.2	3.7	11.8	24	27.2	35.8	10.3	3.4	0.3	7
日期		21	27	10	22	24	31	21	2	5	9	21
年统计	降水量	357.5	降水日数	75								

表 4 乌鲁木齐河源 1 号冰川水文点逐日平均相对湿度表（相对湿度：%）

日\月	1	2	3	4	5	6	7	8	9	10	11	12
1					61	83	50	36				
2					43	62	64	58				
3					36	35	76	46				
4					30	24	58	76				
5					53	32	59	68				
6					51	46	87	66				
7					37	54	77	59				
8					77	38	48	80				
9					48	59	71	45				
10					59	62	83	84				
旬总数					495	495	673	618				
旬平均					50	50	67	62				
11					92	68	50	68				
12					83	44	40	70				
13					62	49	38	64				
14					37	40	44	47				
15					58	66	37	44				
16					61	81	47	82				
17					36	33	59	67				
18					32	46	71	77				
19					40	52	97	77				
20					56	71	92	83				
旬总数					557	550	575	679				
旬平均					56	55	58	68				
21					79	71	96	76				
22					84	55	66	54				
23					84	56	49	70				
24					82	88	66	41				
25					89	64	83	72				
26					78	79	90	71				
27					61	94	63	50				
28					91	88	59	56				
29					75	59	57	65				
30					43	51	76	51				
31					65		78					
旬总数					831	705	783	606				
旬平均					76	70	71	61				
月总数					1883	1750	2031	1903				
月平均					61	58	66	63				
最小					15	6	17	16				
日期					14	11	7	27				
附注	相对湿度只在 5-8 月冰川消融期观测											

表 5 乌鲁木齐河源空冰斗水文点逐日平均流量表（流量：m^3/s）

日＼月	1	2	3	4	5	6	7	8	9	10	11	12
1					0.000	0.120	0.064	0.300				
2					0.000	0.080	0.057	0.315				
3					0.000	0.050	0.080	0.205				
4					0.000	0.064	0.071	0.230				
5					0.000	0.080	0.064	0.160				
6					0.000	0.071	0.120	0.080				
7					0.000	0.071	0.071	0.071				
8					0.000	0.120	0.057	0.080				
9					0.000	0.057	0.050	0.071				
10					0.000	0.018	0.050	0.064				
旬总数					0.000	0.731	0.684	1.576				
旬平均					0.000	0.073	0.068	0.158				
11					0.000	0.120	0.064	0.230				
12					0.000	0.205	0.071	0.230				
13					0.000	0.080	0.064	0.220				
14					0.000	0.120	0.050	0.245				
15					0.000	0.120	0.042	0.205				
16					0.000	0.315	0.042	0.245				
17					0.000	0.270	0.042	0.300				
18					0.000	0.120	0.042	0.245				
19					0.057	0.071	0.071	0.280				
20					0.057	0.064	0.270	0.300				
旬总数					0.114	1.485	0.758	2.500				
旬平均					0.011	0.148	0.076	0.250				
21					0.050	0.064	0.160	0.245				
22					0.018	0.064	0.280	0.300				
23					0.000	0.080	0.230	0.270				
24					0.034	0.050	0.160	0.230				
25					0.080	0.057	0.160	0.245				
26					0.026	0.050	0.160	0.220				
27					0.064	0.050	0.230	0.205				
28					0.071	0.064	0.160	0.160				
29					0.120	0.034	0.080	0.080				
30					0.120	0.064	0.064	0.057				
31					0.160		0.071	0.042				
旬总数					0.743	0.577	1.755	2.054				
旬平均					0.068	0.058	0.160	0.187				
月总数					0.857	2.793	3.197	6.130				
月平均					0.028	0.093	0.103	0.198				
月最大					0.28	0.52	0.6	0.5				
日期					30	16	22	1				
月最小					0.000	0.000	0.018	0.042				
日期					1-18	3	31	10				
年统计	年总数	12.977	最大流量	0.600	7.22	最小流量	0	5.1	平均流量	0.105		
	径流量	1120149	m^3	径流模数	62.74	$L/s.km^2$	径流深度	667	mm			

表 6 乌鲁木齐河源空冰斗水文点逐日平均气温表（气温：℃）

日\月	1	2	3	4	5	6	7	8	9	10	11	12
1	-15.1	-25.9	-17.8	-3.6	-12.0	-1.3	5.1	4.5	-0.2	-2.8	-7.2	-12.8
2	-15.8	-25.3	-14.3	-3.4	-7.6	-1.3	4.3	6.4	1.4	-0.4	-8.4	-15.4
3	-17.4	-20.3	-11.1	-2.3	-4.3	-0.7	5.1	8.2	0.1	-1.7	-9.1	-11.4
4	-17.4	-18.5	-12.2	-3.0	-2.0	2.3	5.8	4.5	-1.1	-3.8	-8.3	-13.6
5	-17.6	-18.4	-10.8	-4.4	-2.6	4.0	6.5	4.3	1.6	-2.7	-5.4	-18.1
6	-16.4	-17.6	-11.3	0.6	-1.3	4.5	0.1	6.0	2.9	-1.3	-8.3	-11.8
7	-17.6	-16.2	-6.7	1.7	4.7	4.2	1.1	4.5	3.1	-1.2	-9.8	-10.2
8	-15.8	-12.2	-0.4	0.9	-1.5	3.8	4.1	0.6	1.9	-7.0	-13.8	-15.2
9	-16.5	-12.3	-9.2	-7.6	-2.9	3.3	3.8	1.5	-1.0	-6.2	-14.9	-13.2
10	-17.7	-12.6	-17.9	-10.8	-3.7	2.7	2.3	-0.1	-1.1	-4.7	-13.7	-13.9
旬总数	-167.3	-179.3	-111.7	-31.9	-33.2	21.5	38.2	40.4	7.6	-31.8	-98.9	-135.6
旬平均	-16.7	-17.9	-11.2	-3.2	-3.3	2.2	3.8	4.0	0.8	-3.2	-9.9	-13.6
11	-14.0	-13.4	-14.6	-11.7	-5.7	-1.1	5.1	1.5	-3.2	-3.5	-11.6	-10.0
12	-9.7	-9.0	-12.8	-12.1	-6.7	1.7	8.4	1.8	2.6	-2.5	-13.6	-7.5
13	-16.2	-6.4	-8.4	-7.0	-7.1	2.4	8.2	1.8	6.9	-2.5	-15.2	-9.0
14	-22.5	-12.8	-7.4	-5.9	-5.0	5.4	8.4	4.4	2.9	-4.2	-13.6	-7.4
15	-17.4	-15.3	-8.8	-3.4	-3.0	3	8.3	6.2	-1.8	-4.4	-10.2	-9.4
16	-13.0	-10.3	-9.1	-1.2	-1.2	3.3	7.9	3.1	-1.7	-7.7	-8.6	-12.1
17	-14.8	-8.3	-5.3	0.6	1.9	4.7	8.3	3.5	-2.5	-8.2	-8.5	-9.9
18	-14.4	-14.1	-8.6	-0.6	4.3	6.3	6.5	3.0	-3.9	-9.8	-9.2	-6.4
19	-17.4	-18.0	-9.3	1.5	4.5	6.3	3.6	3.1	-3.6	-10.4	-11.8	-10.3
20	-16.5	-16.6	-12.7	0	3.4	4	0.6	2.8	-2.3	-12.0	-10.2	-17.7
旬总数	-155.9	-124.2	-97.0	-39.8	-14.6	36.0	65.3	31.2	-6.6	-65.2	-112.5	-99.7
旬平均	-15.6	-12.4	-9.7	-4.0	-1.5	3.6	6.5	3.1	-0.7	-6.5	-11.2	-10.0
21	-14.0	-16.3	-12.9	0.3	1.6	3.5	-3.0	-0.1	0.3	-8.4	-9.7	-20.6
22	-12.3	-16.6	-11.5	1.5	-4.1	3.7	1.9	1.5	-3.8	-7.6	-10.6	-16.8
23	-10.4	-18.6	-13.1	-0.3	-4.3	4.6	5.0	1.0	-4.6	-6.0	-9.0	-17.9
24	-8.3	-15.2	-11.5	-2.9	-1.5	0.5	4.7	1.3	-4.8	-5.5	-10.4	-20.6
25	-10.0	-12.6	-11.5	1.6	-1.1	1.1	2.8	0.0	-2.6	-4.9	-11.2	-22.1
26	-13.0	-9.1	-14.8	4.8	-2.3	1.7	1.0	1.8	-2.7	-4.8	-10.9	-23.6
27	-14.2	-12.9	-13.2	-0.5	-1.8	-0.3	2.6	3.4	-1.6	-4.8	-9.2	-19.8
28	-15.8	-14.3	-12.9	-6.5	-4.1	-1.3	5.0	2.7	-5.8	-11.0	-6.8	-22.5
29	-19.9	-17.1	-9.1	-5.7	-2.4	2.8	5.2	1.4	-8.6	-13.1	-5.2	-18.0
30	-23.2		-10.2	-10.0	1.8	5.2	3.6	2.1	-6.0	-11.6	-9.9	-12.4
31	-22.4		-5.6		1.1		1.2	1.7		-8.2		-12.3
旬总数	-163.5	-132.7	-126.3	-17.7	-17.1	21.5	30.0	16.8	-40.2	-85.9	-92.9	-206.6
旬平均	-14.9	-14.7	-11.5	-1.8	-1.6	2.2	2.7	1.5	-4.0	-7.8	-9.3	-18.8
月总数	-486.7	-436.2	-335.0	-89.4	-64.9	79.0	133.5	88.4	-39.2	-182.9	-304.3	-441.9
月平均	-15.7	-15.0	-10.8	-3.0	-2.1	2.6	4.3	2.9	-1.3	-5.9	-10.1	-14.3
最高	-3.5	-3.0	2.9	9.5	12.0	12.0	14.2	12.5	10.8	6.0	-1.5	-3.0
日期	24	17	8	26	7	19	12	15	13	2	29	18
最低	-25.9	-19.3	-20.0	-16.9	-15.6	-4.5	-5.2	-3.8	-10.2	-17.5	-18.2	-26.0
日期	30	1	1	12	1	1	21	25	29	30	9	26
年统计	最高	14.2	日期	7月12日	最低	-25.9	日期	1月30日	年平均	-5.7		

表 7 乌鲁木齐河源空冰斗水文点逐日降水量表（降水量：mm）

日\月	1	2	3	4	5	6	7	8	9	10	11	12
1								0.0				
2									9.5			
3							8.0					
4							0.3	8.8				
5					1.5			1.0		3.4		
6							6.6					
7							0.3	0.0				
8								6.7				
9					0.8						0.3	
10				3.6		0.5		7.2				
11					9.4	6.4		4.4				
12					3.0			1.4				
13						1.7		12.7				
14					2.3				8.2			
15												
16						9.6		0.9				
17					0.3			14.5				
18												
19							5.7	6.4				
20			0.4			1.0	15.6	7.8				
21		2.2			1.6	2.1	15.8	31.2	9.7			7.0
22					10.1		6.0					
23					1.7							
24				2.4	1.1	22.8	6.1	1.6				
25					0.2	0.2	2.3					
26					2.7		4.5					
27			1.3			5.5	4.1					
28		0.6										
29					3.2	0.5	1.3					
30				6.0			0.2	1.0				
31							26.9					
总量	0	2.8	1.7	12.0	37.9	50.3	103.7	105.6	27.4	3.4	0.3	7.0
降水日数		2	2	3	13	10	15	16	3	1	1	1
最大降水量		2.2	1.3	6	10.1	22.8	26.9	31.2	9.7	3.4	0.3	7
日期		21	27	30	22	24	31	21	21	5	9	21
年统计	降水量	352.1	降水日数	67								

表 8 乌鲁木齐河源空冰斗水文点逐日平均相对湿度表（相对湿度：%）

日\月	1	2	3	4	5	6	7	8	9	10	11	12
1					68	88	74	44				
2					55	65	86	71				
3					46	36	88	57				
4					45	32	68	92				
5					70	47	72	72				
6					71	68	94	63				
7					52	77	78	71				
8					81	60	64	78				
9					59	74	90	54				
10					73	83	88	93				
旬总数					620	630	802	695				
旬平均					62	63	80	70				
11					100	81	58	80				
12					96	49	46	87				
13					88	34	48	75				
14					58	47	52	56				
15					71	84	53	46				
16					78	71	66	82				
17					50	38	69	75				
18					38	48	82	81				
19					52	66	94	81				
20					81	84	98	91				
旬总数					712	602	666	754				
旬平均					71	60	67	75				
21					93	86	100	88				
22					95	78	77	65				
23					89	78	57	83				
24					88	100	84	47				
25					91	71	83	73				
26					48	87	89	79				
27					79	100	65	49				
28					90	100	59	75				
29					93	73	71	74				
30					62	76	87	60				
31					80		89					
旬总数					908	849	861	693				
旬平均					83	85	78	69				
月总数					2240	2081	2329	2142				
月平均					72	69	75	71				
最小					27	22	33	19				
日期					3	12	12	15				
附注	相对湿度只在 5-8 月冰川消融期观测											

表 9 乌鲁木齐河源总控水文点逐日平均流量表（流量：m^3/s）

日＼月	1	2	3	4	5	6	7	8	9	10	11	12
1					0.000	1.280	1.030	1.570				
2					0.000	1.200	1.150	1.350				
3					0.640	1.150	1.150	1.090				
4					0.640	1.200	1.280	1.570				
5					0.580	1.350	1.690	1.150				
6					0.640	1.350	1.570	1.150				
7					0.640	1.690	1.940	1.090				
8					0.820	1.460	1.570	0.880				
9					0.820	1.350	1.350	0.780				
10					0.700	1.460	1.460	0.880				
旬总数					5.480	13.490	14.190	11.510				
旬平均					0.548	1.349	1.419	1.151				
11					0.700	1.940	1.350	0.930				
12					0.700	1.940	1.350	1.030				
13					0.700	1.810	1.570	1.200				
14					0.740	1.460	1.690	1.150				
15					0.740	1.280	1.460	1.030				
16					0.740	1.150	1.280	1.090				
17					0.820	1.200	1.460	1.200				
18					0.980	1.200	1.690	1.150				
19					0.980	1.280	0.980	1.150				
20					1.090	1.280	1.200	1.460				
旬总数					8.190	14.540	14.030	11.390				
旬平均					0.819	1.454	1.403	1.139				
21					1.200	1.280	1.090	1.810				
22					1.150	1.280	1.090	1.350				
23					0.930	1.460	1.150	1.280				
24					0.930	1.460	1.150	0.880				
25					1.150	2.200	1.090	0.880				
26					1.030	1.810	1.030	0.780				
27					1.090	1.810	1.030	0.640				
28					1.090	1.810	1.090	0.580				
29					1.200	1.810	1.090	0.580				
30					1.030	1.030	1.150	0.580				
31					1.280		1.810	0.530				
旬总数					12.080	15.950	12.770	9.890				
旬平均					1.098	1.595	1.161	0.899				
月总数					25.750	43.980	40.990	32.790				
月平均					0.831	1.466	1.322	1.058				
月最大					1.570	2.760	4.400	3.020				
日期					20	25	20	21				
月最小					0.000	0.360	0.700	0.500				
日期					1	3	16	31				
年统计	年总数	143.51	最大流量	4.400	7.20	最小流量	0	5.1	平均流量	1.169		
	径流量	12424908	m^3	径流模数	40.46	$L/s.km^2$	径流深度	430	mm			

表 10 乌鲁木齐河源总控水文点逐日平均气温表（气温：℃）

日\月	1	2	3	4	5	6	7	8	9	10	11	12
1	-18.3	-28.0	-17.2	-1.7	-1.0	0.0	7.1	7.2	2.3	-0.3	-5.7	-10.9
2	-19.6	-27.2	-12.9	-1.6	-5.9	1.3	6.2	8.5	3.4	2.0	-5.1	-9.8
3	-20.2	-22.0	-12.9	0.2	-4.0	1.6	5.8	10.3	2.3	1.0	-6.2	-11.2
4	-20.1	-21.0	-12.4	-1.3	1.1	3.5	6.9	6.1	2.2	-1.5	-5.6	-12.7
5	-19.6	-21.0	-10.8	-1.3	-1.1	4.7	8.1	6.5	4.7	0.2	-3.2	-18.2
6	-18.0	-20.5	-10.3	2.0	0.3	5.5	2.4	8.4	5.1	1.0	-5.4	-12.0
7	-16.9	-16.7	-7.1	3.9	7.2	5.1	3.1	6.2	6.0	0.8	-6.3	-11.3
8	-15.6	-12.1	2.2	0.3	-0.7	4.7	6.8	2.2	4.8	-4.0	-11.0	-14.3
9	-16.4	-12.4	-8.0	-5.7	-1.1	4.3	5.3	3.4	1.1	-4.1	-11.9	-12.3
10	-18.0	-12.8	-16.0	-7.9	-0.7	3.3	4.5	1.7	1.5	-2.5	-12.3	-12.7
旬总数	-182.7	-193.7	-105.4	-13.1	-5.9	34.0	56.2	60.5	33.4	-7.4	-72.7	-125.4
旬平均	-18.3	-19.4	-10.5	-1.3	-0.6	3.4	5.6	6.0	3.3	-0.7	-7.3	-12.5
11	-13.6	-12.4	-12.7	-9.4	-4.1	1.5	7.2	3.2	-0.6	-0.1	-10.1	-8.3
12	-11.9	-9.1	-11.0	-8.2	-4.3	3.8	10.5	4.3	4.1	-0.6	-11.5	-6.7
13	-17.1	-7.6	-6.0	-6.0	-4.3	4.7	10.4	4.5	7.6	-0.8	-12.7	-7.0
14	-20.1	-10.7	-5.4	-3.9	-3.5	6.6	10.9	7.3	2.7	-1.5	-12.9	-6.4
15	-21.5	-14.9	-7.6	-1.3	-0.8	4.7	10.7	7.9	-0.3	-1.7	-11.1	-6.3
16	-16.2	-9.3	-7.1	0.4	1.0	5.3	10.5	5.9	1.0	-5.4	-9.4	-9.9
17	-18.9	-8.5	-3.0	1.1	3.9	6.8	10.8	6.0	-0.4	-6.4	-6.9	-7.2
18	-16.1	-13.5	-8.7	1.9	5.9	6.8	10.5	5.6	-1.2	-7.2	-7.1	-3.6
19	-18.7	-17.9	-7.0	3.1	5.8	7.4	9.4	5.5	-0.5	-10.0	-10.4	-9.3
20	-18.4	-16.4	-11.2	-0.6	4.7	5.8	5.8	5.1	0.3	-10.4	-9.6	-16.2
旬总数	-172.5	-120.3	-79.7	-22.9	4.3	53.4	96.7	55.3	12.7	-44.1	-101.7	-80.9
旬平均	-17.2	-12.0	-8.0	-2.3	0.4	5.3	9.7	5.5	1.3	-4.4	-10.2	-8.1
21	-20.0	-15.2	-10.9	2.6	3.8	6.2	-1.4	2.1	2.6	-6.7	-10.8	-19.2
22	-15.3	-16.4	-9.0	2.9	-1.8	6.4	3.8	4.1	-1.1	-4.6	-9.2	-14.1
23	-12.7	-18.0	-10.1	0.9	-1.0	6.3	7.7	3.8	-1.8	-4.9	-9.8	-14.4
24	-14.3	-14.6	-7.2	-2.1	1.0	2.5	8.1	2.6	-1.4	-4.0	-9.4	-16.2
25	-14.6	-12.7	-8.6	3.5	0.3	3.4	5.4	2.3	1.0	-3.0	-9.1	-20.7
26	-15.0	-9.6	-11	5.4	-0.7	3.6	3.2	2.3	0.2	-3.7	-9.1	-20.1
27	-14.9	-12.9	-9.4	-1.0	0.1	1.6	4.3	4.3	1.4	-4.3	-7.6	-16.1
28	-15.4	-14.8	-9.8	-6.5	-1.1	2.1	7.3	4.4	-2.2	-8.0	-5.4	-23.0
29	-20.2	-16.7	-6.3	-5.0	1.3	4.8	8.7	4.7	-7.2	-9.6	-2.7	-21.9
30	-24.7		-7.4	-8.8	4.5	6.4	6.3	5.3	-3.9	-9.3	-8.0	-16.2
31	-22.7		-2.2		3		3.2	4.8		-5.9		-13.9
旬总数	-189.8	-130.9	-91.9	-8.1	9.4	43.3	56.6	40.7	-12.4	-64.0	-81.1	-195.8
旬平均	-17.3	-14.5	-8.4	-0.8	0.9	4.3	5.1	3.7	-1.2	-5.8	-8.1	-17.8
月总数	-545.0	-444.9	-277.0	-44.1	7.8	130.7	209.5	156.5	33.7	-115.5	-255.5	-402.1
月平均	-17.6	-15.3	-8.9	-1.5	0.3	4.4	6.8	5.0	1.1	-3.7	-8.5	-13.0
最高	-6.3	-1.2	5.0	12.5	14.5	15.6	18.0	16.2	13.2	10.0	1.0	0.0
日期	12	17	8	26	7	19	15	15	13	2	5	18
最低	-29.0	-31.0	-22.5	-16.5	-15.5	-3.0	-3.1	-4.1	-11.8	-15.4	-18.5	-26.5
日期	30	1	1	12	1	3	21	24	29	19	9	29
年统计	最高	18	日期	7月15日	最低	-31	日期	2月1日	年平均	-4.3		

表 11 乌鲁木齐河源总控水文点逐日降水量表（降水量：mm）

日\月	1	2	3	4	5	6	7	8	9	10	11	12
1			0.3			1.5	1.1		9.8			
2							4.4					
3							6.4					
4							1.1	7.0		3.0		
5							0.3	1.7				
6					1.6		6.1					
7							0	5.4				
8					0.5	0.5	0.5	1.5		0.2		
9				1.8							0.3	
10		0.3				1.2	2.1	7.2				
11				1.5	10.5	6.9	2.4	2.0	8.0			
12	0.6			0.7	2.6	0.2	0	4.2				
13					1.4	1.7		10.3				
14												
15		0.3			2.7	1.4		0.6	2.1			
16						3.7		15.5		0.2		
17		0.1			0.5							
18		0.3	0.5				0.7	6.6	3.2			
19						0.3	11.1	13.9	8.1			
20		0.1				0.4	18.9	28.9				
21			0.7		0.3	1.0	11.2					7.0
22					11.0	0.1	0.5					
23			1.2		3.2	0.1						
24				1.8	0.3	25.4	4.9					
25					0.8		4					
26			1.4		2.2	3.1	5					
27		1.5		3.7	6.1	3.5	3.2					
28					0.5							
29		0.3		1.8	1.5		0					
30				0.8			5.6	1.0				
31							25.4					
总量	0.6	2.9	4.1	12.1	45.7	51.0	114.9	105.8	31.2	3.4	0.3	7
降水日数	1	7	5	7	16	16	23	14	5	3	1	1
最大降水量	0.6	1.5	1.4	3.7	11	25.4	25.4	28.9	9.8	3	0.3	7
日期	12	27	26	27	22	24	31	20	1	4	9	21
年统计	降水量	379	降水日数	99								

表 12 乌鲁木齐河源总控水文点逐日平均相对湿度表（相对湿度：%）

日\月	1	2	3	4	5	6	7	8	9	10	11	12
1					64	85	58	49				
2					54	56	65	65				
3					38	33	71	56				
4					36	35	67	93				
5					65	46	69	70				
6					63	60	91	62				
7					49	64	84	70				
8					91	73	56	88				
9					59	77	86	55				
10					58	88	87	93				
旬总数					577	617	734	701				
旬平均					58	62	73	70				
11					96	86	62	90				
12					86	58	47	92				
13					84	62	46	77				
14					57	54	43	58				
15					64	74	44	55				
16					62	73	56	76				
17					51	38	55	70				
18					36	65	78	84				
19					47	61	97	83				
20					75	80	100	94				
旬总数					658	651	628	779				
旬平均					66	65	63	78				
21					79	70	98	87				
22					80	62	68	65				
23					70	73	50	62				
24					76	95	77	56				
25					90	81	84	69				
26					82	87	94	73				
27					68	96	65	63				
28					86	82	65	66				
29					75	68	59	68				
30					49	65	82	66				
31					61		81					
旬总数					816	779	823	675				
旬平均					74	78	75	68				
月总数					2051	2047	2185	2155				
月平均					66	68	70	72				
最小					14	11	26	20				
日期					3	11	11	1				
附注	相对湿度只在 5-8 月冰川消融期观测											

表 13 乌鲁木齐河源后峡基本营地气象场逐日平均气温表（气温：℃）

日\月	1	2	3	4	5	6	7	8	9	10	11	12
1	-14.6	-20.2	-7.3	3.9	1.3	8.1	13.8	13.6	9.8	3.1	0.1	-3.4
2	-13.7	-19.7	-6.3	5.6	2.3	8.9	13.3	15.8	9.5	5.6	-3.2	-10.2
3	-14.0	-17.8	-5.3	6.7	5.0	8.6	14.7	14.0	8.0	6.7	-4.2	-10.1
4	-14.3	-15.7	-2.9	5.2	7.1	9.5	17.0	13.9	7.7	9.0	-1.4	-8.8
5	-15.6	-14.5	-2.7	5.5	6.0	11.4	14.9	14.2	9.7	6.1	1.2	-13.6
6	-14.2	-14.2	-2.9	6.4	10.1	13.8	11.6	15.5	12.3	7.5	-2.2	-11.5
7	-14.0	-13.0	0.5	6.4	11.2	12.0	11.1	11.1	12.8	4.8	-1.6	-8.7
8	-12.8	-8.4	5.5	3.8	6.7	11.9	13.6	9.5	7.9	1.0	-6.9	-9.5
9	-12.4	-7.7	-6.3	1.9	5.8	11.3	11.5	9.6	8.6	-0.2	-9.2	-12.0
10	-12.8	-6.2	-8.5	0.7	3.0	10.2	13.4	9.1	5.2	2.7	-5.6	-8.3
旬总数	-138.4	-137.4	-36.2	46.1	58.5	105.7	134.9	126.3	91.5	46.3	-33.0	-96.1
旬平均	-13.8	-13.7	-3.6	4.6	5.8	10.6	13.5	12.6	9.2	4.6	-3.3	-9.6
11	-11.4	-5.8	-8.4	-0.9	2.0	9.7	16.5	10.7	8.1	3.4	-4.4	-11.0
12	-7.7	-5.3	-4.8	-0.8	3.4	9.8	17.9	10.6	9.9	3.9	-5.4	-8.3
13	-9.5	-4.1	-0.4	2.3	4.9	12.5	18.9	12.2	12.4	4.2	-5.9	-7.4
14	-12.2	-4.2	-1.2	4.4	4.4	14.5	19.9	13.5	8.2	5.3	-6.9	-6.2
15	-18.7	-9.5	-2.1	6.5	8.4	11.5	16.9	15.1	7.9	5.6	-5.9	-6.6
16	-15.6	-1.1	-0.8	8.7	10.1	11.6	19.3	12.5	6.1	0.3	-5.7	-8.1
17	-14.2	-2.5	1.0	9.0	11.6	12.2	18.0	13.0	7.5	-1.4	-3.6	-8.1
18	-11.0	-5.6	-1.0	9.0	14.5	14.2	16.1	14.1	7.0	-1.7	-3.8	-5.2
19	-10.0	-10	-3.4	9.6	13.2	15.8	13.2	13.2	6.6	-2.6	-6.4	-4.8
20	-15.1	-9.3	-4.4	4.9	14.7	16.0	9.8	11.7	7.6	-4.2	-5.2	-9.9
旬总数	-125.4	-57.4	-25.5	52.7	87.2	127.8	166.5	126.6	81.3	12.8	-53.2	-75.6
旬平均	-12.5	-5.7	-2.6	5.3	8.7	12.8	16.6	12.7	8.1	1.3	-5.3	-7.6
21	-14.4	-9.1	-4.9	6.1	11.3	15.8	8.8	11.1	8.4	-2.3	-6.4	-16.2
22	-14.1	-9.9	-4.1	8.8	6.1	15.0	11.6	11.0	6.6	1.0	-6.5	-17.6
23	-13.8	-8.7	-3.1	6.8	7.7	15.1	14.3	8.9	6.4	0.6	-5.8	-19.2
24	-12.3	-9.3	-1.0	6.4	8.2	10.9	14.4	8.4	6.0	1.6	-7.6	-21.4
25	-10.5	-5.5	-1.2	9.5	7.7	11.7	12.0	8.4	6.0	1.7	-8.8	-18.4
26	-8.7	-4.1	-4.7	11.2	7.3	11.8	11.3	8.8	5.7	1.3	-7.6	-19.6
27	-10.9	-5.5	-8.0	4.9	6.4	9.8	11.8	10.0	5.3	0.6	-6.8	-18.5
28	-10.1	-6.8	-5.3	-0.1	9.2	10.3	14.0	10.8	0.5	0.2	-5.8	-19.7
29	-12.0	-7.0	-0.4	1.3	10.4	12.2	15.6	12.2	1.4	-3.5	-3.5	-23.1
30	-17.7		-2.4	-0.3	14.4	12.4	13.5	12.6	0.8	-5.5	-2.2	-20.3
31	-19.0		2.6		10.0		12.6	10.7		0.5		-14.0
旬总数	-143.5	-65.9	-32.5	54.6	98.7	125.0	139.9	112.9	47.1	-3.8	-61.0	-208.0
旬平均	-13.0	-7.3	-3.0	5.5	9.0	12.5	12.7	10.3	4.7	-0.3	-6.1	-18.9
月总数	-407.3	-260.7	-94.2	153.4	244.4	358.5	441.3	365.8	219.9	55.3	-147.2	-379.7
月平均	-13.1	-9.0	-3.0	5.1	7.9	12.0	14.2	11.8	7.3	1.8	-4.9	-12.2
月最高	2.7	11.5	14.0	22.6	24.6	25.8	30.8	29.2	22.4	18.5	12.3	4.2
日期	27	12	8	26	18	19	13	2	13	6	4	14
月最低	-24.1	-26.6	-15.0	-7	-5.5	-0.3	1.9	0.8	-7.4	-12.5	-15.5	-27.7
日期	15	2	11	12	2	3	9	29	30	30	25	29
年统计	最高	30.8	日期	7月13日	最低	-27.7	日期	12月29日	年平均	1.5		

表 14 乌鲁木齐河源后峡基本营地气象场逐日降水量表（降水量：mm）

日\月	1	2	3	4	5	6	7	8	9	10	11	12
1						5.4	2.7		7.5			1.7
2						11.0	1.1					
3								0.6	1.8		0.7	
4				0.2			0.3	4.5				0.1
5					3.8		1.2					0.7
6					0.0		3.0					
7							7.4	1.8				
8					2.1	0.1		4.3		0.2	0.6	
9			0.2	0.8				0				
10			1.1		5.2	3.6		4.9	2.6			
11				2.4	7.0	5.6		0.5	5.4			
12				2.9	0.5	1.9		2.2				
13						0.6		7.2			0.5	
14	0.6				1.0			0.6	2.5			
15						0.8			4.1			0.1
16					0.6	1.7		6.3		0.9		
17												
18		3.8	2.4				5.1		3.0			
19	3.3	0.4	0.0				13.7	6.1	2.6			6.0
20			1.4				21.0	3.2				1.4
21			1.3		3.7	0.6	9.1	20.7				0.2
22					14.1				4.0			
23		0.7	2.2		2.2	1.8			0.9			
24				1.5		13.5	0.7	1.1				
25			3.0		10.7		9.1					
26			3.9			0.1	13.9					
27		1.7		5.3	0.3	7.9	2.4					
28				1	0.4				1.2	0.6		0.5
29	0.1					2				0.7		
30			0.5	0.5		6.6	10.2			0.4		
31							16.5	2.4				
总量	4.0	6.6	16.0	14.6	51.6	63.2	117.4	66.4	35.6	2.8	1.8	10.7
降水日数	3	4	10	8	14	16	16	16	11	5	3	8
最大降水量	3.3	3.8	3.9	5.3	14.1	13.5	21	20.7	7.5	0.9	0.7	6
日期	19	18	26	27	22	24	20	21	1	16	3	19
年统计	降水量	390.7	降水日数	114								

表 15 乌鲁木齐河源后峡基本营地气象场逐日平均相对湿度表（相对湿度：%）

日\月	1	2	3	4	5	6	7	8	9	10	11	12
1	80	82	76	65	62	79	72	66	87	57	64	96
2	75	83	66	59	57	66	79	66	77	62	82	94
3	81	70	65	60	49	43	66	84	86	68	98	82
4	79	74	62	82	49	52	48	81	76	64	78	86
5	75	69	66	77	65	48	65	69	74	61	74	96
6	72	72	72	59	59	48	74	69	65	58	92	82
7	73	69	66	65	64	61	79	90	61	70	73	67
8	75	71	68	80	89	72	65	90	82	85	87	88
9	77	76	84	95	71	72	71	80	70	77	79	82
10	85	80	80	88	87	82	57	87	85	66	66	77
旬总数	772	746	705	730	652	623	676	782	763	668	793	850
旬平均	77	75	70	73	65	62	68	78	76	67	79	85
11	83	74	79	92	91	76	57	81	76	71	66	80
12	81	66	72	83	84	75	57	81	67	65	80	73
13	95	63	62	71	75	60	50	76	58	72	85	87
14	92	85	70	64	75	54	49	70	78	67	88	82
15	91	78	77	59	63	67	53	66	73	63	64	90
16	82	52	79	50	51	72	64	77	70	86	57	93
17	90	81	74	55	54	66	67	73	61	70	57	80
18	88	94	87	63	37	57	82	65	88	71	62	84
19	98	83	90	60	47	49	92	72	77	83	75	96
20	98	79	92	80	56	53	90	82	71	67	75	94
旬总数	898	755	782	677	633	629	661	743	719	715	709	859
旬平均	90	76	78	68	63	63	66	74	72	72	71	86
21	86	77	84	72	83	64	78	80	67	53	80	96
22	81	83	76	65	85	54	76	68	87	52	72	96
23	83	80	87	68	75	56	69	82	78	57	76	96
24	78	72	67	79	77	84	70	73	71	58	73	94
25	82	68	80	60	84	76	85	78	70	59	63	94
26	79	75	88	56	80	71	84	72	73	54	59	92
27	83	88	85	91	81	81	72	68	69	59	60	90
28	87	81	72	84	78	73	65	65	77	84	58	89
29	96	82	66	79	63	67	70	60	61	90	50	92
30	84		90	87	42	75	84	59	55	83	73	90
31	75		65		68		80	75		69		90
旬总数	914	706	860	741	816	701	833	780	708	718	664	1019
旬平均	83	78	78	74	74	70	76	71	71	65	66	93
月总数	2584	2207	2347	2148	2101	1953	2170	2305	2190	2101	2166	2728
月平均	83	76	76	72	68	65	70	74	73	68	72	88
最小	47	33	19	17	13	24	23	23	16	16	23	44
日期	24	16	24	16	18	4	5	29	30	21	1	3
附注												

乌鲁木齐河源 1 号冰川表面运动速度和冰舌末端变化

（2002/2003 和 2003/2004 年度）

井哲帆

（中国科学院寒区旱区环境与工程研究所，甘肃 兰州 730000）

1 观测与说明

2003 年 8 月底对冰川表面的运动点按照其运动量的多少又重新插设了标杆，基本恢复到上一年度消融期末各个点的位置。对运动点的观测是使用全站仪进行观测的。

表 1 为 2002/2003 年度的运动速度，表 2 为 2003/2004 年度的运动速度，表 3 为 1 号冰川东、西支冰舌的年进退变化量，表 4、5 为 2003 和 2004 年度的各流速点的空间坐标。

坐标系统仍为独立坐标系。X 为纵坐标，Y 为横坐标，Z 为竖直向上的坐标。U_X、U_Y、U_Z是分别平行于 X、Y 和 Z 轴的速度分量，U_{XY}为速度的水平分量，a 为运动速度的方向。

2 运动速度的初步分析

在计算和整编运动速度资料的过程中，经过对比和分析得出以下结果：

（1）1 号冰川 2003 年度和 2004 年度的表面运动与前几年运动速度相比变化基本不大，均有所减小，从表 1 和表 2 中可以看出，东支冰川 2004 年度最大流速点为 E3′，其年流速为 4.68 米，2003 年度流速最大点仍为 E3′ 点，其年流速为 4.72 米。西支冰川 2004 年度最大流速点为 E2 点，其年流速为 6.12 米，2003 年度最大流速点还是 E2 点，其年流速为 6.03 米。最大流速点位与往年相同。

（2）运动速度垂直分量 U_Z 的年度变化规律同往年的变化规律完全相同。即消融区的显出流作用和积累区的显入流作用。

（3）冰川末端进退的观测方法仍同以往。表 3 反映了 2003 年度和 2004 年度的冰舌退缩量，从表中可以看出，东支冰舌保持了较稳定的退缩速率。2003 年度西支冰舌的退缩量相对 2002 年度有所减小，而到 2004 年度东、西支冰舌的退缩量度均比 2003 年度略大一些。

表 1 年运动速度（观测日期：2002.08.26—2003.08.23）

点名	U_x（m）	U_y(m)	U_{xy}(m)	U_z(m)	a(°	′)	U_{xy}(m/a)
A′	0.39	2.72	2.74	-0.08	80	23	2.76
B2′	1.21	3.12	3.35	-0.06	68	34	3.36
B3′	-0.27	4.45	4.46	-0.05	93	40	4.48
C1′	2.45	3.20	4.03	-0.17	52	52	4.05
C2′	2.54	3.31	4.17	-0.17	53	04	4.20
C3′	2.51	3.06	3.96	-0.53	51	23	3.98
D1′	3.37	1.13	3.55	-0.14	19	21	3.57
D2′	3.53	1.10	3.69	-0.04	17	25	3.71
D3′	3.28	1.25	3.51	-0.05	21	22	3.53
E1′	0.68	0.03	0.68	-0.05	3	17	0.68
E2′	4.01	0.47	4.03	-0.54	7	31	4.04
E3′	4.67	0.50	4.70	-0.73	6	11	4.72
F1′	0.82	0.25	0.86	-0.15	18	28	0.86
F2′	3.64	0.50	3.67	-0.62	7	39	3.69
F3′	4.27	0.53	4.30	-0.72	7	04	4.33
G1′	0.33	0.18	0.38	-0.04	25	16	0.38
G2′	3.02	1.02	3.19	-0.41	18	06	3.20
G3′	3.37	1.07	3.54	-0.67	18	38	3.55
H1′	0.81	1.01	1.29	-0.12	48	24	1.30
H2′	1.83	0.51	1.90	-0.49	17	12	1.91
A	-0.90	0.62	1.09	-0.29	143	32	1.10
B	-1.81	5.21	5.51	-0.90	109	31	5.54
C1	0.14	3.63	3.63	-0.69	85	02	3.65
C2	-0.12	5.50	5.50	-0.67	93	14	5.53
C3	-0.12	5.38	5.38	-0.46	93	19	5.41
D1	0.05	2.40	2.40	-0.42	90	03	2.41
D2	0.83	4.89	4.96	-0.85	79	52	4.99
D3	0.46	5.67	5.69	-0.88	85	28	5.72
E1	0.94	5.90	5.97	-0.87	80	46	6.01
E2	1.53	5.80	6.00	-1.34	75	16	6.03
E3	2.02	5.34	5.71	-0.49	69	09	5.74
F1	2.13	4.10	4.62	-0.82	62	05	4.64
F2	2.14	4.56	5.03	-0.80	64	22	5.06
F3	1.92	4.11	4.54	-0.77	64	42	4.56
G1	0.10	0.31	0.33	-0.08	71	14	0.33
G2	1.60	4.50	4.77	-0.40	69	31	4.80
G3	2.01	4.73	5.14	-0.64	67	15	5.17
H1	0.04	0.25	0.25	-0.06	79	38	0.25
H2	2.04	3.87	4.37	-0.46	61	15	4.39
H3	2.45	4.06	4.74	-0.96	58	21	4.77
L1	3.53	2.90	4.57	-2.52	39	22	4.59
L2	4.42	3.21	5.46	-2.92	36	07	5.49

表 2　年运动速度（观测日期：2003.08.23—2004.8.22）

点名	U_x（m）	U_y(m)	U_{xy}(m)	U_z(m)	a(°	′)	U_{xy}(m/a)
A′	0.40	2.74	2.77	-0.07	80	32	2.77
B2′	1.20	3.15	3.37	-0.06	68	41	3.37
B3′	-0.28	4.45	4.46	-0.04	93	44	4.46
C1′	2.44	3.22	4.04	-0.18	52	50	4.04
C2′	2.55	3.34	4.20	-0.18	53	09	4.20
C3′	2.52	3.06	3.96	-0.51	51	19	3.96
D1′	3.38	1.14	3.57	-0.12	19	28	3.57
D2′	3.50	1.12	3.67	-0.03	17	30	3.67
D3′	3.27	1.25	3.50	-0.05	21	29	3.50
E1′	0.67	0.03	0.67	-0.04	3	11	0.67
E2′	4.02	0.48	4.03	-0.55	7	23	4.03
E3′	4.65	0.50	4.68	-0.78	6	21	4.68
F1′	0.81	0.26	0.85	-0.18	18	22	0.85
F2′	3.63	0.52	3.67	-0.66	7	34	3.67
F3′	4.25	0.53	4.28	-0.70	7	12	4.28
G1′	0.30	0.19	0.36	-0.03	25	24	0.36
G2′	3.03	1.04	3.20	-0.44	18	14	3.20
G3′	3.32	1.07	3.49	-0.70	18	38	3.49
H1′	0.82	1.02	1.30	-0.15	48	35	1.30
H2′	1.78	0.52	1.85	-0.47	17	24	1.85
A	-0.91	0.56	1.07	-0.26	143	38	1.07
B	-1.82	5.20	5.51	-0.95	109	23	5.51
C1	0.15	3.64	3.64	-0.66	85	15	3.64
C2	-0.12	5.52	5.52	-0.61	93	27	5.52
C3	-0.13	5.39	5.39	-0.40	93	26	5.39
D1	0.06	2.40	2.40	-0.42	90	16	2.40
D2	0.85	4.90	4.97	-0.88	79	44	4.90
D3	0.48	5.67	5.69	-0.87	85	39	5.67
E1	0.97	5.98	6.06	-0.87	80	41	5.98
E2	1.50	5.93	6.12	-1.33	75	28	6.12
E3	2.04	5.44	5.81	-0.46	69	02	5.81
F1	2.11	4.12	4.63	-0.80	62	19	4.63
F2	2.12	4.55	5.02	-0.77	64	33	5.02
F3	1.90	4.09	4.51	-0.73	64	47	4.51
G1	0.11	0.30	0.32	-0.08	71	26	0.32
G2	1.58	4.51	4.78	-0.40	69	39	4.78
G3	2.03	4.68	5.10	-0.65	67	24	5.10
H1	0.04	0.24	0.25	-0.05	79	25	0.25
H2	2.05	3.83	4.34	-0.43	61	13	4.34
H3	2.38	4.02	4.67	-1.00	58	28	4.67
L1	3.54	2.91	4.58	-2.51	39	36	4.58
L2	4.34	3.23	5.41	-2.94	36	03	5.41

表 3 东西支冰舌进退变化量

冰舌进退值（米）		
时间	东支冰舌	西支冰舌
2002.08.26—2003.08.23	-3.10	-6.10
2003.08.23—2004.08.22	-3.23	-6.28

表 4 流速点坐标（观测日期：2003.08.23）

东支点名	X（m）	Y(m)	Z(m)	西支点名	X(m)	Y(m)	Z(m)
A′	5145.34	3767.40	3724.84	A	5292.05	3391.73	3833.61
B2′	5150.42	3625.76	3804.43	B	5388.90	3408.35	3857.64
B3′	5071.12	3678.32	3801.38	C1	5436.59	3274.36	3902.82
C1′	5119.31	3347.14	3848.95	C2	5384.64	3271.77	3910.90
C2′	5065.18	3440.42	3850.68	C3	5342.21	3252.52	3921.47
C3′	4992.04	3504.27	3844.21	D1	5489.45	3248.54	3932.34
D1′	4884.17	3228.22	3891.14	D2	5435.89	3165.93	3926.92
D2′	4838.28	3314.91	3893.44	D3	5366.03	3161.70	3934.11
D3′	4789.68	3404.39	3894.46	E1	5441.28	3020.12	3971.14
E1′	4568.11	2999.24	3924.72	E2	5371.97	3011.62	3974.53
E2′	4562.42	3097.56	3923.18	E3	5298.38	2998.74	3993.80
E3′	4532.53	3186.33	3920.88	F1	5390.83	2820.98	4011.15
F1′	4350.84	2966.47	3966.86	F2	5311.82	2832.60	4015.53
F2′	4344.53	3042.37	3964.44	F3	5234.06	2835.18	4024.72
F3′	4319.62	3109.29	3962.50	G1	5405.36	2597.76	4057.91
G1′	4153.73	2900.49	4014.45	G2	5334.19	2665.73	4052.30
G2′	4147.19	2971.04	4008.70	G3	5254.57	2698.12	4043.73
G3′	4122.32	3034.57	4002.83	H1	5344.56	2435.35	4076.82
H1′	3946.79	2791.38	4065.13	H2	5278.10	2518.52	4072.26
H2′	3905.07	2932.14	4040.76	H3	5197.33	2570.83	4066.87
				L1	5148.79	2499.87	4080.21
				L2	5075.58	2430.15	4129.04

表 5 流速点坐标（观测日期：2004.08.22）

东支点名	X（m）	Y(m)	Z(m)	西支点名	X(m)	Y(m)	Z(m)
A′	5145.74	3770.14	3724.77	A	5291.14	3392.29	3833.35
B2′	5151.62	3628.91	3804.37	B	5387.08	3413.55	3856.69
B3′	5070.84	3682.77	3801.34	C1	5436.74	3278.00	3902.16
C1′	5121.75	3350.36	3848.77	C2	5384.52	3277.29	3910.29
C2′	5067.73	3443.76	3850.50	C3	5342.08	3257.91	3921.07
C3′	4994.56	3507.33	3843.70	D1	5489.51	3250.94	3931.92
D1′	4887.55	3229.36	3891.02	D2	5436.74	3170.83	3926.04
D2′	4841.78	3316.03	3893.41	D3	5366.51	3167.37	3933.24
D3′	4792.95	3405.64	3894.41	E1	5442.25	3026.10	3970.27
E1′	4568.78	2999.27	3924.68	E2	5373.47	3017.55	3973.20
E2′	4566.44	3098.04	3922.63	E3	5300.42	3004.18	3993.34
E3′	4537.18	3186.83	3920.10	F1	5392.94	2825.10	4010.35
F1′	4351.65	2966.73	3966.68	F2	5313.94	2837.15	4014.76
F2′	4348.16	3042.89	3963.78	F3	5235.96	2839.27	4023.99
F3′	4323.87	3109.82	3961.80	G1	5405.47	2598.06	4057.83
G1′	4154.03	2900.68	4014.42	G2	5335.77	2670.24	4051.90
G2′	4150.22	2972.08	4008.26	G3	5256.60	2702.80	4043.08
G3′	4125.64	3035.64	4002.13	H1	5344.60	2435.59	4076.77
H1′	3947.61	2792.40	4064.98	H2	5280.15	2522.35	4071.83
H2′	3906.85	2932.66	4040.29	H3	5199.71	2574.85	4065.87
				L1	5152.33	2502.78	4077.70
				L2	5079.92	2433.38	4126.10

参考文献

[1] 井哲帆,1999.乌鲁木齐河源 1 号冰川表面运动速度和冰舌末端变化(1996/1997 和 1997/1998 年度). 中国科学院天山冰川观测试验站年报，15：154－159

[2] 井哲帆,1999.乌鲁木齐河源 1 号冰川表面运动速度和冰舌末端变化(1998/1999 和 1999/2000 年度). 中国科学院天山冰川观测试验站年报，16：

[3] 井哲帆,2002.乌鲁木齐河源 1 号冰川表面运动速度和冰舌末端变化(2000/2001 和 2001/2002 年度). 中国科学院天山冰川观测试验站年报，16：

天山奎屯河哈希勒根 51 号冰川表面运动速度和冰舌末端变化

（2002/2003 和 2003/2004 年度）

井哲帆

（中国科学院寒区旱区环境与工程研究所，甘肃 兰州 730000）

1 观测与说明

2003 年 9 月和 2004 年 8 月，对天山奎屯河哈希勒根 51 号冰川的运动变化又进行了观测。本文公布了 2003 年度和 2004 年度的冰川表面运动观测资料。

冰川表面运动速度的观测是使用全站仪进行测量的，从控制点 K1、K2 上对布设在冰川表面的测杆进行观测的，以座标法计算出冰体单位时间内的空间位移.。冰舌末端变化测量采用距离丈量法观测.。

2003 年 9 月对冰川表面的运动观测点又重新进行了调整布设，坐标系采用北京 54 坐标系。

表 1、2 分别为 2002/2003、2003/2004 年度的冰川表面运动速度，表 3 是冰舌末端的年进退变化量， 表 4 是观测运动点的坐标值。

2 运动速度的年际变化

奎屯河 51 号冰川 2002/2003 年度和 2003/2004 年度的表面运动速度值 U_{xy} 还是不大，从表 1 中可以看出，该冰川 2002/2003 年度的最大流速点为 E1 点，高度在平衡线 3600 m 处，其年流速为 3.00m。

由于在 2003 年 9 月对运动点位重新进行了调整，与 2002 年度的点位不可进行同名点比较，但总体上该冰川 2003/2004 年度的运动速度值不大，最大流速点为 E3 点，其速度值为 2.99m.a^{-1}，运动速度垂直分量 U_Z 的变化规律同往年冰川的变化规律完全相同. 即消融区的显出流作用和积累区的显入流作用.

3 冰舌末端变化

冰川末端进退的观测方法是通过在 GPS 测定的控制观测点进行重复距离丈量得出的。2002/2003 年度的平均退缩量为 5.13 m，2003/2004 年度的平均退缩量为 5.15m。

表1 年运动速度（观测日期：2002.09.06—2003.09.03）

点名	U_x（m）	U_y(m)	U_{xy}(m)	U_z(m)	a(° ′)	U_{xy}(m/a)
A1	-0.97	-2.40	2.58	-1.42	248 05	2.60
A2	-1.06	-2.37	2.60	-1.40	245 22	2.62
A3	-1.03	-2.35	2.56	-1.48	243 31	2.58
B1	-1.38	-1.60	2.11	-1.16	227 44	2.13
B2	-1.32	-1.43	1.95	-1.17	226 29	1.97
B3	-1.30	-1.46	1.95	-1.17	226 46	1.97
C1	-1.05	-1.27	1.65	-1.10	228 45	1.66
C2	-1.06	-1.21	1.61	-1.12	228 23	1.62
C3	-1.02	-1.15	1.54	-1.10	227 43	1.55
C4	-1.12	-1.13	1.59	-1.06	222 13	1.60
D1	-1.21	-1.40	1.85	-1.03	228 12	1.87
D2	-1.18	-1.47	1.88	-1.02	230 34	1.90
D3	-1.33	-1.20	1.79	-1.11	221 19	1.81
D4	-1.84	-1.17	2.18	-1.46	211 14	2.20
E1	-2.70	-1.25	2.98	-2.08	204 21	3.00
E2	-2.74	0.80	2.85	-1.03	164 32	2.88
E3	-2.68	0.82	2.80	-1.27	163 13	2.82
F	-1.50	-0.60	1.61	-1.30	201 33	1.63

表2 年运动速度（观测日期：2003.09.03—2004.08.26）

点名	U_x（m）	U_y(m)	U_{xy}(m)	U_z(m)	a(° ′)	U_{xy}(m/a)
A1	-0.95	-2.35	2.53	-1.40	247 59	2.58
A2	-1.04	-2.33	2.55	-1.41	245 56	2.60
A3	-1.01	-2.32	2.53	-1.45	246 28	2.58
B1	-1.36	-1.57	2.08	-1.13	229 05	2.12
B2	-1.30	-1.40	1.91	-1.15	227 07	1.95
B3	-1.28	-1.44	1.93	-1.15	228 22	1.96
C1	-0.94	-1.22	1.54	-1.11	232 23	1.57
C2	-1.01	-1.21	1.58	-1.13	230 09	1.60
C3	-0.96	-1.12	1.48	-1.11	229 24	1.50
C4	-1.03	-1.11	1.51	-1.08	227 08	1.54
C5	-0.95	-1.13	1.48	-1.10	229 56	1.50
C+1	-0.96	-1.15	1.50	-1.06	230 08	1.53
C+2	-0.98	-1.17	1.53	-1.04	230 03	1.56
D1	-1.21	-1.36	1.82	-1.04	228 20	1.86
D2	-1.14	-1.42	1.82	-1.02	231 14	1.86
D3	-1.20	-1.32	1.78	-1.09	227 43	1.82
D4	-1.38	-1.59	2.11	-1.01	229 03	2.15
D5	-1.33	-1.48	1.99	-1.05	229 03	2.03
D6	-1.52	-1.21	1.94	-1.36	218 31	1.98
E1	-2.51	-0.83	2.64	-1.14	198 18	2.69
E2	-2.62	0.80	2.74	-1.03	163 01	2.79
E3	-2.68	-1.20	2.94	-1.97	204 07	2.99
E4	-2.72	0.82	2.84	-1.00	163 13	2.90
E5	-2.64	0.80	2.76	-1.23	163 09	2.81
F1	-2.27	-0.74	2.39	-1.12	198 03	2.43
F2	-1.44	-0.67	1.59	-1.25	204 57	1.62

表 3 冰舌末端变化量(观测日期：2000.08.22—2002.09.06)

时 间	2002.09.06—2003.09.03	2003.09.03—2004.08.26
末端变化(m)	-5.10	-5.05
年平均变化(m)	-5.13	-5.15

注：“—”表示为后退

表 4 运动速度点坐标

观测时间			2003.09.03			2004.08.26
点名	X(m)	Y(m)	Z(m)	X(m)	Y(m)	Z(m)
A1	90273.52	47716.48	3507.47	90272.57	47714.13	3506.07
A2	90362.45	47637.40	3508.83	90361.41	47635.07	3507.42
A3	90441.24	47499.66	3507.42	90440.23	47497.34	3505.97
B1	90126.35	47636.26	3534.24	90124.99	47634.69	3533.11
B2	90263.54	47554.04	3535.22	90262.24	47552.64	3534.07
B3	90365.13	47446.25	3535.05	90363.85	47444.81	3533.90
C1	89870.22	47575.53	3550.66	89869.28	47574.31	3549.55
C2	89999.61	47511.26	3557.45	89998.60	47510.05	3556.32
C3	90106.27	47447.24	3555.30	90105.31	47446.12	3554.19
C4	90224.53	47394.47	3556.84	90223.50	47393.36	3555.76
C5	90330.48	47330.52	3556.73	90329.53	47329.39	3555.63
C+1	89896.47	47450.12	3567.15	89895.51	47448.97	3566.09
C+2	89986.08	47395.51	3775.03	89985.10	47394.34	3773.99
D1	89709.42	47459.50	3581.22	89708.21	47458.14	3580.18
D2	89821.56	47380.46	3577.46	89820.42	47379.04	3576.44
D3	89942.61	47330.66	3580.38	89941.41	47329.34	3579.29
D4	90079.05	47283.55	3585.39	90077.67	47281.96	3584.38
D5	90189.26	47254.63	3585.57	90187.93	47253.15	3584.52
D6	90294.44	47189.23	3584.63	90292.92	47188.02	3583.27
E1	89768.58	47263.18	3616.38	89766.07	47262.35	3615.24
E2	89870.52	47190.59	3614.83	89867.90	47191.39	3613.80
E3	89468.24	47115.47	3613.15	89465.56	47114.27	3611.18
E4	90103.63	47060.22	3612.23	90100.91	47061.04	3611.23
E5	90231.41	47035.56	3611.16	90228.77	47036.36	3609.93
F1	89649.47	47236.32	3631.62	89647.20	47235.58	3630.50
F2	90113.42	46844.67	3440.27	90111.98	46844.00	3439.02

参考文献(References):

1] 井哲帆，叶柏生，焦克勤，杨惠安。天山奎屯河哈希勒根 51 号冰川表面运动特征分析[J]. 冰川冻土 2002，24（5）：566—569.

2] 井哲帆，2002.天山奎屯河哈希勒根 51 号冰川表面运动速度和冰舌末端变化(2000/2001 和 2001/200 年度). 中国科学院天山冰川观测试验站年报，16：71－74.

天山乌鲁木齐河源 1 号冰川过程研究资料整编说明

本资料为天山冰川观测试验站过程研究小组（简称 PGPI）自 2002 年 9 月 14 日至 2004 年 12 月 14 日期间所挖取的 118 个连续雪坑剖面。PGPI 取样点位于 1 号冰川东支海拔 4130m 处的粒雪盆厚壁，取样频率为每周一次。

雪层剖面资料

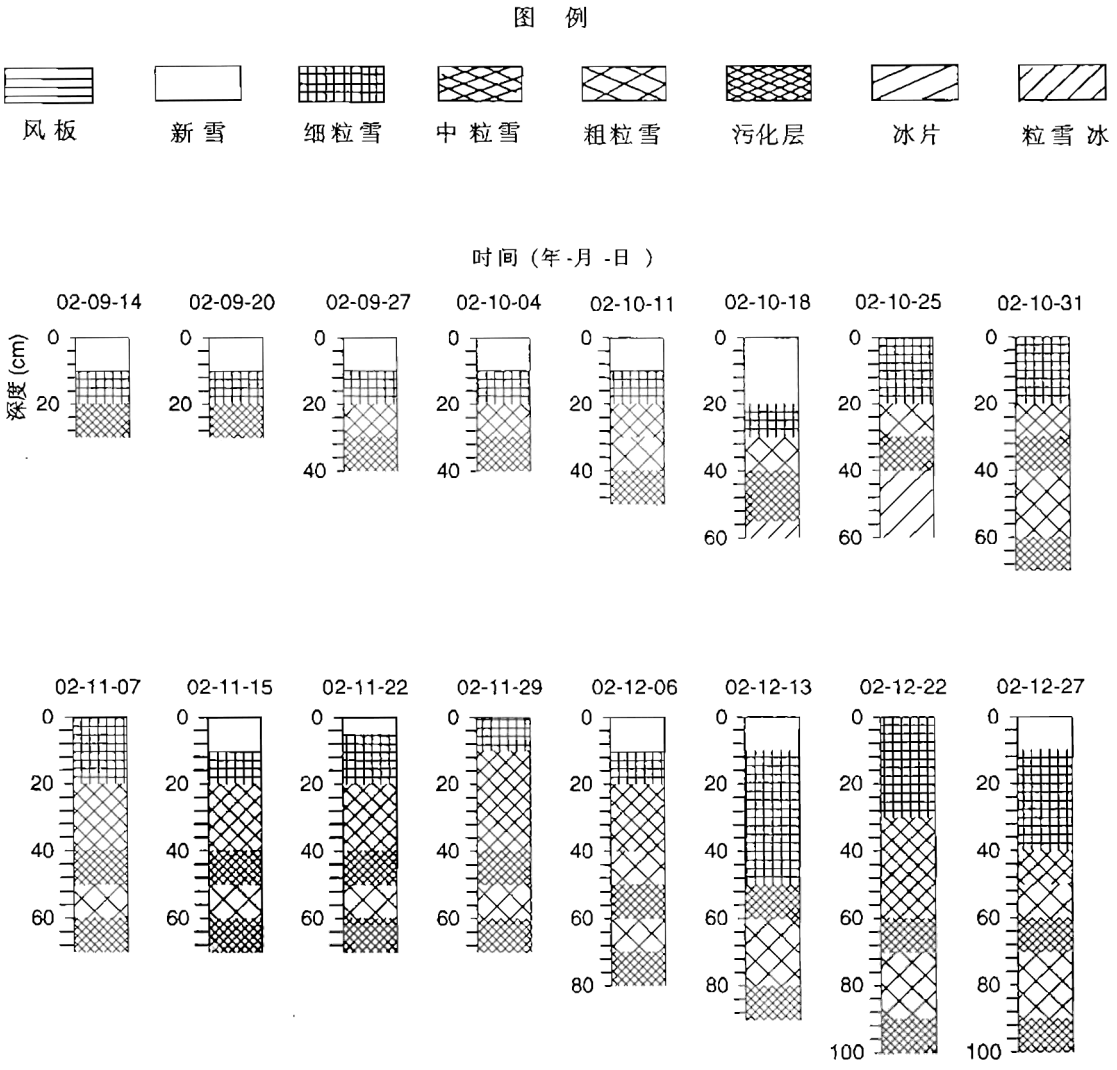

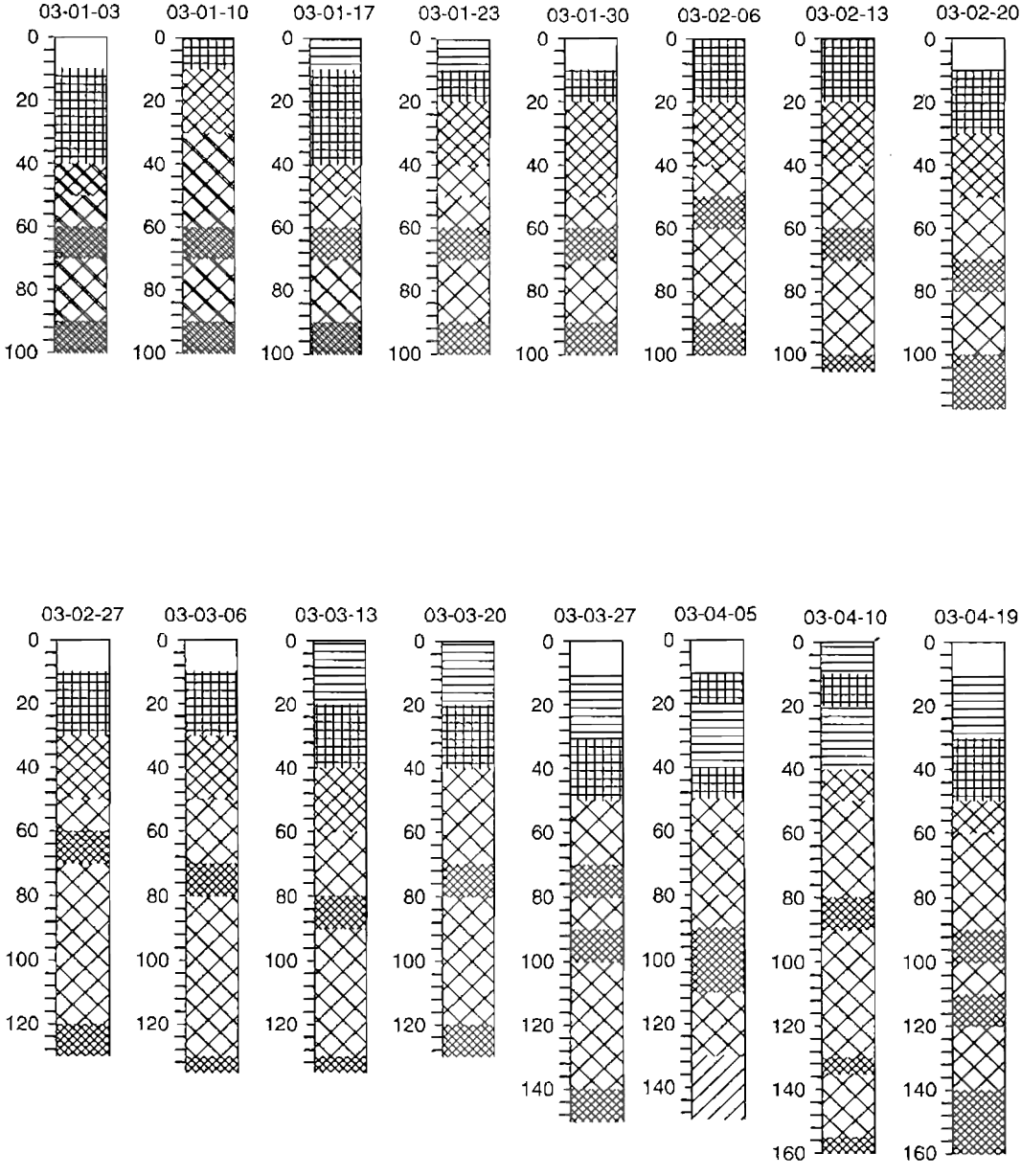
03-01-03
03-01-10
03-01-17
03-01-23
03-01-30
03-02-06
03-02-13
03-02-20
03-02-27
03-03-06
03-03-13
03-03-20
03-03-27
03-04-05
03-04-10
03-04-19

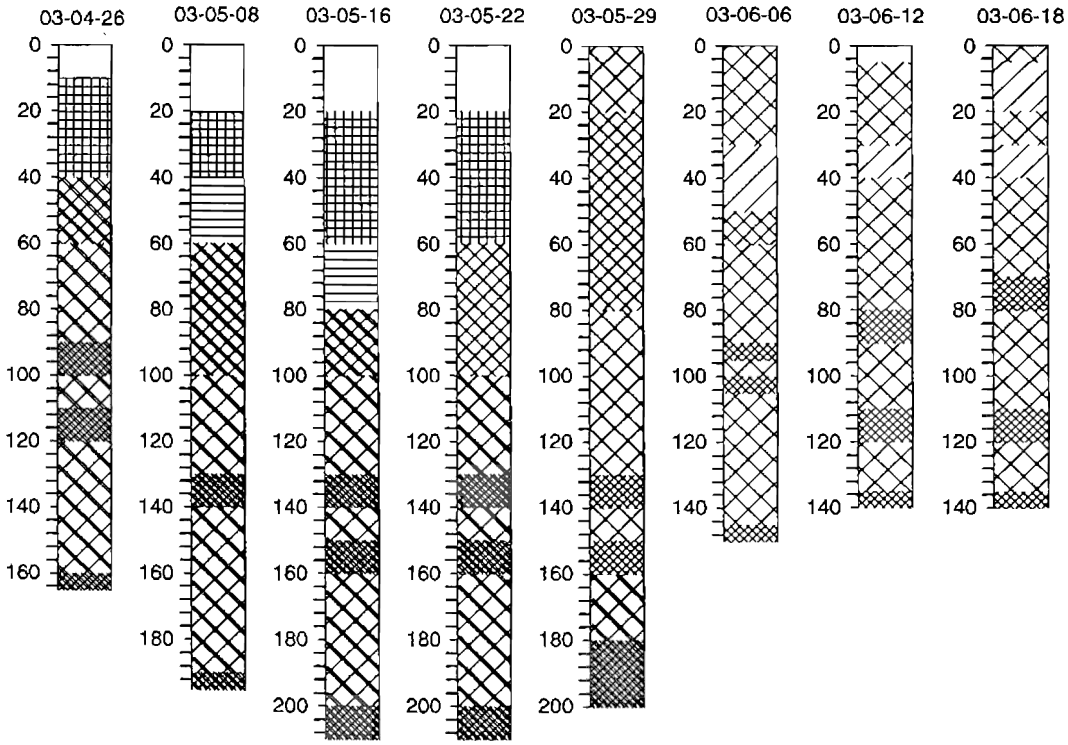
03-04-26
03-05-08
03-05-16
03-05-22
03-05-29
03-06-06
03-06-12
03-06-18
0
20
40
60
80
100
120
140
160
180
200

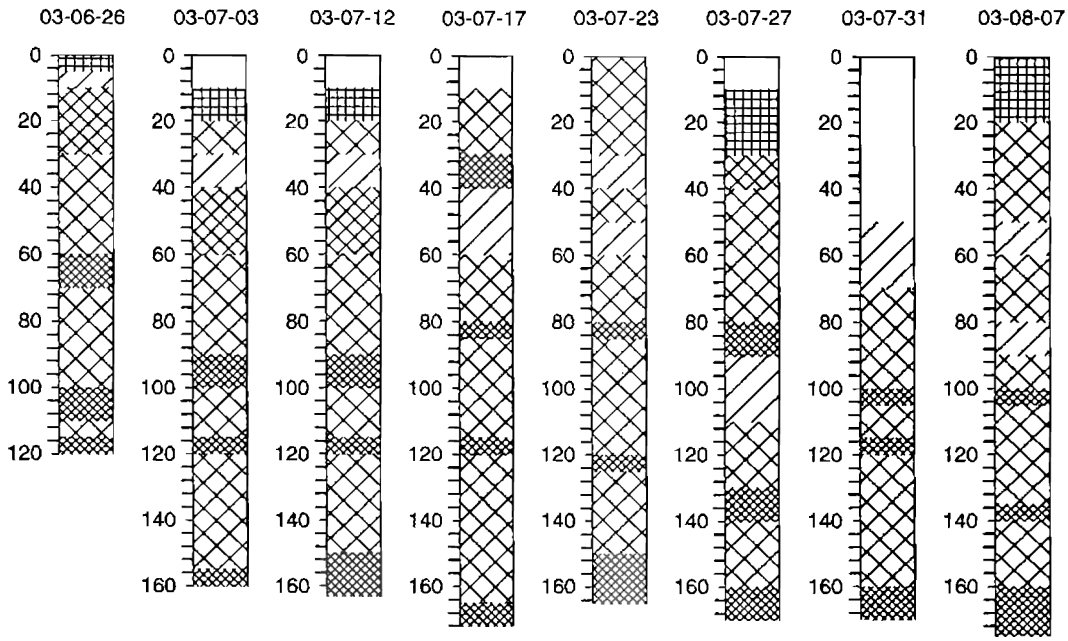
03-06-26
03-07-03
03-07-12
03-07-17
03-07-23
03-07-27
03-07-31
03-08-07
0
20
40
60
80
100
120
140
160

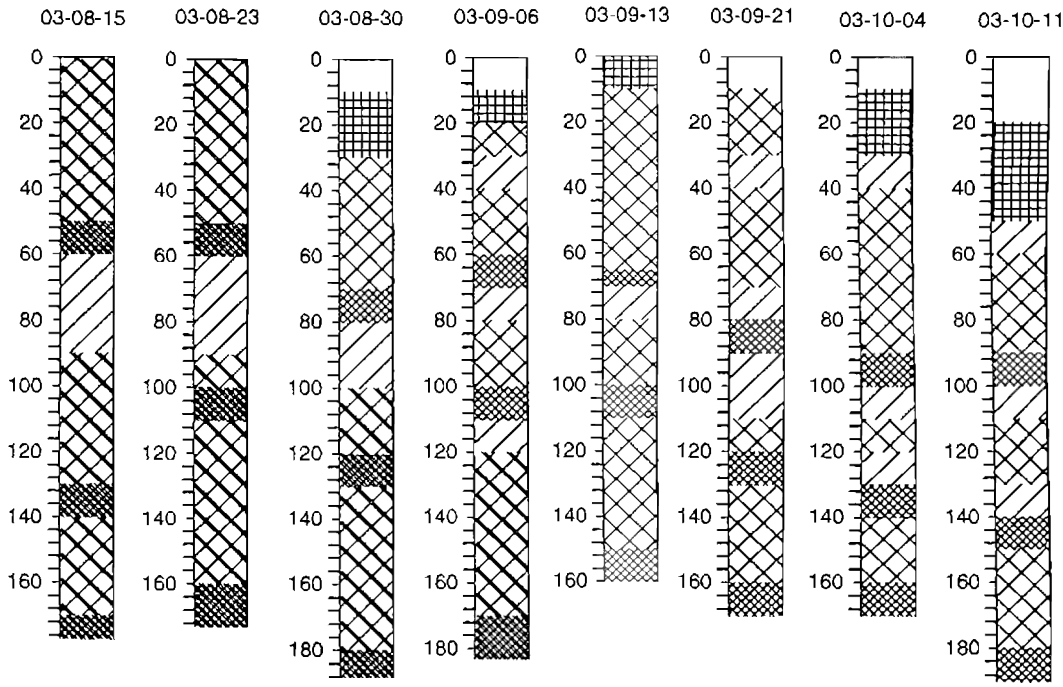
03-08-15
03-08-23
03-08-30
03-09-06
03-09-13
03-09-21
03-10-04
03-10-11

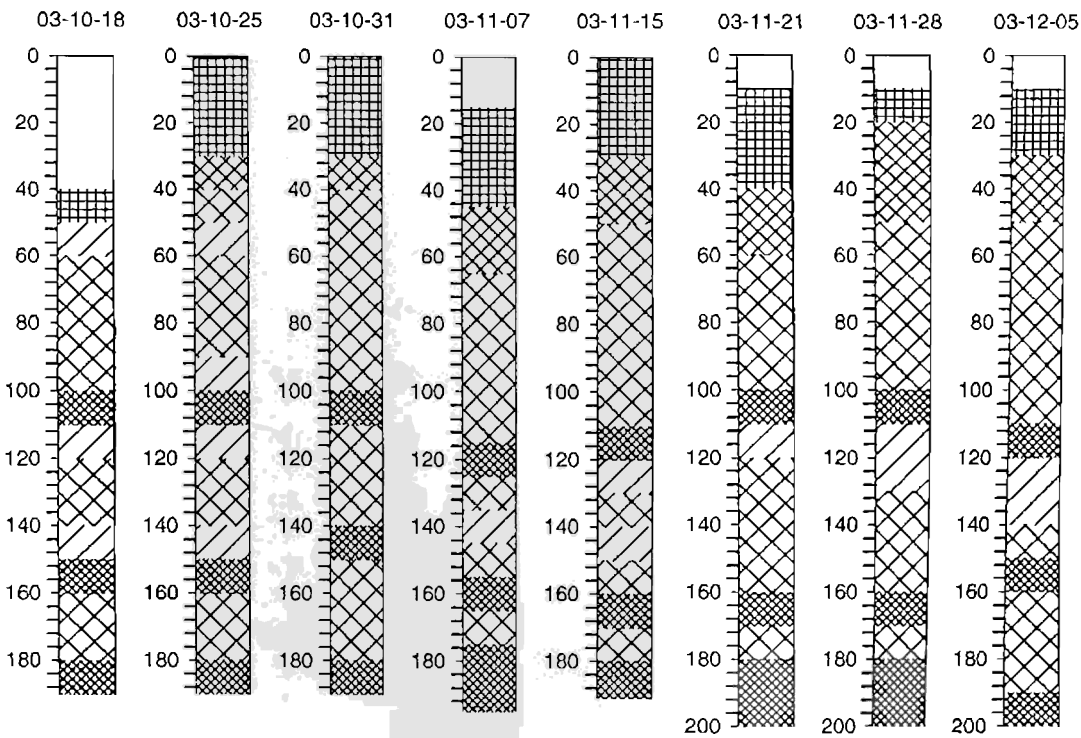
03-10-18
03-10-25
03-10-31
03-11-07
03-11-15
03-11-21
03-11-28
03-12-05

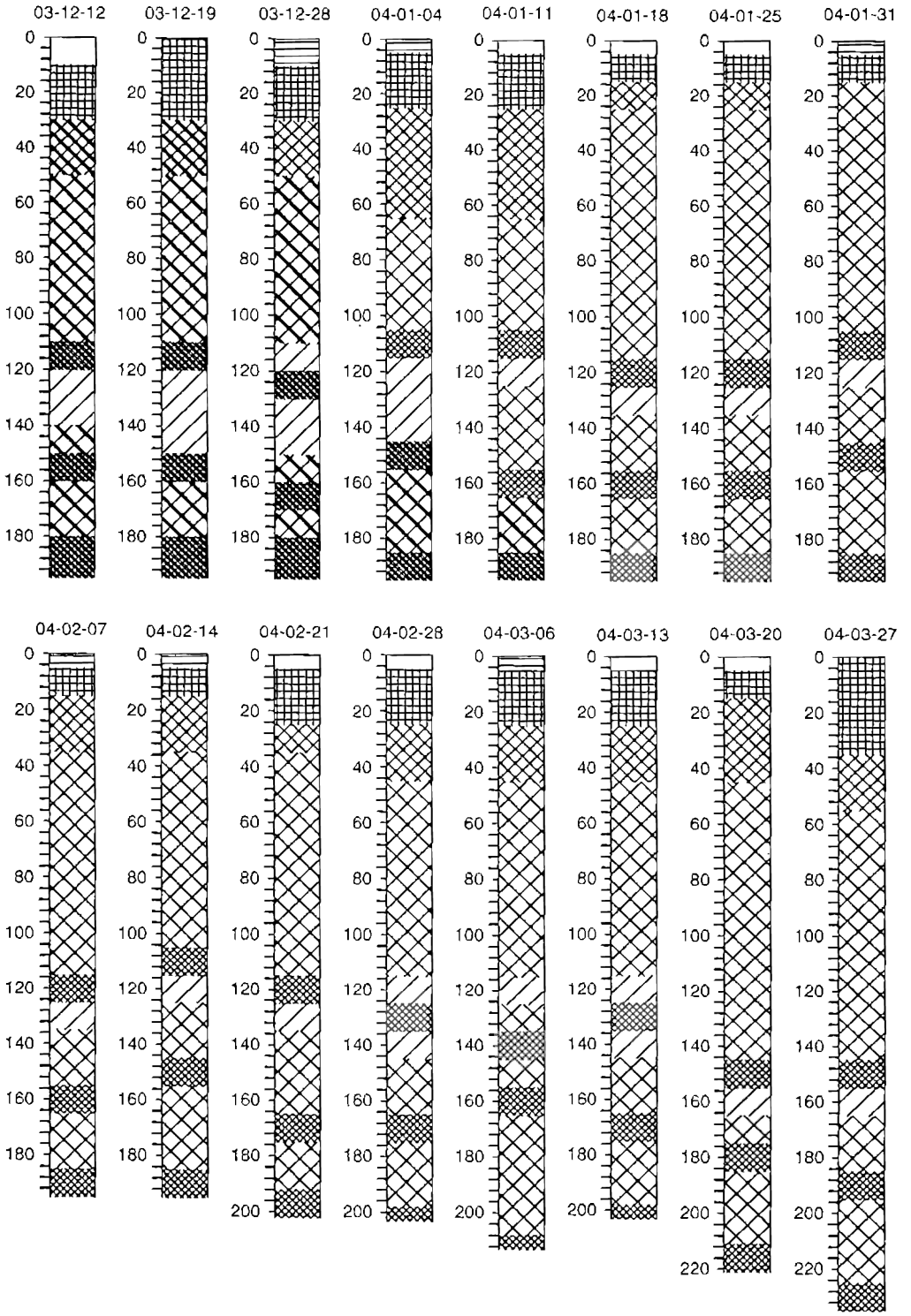
03-12-12
03-12-19
03-12-28
04-01-04
04-01-11
04-01-18
04-01-25
04-01-31
04-02-07
04-02-14
04-02-21
04-02-28
04-03-06
04-03-13
04-03-20
04-03-27

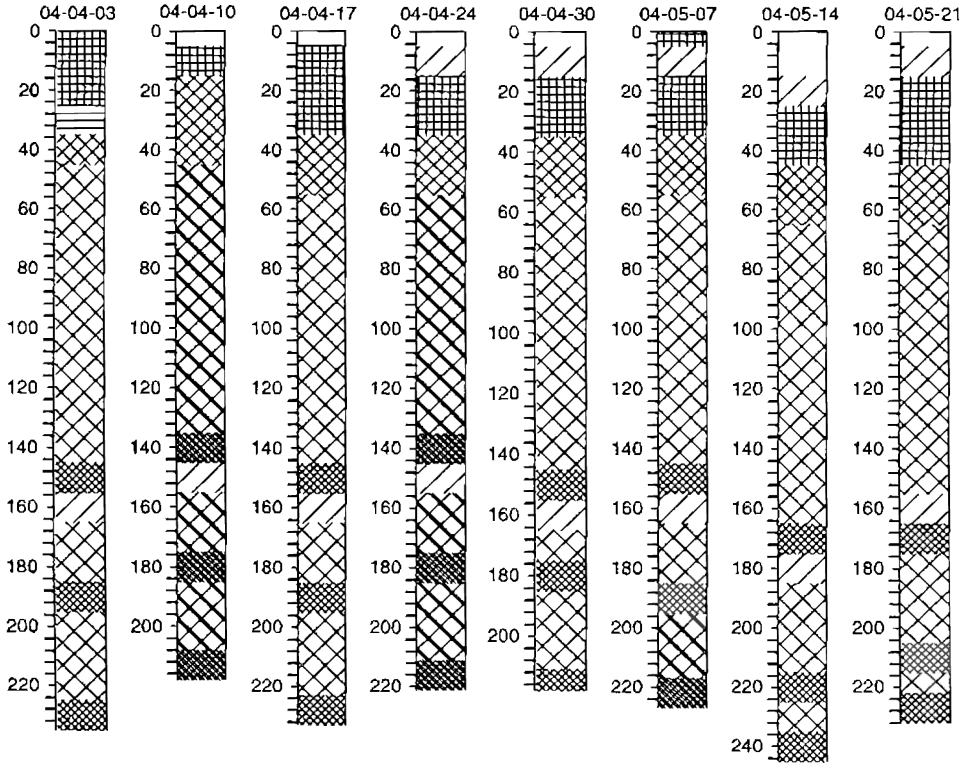
04-04-03
04-04-10
04-04-17
04-04-24
04-04-30
04-05-07
04-05-14
04-05-21

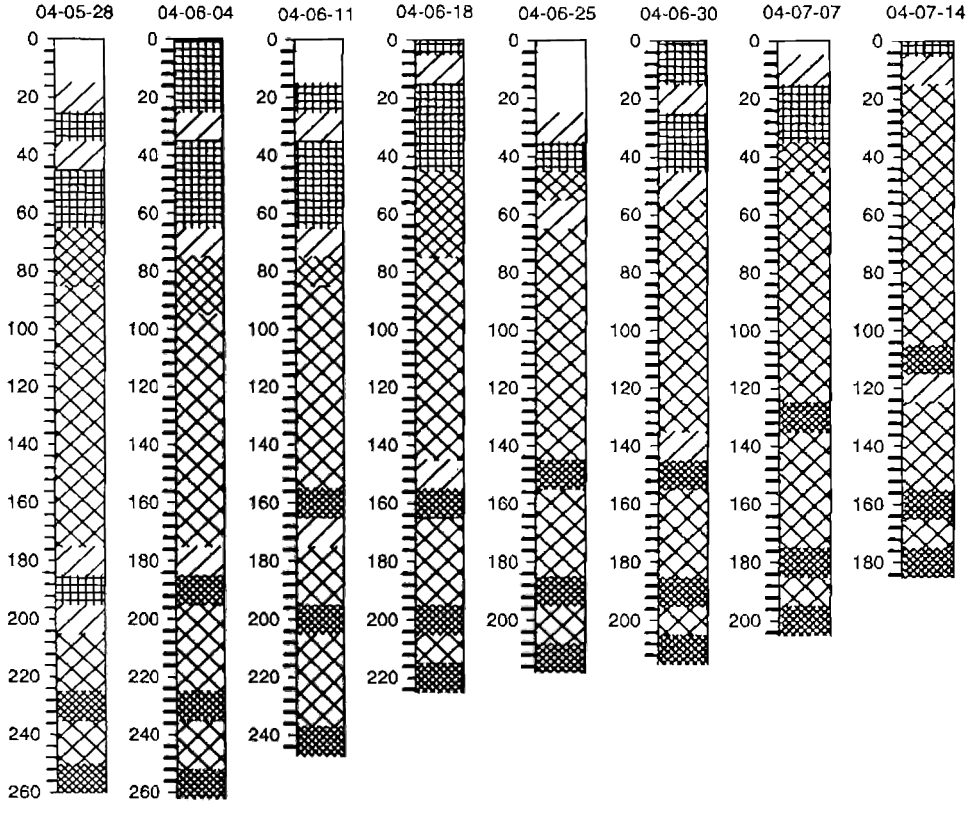
04-05-28
04-06-04
04-06-11
04-06-18
04-06-25
04-06-30
04-07-07
04-07-14

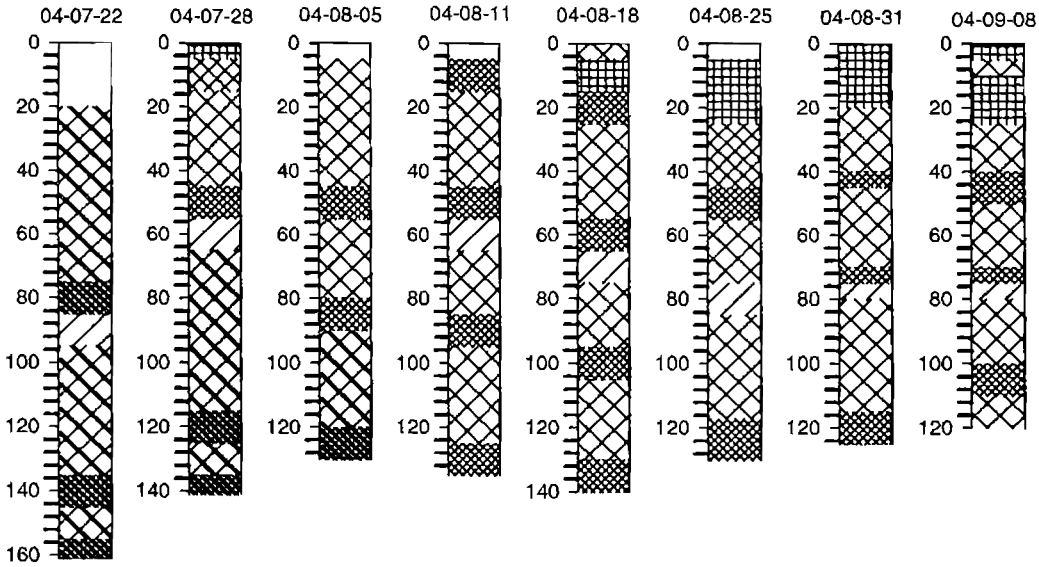
04-07-22
04-07-28
04-08-05
04-08-11
04-08-18
04-08-25
04-08-31
04-09-08

竹板资料

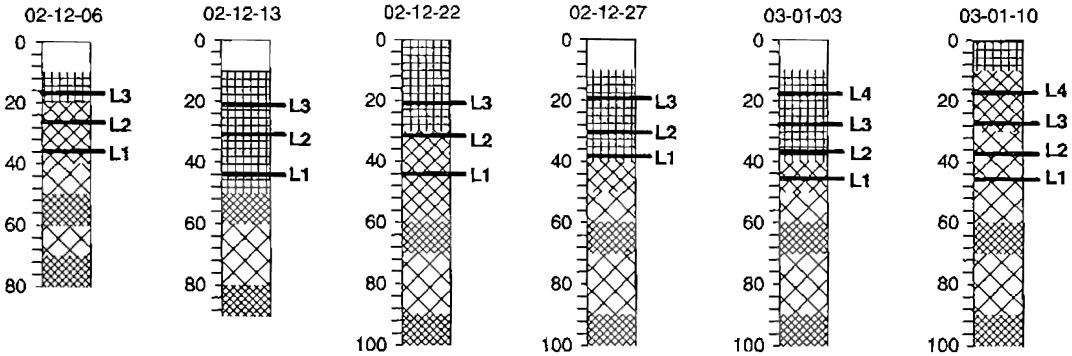
02-12-06
02-12-13
02-12-22
02-12-27
03-01-03
03-01-10
L1
L2
L3
L4

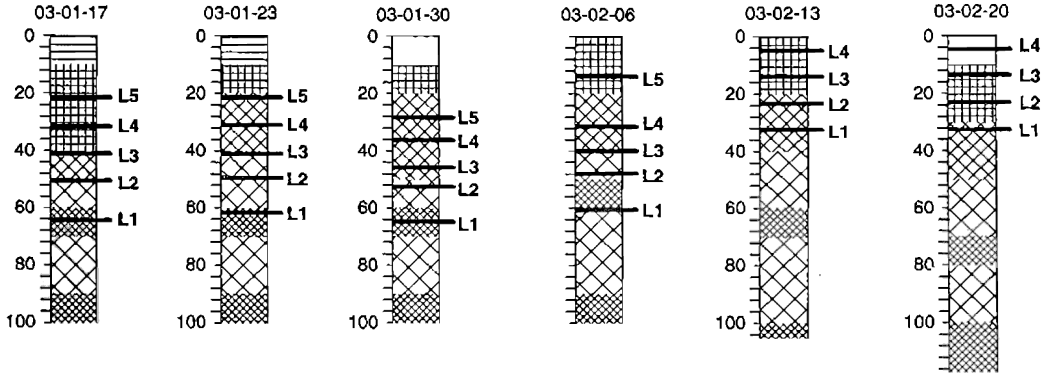
03-01-17
0
20
40
60
80
100
L5
L4
L3
L2
L1
03-01-23
0
20
40
60
80
100
L5
L4
L3
L2
L1
03-01-30
0
20
40
60
80
100
L5
L4
L3
L2
L1
03-02-06
L5
L4
L3
L2
L1
03-02-13
0
20
40
60
80
100
L4
L3
L2
L1
03-02-20
0
20
40
60
80
100
L4
L3
L2
L1

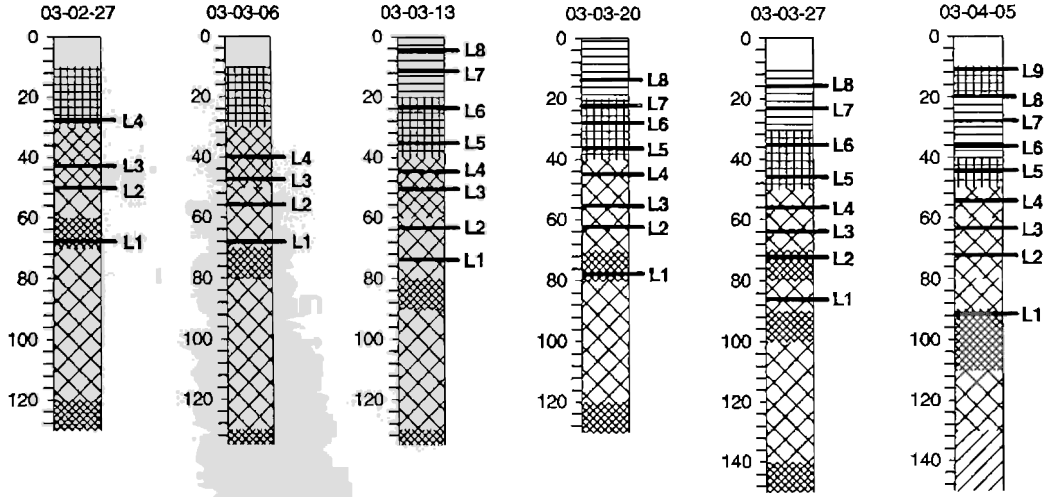
03-02-27
0
20
40
60
80
100
120
L4
L3
L2
L1
03-03-06
0
20
40
60
80
100
120
L4
L3
L2
L1
03-03-13
0
20
40
60
80
100
120
L8
L7
L6
L5
L4
L3
L2
L1
03-03-20
0
20
40
60
80
100
120
L8
L7
L6
L5
L4
L3
L2
L1
03-03-27
0
20
40
60
80
100
120
140
L8
L7
L6
L5
L4
L3
L2
L1
03-04-05
0
20
40
60
80
100
120
140
L9
L8
L7
L6
L5
L4
L3
L2
L1

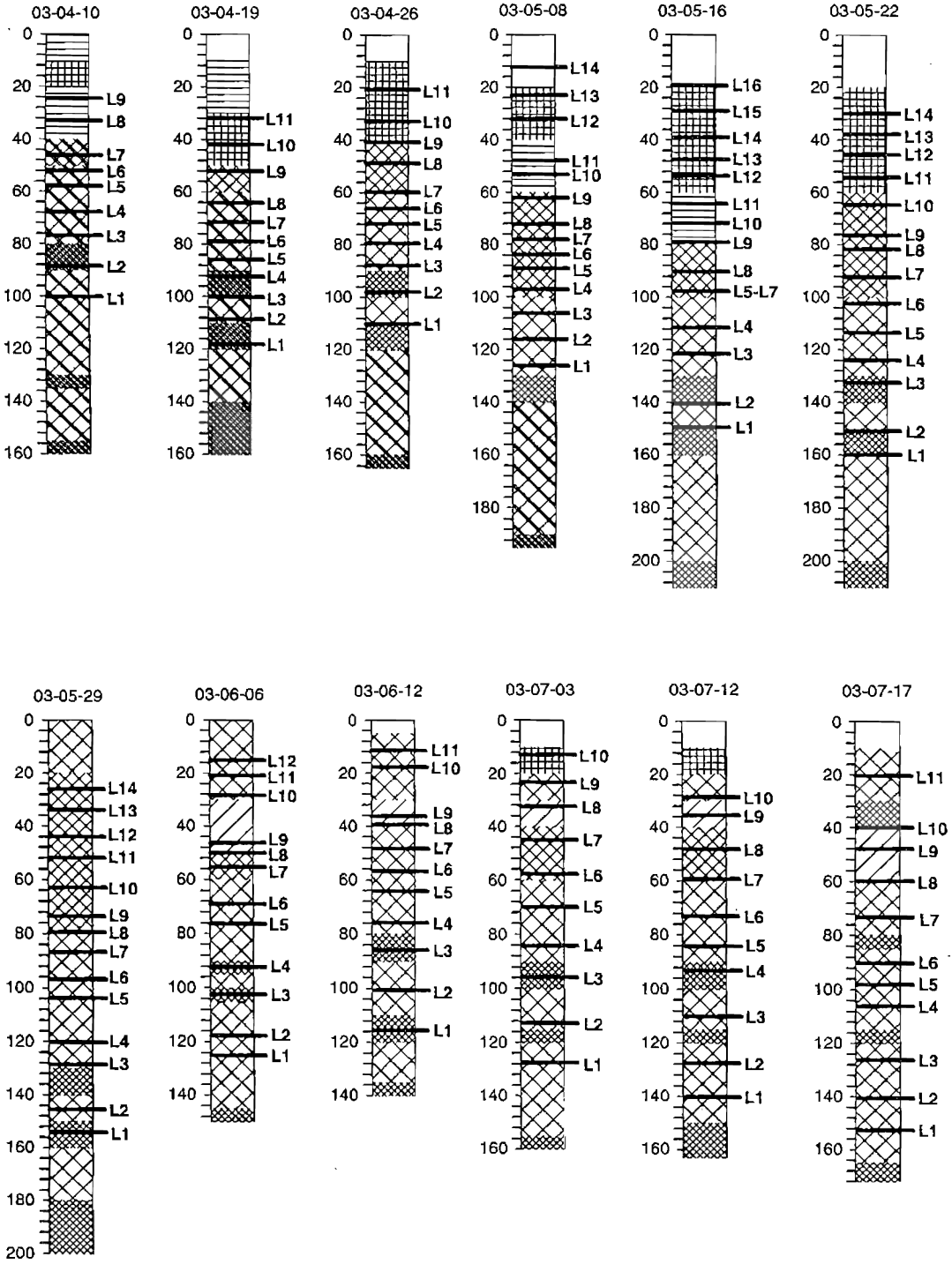
03-04-10
03-04-19
03-04-26
03-05-08
03-05-16
03-05-22
03-05-29
03-06-06
03-06-12
03-07-03
03-07-12
03-07-17

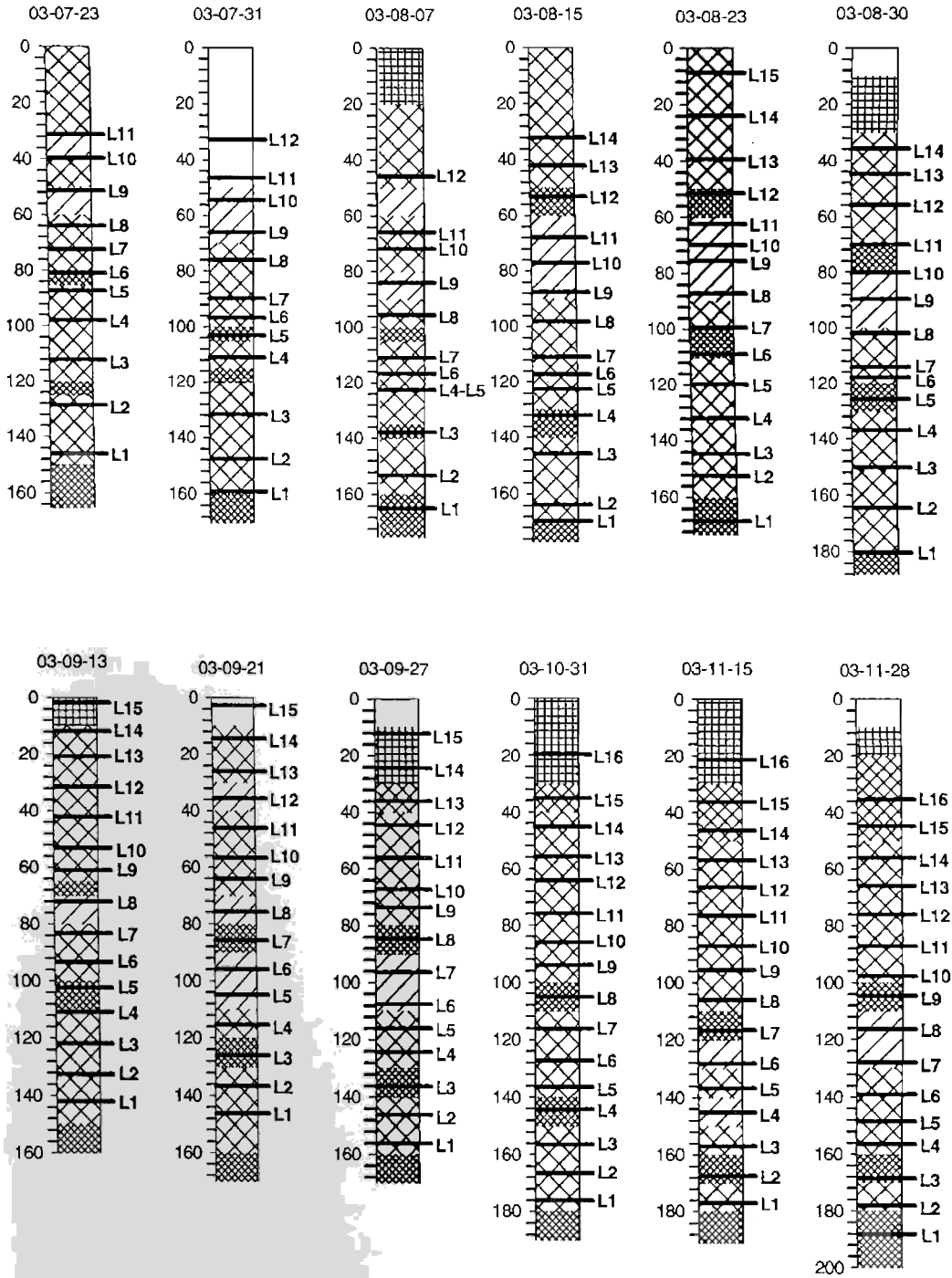
03-07-23
03-07-31
03-08-07
03-08-15
03-08-23
03-08-30
03-09-13
03-09-21
03-09-27
03-10-31
03-11-15
03-11-28

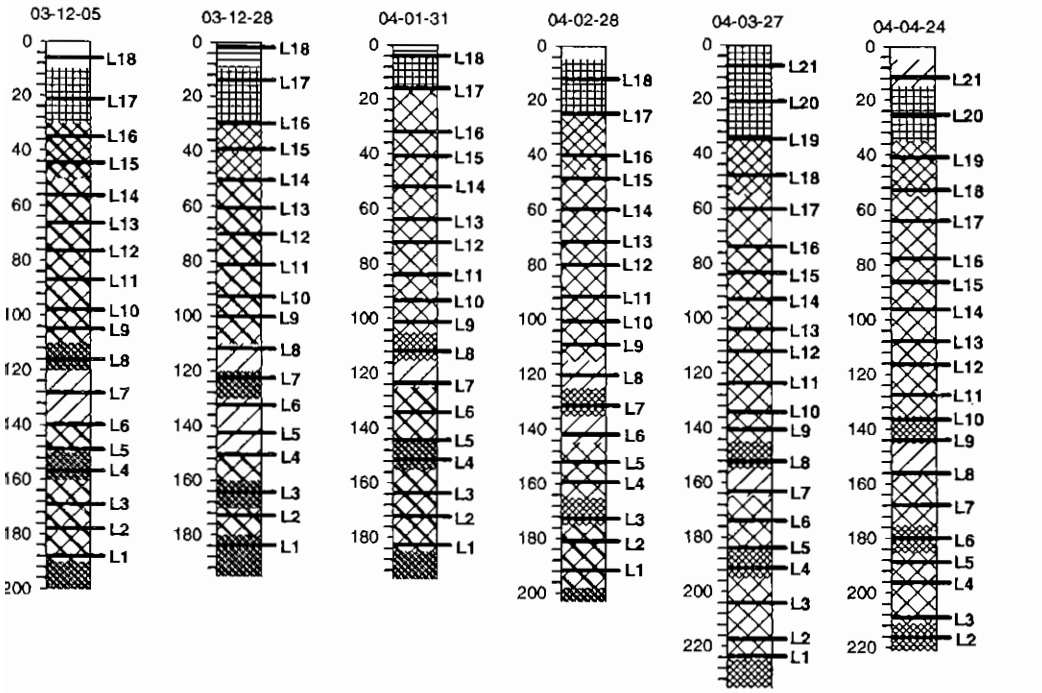
03-12-05
03-12-28
04-01-31
04-02-28
04-03-27
04-04-24

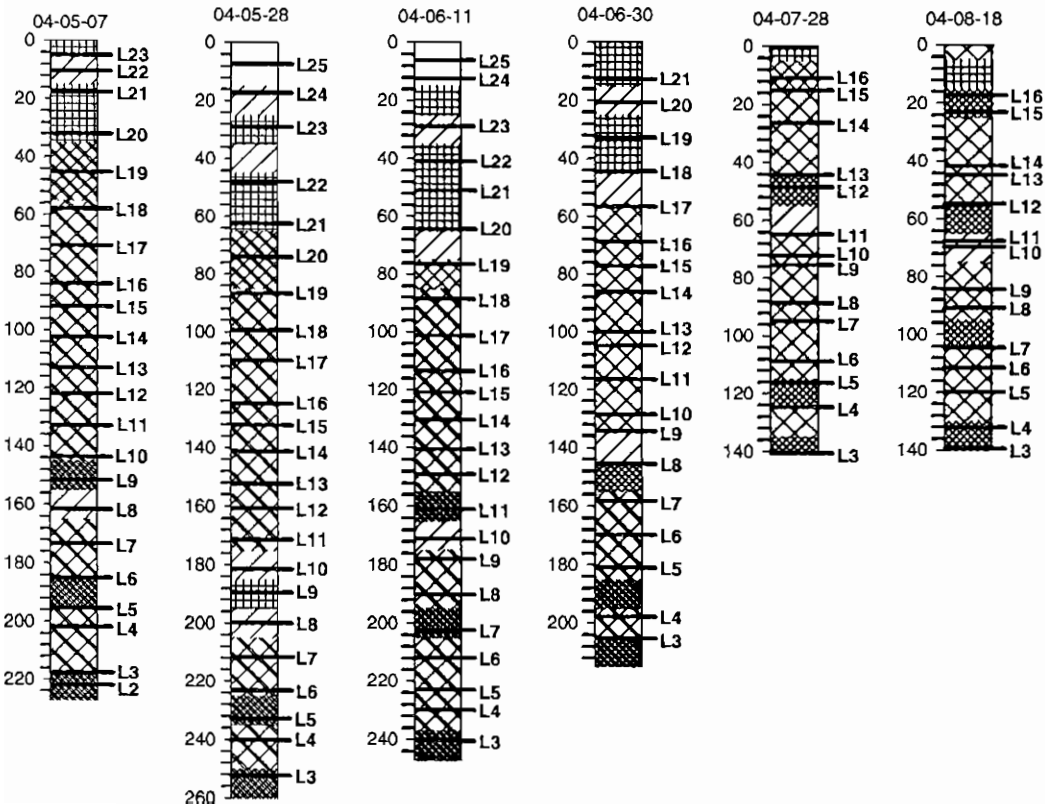
04-05-07
04-05-28
04-06-11
04-06-30
04-07-28
04-08-18